EFFECTS OF TIME VARYING AND CONSTANT LOADS ON EFFECTIVENESS OF FAULT DETECTION METHODS OF ELECTRICAL MACHINE

THESIS

submitted in fulfillment of the requirement of the degree of

DOCTOR OF PHILOSOPHY

to

J.C.BOSE UNIVERSITY OF SCIENCE & TECHNOLOGY,

YMCA, FARIDABAD

by

KALPANA SHEOKAND

Registration No: YMCAUST/Ph23/2011

Under the Supervision of

Dr. NEELAM TURK

PROFESSOR

Department of Electronics Engineering

Faculty of Engineering and Technology

J.C. Bose University of Science & Technology, YMCA

Sector-6, Mathura road Faridabad, Haryana, India

OCTOBER, 2021

DECLARATION

I hereby declare that this thesis entitled **EFFECTS OF TIME VARYING AND CONSTANT LOADS ON EFFECTIVENESS OF FAULT DETECTION METHODS OF ELECTRICAL MACHINE** by **KALPANA SHEOKAND,** being submitted in fulfilment of the requirement for the Degree of Doctor of Philosophy in **ELECTRONICS ENGINEERING** under Faculty of Engineering of J. C. Bose University of Science and Technology, YMCA , Faridabad, during the academic year 2020-2021, is a bona fide record of my original work carried out under guidance and supervision of **Dr. NEELAM TURK, PROFESSOR, DEPARTMENT OF ELECTRONICS ENGINEERING,** J. C. Bose University of Science and Technology, YMCA, Faridabad and has not been presented elsewhere.

I further declare that the thesis does not contain any part of any work which has been submitted for the award of any degree either in this university or any other university.

Kalpana Sheokand

Registration No. YMCAUST /Ph 23/2011

CERTIFICATE

This is to certify that this thesis entitled **EFFECTS OF TIME VARYING AND CONSTANT LOADS ON EFFECTIVENESS OF FAULT DETECTION METHODS OF ELECTRICAL MACHINE by KALPANA SHEOKAND**, submitted in fulfilment of the requirement for the Degree of Doctor of Philosophy in **ELECTRONICS ENGINEERING** under Faculty of Engineering of J. C. Bose University of Science and Technology, YMCA, Faridabad, during the academic year 2020-2021, is a bona fide record of the work carried out under my guidance and supervision.

I further declare that to best of my knowledge the thesis does not contain any part of any work which has been submitted for the award of any degree either in this university or any other university.

Dr. Neelam Turk
Professor
Department of Electronics Engineering
Faculty of Engineering and Technology
J.C. Bose University of Science and Technology,
YMCA, Faridabad

Dated:

ACKNOWLEDGEMENT

First of all, I sincerely acknowledge my gratitude to **ALMIGHTY** whose blessings have bestowed in me the will power and confidence to carry out my project. It is both an elevating and humbling experience to have the opportunity to acknowledge all the peoples involved in this thesis work.

I have a great pleasure to express my deep sense of respect and sincere gratitude to my supervisor ***Dr. Neelam Turk***, Professor, Electronics Engineering Department, J. C. Bose University of Science & Technology, YMCA, Faridabad, Haryana, for her guidance, motivation, and inspiration. She has been my inspiration as I hurdle all the obstacles in the completion of this research work. Her encouragement and attention in every stage of my research work provided me with the spirit to complete this research.

I also wish to express my sincere gratitude to ***Prof. (Dr.) Neelam Turk***, Chairperson, Electronics Engineering Department, J. C. Bose University of Science & Technology, YMCA, Faridabad, Haryana for her sincerely help and providing me the necessary research facilities for the completion of the work.

I am grateful to the Vice-Chancellor ***Prof. Dinesh Kumar***, J. C. Bose University of Science & Technology, YMCA, Faridabad and ***Prof. M. L. Agarwal***, Dean (Engineering and Technology) for their support and encouragement during my course of study.

I am very much thankful to ***Prof. (Dr.) Munish Vashishath***, Professor, Electronics Engineering Department, J. C. Bose University of Science & Technology, YMCA, Faridabad, Haryana, who has been a constant support to me and helped me for understanding the complex mathematical modeling during my research work.

I am also thankful to the all faculty members and staff of Electronics Engineering Department of J. C. Bose University of Science & Technology, YMCA, Faridabad for their continuous support and co-operation.

Though inept, I would like to express my deep gratitude to my **parents**, for being supportive, understanding, patient, and for having shaped me into who I am. They have always encouraged my academic endeavour which is my greatest motivation in the study.

I also express my deep appreciation to my husband ***Mr. Sudhir Sheokand*** and loving daughters ***Tanishka, Anvika*** and son ***Lakshiv*** whose constant inspiration, patience, understanding and moral support have greatly contributed to the realization of this work.

I feel indebted to all well-wishers, whose names remain unmentioned but who have never retraced back from helping me whenever the need arose.

Kalpana Sheokand

Registration No. YMCAUST /Ph 23/2011

ABSTRACT

Health monitoring involves taking measurements on an Induction Motor (IM) while it is operating in order to detect faults. For this purpose normally a single sensor type, for example current is used to detect the broken rotor bar using fault frequency components only under the full load condition or a limited number of load cases. The correlations among the different types of sensors and their ability to diagnose single and combined faults over a wide range of loads or dynamic change in the load have not been the focused part in the previous research work. Furthermore, to detect fault in Squirrel Cage Induction Motor (SCIM) using any fault frequency components, it is important to investigate the variability in its amplitude to other effects apart from fault severity and load this area of research has also been neglected in the literature of IM condition monitoring.

The main emphasizes of this research work is to find a methodology which effectively detects faults in induction machine under different constant and time varying loading conditions at an early stage in order to avoid its catastrophic failure which may further lead to system failure. In this research work, the stator current with vibration signals is used for feature selection and deep learning methods are used for classification of faults with its type and severity.

Deep learning methods are advance algorithms of artificial intelligence domain. Since after the introduction of deep learning algorithms it over shadows the other machine learning algorithms and are being extensively used in various applications due to its higher accuracy and adaptability to handle data.

This research work aims to improvise SCIM machine fault diagnosis and proposed the reliable methods to detect single and combined faults (other fault in presence of one fault) over a wide range of load conditions i.e. no load, 25%, 50% , 100% and under time varying load condition. The behavioral analysis of SCIM is analyzed using ANSYS software tools. By using RMxprt, a 5kW three-phase SCIM is designed. Consequently, the designed motor is transferred from ANSYS RMxprt to Maxwell 2D software tool to apply accurate Finite Element Method (FEM) for analysis purpose.

The SCIM model further put under 2D different failure's modes like (broken rotor bars,

stator fault, eccentricity faults) which are examined under different loading conditions. Fault generation and its effects are successfully investigated in ANSYS RMxprt & Maxwell 2D software tools. To achieve the Fault Detection (FD) and examined effects of load under time varying loading conditions, MATLAB software tool is used. The mathematical model of SCIM is designed and extensively executed under wide range of constant load variations and time varying loading scenarios and results are obtained after applying soft computing techniques like Support Vector Machine (SVM), Random Forest (RF) and Deep Belief Neural Networks (DBNN) under various type of rotor broken bar faults, stator winding faults, eccentricity faults and combined faults.

SVM and RF are applied for the comparative analysis of new age deep learning classifier with conventional SVM and RF classifier. All the techniques are applied to detect the faults in IM using DWT. This technique relies on the instantaneous reactive power signal decomposition, from which detail coefficients and wavelet approximations are extracted which is termed as features. In order to obtain a robust diagnosis, feature vectors are extracted from DWT analysis of power signals using DBNN to distinguish the motor state. Subsequently, in order to validate the proposed approach, a three phase SCIM is designed under MATLAB software.

To check the effectiveness of the proposed method in fault diagnosis, the motor is run under various operations of healthy and faulty conditions for different constant loads and time varying load. Promising results are obtained and proposed framework of DBNN is performed well with achieved detection accuracy 99.83%. The accuracy is calculated in terms of number of times the fault detected and classified correctly. So, in case of DBNN the accuracy achieved is higher than other algorithms like SVM and RF which are also used for FD in this research work. Finally, comparison with SVM, RF and other previous research work existing algorithms proves the efficacy of proposed deep learning algorithm which is more robust in diagnosing the faults in motor.

In future the work can be carried in the area of real-time intelligent system which would process the condition of the IM and issue the suitable command accordingly.

TABLE OF CONTENTS

LIST OF TABLES

LIST OF FIGURES

LIST OF ABBREVIATIONS

AC	Alternating Current
DWT	Discrete Wavelet Transform
EMF	Electro Magnetic Force
MCSA	Motor Current Signature Analysis
HMI	Human Machine Interface
FEM	Finite Element Method
DBNN	Deep Belief Neural Network
SVM	Support Vector Machine
FEA	Finite Element Analysis
IM	Induction Motor
SE	Static Eccentricity
NN	Neural Network
FDP	Failure Developing Period
MIMO	Multi Input Multi Output
FD	Fault Detection
EMWFA	Extension of the Modified
MMF	Magneto-Motive Force
OE	Output Error
GMM	Gaussian Mixed Model
RPS	Reconstructed Phase Space
MRF	Markov Random Field
RBF	Radial Basis Function
LOO	Leave-One-Out
RF	Random Forest
ROC	Receiver Operating Characteristic
KNN	K-Nearest Neighbor
MLP	Multilayer Perceptron

CHAPTER 1

INTRODUCTION

1.1 OVERVIEW

The electric motor is an electromechanical device that converts electrical energy into mechanical energy. As a very important part of modern industry, Induction Motors play an important role in important applications such as pump systems, fans, lifting systems, electric vehicles, crushers, cement plants, and many other industrial segments. An asynchronous motor, which is actually an AC motor in which the current required to generate torque, is induced by electromagnetic induction of the magnetic field of the stator winding [1]. Therefore, induction machines generally do not require external mechanical switching, individual excitation, or even self-excitation for part of the energy transferred from the stator to the rotor. The rotors of numerous electrical components in operating induction machines are highly prone to system failure [2].

With a squirrel cage rotor [3], its bars can be damaged by mechanical stresses on the machine. Meanwhile, the bearings in the IM can be affected by extreme wear and fragmentation caused by improper lubrication, unbalanced load on the motor, misalignment of the bearing components with the rotor, etc. Traditionally, most manufacturers and users trust it in a very traditional way approaches to IM protection such as overcurrent or overvoltage estimation to ensure reliable system operation. Fast and immensely complex IM applications in modern industrial applications are alarming for optimized system monitoring and monitoring for induction machines [3]. Even the reduction of the man-machine interface requires requirements for on-line detection, with which motor faults can be diagnosed effectively without danger or process interruptions. The IMs low cost and miniaturized size, low maintenance cost robustness and flexible operation with minimal power supply make this system highly efficient and useful in modern industrial process. Detecting faults in the IM in advance and diagnosing them optimally makes it easier for industry to work with the least unexpected industrial shutdown or maintenance mechanism [4]. This minimizes lost production, financial waste, and even prohibits catastrophic penalties. Condition monitoring and fault diagnosis mechanisms are necessary to formulate a well-defined and qualified map between the motor signals and the IM fault condition indications [4].

Various failure detection methods have been developed and effectively applied to detect machine failures at different stages using various machine variables such as current, voltage, speed, efficiency, temperature, and vibration [5]. Therefore, for economic and safety reasons, it is important to control the behavior of motors of different sizes. As an approach to condition monitoring, a very effective scheme can be offered that can provide the warning device at an early stage and efficiently predict the possibility of errors at an early stage of operation [6]. The monitoring system retrieves the details of the machines in use as raw data or raw details. By implementing advanced and highly efficient signal processing approaches, communicating diagnostic information to operators becomes very easy and straightforward, even well before the catastrophic machine failure. The challenging problem with this approach is that this mechanism requires continuous surveillance with human presence. Automation in the diagnostic process could include the logical progression of condition monitoring methods. To automate the diagnostic process, a series of soft computational diagnostic techniques using fuzzy logic [7, 8], NN [9] and machine learning algorithm [10] have recently been implemented.

In view of the need for a robust and highly efficient system for the detection of faults in IM, the approaches based on the Fourier transform and the wavelet transform can play a decisive role. The precision and spontaneous diagnostic potential of these signal processing approaches make them robust and efficient candidates for use in most induction machine fault detection applications [11]. The work presented considers the Discrete Wavelet Transform (DWT) technique with machine learning algorithms to achieve the objective of detection of errors in IM.

A number of approaches and systems are there for monitoring the IM functions for ensuring the higher consistency. Few leading approaches are as follows [12, 13]:

1. EMF monitoring systems,
2. Systems based on temperature estimation,
3. Monitoring approach based on radio frequency emissions analysis,

4. Approaches based on the estimation of noise and vibration in IM,
5. Approaches considering the speed and torque of rotor,

Despite these approaches and tools mentioned above, there are a number of companies that suffer from unexpected system failures that ultimately result in lower productivity in the industry. Various issues such as the environment, features, and system facilities can cause the system to fail in their combined form. Therefore, any type of optimization and improvement of the system could be of great interest to everyone.

1.2 BACKGROUND

Extensive research has been conducted over the past 20 years to develop new diagnostic and Fault Detection techniques for IM. The review also covers a wide range of literature in the field including machine modeling, conditioning monitoring, machine health assessment, types of faults in IM and FD techniques. In addition to the methods mentioned above, this literature survey also takes into account the most important developments in this area in recent years. This overview covers techniques related to model-based fault detection techniques, techniques based on signal processing, and techniques based on soft computing.

1.2.1 Model Based Techniques

In the recent past numerous researches have been conducted and numerous Fault Detection (FD) techniques like Finite Element Method (FEM), and others have been employed by the researchers for fault diagnosis. The major developments in these fields are covered in the review, from early research to the most recent.

Nandi et al. [14] has a broad distribution of the major electrical machines faults:

- Abnormal connection of the stator winding,
- Broken rotor bars or cracked end rings,
- Static and/or dynamic air-gap eccentricities,
- Bent shaft,
- Shorted rotor field winding,

- Bearing and gearbox failures.

These faults produce one or more of the following symptoms [14]:

- Unbalanced voltages and line currents,
- Increased torque pulsation,
- Decreased average torque,
- Increased losses and reduction in efficiency,

Transient analysis of an IM using FEA with predicted transient powers when starting the motor without load [15], when operating the motor with asymmetric stator excitation and during the turn-by-turn fault state, the geometric dimensions of the IM are modeled in the area of the finite elements. Diagnosis and characterization of the influence of broken rotor bars and connectors in squirrel cage motors using the state space sampling method for finite elements in connection with the temporal resolution method, diagnostic effects and characterization of elongation of broken bars and connectors [16]. The models are used to calculate/predict the characteristic frequency components that characterize bus bar and connector breakage. The behavior of electromagnetic properties is also analyzed using the FEM analysis for the occurrence of bus failure [17]. In other research work, flux density and mechanical stress were used to capture motor shaft failure in the mainline fed FEM model [18].

Most of the FD techniques available in the literature are based on the analytical model, which includes various assumptions for current spectrum analysis that does not take into account saturation, non-linear core materials and natural effects etc. To address this problem, the Equivalent Magnetic Circuit (EMC) model [19] was used to take into account the effects of magnetic saturation, the non-linear behavior of the material and the real representation of the air distribution in the stator and grooves rotor. Online diagnosis of squirrel cage motor failures using FEM suggests an approach based on the signature of global and external variables that is used to solve problems related to broken rotor bar and terminal ring [20]. This enables finer analysis using finite element-based implementation, higher precision, and an easier form of recognition. The use of finite element techniques to improve early fault detection techniques in three-phase IM describes how commercial finite element packages can be used to simulate rotor failures and thus improve the capacity of practical condition monitoring systems [21]. Accurate models of machines under failure conditions are developed using finite element packages with fixed mesh and timing. In Martin et al. [22], the influence of non-consecutive line breaks in MCSA to diagnose rotor faults in IM provides modeling to investigate the influence of the number and position of faulty bars on the diagnostic method of traditional MCSA. The analysis is based on the fault current and space vector theory, which provides a physical interpretation of the appearance of the left sideband component at a fraction of two extremes. In other studies, the static two-dimensional analysis of the fault and the results of the stator windings was compared with a healthy motor [23].

Vaseghi et al. [24] proposed IM model with stator winding fault and the model is validated using time steps FEA. The designed model is used to analyze the behavior of the machine under fault conditions. An IM analysis using time-step techniques shows that the equivalent circuit approach generally provides reasonable predictions about torque and current, but not information about flux distribution. This deficiency is remedied by a numerical approach using a nonlinear, time-shifted 2D finite element method to drive a constant voltage source [25]. Comparison of no-load stator current and other load conditions shows good agreement with test values at a large IM.

Ebadi et al. [26] introduced the FEM, a numerical method to solve a differential or integral equation. This is true for a number of physical problems where the relevant differential equations exist. The FEM consists of a continuous function in parts for the solution, so that the fault in the solution is reduced. Ali Ebadi describes the performance evaluation of the three phase squirrel cage induction machine according to FEM.

Lombard et al. [27] discussed some of the benefits of Finite Numerical Method(FEM), widely used for numerically solving differential equations in two or three space variables including higher precision, better design and understanding of critical design parameters, virtual prototypes, fewer hardware prototypes, a faster and more economical design cycle, higher productivity, and more revenue. The basic theory of conventional electromagnetic and direct EMF is given by P Lombard et al. In some research papers, modeling based on state space equations is used to determine the stator current in the IM for FD using the FEA [28].

Fireteanu et al. [29] provide detailed information on the effects of SE on IM in a series of experiments with different strains and eccentricity levels. While this helps to understand the effect of SE, it cannot be used directly to detect eccentricity errors because detailed error testing is not possible on an industrial motor. Researchers have also tried signature (current and air gap magnetic flux) analysis to identify eccentricity failure [30], where the coil sensors are arranged in a different orientation to identify faults. The severity of SE in induction machines diagnosed using the magnetic flux density of airspace [31]. However, due to the difficulty of obtaining air gap magnetic induction, no experimental results were provided to validate the results. The document does not even offer a solution to implement it. An analysis based on flow patterns is presented in some studies [32]. Flow pattern analysis is quite simple and completely non-invasive. In addition, it is more effective than conventional motor current analyzes in identifying the rotor and stator in induction machines.

Isermann [33] presented model-based consistent progressive fault identification and prediction for Multiple Input Multiple Output (MIMO) nonlinear discrete time systems. The proposed scheme handles state and output errors considering separate time profiles. Occurring or abrupt errors are modeled on the basis of the input and output signals of the system. The asymptotic stability of the Failure Detection and Prediction (FDP) scheme improves detection and accuracy of time to failure. The robustness of the proposed method is demonstrated using a MIMO (fourth order) satellite system.

Arkan et al. [34] presented two orthogonal wave models of a tri-phasic IM. Of these two models, the first has asymmetrical windings and the other has inter-turn shorts in the stator winding. The motor is modeled using classical two-axis theory and the equations are modified to account for faults between the stator windings. A form of the system state space is presented for dynamic modeling. The results of the execution of the models are compared with the experiment carried out on a special wound motor with bushings to shorten a different number of turns. Previous models were used successfully to investigate steady-state and transient behavior of IM in short-circuits windings.

Sahraoui et al. [35] have presented an advanced mathematical model for induction machines that operates short circuits between the stator windings. The model is based on the multiple coupled proximity circuit. Inductances are calculated in a 2D extension of the Modified Winding Function (EMWFA) approach, in which spatial harmonics across the slots are taken into account in addition to the effects of rotor bar preload and increasing linear MMF. The results show that the short circuit between the windings causes some spectral components that appear in the spectral line of the current.

Bachir et al. [36] have proposed a new model of squirrel cage motors for stator and rotor failure. First, they processed a model that takes into account the effects of faults between turns that cause a short circuit in one or more stator phase winding circuits. They then propose a new faulty model dedicated to detecting broken rotor bars. The appropriate diagnostic method is proposed based on the estimation of the defective model parameters of the stator and rotor.

1.2.2 Signal Processing Techniques

Signal processing techniques have been widely used in recent years to identify various instant messaging errors. These techniques successfully detect certain faults in the IM by analyzing the characteristics or specific parameters generated in the data being sampled. A new method has been introduced to analyze the signature of inductive motors, namely the real-time performance [37]. In this document, real-time energy is used instead of stator current to analyze the motor signature and identify mechanical defects in the drive system. The information carried by energy in real time is the product of voltage and current which is greater than the currently deductible capacity. In the current fixed power spectrum, the highest value is -52 dB, and in the current power spectrum the highest value is -47 dB. From the above, it can be seen that the real-time power is 5 dB greater than the power of the decentralized spectral component. A wavelet package has been proposed to extract useful information from IM vibration signals [38]. Although the measured vibration signals contain a transient part, the Fourier Transform cannot provide enough information to detect some machine faults. The results of using the wavelet packet are used by the statistical feature selection criteria to discard feature components that contain less discriminatory information. The extracted vector with reduced dimensional properties is used as input to the NN classifier. The results show an improvement in the ability to generalize the NN and a significant reduction in training time. The current approach is used to analyze signatures to detect instant messaging errors. This approach uses a power signature to determine that the author has detected many errors, such as breaking rotor bars in the IM squirrel and detecting short revolutions in an industrial motor. In this article, the author has created four case studies that identify various faults in the induction machine. Based on the results, the author made it clear that kinetic current analysis is a powerful technique for monitoring the status of triphasic IMs [39].

Kim et al. [40] has developed a fault diagnosis system without speed sensor for asynchronous motors. In this document, the proposed system is used to detect electrical elements (short circuit in the stator winding) and mechanical elements (broken rotor bars, eccentric air gap, bearings). Here, they used a combination of repetitive NNs and signal processing algorithms, such as wave-based and Fourier-based techniques, to detect faults in IMs. The voltage and currents from the terminals of motors were used as inputs to the diagnostic system. Fourier-based signal processing technology is applicable when the device is in a stable state, and wave-based signal processing technology is applicable when the device is in transition mode.

Douglas et al. [41] introduced a new algorithm that uses the gradient descent method to minimize least squares errors in a series of equations that change with time. The algorithm is used for the analysis of the current signature of the transient motor using waves. Here, the residual currents are analyzed with wavelets to detect broken rotor bars. The advantage of this method is that no parameters such as speed or number of rotor bars are required. In this method, a higher order notch filter is used to separate the fundamental frequency from the rotor bar frequencies. Once the fundamental frequency has been removed, the residual current can be examined using a DWT analysis. Therefore, the 8 Daubechies wavelets are used as a function of the mother wavelet. It can be seen from the results that the rotating rotor bar can be detected using transients measured at maximum current.

T.Yang et al.[42] proposed feature based online diagnostic approach for FD in IM using MCSA with advanced signal processing algorithms. The previously planned system was ready to diagnose IM with four types of defects such as broken rotor bars and also finishing rings, shorting of stator coil windings, bearing cracks and eccentricity defects of the air gap. Motor diagnosis with MCSA is dependent on slip. If the detected slip shows an error, the machine diagnostic results are incorrect. Therefore, to find the correct slip, the best slip hold algorithm estimator supported by the theorem estimation method is used.

A.M. da Silva et al. [43] has presented an IM fault diagnosis method that uses three-phase stator current envelopes for broken rotor bars and shorts between the windings in the stator windings. The above methods not only identify an IM as healthy or faulty, but also identify the severity of the failure by identifying the number of broken bars or the number of short turns in the stator windings. The training and test sets are generated from the tri phasic stator current of an IM under both healthy and faulty operating conditions using Gaussian Mixture Models (GMM) of reconstructed phase space transformations. The author has claimed that the proposed method can be a powerful troubleshooting tool for induction machines due to its higher precision.

M. Riera Guasp [44] proposed a technique based on the transformation of discrete wavelets for the detection of asymmetries in the rotor of an IM using the starting current and the stop-stop current, as well as the mixed eccentricities using the starting current. The author used Daubechies-44 as stem waves for the DWT analysis. To avoid an overlap between two neighboring frequency bands, a higher order mother wavelet was used. The author also found the parameters to quantify the severity of the failure in the case of starter rotor asymmetry and clogged rotor asymmetry.

1.2.3 Soft Computing Techniques

Various applications of using soft computing techniques in motor fault detection and diagnosis have been published across the different verticals of the industry journals. In most applications, the stator current is used with one of the soft computing classification algorithms to obtain FD accuracy. The Park vector patterns are based on the detection of different types of supply failures, such as voltage imbalance and single-phase adjustment [45]. Furthermore, a NN based back propagation algorithm is used to obtain the state of the machine by testing the shape of the vector patterns of the park. Two NN-based approaches were used, classical and decentralized. The generality of the proposed methodology has been experimentally tested and the authors state that the results provide a satisfactory level of precision. Applications of artificial intelligence in machine monitoring and fault diagnosis are examined in detail [46]. The expert system was used as a tool for the diagnosis of failures and the validity of the use of NN together with the fuzzy logic for the identification of failures and the evaluation of their severity.

Other research introduced a comprehensive adaptive neuro-fuzzy inference system to identify stator shorts in brushless DC motors, with fault diagnosis performed by two independent ANPHYSES. The first is used to find out the shorted turns and the second is used to identify the faulty phase [47]. The inputs to the first Adaptive Fuzzy Neural Inference System (ANFIS) are the diagnostic indices for determining the number of turns shorted, while the output was set to zero during normal operation and integers under fault conditions. The input to the second ANFIS were the identification indices of three phases and its output was an integer indicating the defective phase. In some applications, a generic approach based on a neuro-fuzzy model is based on the detection of flaws in the breaking bar of the rotor in an IM [48]. The data to train the neuro-fuzzy system to model the generic static torque-speed relationship of the IM class used in the practical evaluation of the fault detector. A modeling error was found when comparing the output speed of the neuro-fuzzy model and the speed obtained from the experimental torque-speed equation. This approach overcomes the practical limitations of model-based strategies by reducing the amount of experimental data required to design the flaw detector. This method can also identify the absence / presence of cracked rotor bars under various load conditions.

Ballal et al. [49] proposes ANFIS to detect bearing and insulation wear defects in IM. Here, the authors have given ANFIS five contributions which are as motor input current, speed, winding temperature, bearing temperature, and noise generation. Fuzzy neural architecture takes into account both Artificial Neural Network (ANN) and fuzzy logic technology. Authors have used a multilayer feed forward network as fuzzy rules of the ANN type and fuzzy inference systems.

Rodríguez and Antero Arkkio [50] used a method to detect faults in the stator winding in IM. In this work, the tri phasic mean square values of the stator and the variance were used as input for the fuzzy logic system. The input data is generated by FEM analysis with the engine running under various load conditions. The fuzzy logic method was able to record the state of the motor with and without noise with high precision. The disadvantage of the method is that a current imbalance generated by the power supply can be identified as a motor fault condition.

R.H. Abiyev and O. Kaynak [51] integrated both fuzzy logic systems with NN wavelet for the identification and control of an insecure system. In this article, they used the decent gradient algorithm for parameter settings. Two implementation examples were presented to identify and monitor performance. It was shown that diffuse wave NNs can converge faster and are more adaptable to new data.

Bouzid et. al [52] proposed NN approach for the automatic detection and localization of a short circuit fault between the windings in the stator of an IM. In this, they used a feed-forward multilayer NN perceptron that is trained by the back propagation technique. The phase shift between the phase voltage and the line current of an IM is used as an input to the NN. The desired output is set to one or zero. If a short is detected and it is in one of the three phases, the corresponding output NN is set to one otherwise it is zero.

J. Kurek and S. Osowski [53] presented an automated computerized system for diagnosing the rotor bars of the induction electric motor using the SVM. Two diagnostic system solutions have been developed. The first, called error detection, only detects when an error occurs. The second complex diagnosis can determine which bars have been damaged. The main problem is related to the generation and selection of diagnostic characteristics from which the condition of the rotor bars is detected.

Feng Jia et al. [54] aims to process massive error data immediately and automatically provide accurate diagnostic results. Numerous studies have been carried out on the intelligent diagnosis of failures in rotating machinery. Commonly used among these studies are ANN -based methods that use signal processing techniques to extract features and then input the features into ANN to classify faults.

Zhang W et al. [55] proposed a novel method called deep convolutional neural networks with broad first-layer nuclei. The proposed method uses raw vibration signals as input (data expansion is used to generate more inputs) and uses the wide cores in the first convolution layer to extract characteristics and suppress high frequency noise.

X Yang et al. [56] proposed an effective and practical fault diagnosis algorithm for induction machines, which is based on adaptive weighted votes from various RF classifiers. First, the vibration signals and the stator current signals are obtained and analyzed. The energy characteristics at various characteristic frequencies related to motor failures of each type of signal are extracted and used as input to the appropriate RF classifier. Cluster analysis is then applied to the test and training samples to determine the weight of each classifier to make decisions about the diagnostic result.

T. dos Santos et al. [57] proposed an approach to detect short circuit faults in the stator winding in SCIM based on RF. This is accomplished by evaluating the imbalance in the current and voltage waveforms, as well as in the park's vector for both current and voltage.

Aydin et al. [58] introduced the new feature vector based on park's vector approach. The phase space of this feature vector is constructed using nonlinear time series analysis. Faulty short circuit faults in the rotor rod and stator are rated with SVM in the combined phase space. The experimental data come from a three-phase IM. One, two and three broken rotor bars faults and a 10% short circuit of stator faults are successfully detected. The MCSA technique is based on the analysis of stator current under healthy and faulty conditions. This technique suggested diagnosing stator-to-turn failure in IM using wavelet transform and SVM as tools [59]. The fault diagnosis system using SVM-based classification techniques was developed for the diagnosis of rotor failures of cage induction machines. Subsequently, a classifier based on SVM for various classes will be developed and applied in order to distinguish health status from various rotor failure states [60].

Research based on deep learning is carried out to diagnose and classify the different types of faults in induction machines. For sensitive identification of faults between shifts in IM using deep learning-based methods, the model is trained and tested early on an induction machine to mainly detect short circuit faults between the windings. In the proposed work, models of Convolutional Neural Networks (CNN), recurrent NNs. Long-term Short-term Memory (LSTM), included for Fault Detection. Furthermore, the results show that CNN is superior to LSTM in accuracy, which provides good classification performance for FD in the early stages of fault development [61].

E. Pandarakone et al. [62] took into account the practical occurrence of faults and introduced the scratch on the outer race of the bearing. An online bearing diagnostic method is proposed using a deep learning based approach. The CNN architecture is originally used for fault characterization. In particular, a FFT analysis is performed using the stator load current, followed by the extraction of characteristics of selected frequency components that are used to train the CNN algorithm.

Heydarzadeh et al. [63] in, deep NNs are employed to diagnose five classes of transmission faults that apply to three common supervisory signals, i.e vibration, acoustics, and torque. DWT is used to provide the initial functions as inputs to the network. To validate the proposed method, a test bench built based on a 250W three-phase SCIM shaft which is connected to a single-stage helical gear drive.

John Grezman et al. [64] in, the authors examine the performance of a CNN that is trained using images of time-frequency spectra of vibration signals measured in an IM. The results show that the patterns learned by the CNNs in the time-frequency spectrum images are intuitive and consistent with respect to network retraining.

Mohammad Zawad Ali et al. [65], in this research work, stator currents and vibration signals from motors are selected to develop fault detection methods. Additionally, two signal processing techniques (Matching Pursue and DWT) are selected for feature extraction. Three classification algorithms, SVM, KNN, and Ensemble, with 17 different classifiers offered in the MATLAB toolbox, are used in the modeling to evaluate the performance and suitability of different classifiers for diagnosis of failures.

Tarannum Khan et al [66] in, author suggested Motor Current Signature Analysis (MCSA) using deep learning based one dimensional Convolutional Neural Network(1D-CNN) model and Long Short Term Model (LSTM). The results using these two methods have been compared, and this initial investigation shows that CNN is found to be more suitable than LSTM, for incipient fault diagnosis.

Lots of quality research on fault diagnosis of induction machine and algorithm based detection have been examined. To detect and classify various machine learning based model, fuzzy based model have been implemented and posted commendable results. The literature survey indicates that the individual faults have been the main focused area and combined fault analysis is still an unexplored area. Furthermore, the time varying load operating conditions of IMs are not much researched. Need of considering combination of faults which could be hazardous for the motor is at most.

1.3 RESEARCH GAPS

Previous research has addressed several aspects related to Fault Detection techniques used for fault diagnosis of Induction Motor like the model based techniques, signal processing techniques and soft computing techniques.

However, majority of the research work which provides outstanding results mainly suggested Motor Current Signature Analysis(MCSA) with stator current as single signature analysis with signal processing techniques like FFT, STFT, Gabor and Hilbert transform etc. to detect presence of fault. But, each technique has some advantages and disadvantages like in case of FFT it has been observed that it cannot diagnose fault in non-loading condition unlike DWT. However, by changing the wavelet transform only a limited amount of work has been done get out.

In addition, model based approaches have their own limitation of characterization of the faults, these methods detect the severe faults and neglect the early stage failure or the faults with diminished magnitude. Previous research suggested primarily fuzzy logic , expert system and ANN soft computing associated with single stator current used for feature extraction. But, rigorous mathematical calculations are done in fuzzy system for fault diagnosis and further, both expert and fuzzy systems have lack of self learning.

Furthermore, the previous research works mainly focus on identification of different types of faults in IM and various methods used to detect these faults using various condition monitoring techniques but the use of advance machine learning techniques in this field still a thrust area now a days. Moreover, earlier research has emphasized largely on fault diagnosis of machine using single stator current signature analysis under full load conditions.

But, the use of multiple signature analysis with signal processing techniques in order to carry out fault detection is still a challenging task.Very little research has been carried out on diagnosis and detection of combined faults and fault detection based on time varying load conditions. Few researchers have used machine learning and deep learning methods for health monitoring of IM.

However, due to the complexity and importance of the systems, there is a need to further improve existing Fault Detection techniques. A major key to the success in FD is the ability to use appropriate technology to effectively fuse the relevant information to provide accurate and reliable results. The advancement in technology will provide opportunities for improving existing FD schemes.

The advance algorithms with feature extraction technique DWT, considering both vibration and stator current signals have not yet been used in this domain of fault diagnosis and detection. The individual faults have been the main focused area and combined fault analysis is still an unexplored area.

Considering the above facts, this present research work includes behavior analysis of motor under healthy and faulty conditions for both individual fault as well as combined faults under different constant and time varying loading conditions in order to validate designed model of IM for carrying out further research work.

The proposed research used hybrid approach of advance machine learning and deep learning algorithms with feature extraction technique applied on both vibration and stator current signals in order to get enhanced accuracy under constant and time varying loading conditions for fault detection of single and combined faults . This approach can identify and aggregate the pertinent information for accurate and authentic motor fault detection and further confirms its effectiveness of fault diagnosis under both constant and time varying loading conditions.

1.4 MOTIVATION

Induction Motor maintenance is one of the severe problem encounters by various utilities and industries. A number of researches have been done for the issues of automatic and on-line detection of faults in IM. Few of the main research work and recommendations were like, Electric Power Research Institute motor literature of reliability as per the reference [67], states that stator faults are liable for 36% of the IM failures. According to Neale [68], the installation and purchasing cost of the equipment’s usually cost less than half of the total expenditure over the life of the machine for maintenance. According to Wowk [69], maintenance expenditure typically presents 15% to 40% of the total cost and it can be up to 80% of the total cost.

The motivation behind this work is to find a methodology which effectively detects faults in induction machine under different constant and time varying loading conditions at an early stage in order to avoid its catastrophic failure which may further lead to system failure. In addition to this, research work involves the stator current with vibration signals for feature selection and proposed framework of novel architecture of DBNN for effective detection of faults under time varying load.

Deep learning techniques are foremost algorithms of artificial intelligence domain. Since after the introduction of deep learning algorithms it over shadows the other machine learning algorithms and are being extensively used in various applications due to its higher accuracy and adaptability to handle data. The ability of the deep neural network's techniques to perform complex correlation among speech signal features, which enhances its performance over traditional approaches.

The deep learning method is the advanced version of the Neural Networks (NNs) which falls under machine learning category and machine learning methods SVM and RF are applied for the comparative analysis of new age deep learning classifier with conventional SVM and RF classifier.

Investigations related to different types of faults like broken rotor bars, stator and eccentric faults in induction machines and various methods to detect these faults are discussed elaborately in the research work.

In this research work, the ANSYS RMxprt & Maxwell 2D and MATLAB software tools were examined using numerous machine learning techniques to diagnose faults in SCIM and identify rotor, stator, eccentric, and combined faults under constant and time-varying load conditions.

After analyzing faults in all conditions, it was concluded that wavelet transformation with machine learning in conjunction with deep learning techniques is very effective in diagnosing various fault related problems. Implementing deep learning methods with DWT can be an important step in optimizing overall system performance.

The idea is to develop a framework to detect and diagnose faults in IM at an early stage. Using deep learning with signal processing technique such as DWT technique can improve the performance of the framework as in Dis short time wavelets allow information to be extracted from high frequency components, which can also diagnose the severity of the fault and its type.

1.5 RESEARCH OBJECTIVES

The objective of this research work is to develop health monitoring system that can detect and diagnose common faults which are generally occurred in three-phase Squirrel Cage Induction Motor. The main aim is to investigate the use of machine learning and deep learning techniques in the area of motor health monitoring. Since this is an electromechanical system application, the author's objective is to develop a health monitoring system that can detect, classify and diagnose common failures that commonly occur in electrical and mechanical parts of three-phase asynchronous motors. To achieve this objective, the following objectives were established:

- To design and develop the Induction Motor implementation model for behavioral analysis of motor.
- To investigate the motor under various faults like broken rotor bar faults and stator faults under different loading conditions.
- Investigation of eccentricity faults in Induction Motors. Sometimes multiple faults may occur simultaneously in IM during working condition. Less research work has been done on investigation of multiple or combined faults. The new concept of combined fault is introduced and examined under load conditions.
- The implemented model put under varied load conditions and faults conditions to apply machine learning techniques like Deep Belief Neural Network (DBNN), Support Vector Machine (SVM) and Random Forest (RF) to detect and classify the motor faults under different faulty conditions.
- Investigations carried out on effectiveness of proposed fault detection method in research work for detecting how the presence of multiple faults as well as common faults, such as rotor bar fault, stator winding fault, air gap eccentricity

and their combinations affects performance of IM under different constant and time varying load conditions.

1.6 RESEARCH METHODOLOGY

The strategy adapted to carryout research work has been depicted in the Figure 1.1.

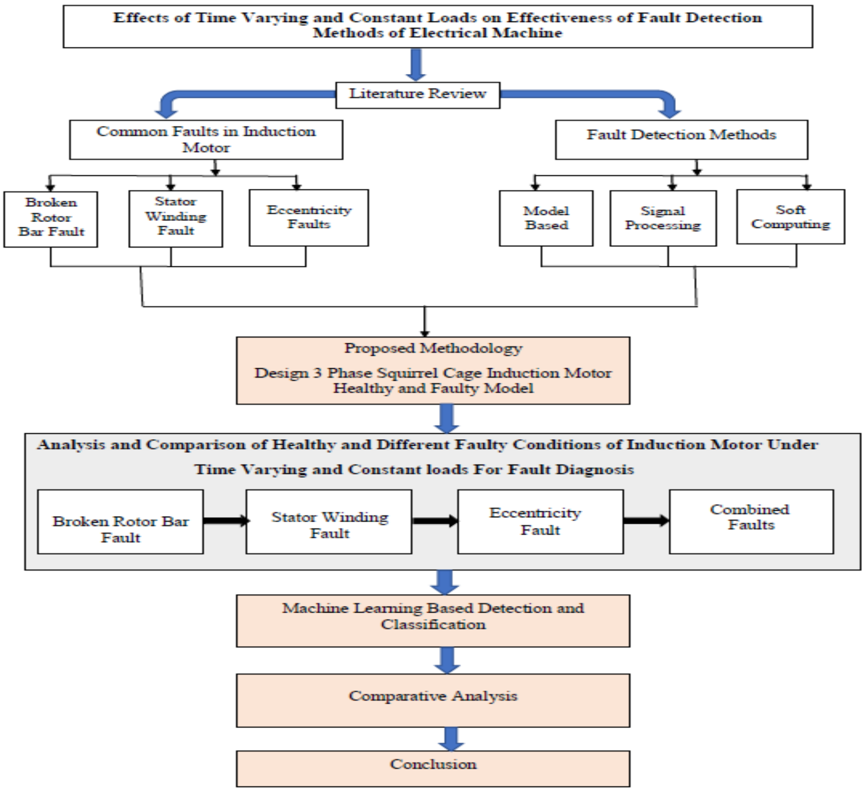

Figure 1.1: Research plan

Further, the following steps provide a brief overview about the work:

- The previous research works mainly focus on identification of different types of faults in IM and various methods used to detect these faults but the use of advance machine learning techniques in this field still a thrust area now a days. In general, broken rotor bars, stator, eccentric and combined faults are discussed elaborately in the research work. Need for monitoring dynamic behavior of the induction machines and combination of the consideration were the two general outcomes of the literature review. In this research work, first the ANSYS RMxprt and Maxwell 2D software tools are used to design the induction machine. The IM healthy characteristics are obtained using the designed model. Parameters like torque, current, and power are analyzed at constant loading condition. Furthermore, various faulty conditions are generated in ANSYS RMxprt designed model and the characteristics of the motor are noted under each fault. The faults considered are rotor broken faults, stator faults, and eccentric faults.

- Analyzed performance characteristics results of healthy and faulty IMs are compared for fault identification under constant loading condition. The MATLAB SCIM model is designed to obtain the health motor performance parameters like torque, speed, stator current and rotor current under time varying load and different constant loading conditions like 100% loading, 50% loading, 25% loading and no loading. Obtained performance characteristics of SCIM healthy and faulty models of rotor bar fault, stator winding fault, eccentric fault and combined faults are compared for fault identification under time varying and different constant loading conditions for further effective fault detection using machine learning methods. Motor vibration and stator current distortion is taken into consideration to detect and diagnose the faulty condition in SCIM. Motor performance degrades as the level of fault increases. So, the DWT is used to extract features of the motor stator current under various faulty conditions like broken rotor bar fault, stator fault, eccentric fault and combination of faults (rotor-stator, stator –eccentric & rotor eccentric).

- To detect and diagnose the type of fault, machine learning algorithms Support Vector Machine and Random Forest are applied on features extracted from analyzed behavior of IM under healthy and faulty conditions for all constant and time varying loading conditions. The accuracies achieved are 96.5% and 97.5% from RF and SVM respectively. The deep learning methods are advanced version of NNs which fall under the machine learning category. These methods are used for effective detection and classification of faults with its type and severity. To enhance the accuracy of detection of fault and its specific type on the results, deep learning techniques are explored. Proposed framework of Deep Belief Neural Network (DBNN) is applied on the extracted features which are based on stator current and vibration of IM. Finally, FD with 99.83% accuracy is achieved from DBNN. The results obtained are compared with other research work for validation.

1.7 THESIS ORGANIZATION

This thesis includes six chapters and these chapters are summarized as:

CHAPTER 1: INTRODUCTION

This chapter is all about the importance of motors in industry and introduction of motor faults diagnosis methods which can detect the type of faults in motor. This chapter also includes background of a research work which signifies the foundation of research optimization. Numerous reviews have been presented based on systems proposed with Fault detection methods or techniques like model based methods, MCSA with associated signal processing techniques and soft computing based approaches, which performed well in a certain way, but could not get the optimum solution for fault detection and diagnosis optimization. Therefore, research gaps are also mentioned in order to find out the best optimum solution for fault detection with high accuracy. Further, the motivation of the thesis, the research objectives and research methodology are presented in this chapter.

CHAPTER 2: MODELING AND PERFORMANCE OF SQUIRREL CAGE INDUCTION MOTOR UNDER HEALTHY CONDITION

This chapter presents the mathematical modeling of Induction Motor (squirrel cage). The ANSYS RMxprt and Maxwell 2D software tools are used to design the induction machine and furthermore, MATLAB software is used to apply model the mathematical equation of IM and implementation model is designed. Both the software's virtualizes the induction machine for carrying out the further research. Implemented models are operated under healthy operating condition and performance of motor is analyzed in terms of voltage, speed, current and torque. The designed model is subjected to various constant and time varying loading conditions.

CHAPTER 3: FAULT TYPES AND DIAGNOSIS & CLASSIFICATION TECHNIQUES

In this chapter, various faults are discussed in detail which may occur during the operating condition of motors and can cause catastrophic failure of motors if not detected and classified at an early stage. The utilization of classification techniques like SVM and RF in fault detection and classification in motors are discussed. All machine learning algorithms applied to detect the different type of faults generated in the SCIM. Deep learning method like DBNN has performed well as compared to the other machine learning techniques.

CHAPTER 4: BEHAVIORAL ANALYSIS OF INDUCTION MOTOR UNDER DIFFERENT FAULTS

This chapter includes the results obtained from the behavioral analysis of induction machine under different faults such as broken rotor bar faults, stator winding faults, eccentric fault and combined faults like eccentric with stator fault, rotor with stator fault and eccentric with rotor fault. ANSYS RMxprt and Maxwell 2D designed model with different faults discussed and executed. MATLAB model is operated under different faulty conditions and its characteristics performance are analyzed and evaluated under various constant and time varying loading conditions. Loading conditions considered are no load, 25% load, 50% load and 100% load. In order to diagnose the effects of number of broken rotor bars, power spectrum is also obtained for different conditions. Comparison of healthy and faulty conditions is done on the basis of IM parameters current, voltage, speed and torque. It is noted that the motor speed, current and torque distortions increases on account of faults and under heavy loading conditions. Furthermore, the variation of stator current is utilized as features in the Fault Detection and classification.

CHAPTER 5: MACHINE LEARNING ALGORITHM BASED FAULT DIGNOSIS EXPERIMENTATION

This chapter proposes the fault diagnosis of induction machine using Support Vector Machine (SVM), Deep Belief Neural Network (DBNN) and Random Forest (RF) using DWT features of the stator current and vibration signals. The feature extraction process using stator current is described. The dataset prepared of current signature of all the types of faults like rotor faults, stator faults, eccentric faults and combined faults under different constant (100%, 50%, 25% and no load) and time varying loading conditions. The machine learning algorithms are applied on the dataset dividing the complete dataset into training and testing dataset. The total dataset generated is 4000 samples in which 1000 are of healthy operating condition, 500 is of rotor bar faulty condition, 500 samples stator faults, 500 eccentric faults, 500 rotor-stator combined faults, 500 rotor-eccentric combined faults, 500 stator-eccentric combined faults and then the whole dataset is divided into 70% training and 30% testing. On the training and testing dataset the classification approaches DBNN, SVM and RF are applied to get the effectiveness of each algorithm on detection and classification of faults in IM. The comparison is done on the basis of accuracy of fault type detection and time taken in detecting the fault.

CHAPTER 6: CONCLUSIONS, CONTRIBUTIONS AND FUTURE WORK

This chapter covers the benefits that can be derived from the research work undertaken and also concludes the various results obtained during different faults generation and fault diagnosis of induction machine under different constant loads and time varying loading condition. The chapter includes benefactions of the present work in the field of Fault Detection and diagnosis in Induction Motor by applying advanced algorithms of machine learning and deep learning and addresses the future scope to continue with this line of research and development in the field of fault detection and classification of induction machine.

CHAPTER 2

MODELING AND PERFORMANCE OF SQUIRREL CAGE INDUCTION MOTOR UNDER HEALTHY CONDITION

2.1 INRODUCTION

In recent decades, a large number of mathematical models for triphasic Induction Motors have been intensively investigated [70]. IM models are created on the basis of suitable mathematical descriptions that have a relevant dynamic characterization of the processes associated with IM operation under fault-free and error-free conditions. Model-based methods have been widely implemented for parameter estimation of induction machines [71], condition monitoring, and protection [72]. The advantages of model-based methods are: they are not intrusive and application costs tend to be low.

The chapter emphasizes on design of three-phase IM mathematical model and performance analysis that can be further used to detect and classify rotors, stator, eccentricity, and combined faults using machine learning detection methods.

2.2 MODELING OF INDUCTION MOTOR IN ANSYS

Induction Motor model design is implemented in ANSYS RMxprt software tool and the FEM analysis is done in Maxwell 2D software tool.

2.2.1 ANSYS RMxprt

Engineers designing electrical machines and generators now have the advantage of expanding ANSYS Maxwell with ANSYS RMxprt, a template-based design tool. Together, Maxwell and RMxprt have succeeded in developing a truly bespoke machine design to meet the market demand for lower cost and above average efficiency machines. RMxprt uses classical analytical motor theory and equivalent magnetic circuit methods and can therefore calculate machine performance, make initial sizing decisions, and perform hundreds of "what-if" analyzes in seconds. A great advantage of RMxprt is that it can automatically configure a complete Maxwell project (2-D / 3-D), which can also contain geometry, materials, and boundary conditions.

The motor with rating of 5kW power and 415V rated voltage is taken into consideration while designing the complete parameter list is shown in Table 2.1

Table 2.1 Squirrel Cage Induction Motor parameters

Parameters	Value
Rated Power	5kW
Rated Voltage	415V
Rated Speed	1462.7 rpm
Frequency	50Hz
Number of stator slots	36
Number of rotor slots	28
Number of poles	4
Stator Outer Diameter	219.8mm
Stator Inner Diameter	136mm
Rotor Outer Diameter	135.42mm
Rotor Inner Diameter	44.85mm

2.2.2 Squirrel Cage IM Design Using RMxprt

RMxprt is a template-based design tool that makes it easy for electrical machine designers. Maxwell 2D and RMxprt together can result in individual machine design according to specific requirements (high efficiency, low cost, good power factor).

Machine performance calculations and initial size decisions can be made in seconds that would have otherwise taken days to calculate by hand. The motor is designed using above parameters as shown above in Table 2.1 using RMxprt tool of ANSYS. The RMxprt design can be imported into Maxwell, including geometry, materials, and boundary conditions.

AC motors generally use a squirrel cage. The ironically shaped motor cast aluminum or copper that melted between the iron laminates of the rotor. Considerable fragments of the rotor currents flow through the lacquered bars and laminates. A 5kW three-phase SCIM is designed in RMxprt and analyzed using Maxwell 2D. The assigned stator windings are made of copper. The FEM model proposed of IM is shown in Figure 2.1, which is almost identical to the real machine in terms of its geometry and magnetic circuit.

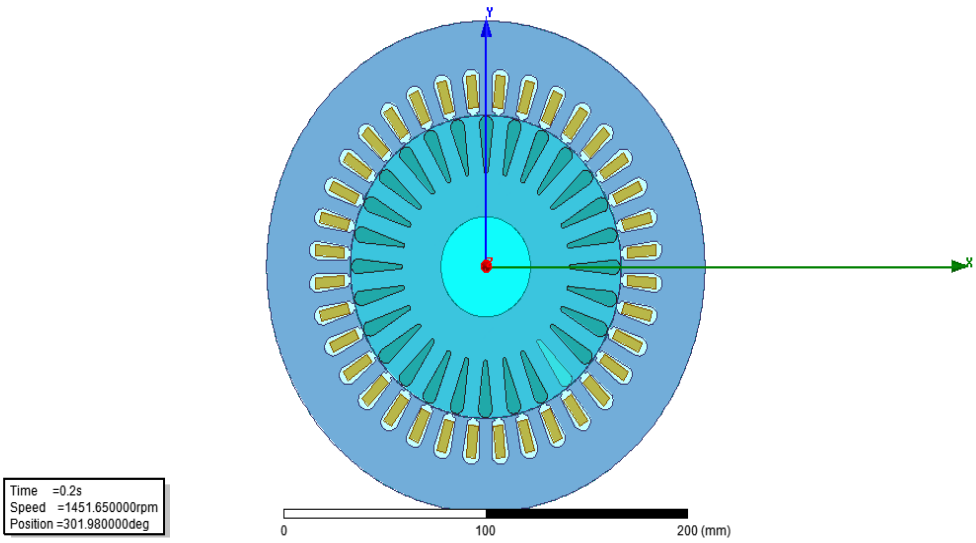

Figure 2.1: Induction Motor model for healthy condition

2.2.3 ANSYS Maxwell 2D

ANSYS Maxwell is the inexpensive electromagnetic field modeling software for designers manufacturing and analyzing 3D and 2D electromagnetic and electromechanical devices, including motors, actuators, transformers, sensors, and coils. Maxwell 2D that uses Finite Element Analysis (FEA) to identify electrical, magnetostatic, eddy current, and transition problems. Maxwell 2D determines the electromagnetic field problems for a given model with pertinent materials, boundaries and source conditions applying Maxwell's equations over a finite region of space [73-74].

Differential forms of Maxwells equations are as follows:

$$Faraday'sLaw\ of\ Induction\ \nabla XE = -{}^{dB}/_{dt} \tag{2.1}$$

$$Gauss's\ Law\ for\ Magesium\ \nabla \cdot B = 0 \tag{2.2}$$

$$Ampere's\ Law\ \ \nabla XH = J + {}^{dD}/_{dt} \tag{2.3}$$

$$Gauss's\ Law\ of\ Electricity\ \nabla \cdot D = P \tag{2.4}$$

2.2.4 Finite Element Analysis Using Maxwell

With an aim to glean the set of algebraic equations which is to be solved, the geometry of the problem is discretized on its own into infinitesimal elements (e.g. triangles in 2D). All the model solids will be meshed on its own by the mesher. FEM approach is used to analyze the IM under various conditions [75].

The Finite Element Method (FEM) is a numerical method for solving a differential or integral equation.. The motor specified above is relocated with a direct channel from RMxprt to Maxwell. Maxwell uses precise EMF to determine static, frequency domain, and time-varying electric and electromagnetic fields. The motor parameters are the same as shown in Table 2.1. The graph for the magnetic flux density analysis is shown in Figure 2.2.

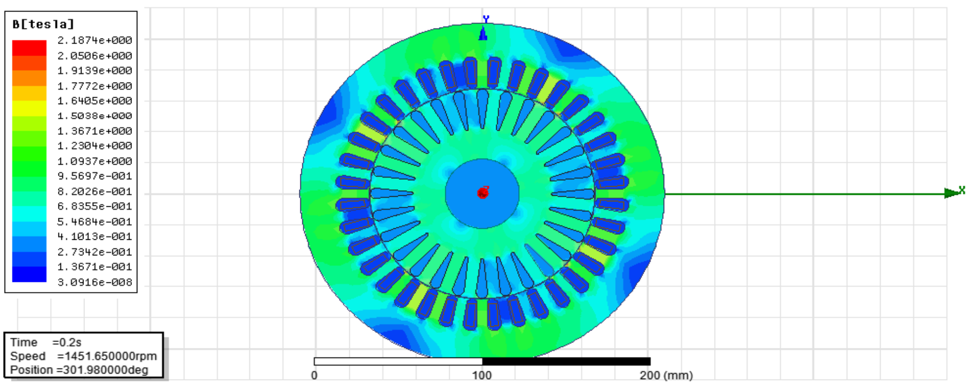

Figure 2.2: Magnetic flux density model of IM

Figure 2.2 shows motor performance through the magnetic flux of a healthy motor under normal operating conditions.

2.2.5 Induction Motor Performance Under Normal Healthy Conditions

The 5kW SCIM is designed and analyzed using FEM model. Initially healthy motor parameters are investigated under normal operating condition.

The symmetric distribution of flux density over the various parts of stator and rotor of the healthy machine can be seen in Figure 2.3. From Figure, it can be clearly seen that the flux is uniformly distributed over all the parts of the rotor and the stator. The current density plot is shown in Figure 2.4, which shows the uniformity of the current density. So, in healthy operation the current are symmetrical in all parts of the stator and rotor there is no ambiguity and there is no effect on any part while operation.

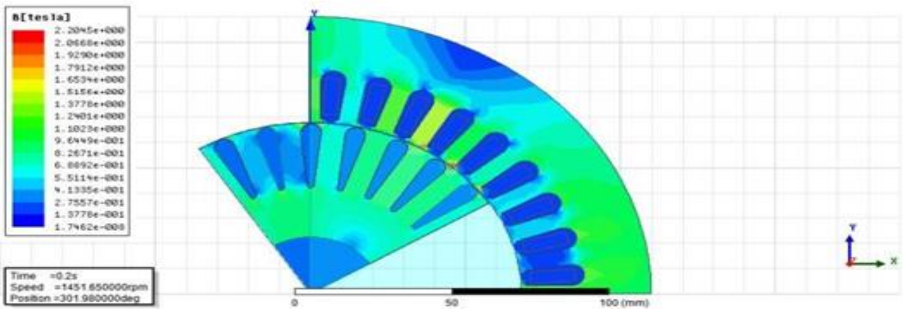

Figure 2.3: Induction Motor flux density distributions during normal condition

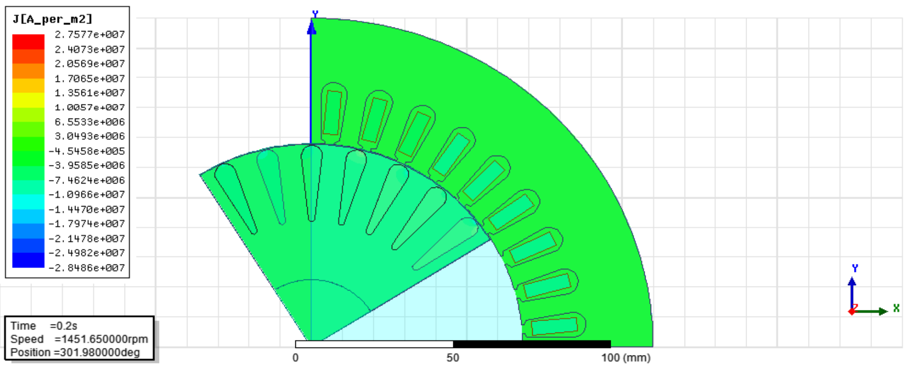

Figure 2.4: Current density plot of IM during normal condition

Under normal operating condition torque produced has transients in positive and negative direction which tends elevate as the fault occur in motor. Figures 2.5, 2.6, 2.7 and 2.8 show the motor characteristics under normal operating conditions. Figure 2.5 shows the torque response of the SCIM over the period of time during the normal condition. The average load torque in normal operating condition is 33.4175Nm. Figure 2.6 illustrates the FEM IM model stator current response under normal condition the three phase current showing minimal distortion. But during the starting the current peaks are high and gets stable at around 60 sec operating time. Figure 2.7 illustrates the flux linkage response of the IM model, from the figure it can be clearly seen that the stability of the IM is achieved after 60sec of the operation. Figure 2.8 illustrates the average power in watts under normal operating condition. The average power obtained is 5080.111watt and the major transient effective points are there at the starting of the motor as the time passes around after 75secs the transient stabilises.

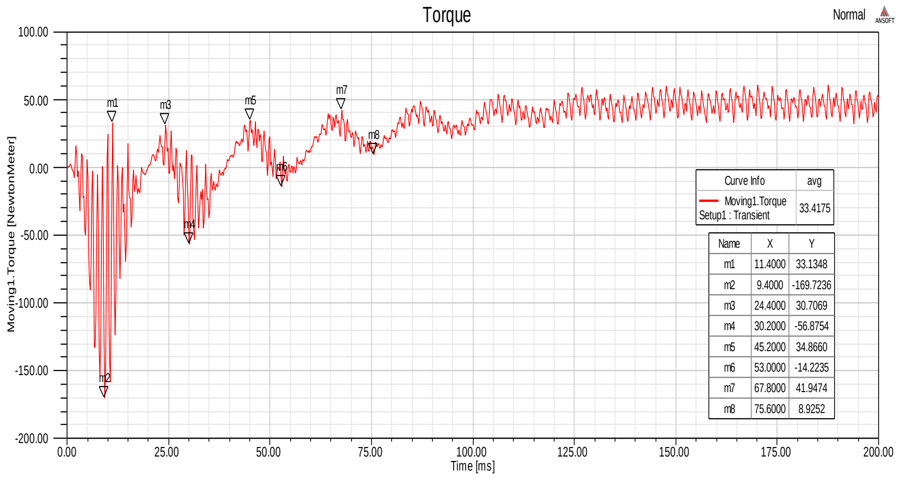

Figure 2.5: Induction Motor torque response over period of Time during normal condition

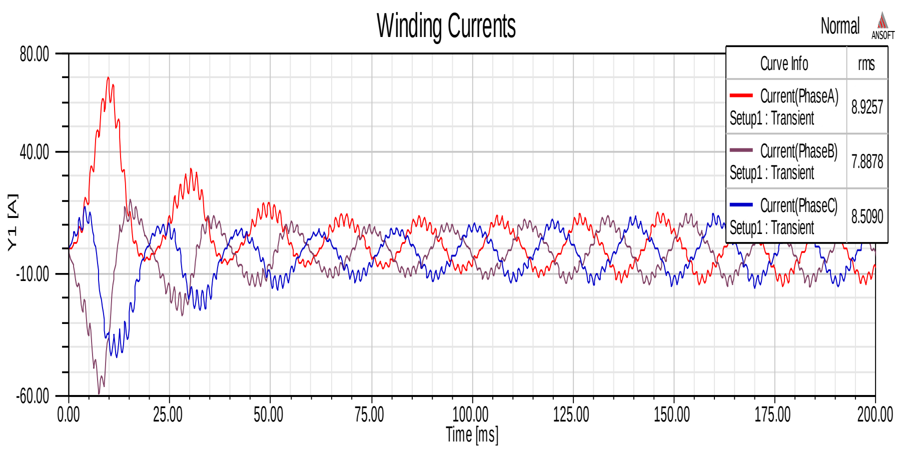

Figure 2.6: Induction Motor current response during normal condition

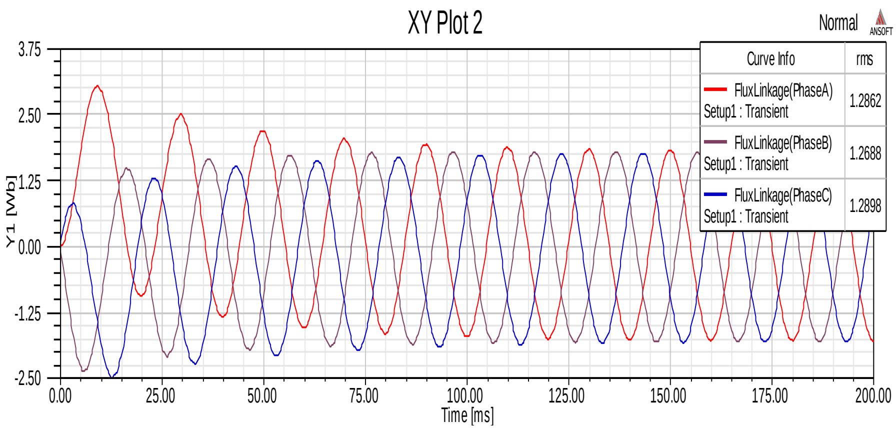

Figure 2.7: Flux linkage response of IM during normal condition

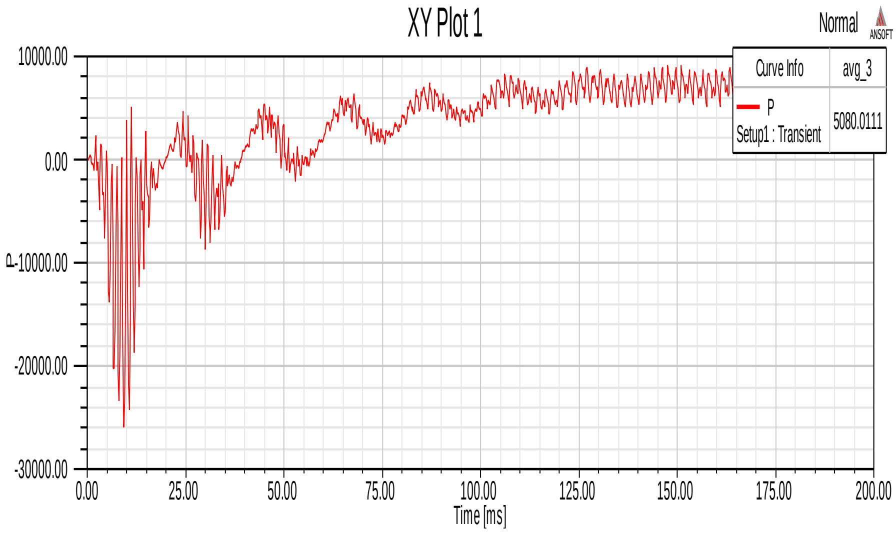

Figure 2.8: Induction Motor output power response during normal condition

2.3 MATHEMATICAL MODELING OF THREE PHASE INDUCTION MOTOR

The modeling of the three-phase induction machine relies on the following hypotheses and assumptions [76]:

1. The machine air gap has supposed constant thickness. So, the notching effects and generating space harmonic can be ignored;
2. The magneto motive forces created by stator and rotor phases are spread in a sinusoidal way along the air gap;
3. The slotting in stator and rotor produces negligible variation in respective inductances;

4. The magnetic field is not saturated and has a constant permeability;
5. The skin effect, hysteresis and eddy effects are not taken into account;
6. The harmonics in voltages and currents are neglected;
7. The temperature of motor stays constant resulting in constant parameters in the mathematical models.

These hypotheses allow the development of a practical mathematical model with a limited complexity.

2.3.1 Induction Motor Model in abc Coordinates

The proper selection of an IM model structure and its parameterization are critical since they influence both the observation and identification ability. The dynamic mathematical model of an IM is usually represented in the stationary a, b and c reference frame in terms of voltage, current and flux linkage as follows :

$$\begin{bmatrix} v_{as} \\ v_{bs} \\ v_{cs} \end{bmatrix} = R_s \begin{bmatrix} i_{as} \\ i_{bs} \\ i_{cs} \end{bmatrix} + \frac{d}{dt} \begin{bmatrix} \lambda_{as} \\ \lambda_{bs} \\ \lambda_{cs} \end{bmatrix}, \tag{2.5}$$

$$0 = R_r \begin{bmatrix} i_{ar} \\ i_{br} \\ i_{cr} \end{bmatrix} + \frac{d}{dt} \begin{bmatrix} \lambda_{ar} \\ \lambda_{br} \\ \lambda_{cr} \end{bmatrix}, \tag{2.6}$$

$$\begin{bmatrix} \lambda_{as} \\ \lambda_{bs} \\ \lambda_{cs} \end{bmatrix} = L_{sr} \begin{bmatrix} i_{ar} \\ i_{br} \\ i_{cr} \end{bmatrix} + L_{ss} \begin{bmatrix} i_{as} \\ i_{bs} \\ i_{cs} \end{bmatrix}, \tag{2.7}$$

$$\begin{bmatrix} \lambda_{ar} \\ \lambda_{br} \\ \lambda_{cr} \end{bmatrix} = L_{rr} \begin{bmatrix} i_{ar} \\ i_{br} \\ i_{cr} \end{bmatrix} + L_{rs} \begin{bmatrix} i_{as} \\ i_{bs} \\ i_{cs} \end{bmatrix}, \tag{2.8}$$

Where,

V_{abcs}, i_{abcs} and λ_{abcs} stator voltage, current and flux,

$\mathrm{i}_{\mathrm{abcr}}$ and λ_{abcr} rotor current and flux,

R_s and R_r stator and rotor resistance,

The stator to stator winding inductances *Lss*, rotor-to rotor winding inductances *Lrr* and stator-to-rotor mutual inductances *Lsr* are presented as

$$L_{ss} = \begin{bmatrix} L_{ls} + L_s & L_{sm} & L_{sm} \\ L_{sm} & L_{ls} + L_s & L_{sm} \\ L_{sm} & L_{sm} & L_{ls} + L_s \end{bmatrix} \tag{2.9}$$

$$L_{rr} = \begin{bmatrix} L_{lr} + L_s & L_{rm} & L_{rm} \\ L_{rm} & L_{lr} + L_s & L_{rm} \\ L_{rm} & L_{rm} & L_{lr} + L_r \end{bmatrix} \tag{2.10}$$

$$L_{ss} = L_{sr} \begin{bmatrix} \cos(\theta_r) & \cos(\theta_r + \frac{2\pi}{3}) & \cos(\theta_r - \frac{2\pi}{3}) \\ \cos(\theta_r - \frac{2\pi}{3}) & \cos(\theta_r) & \cos(\theta_r + \frac{2\pi}{3}) \\ \cos(\theta_r + \frac{2\pi}{3}) & \cos(\theta_r - \frac{2\pi}{3}) & \cos(\theta_r) \end{bmatrix} \tag{2.11}$$

Where, Lls, Ls and Lsm are the per phase stator leakage inductance, self- inductance of the stator winding and mutual inductance between stator windings, respectively; Llr, Lr and Lrm are the per phase rotor leakage inductance, self-inductance of the rotor winding and mutual inductance between rotor windings, respectively; Lsr is the mutual inductance between stator and rotor windings; θr is rotor angular position. The peak value of stator-to-rotor mutual inductances Lsr is equal to the transpose of rotor to-stator mutual inductances Lrs, i.e. Lsr = LT

Based on the hypotheses at the beginning of this section, the inductances of Induction Motor can be expressed in terms of the per phase total equivalent stator winding turns Ns, equivalent rotor winding turns Nr and air-gap permeance Pg. Thus, the sum of inductances can be represented by Ls to reduce the number of variables,

Where, L_{ls}, L_s and L_{sm} are the per phase stator leakage inductance, self- inductance of the stator winding and mutual inductance between stator windings, respectively; L_{lr}, L_r and L_{rm} are the per phase rotor leakage inductance, self-inductance of the rotor winding and mutual inductance between rotor windings, respectively; L_{sr} is the mutual inductance between stator and rotor windings; θ_r is rotor angular position. The peak value of stator-to-rotor mutual inductances L_{sr} is equal to the transpose of rotor to-stator mutual inductances L_{rs}, i.e. $L_{sr} = L_{rs}^T$

Based on the hypotheses at the beginning of this section, the inductances of Induction Motor can be expressed in terms of the per phase total equivalent stator winding turns N_s, equivalent rotor winding turns N_r and air-gap permeance P_g. Thus, the sum of inductances can be represented by Ls to reduce the number of variables,

$$L_{sm} = -\frac{L_{rs}}{2};\ L_{rm} = -\left(\frac{N_r}{N_s}\right)^2 \frac{L_{rs}}{2} \tag{2.12}$$

$$L_{sr} = -\frac{N_r}{N_s} L_s;\ L_r = -\left(\frac{N_r}{N_s}\right)^2 L_{rs} \tag{2.13}$$

In this research, the motor parameters are estimated based on both transient response and steady state condition.

2.3.2 Induction Motor Model in *αβ* Coordinates

The three-phase quantities (voltages and currents) are transformed from *abc* to *αβ* co-ordinates to reduce computational complexity. The transformation matrices of stator and rotor variables from *abc* to *αβ* are defined as follows [77]:

$X_{\alpha\beta s} = T_{\alpha\beta} X_{abcs}$ stator variables

$X_{\alpha\beta r} = T_{\alpha\beta}\, X_{abcr}$ rotor variables

Where,

$$T_{\alpha\beta} = \sqrt{\frac{2}{3}} \begin{bmatrix} 1 & -1/2 & -1/2 \\ 0 & \sqrt{3/2} & -\sqrt{3/2} \end{bmatrix},$$

$$T_r(\theta_r) = \begin{bmatrix} \cos\theta_r & -\sin\theta_r \\ \sin\theta_r & \cos\theta_r \end{bmatrix}$$

Applying these two transformation matrices to equations (2.10) - (2.13) and replacing L_{sm}, L_r, L_{rm} and L_{sr} with L_s using equation (2.8), the mathematical model of an IM in the *αβ* reference frame is presented as,

$$\begin{bmatrix} v_{\alpha s} \\ v_{\beta s} \end{bmatrix} = R_s \begin{bmatrix} i_{\alpha s} \\ i_{\beta s} \end{bmatrix} + \frac{d}{dt} \begin{bmatrix} \lambda_{\alpha s} \\ \lambda_{\beta s} \end{bmatrix}, \tag{2.14}$$

$$o = R'_r \begin{bmatrix} i'_{\alpha r} \\ i'_{\beta r} \end{bmatrix} + \frac{d}{dt} \begin{bmatrix} \lambda'_{\alpha r} \\ \lambda'_{\beta r} \end{bmatrix} - \omega_r T_r\left(\frac{\pi}{2}\right) \begin{bmatrix} \lambda'_{\alpha r} \\ \lambda'_{\beta r} \end{bmatrix}, \tag{2.15}$$

$$\begin{bmatrix} \lambda_{\alpha s} \\ \lambda_{\beta s} \end{bmatrix} = L_{ls} \begin{bmatrix} i_{\alpha s} \\ i_{\beta s} \end{bmatrix} + L_{ls} \left(\begin{bmatrix} i_{\alpha s} \\ i_{\beta s} \end{bmatrix} + \begin{bmatrix} i'_{\alpha r} \\ i'_{\beta r} \end{bmatrix} \right), \tag{2.16}$$

$$\begin{bmatrix} \lambda'_{\alpha r} \\ \lambda'_{\beta r} \end{bmatrix} = L'_{lr} \begin{bmatrix} i'_{\alpha r} \\ i'_{\beta r} \end{bmatrix} + L_m \left(\begin{bmatrix} i_{\alpha s} \\ i_{\beta s} \end{bmatrix} + \begin{bmatrix} i'_{\alpha r} \\ i'_{\beta r} \end{bmatrix} \right) \tag{2.17}$$

Where $R'_r = \left(\frac{N_s}{N_r}\right)^2 R_r$, $i'_{\alpha\beta r} = \frac{N_r}{N_s} i_{\alpha\beta r}$, $\lambda'_{\alpha\beta r} = \frac{N_s}{N_r} \lambda_{\alpha\beta r}$, $L'_{lr} = \left(\frac{N_r}{N_s}\right)^2 L_{lr}\ and\ L_m = \frac{3}{2} L_s$.

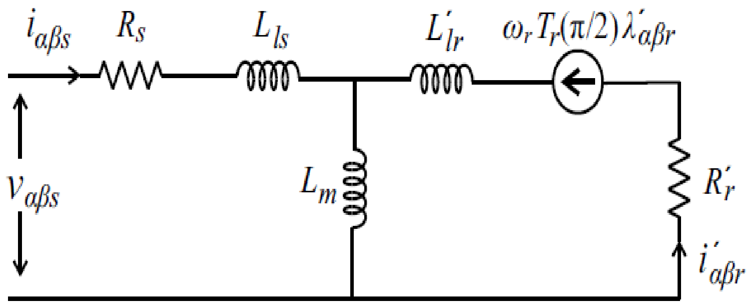

Figure 2.9: Equivalent circuit representation of IM in αβ reference frame

Figure 2.9 shows the equivalent circuit model of a three phase IM in the αβ reference frame. This model is the base of generating the modeling in the MATLAB environment.

2.4 MATLAB MODEL OF SCIM

The mathematical equations described in section 2.3 are modeled with MATLAB software. The MATLAB development environment offers convenient free-body diagram programming, where components are dragged and dropped into a GUI and the connection is established according to the equation. In addition to mathematical modeling of the IM with different operating conditions, MATLAB can be conveniently used to set up a suitable solution method and analyze the results.

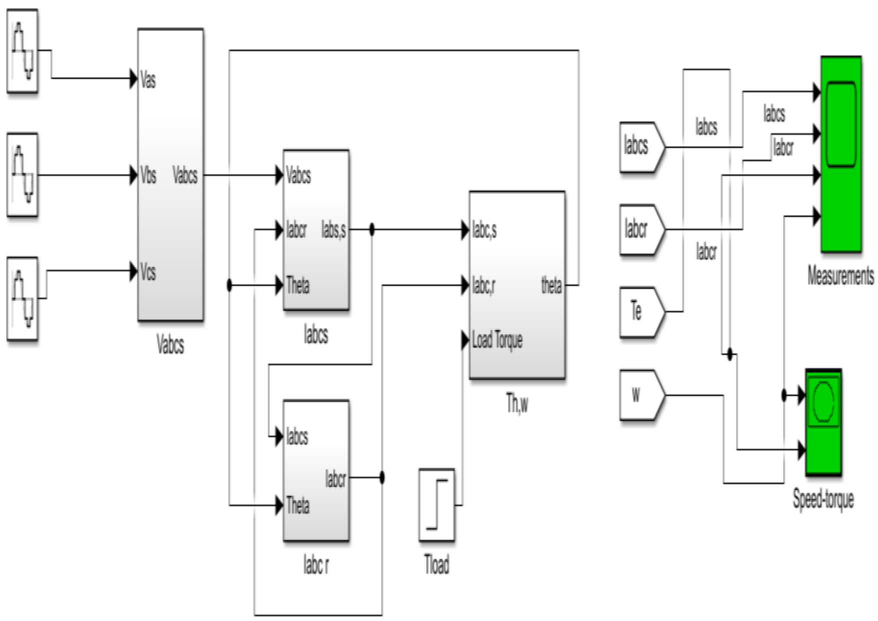

Figure 2.10: MATLAB model of SCIM (Healthy condition)

Figure 2.10 shows the complete SCIM MATLAB model with a separate subsystem for calculating stator voltage, stator current, rotor current, torque, and speed. Each subsystem is discussed in the next part of this section. The three-phase IM is provided with a three-phase power supply, which is generated by a signal generator in the MATLAB block, which is produced with a phase difference of 120 ° from each other with 50 Hz as the base frequency. The three-phase supply is fed to the stator voltage block, which generates the three-phase stator voltage. Then the Vabcs is connected to the Iabcs three-phase stator current subsystem and also the torque and speed generation block is connected to Iabcs and Iabcr, i.e stator current block and rotor current. The oscilloscope blocks are used to obtain real-time operational output.

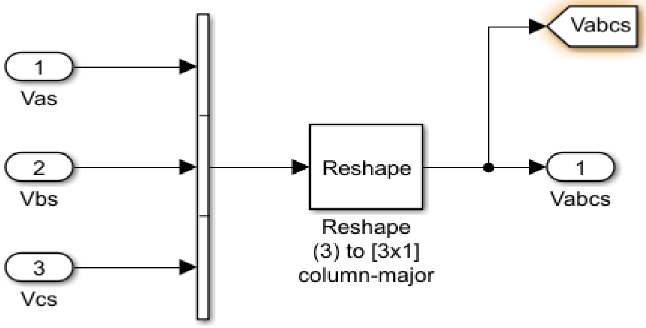

Figure 2.11: Phase stator voltage matrix subsystem (Vabcs)

Figure 2.11 shows the subsystem of the stator voltage matrix creation from equations (2.5) – (2.7), the 3-phase stator voltage matrix is created using the input blocks to take the Va, Vb and Vc all three phases of the stator and convert it into matrix form using reshape block.

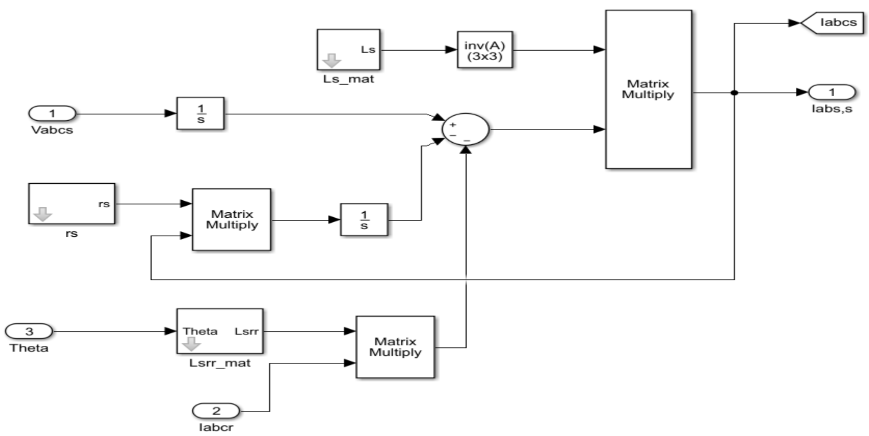

Figure 2.12: Phase stator current calculation subsystem (Iabcs)

The stator current calculation from equations (2.6) – (2.10) is done in subsystem of Iabcs. Mutual inductance calculation, rotor resistance and stator resistance all calculation is done using matrix multiply block, integrator block, inverse block and add/subtract block generating the Iabcs stator current at the output of Figure 2.12 subsystem.

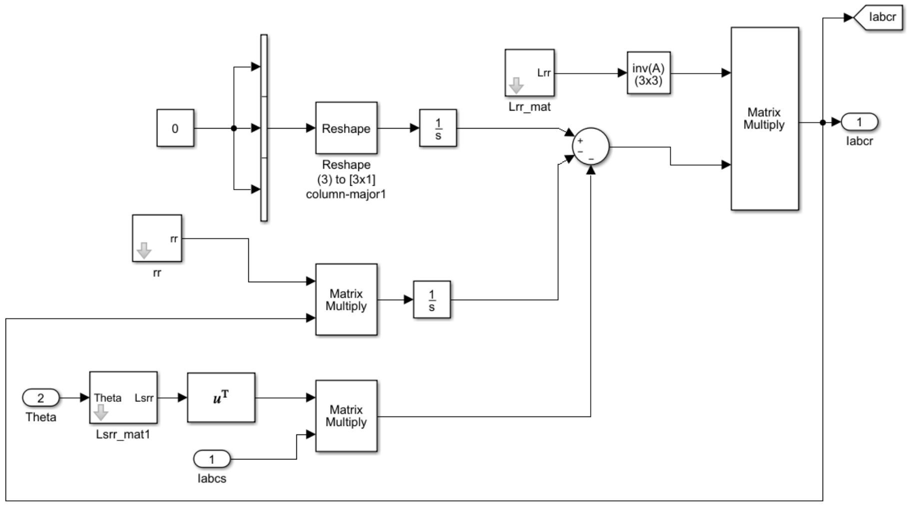

Figure 2.13: Phase rotor current calculation subsystem (Iabcr)

The rotor current calculation from equations (2.6) – (2.10) is done in subsystem of Iabcr. Mutual inductance calculations, rotor resistance and stator resistance all calculations are done using matrix multiply block, integrator block, inverse block and add / subtract block generating the Iabcr rotor current at the output of Figure 2.13 subsystem.

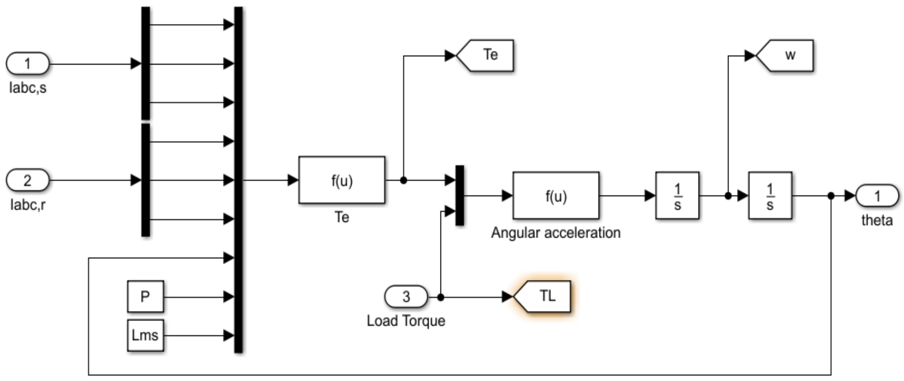

Figure 2.14: Torque and speed calculation subsystem

Figure 2.14 illustrates the torque and speed calculation subsystem model of the SCIM. Majorly function block, integrator block and parameter configuration block is utilized to model the equation.

2.4.1 MATLAB Model Results of Healthy SCIM

This section describes all the results obtained from the MATLAB model as worked under various load conditions. Four load situations, i.e. no load, 25%, 50% load and 100% load, are taken into account and the impact on rotor current, stator current, torque and speed is evaluated in graphical form.

- **SCIM at No Load Condition**

The model of IM is examined first by running the motor at no load condition during the starting of the motor and the obtained results are shown in Figures 2.15, 2.16 and 2.17. The rotor of the motor initially tends to rotate with minimal jerk and achieve the synchronous speed 1470 after 1.15 sec of time. The stability of the system is achieved after 1.15 seconds of operating time. The initial overshoot is experienced in the torque as well as in the stator and rotor currents as shown in Figures 2.15 and 2.16 is due to the initial friction of the SCIM. Figure 2.17 displays the IM signature frequency spectrum at no load normal healthy operating condition. From the figure, it can be seen that the spectrum is completely free of any current components around the main supply frequency and consequently, the frequency range in which current components due to broken rotor bars are expected is empty. The motor thus shows no signs of broken rotor bars.

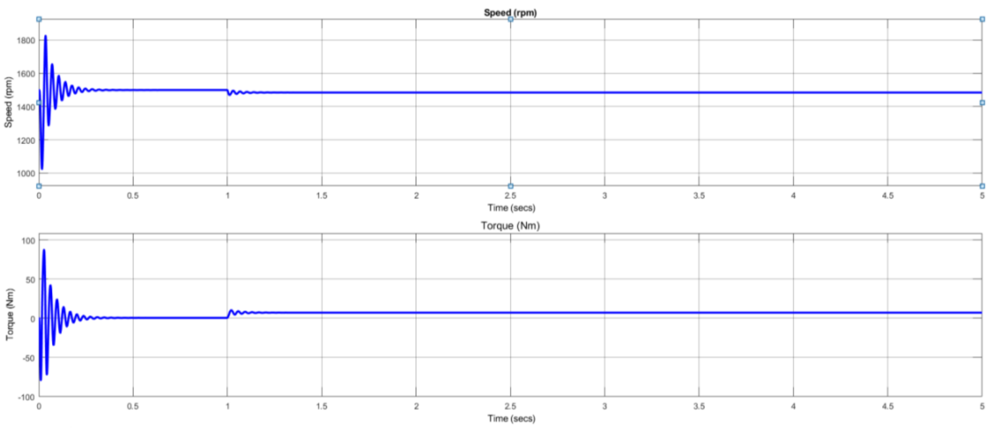

Figure 2.15: Speed (rpm) & torque (Nm) at no load condition

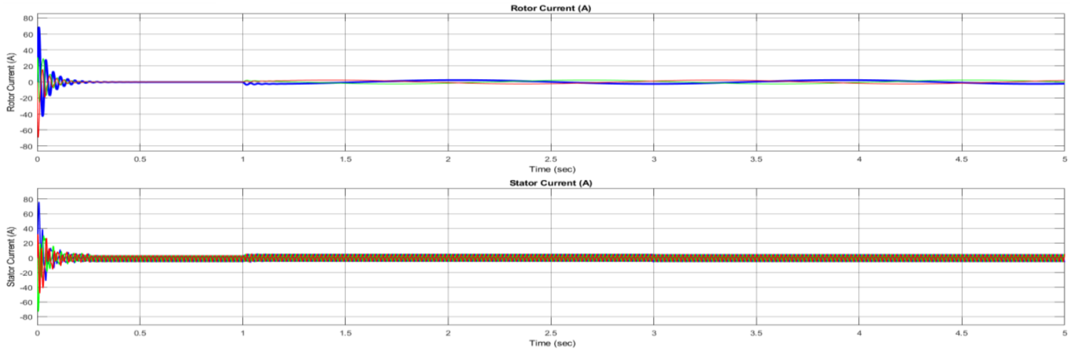

Figure 2.16: Rotor and stator current (A) at no loading condition

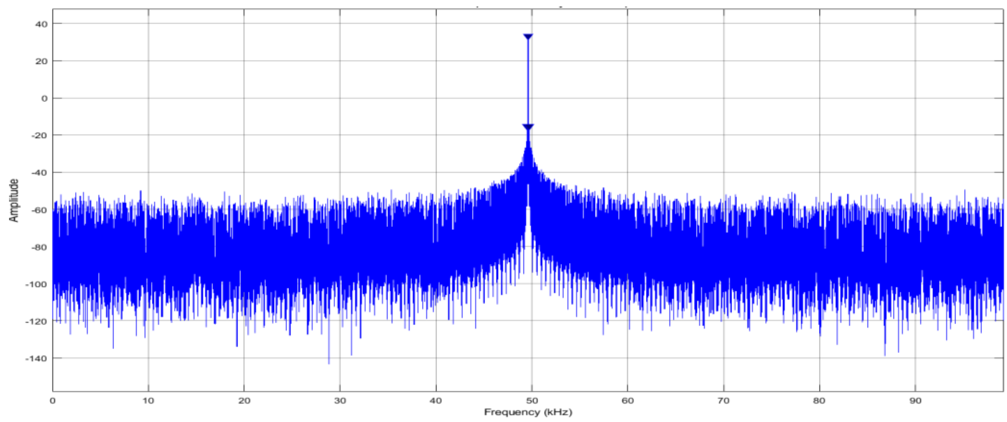

Figure 2.17: Power spectrum of motor stator current at healthy condition

- **SCIM at 25% Loading Condition**

Secondly, the IM is executed at operating condition of 25% loading condition all characteristics of the motor are observed and depicted in Figures 2.18 and 2.19. Figure 2.18 depicts the motor speed generated and torque produced. Figure 2.19 shows rotor and stator current flows at 25% loading state.

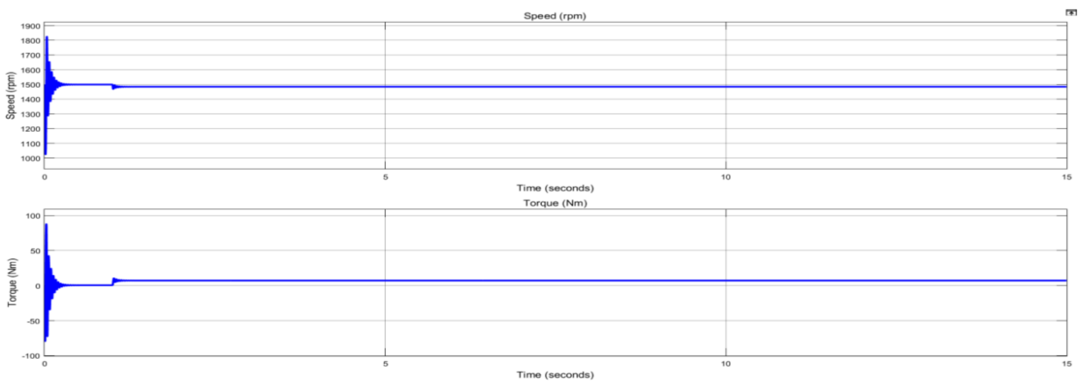

Figure 2.18: Speed (rpm) and torque (Nm) at 25% loading condition

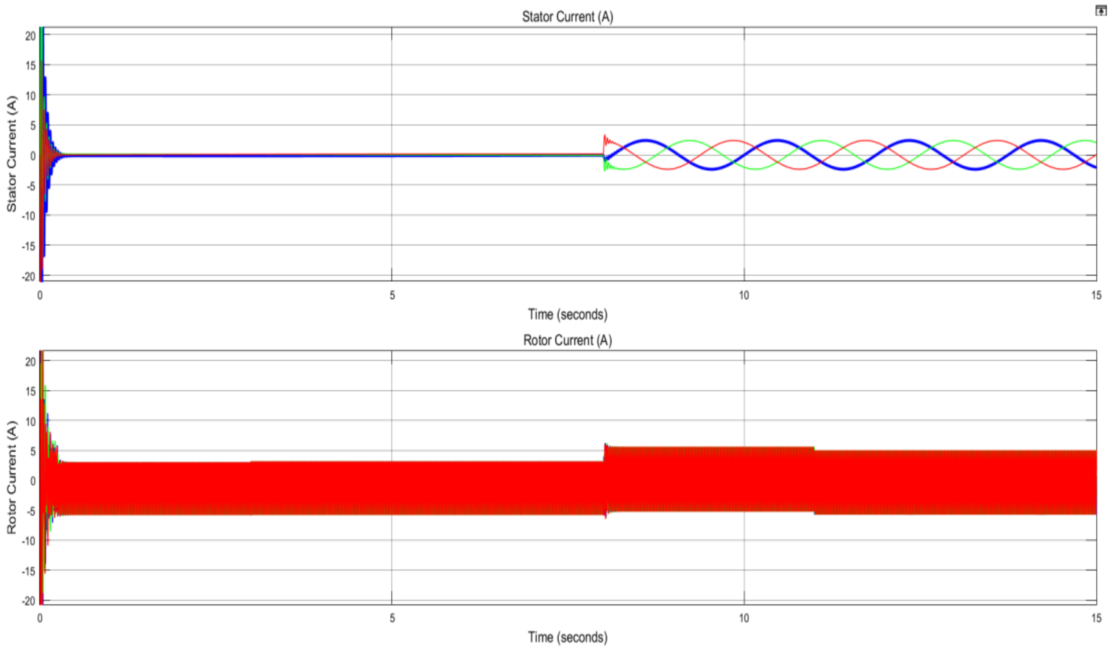

Figure 2.19: Rotor and stator current (A) at 25% loading condition

- **SCIM at 50% Loading Condition**

Secondly, the IM is executed at operating condition of 50% loading condition all characteristics of the motor are observed and depicted in Figures 2.20 and 2.21.

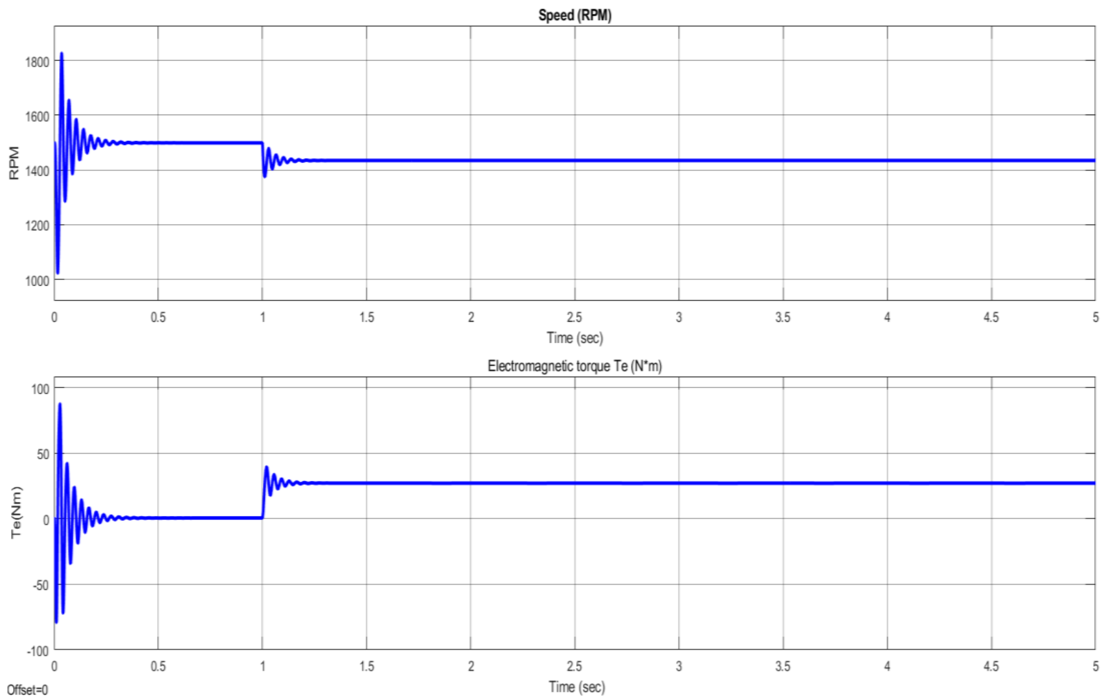

Figure 2.20: Speed (rpm) and torque (Nm) at 50% loading condition

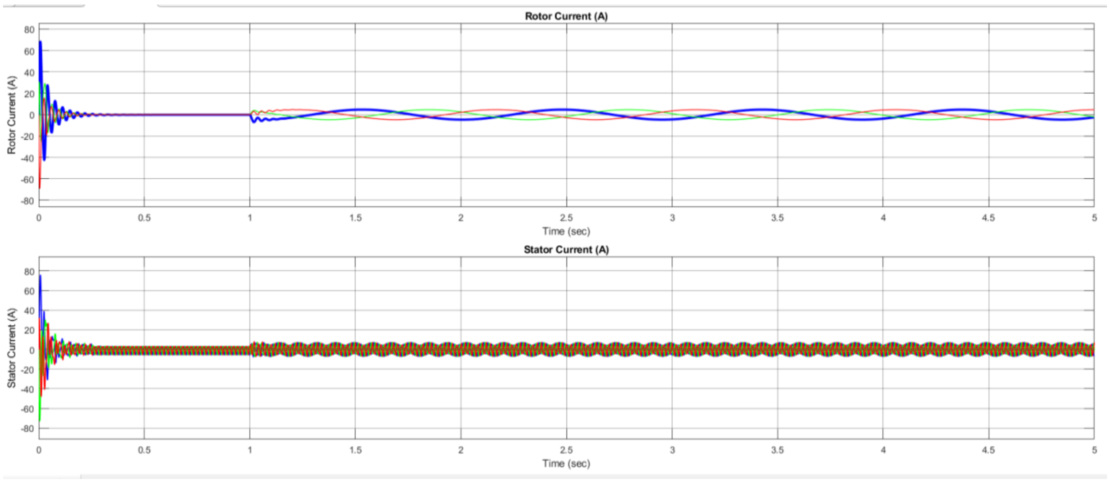

Figure 2.21: Rotor and stator current (A) at 50% loading condition

- **SCIM at 100% Loading Condition**

The IM is executed at operating condition of 100% load illustrated in Figures 2.22 and 2.23 where the graph of speed, torque, stator current and rotor current are presented. From the Figure 2.22, it can be clearly seen that at 100% loading the motor is taking relatively higher time to reach to the synchronous speed. Here, in this implementation the motor took more than 1.2 seconds to reach to the maximum speed which is again around 1435 rpm which is lower as compared to 50% and no load scenario. As the load on the motor increases the motor currents increases and the synchronous speed decreases and which is a slight wear and tear of the motor and over the period of time tends to get faulty. However, the diagnosis of the fault at an early stage in the motor will results in reducing the deterioration of the motor and increase the lifespan of the motor.

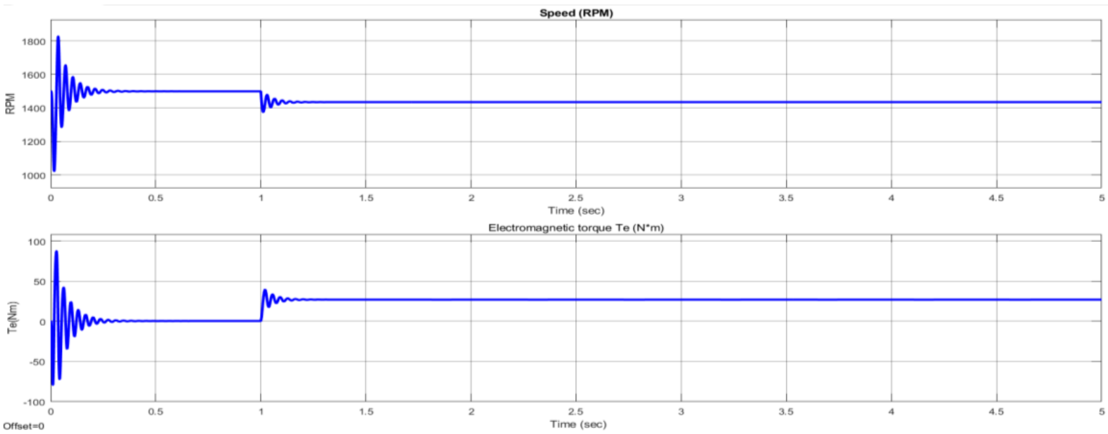

Figure 2.22: Speed (rpm) and torque (Nm) at 100% loading condition

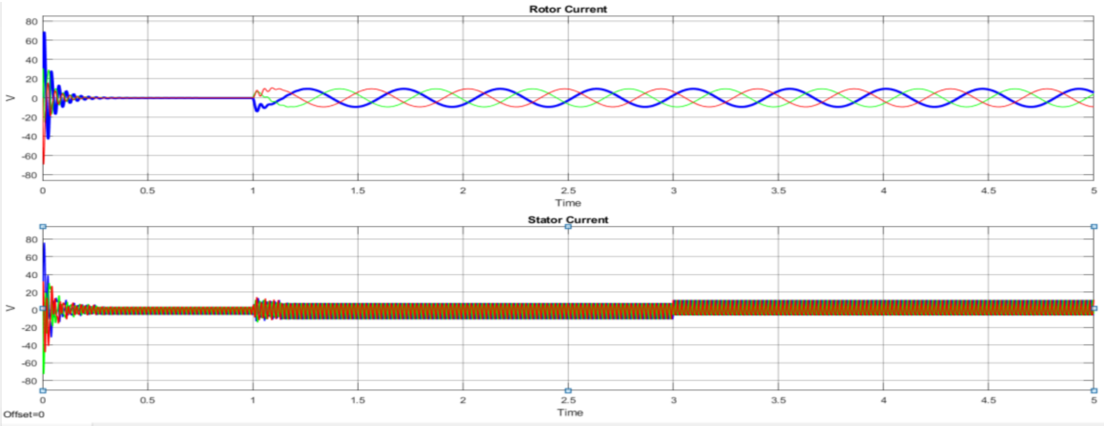

Figure 2.23: Rotor and stator current (A) at 100% loading condition

Table 2.2 illustrates the behavior of healthy motor under varied loading conditions. The torque is maximum at full load condition i.e. 27.17Nm and speed is minimum at around 1435 rpm, the speed tends to increase as the load decreases on the motor. The motor characteristics have been obtained affectively and MATLAB IM model performance at different loading conditions varied as per the theoretical formulation of the IM. Thus, validated the MATLAB designed model.

Table 2.2: Three-phase SCIM performance at different loading conditions

Loading Conditions	Torque (Nm)	Speed (rpm)
Full Load	27.17	1435
Half Load	13.82	1468
Quarter Load	7.14	1484

2.4.2 Healthy Induction Motor Under Time Varying Loading Condition

The MATLAB model of the IM has been tested under different loading conditions and furthermore, it has been analysed on the time varying loading condition during runtime. For this experimentation, the model is operated under varied loading at different time intervals and its results have been displayed in Figures 2.24 and 2.25. The variation of speed and torque is varied as per the on-demand loading conditions during runtime is being displayed in Figure 2.24.

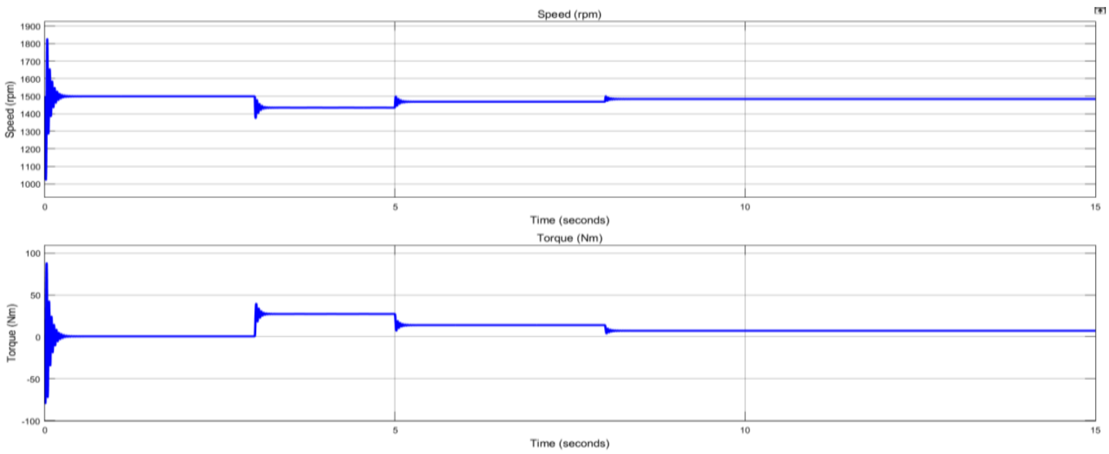

Figure 2.24: Speed (rpm) and torque (Nm) at different time varying loading conditions

The load on the motor is applied as from 0-3 seconds it's no load, 3-5 seconds it's full load, 5-8 seconds it's half load, 8-11 seconds its quarter load and 11-15 seconds it's no load. The designed model provided efficiently all the required torque and speed as per the variation of the loading condition during runtime.

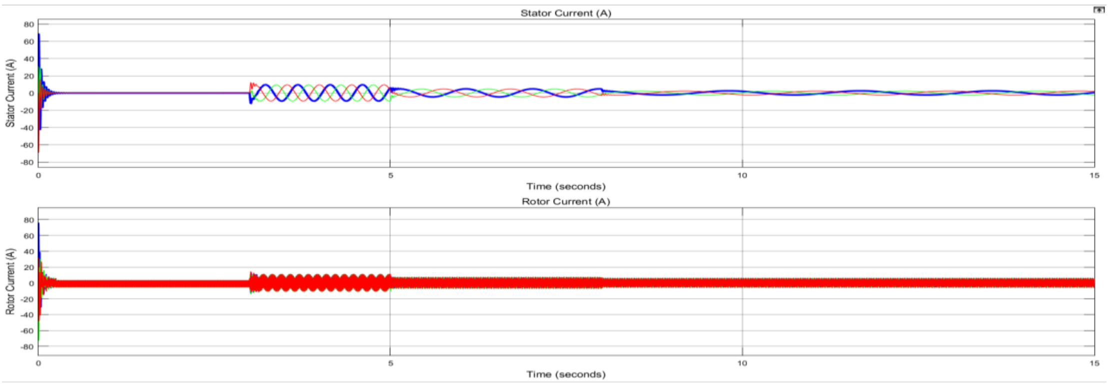

Figure 2.25: Rotor and stator Current (A) at different time varying loading condition

2.5 SUMMARY

The proper selection of an IM model structure and its parameterization are critical since they influence both the observation and identification ability. So, the main challenging task was to design base model of healthy IM whose behavior resembles real motor which is successfully accomplished using Rmxprt a template based designed tool and mathematical model of a three phase SCIM implemented in MATLAB in the presented chapter .

The behavior of motor in terms of its characteristics like torque, power, and current can be done in Maxwell 2D using FEA. The Finite Element Method (FEM) is a numerical method for solving a differential or integral equation used for analysis purpose and briefly discussed in this chapter.

Moreover, for the FD and diagnosis, the IM model is implemented in MATLAB software tool which will be utilized for further fault analysis and classification of faults. The motor characteristics have been obtained affectively and MATLAB IM model performance at different loading conditions varied as per the theoretical formulation of the IM. Thus, validated the MATLAB designed model. The motor parameters and characteristics can be precisely calculated. Further, the designed model is subjected to various constant and time varying loading conditions in order to carry out research work.

CHAPTER 3

FAULT TYPES AND DIAGNOSIS & CLASSIFICATION TECHNIQUES

3.1 INTRODUCTION

This chapter provides a brief description of the different types of faults that occur in SCIM. The most common faults are broken rotor bar faults, stator, and eccentric faults. Then the fault diagnosis approaches in SCIM are discussed. Signal processing based approach, model based approach and vibration signal based approach. The DWT-based approach is taken into account in this research work. In addition, various soft computing techniques are being developed to autonomously identify and classify the fault and its type. The work was mainly focused on the DBNN deep learning method but the SVM and RF machine learning methods are also used further for detection for comparative analysis.

3.2 FAULT DIAGNOSIS METHODS

A number of mechanisms and approaches have been developed to diagnose the faults in IM. Numerous approaches have achieved impressive results for detecting and diagnosing the faults. However, there is still a large gap for further development and improvement.

This research work examines some of the essential techniques with machine learning and deep learning approaches, and it has been found that the signal processing based approach may be the optimal one of all the different approaches that will meet all of the related requirements for the same. Some of the troubleshooting methods are listed below.

1. Park's Vector Approach
2. Fast Fourier Transformation
3. FFT enabled monitoring and diagnosis
4. Discrete Wavelet Transform
5. Fault Signature Analysis through vibrations and currents

6. Discrete Wavelet Transform

3.2.1 Discrete Wavelet Transform

The wavelet transform has established itself as a robust tool for dealing with certain transient signals, such as waveforms of vibration signals, in numerous applications. The approach allows for very accurate and efficient interpretation of time domain and frequency domain signals at the same time with the goal of examining all components, such as local, transient, or intermittent. In fact, the wavelet transform can be of two types, discrete or continuous.

The wavelet transform of the continuous type shows more significant information of a signal compared to DWT, but unfortunately it has a longer computation time than the discrete one. On the other hand, signal processing with much higher processing speed and efficiency is required for most applications and especially for industrial applications. Hence, DWT becomes a potential player for such applications. The DWT takes into account a dyadic grid and orthonormal wavelet base functions, which ultimately have no redundancy. DWT estimates wavelet coefficients at certain particular discrete intervals of time components and scales. The estimated coefficients of DWT can be used to construct a set of characteristics that explicitly represent different types of signals.

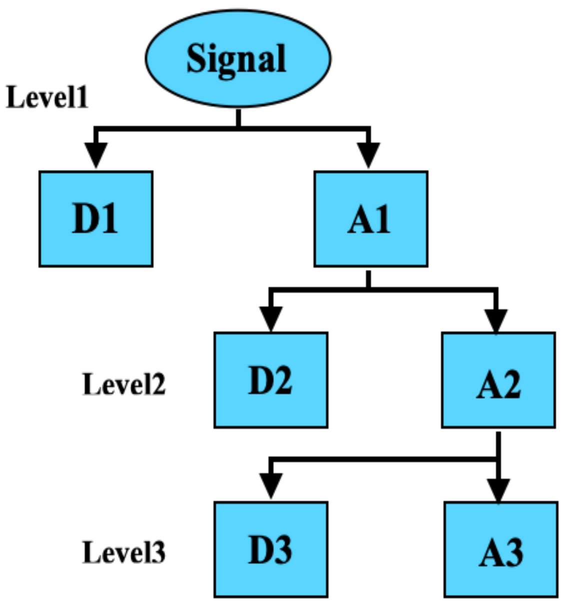

Figure 3.1: Filter bank representation of the DWT [78]

At each level in filter bank the signal is decomposed into lower and higher frequencies. A function in DWT known as a dilation function can be expressed as a tree of high and low pass filters, with each individual pass converting the low pass filter into additional lower and higher frequency signal components. The graphical representation of such a transformation is shown in Figure 3.1[78]. The filter bank implementations can be explicated as computing the wavelet coefficients of a discrete set of child wavelets for a given mother wavelet ψ(t). The mother wavelet is shifted and scaled by power of 2 in the case of Discrete Wavelet Transform as given in equation (3.1).

$$\psi_{j,k}(t) = \frac{1}{\sqrt{2^j}}\psi\left(\frac{t-k2^j}{2^j}\right) \tag{3.1}$$

Both j and k are integers, where k is the shift parameter and j is the scale parameter. Wavelet coefficient of signal x(t) length of 2^N is in the case of child wavelet in the discrete family is :

$$\gamma_{jk} = \int_{-\infty}^{\infty} x(t)\frac{1}{\sqrt{2^j}}\psi\left(\frac{t-k2^j}{2^j}\right)dt \tag{3.2}$$

Where in equation (3.2), γ_{jk} is expressed as convolution of x(t) with a dilated, reflected, and normalized version of the mother wavelet sampled at points $1, 2^j, 2^{2j}, ___, 2^N$by fixing j at a particular scale which gives detail coefficient of filter bank correspond exactly to a wavelet coefficient of a discrete set of child wavelets for a given mother wavelet ψ .

The signal decomposition process takes place with the original signal introduced through successive decomposition into various components of the signal with lower resolution. In other words, components with a higher frequency are not processed for analysis in later steps. In the DWT, the components with the lowest frequency of the signal are given as approximate values, while on the other hand the components with the highest frequency are given as details.

Time-frequency representation of a digital signal can be achieved using digital filter approaches. Filters with different cutoff frequencies are used to analyze signals with varying frequencies. The input signal is processed or passed through a sries or series of high-pass filters for the analysis of high-frequency signals and similarly passes through low-frequency filters for the analysis of low-frequency signals [78].

Most researchers have provided sophisticated expressions for fault frequency components. However, they have not provided the most accurate diagnostic model for stator current analysis. Machine models based on numerical calculations for error detection are used in many research projects. However, they do not provide the methodological expressions of stator current that are important in choosing the appropriate approaches to signal analysis and FD. The most common approach to stator current output under these circumstances is to estimate the spectrum.

The frequency component that is most important in your original signal would have a high amplitude in the region of the DWT signal. This signal consists of specific frequencies. One of the main advantages of DWT over fourier transformation is that DWT does not lose any temporal location of the considered frequencies.\

In general, the power spectral density (PSD) for the stator current is calculated using Fourier transform approaches. However, there is a need for advanced and very robust approaches to analyzing the transient signal. In this research work, stator current signals and vibration signals of healthy and faulty IM under different loading conditions are considered in order to detect the presence of fault like stator winding faults , eccentric faults and broken rotor faults. Further, DWT is used for feature extraction of both the signals and extracted features are act as input for the fault detection and classification methods.

3.2.2 Fault Signature Analysis Through Vibrations and Currents

Vibration monitoring technology is one of the most important approaches to monitoring mechanical errors or system failures. Due to the nature of mechanical failure, vibration occurs in related components of machines. Since mechanical vibration causes the generation of acoustic noise, it facilitates the possibility of noise monitoring.

Current monitoring techniques are usually applied to detect the various types of induction motor faults such as rotor fault, short winding fault, air gap eccentricity fault, bearing fault, load fault etc. While neither of these approaches is economical, given that the cost of the converters used are higher, these approaches could only be implemented with large machines or highly critical industrial applications.

To have a complete monitoring system, a large number of transducers intended for vibration measurement must be connected to various system devices that can fail, such as bearings, gear machines, stator racks, and load components. So a severe mechanical defect in a component affects the electrical machine throughout the load torque and shaft speed. This shows that the machines or the motor can be seen as an intermediate converter component which is a collection of effects. This severely limits the number of sensors or transducer components required.

3.3 DIFFERENT TYPES OF FAULTS IN INDUCTION MOTOR

Mechanical mechanisms that are in motion in an induction motor are particularly giving problem from wear, corrosion, erosion, fatigue, contamination, abuse, etc. Electrical components and/or systems tend to suffer from wear, insulation deterioration, aging of plastic parts, fatigue from flexing, dirt and moisture contamination, terminations becoming loose, etc.

In general, IM faults can be divided into electrical and mechanical faults. All types of faults are summarized in the block diagram in Figure 3.2.

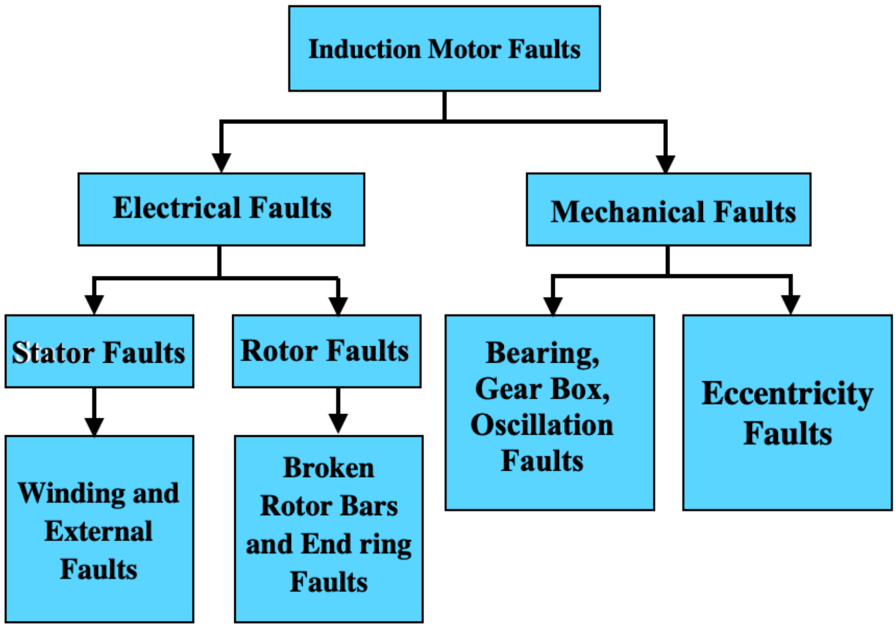

Figure 3.2: Block diagram of Induction Motor faults

Electrical faults are further divided into stator and rotor faults. Although the motors are reliable electrical devices, they can be prone to numerous types of failure. These electrical faults include the short circuit between the turns in the stator windings, faults in the stator windings caused by open circuit, faults in broken rotor bars and some other faults like broken end rings, rotor eccentricity mechanics. Several studies have shown that 30-40% of IM failures are due to a broken insulation in the stator winding. The materials used for insulation purposes generally suffer from the degradation due to continuous change, instantaneous tension, and system overload caused by mechanical as well as environmental situations.

For all of these possible reasons, the thermal stresses are the most important that cause the insulation material of the stator winding to degrade. Even so, the most effective insulation fails quickly even if the system operates above the threshold temperature and, for every 10°C increase in temperature, the service life of the insulation used shortens by 50%. The presence of this type of fault in the IMs results in unstable stator voltages and currents, torque fluctuations, a decrease in power efficiency, overheating of the system, extreme vibrations, and a decrease in torque. In addition, such machine faults can increase the size of certain harmonic components [79, 80].

3.3.1 Stator Faults

Stator faults mainly occur due to the stator winding-related faults. Stator faults are mostly responsible for 38% of the failures in an IM. A number of research works have demonstrated that the prevalence of failure of IM stator winding, caused due to the destruction of the turns insulation. The failures related to the stator winding could be classified into five main groups shown in Figure 3.3.

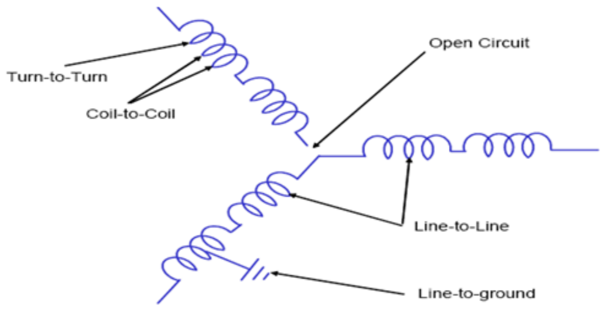

Figure 3.3: Star connected stator showing possible failure mode

1. Line-to-line,
2. Turn-to-turn,
3. Line-to-ground,
4. Coil-to-coil and
5. Single or multi-phase windings open circuit faults.

The idle error may be due to other reasons such as: a mechanical failure of a machine terminal connector, an internal winding break, or an electrical failure in one of the inverter phase branches. Therefore, an idle fault can be considered one of the most common failures in IM units. The most undesirable result of an open circuit fault would be a serious accident that could injure people's lives and immediately shut down the drive.

In general, the stator winding of an induction machine is subject to stresses caused by a number of factors, such as thermal overloads, mechanical vibrations, and voltage spikes generated by variable frequency drives. Few of the major causes of stator winding failure are:

- Due to Loose bracing for end windings
- Due to high stator core or winding temperatures
- Due to short circuits
- Due to Contaminations caused by oil, moisture, etc.
- Due to starting stresses
- Due to leakage of cooling systems
- Due to electrical discharges

3.3.2 Rotor Related Faults

Breaking the rotor bar is one of the most common machine failures. Several factors can contribute to this error, including: hot spots, sparks and thermal imbalance, chemical contamination, moisture abrasion of rotor materials, manufacturing defects, frequent starts at nominal voltage, thermal stresses and / or mechanical stresses caused by bearing errors and metal fatigue [81]. The broken bar can also be partially or totally cracked. The resistance due to a broken bar would increase, adding another resistance and thus generating more heat. The bar would crack completely and an electric arc would occur over the cracked area. This bending or arcing damages the lamination of the rotor. Adjacent bars carry increased current and are exposed to high voltages, which ultimately leads to failure of the rotor bars. In short, it can be said that centrifugal forces aggravate damaged or broken bars and can also damage the stator winding.

The cage of an IM consists of rotor bars and end rings. A broken bar can be incompletely or completely broken. These types of bars can be due to manufacturing defects, repetitive starts at nominal voltage, stresses due to thermal irregularities and mechanical stresses. A broken rotor bar can cause various effects on IMs. The manifestation of the components of the lateral ligament is one of the common effects of a broken bar. The sideband components are located in the power spectrum of the stator current on the left and right side of the fundamental frequency component. The left sideband component is caused by electromagnetic asymmetries in the rotor cage, and on the other hand, the right sideband component is generated due to the resulting speed ripples caused by the resulting torque pulsations. Sideband frequencies can be expressed as in equation 3.3[82, 83]:

$$f_{br} = (1 \pm 2s)f_s \tag{3.3}$$

Where f_{br} is fault frequency components due to broken bars and f_s, the supply frequency.

Other effects of broken rotor bars, for classification purpose in IM are the speed oscillations torque ripples, instantaneous stator power oscillations and stator current envelopes.

3.3.3 Eccentricity Related Faults

The eccentricity of the machine can be defined as the location of the asymmetric air gap that remains between the stator and the rotor stem. In fact, there is usually a certain eccentricity in rotating electrical machines. Few users give a maximum value of 5%, in some cases 10% of the air gap length is admissible or tolerable [84]. On the other hand, in general applications and in manufacturing, it is always attempted to reach the full eccentricity level or keep it smaller to reduce the total mechanical vibration that causes noise and ultimately leads to reduced magnetic force. Because the air gap of an induction machine is significantly smaller compared to other categories of electrical machines used for similar applications, these types of machines are more sensitive to changes in the length of the air gap. In general, there are two types of eccentricity of the air gap [84]:

1. Static Eccentricity (SE)

2. Dynamic Eccentricity (DE)

In the first case of eccentricity, the arrangement of the nominal length of the radial air space in the space is permanent, while in the second scenario the center of the rotor is not in the middle of the circulation and the arrangement of the air space spin with the rotor. Until it is detected at an early stage, the eccentricity becomes much larger, creating higher imbalances in the radial forces that could cause friction from the stator to the rotor and, ultimately, this leads to a major failure of the electrical machine.

3.4 DEEP BELIEF NEURAL NETWORK FRAMEWORK

The deep learning methods are advanced version of NNs which fall under the machine learning category. The DBNN is a deep learning architecture with several hidden levels that is able to automatically learn hierarchical representations in an unsupervised manner and at the same time perform a classification. To precisely structure the model, there is both an unsupervised pre-training process and a supervised fine-tuning strategy. Because of the vanishing gradient problem, it is often difficult to learn a large number of parameters in a deep learning model that has multiple hidden layers. To solve this problem, an improved training algorithm is used that processes and learns one layer at a time, and each pair of layers is considered to be an RBM model. RBM is the basic unit of DBNN, so RBM is introduced first.

3.4.1 Restricted Boltzmann Machine

The RBM is a mathematical model that is often used in probability statistics and follows the random field theory of logarithmic linear Markov Random Field [85, 86], which has several special forms, and the RBM is one of them. RBM model has two levels: one level is the entry level, also known as the visible level, and the other level is the exit level, also known as the hidden level. All visible units in the RBM are fully connected to hidden units, while units within layers have no connection to each other. The architecture of an RBM is shown in Figure 3.4.

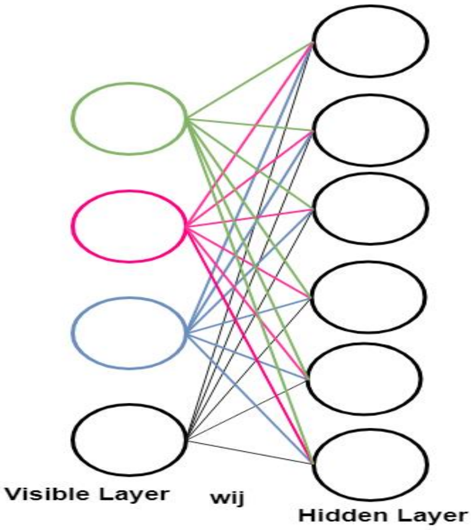

Figure 3.4: RBM architecture [85].

3.4.2 Training of RBM

In order to set the model parameters, the RBM needs to be trained using training dataset. In the procedure of training a RBM model, the learning rule of stochastic gradient descent is adopted. The log-likelihood probability of the training data is calculated, and its derivative with respect to the weights is seen as the gradient shown in equation (3.4).

$$\frac{\partial \log p(v)}{\partial w_{ij}} = < v_i h_j >_{data} - < v_i h_j >_{model} \tag{3.4}$$

Parameter update rules are originally derived by Hinton and Sejnowki shown in equation (3.5):

$$\Delta_{w_{ij}} = \varepsilon\big(< v_i h_j >_{data} - < v_i h_j >_{model}\big) \tag{3.5}$$

Where, ε is the learning rate, the symbol$<.>_{data}$ represents an expectation from the data distribution while the symbol >*model* is an expectation from the distribution defined by the model.

$$\Delta_{w_{ij}} = \varepsilon\big(< v_i h_j >_{data} - < v_i h_j >_{recon}\big) \tag{3.6}$$

Reconstruction model with Gaussian-Bernoulli RBM to deal with the real valued data in practical problems is shown in equation (3.6) where in visible units are updated in parallel to get a reconstruction and the model updated using equation (3.6).

3.4.3 Architecture of DBNN

The DBNN model is a deep faith neural network architecture in a deep learning domain with multiple hidden layers containing multiple non-linear representations. It is a probabilistic generative model and can be formed from RBM, as shown in Figure 3.5 that shows how an RBM is stacked on top of one another. The DBNN architecture can be built by stacking multiple RBMs in a row to form a deep network architecture.

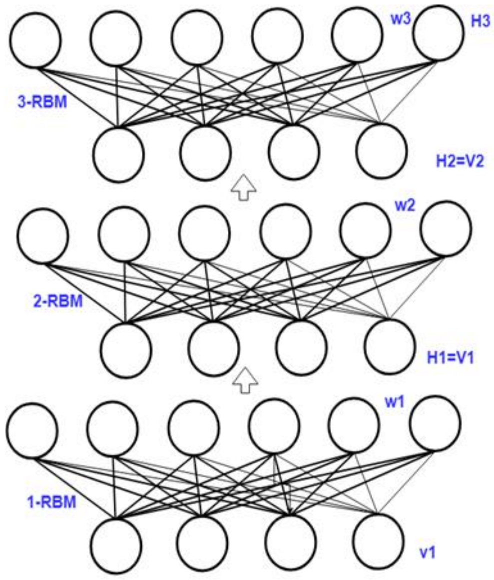

Figure 3.5: DBNN architecture [87]

As DBNN has multiple hidden layers, it can learn from the input data and extract hierarchical representation corresponding to each hidden layer. Joint distribution between visible layer v and the l hidden layers h^m can be calculated mathematically from conditional distribution $\prod_{m=1}^{n-1} P(h^{m-1}|h^m)$ for the $(m–1)^{\text{th}}$ layer conditioned on the m'th layer and visible hidden joint distribution $P(h^{n-1}, h^n)$ as shown in equation (3.7)

$$P(v, h^1, \dots., h^n) = (\prod_{m=1}^{n-1} P(h^{m-1}|h^m))P(h^{n-1}, h^n). \tag{3.7}$$

For deep NNs, learning such a set of parameters using a conventional supervised training strategy is impractical because the errors transmitted in low-level layers are weakened by multiple hidden layers and the ability to adjust the parameters is weak for conventional back propagation methods. It is difficult for the network to generate optimal parameters globally. Here, the greedy layer-by-layer method of unsupervised pre-training is used to train DBN. This process can be represented as follows. The first step is to train the input units (v) and the first hidden layer (h1) using RBM rule (denoted as RBM1). Next, the first hidden layer (h1) and the second hidden layer (h2) are trained as a RBM (denoted as RBM2) where the output of RBM1 is used as the input for the RBM2. Similarly, the following hidden layers can be trained as RBM3, RBM4,…, RBMn until the set number of layers are met. It is an unsupervised pre-training procedure, which gives the network an initialization that contributes to convergence on the global optimum. For classification tasks, fine-tuning all the parameters of this deep architecture together is needed after the layer wise pre-training. It is a supervised learning process using labels to eliminate the training error and improve the classification accuracy.

3.4.4 Fault Diagnosis Based on DBNN

The stator current waveform signals are selected as input to the entire system for fault diagnosis because they generally contain useful information that can reflect the operating conditions of IMs.

However, there is a correlation between the sampled data points. This is difficult to model for the DBNN architecture as it is unable to work out the correlation between the input units that can affect the next classification task. Therefore, in this research, the stator current signals are processed with a Discrete Wavelet Transform to convert the stator current signals with two DWT levels from the time domain to the frequency domain, and then the wavelet of each signal is used as the input to the DBNN Architecture. This is beneficial for the classification task during the training process. In particular, DBNN learns a model that generates input data that can get more intrinsic properties from the input, ultimately improving the accuracy of the classification.

In this module, DBNNs are created using a series of stacked RBMs and then train by training a data set from the data preparation module to obtain the model parameters. The input parameters of the architecture are initialized first, including a series of numbers of neurons and numbers of hidden layers, as well as training epochs. Then each layer in the architecture is trained as an RBM entity, and the output of the lower layer RBM is used as the training input for the RBM of the next layer.

After learning in layers, the synaptic weights and distortions are established and the basic structure is determined. The classification process is then followed to predict the failure category. It is a supervised fine-tuning process as shown in Figure 3.6, and the proposed method uses the back propagation training algorithm to implement fine-tuning in which the marked data is used for training to improve the discrimination ability for the classification task.

The unattended training process trains one RBM at a time and then monitors the fit process using labels to fit the weights of the entire model. The difference between the DBNN outputs and the destination tag is considered a training error.

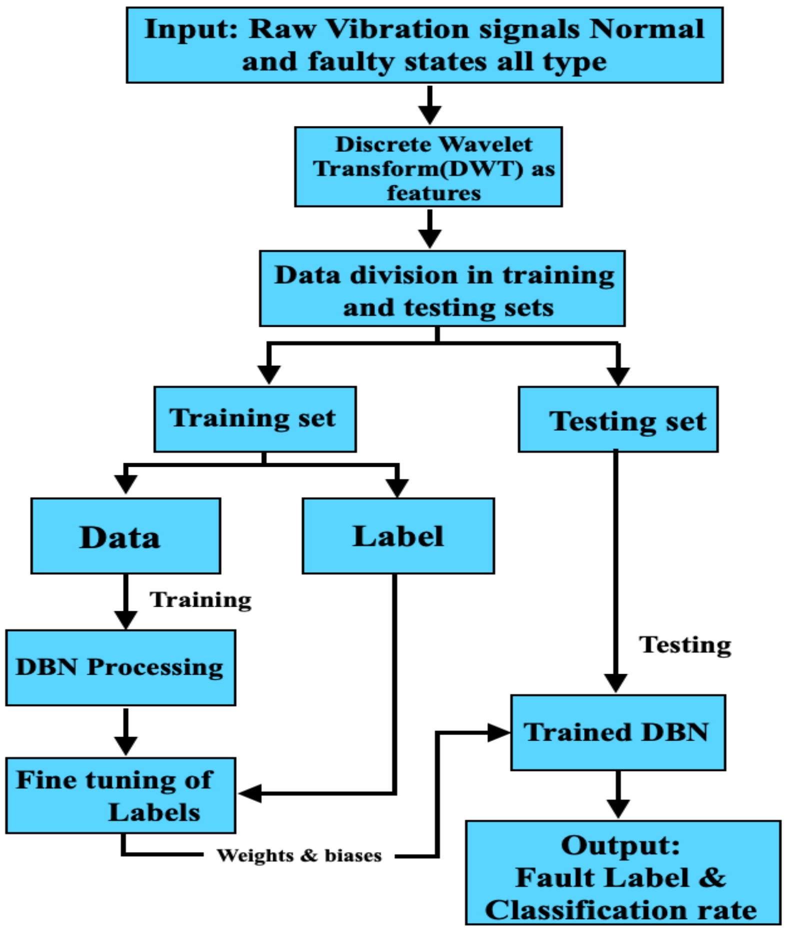

Figure 3.6: Supervised fine tuning process of DBNN

To obtain the minimum error, the deep network parameters are updated based on the learning rules. After training the DBNN model, all the DBNN parameters are set and the next procedure is to test the classification ability of the trained DBNN model and the classification rate is calculated as an index for evaluation as Figure 3.7 demonstrates the testing process to get the accuracy. The current signal from the stator is the input of the established fault diagnosis system, and its output indicates the operational status of the IM.

After the layered synaptic learning loads, the twists and turns are resolved to determine the essential structure. In this way, the bundling process continues to anticipate the failure class. It is a regulated optimization strategy and the proposed technique receives the computation to prepare for the de-spreading to perform the adjustment using information that has been established for the preparation to improve the separation capacity for the grouping task. Unattended setup processes each train in an RBM and then verifies the calibration process using names that change the severity of the entire model.

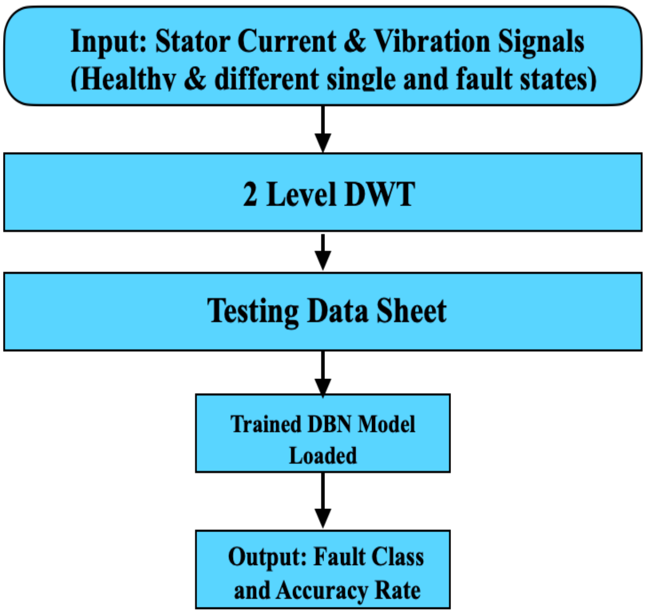

Figure 3.7: Testing process for fault diagnosis

The distinction between DBNN yields and the target label is considered a preparatory error. To get the basic error, the learning rules update the deep system parameters. After preparing the DBNN model, all the DBNN parameters are configured. At this time, the clustering limit of the prepared DBNN model is tested and the disposition rate is determined as a data set for evaluation. The current stator signal is the contribution of the processed frame in the defect processing frame, and its output shows the working conditions of the induction machine.

3.5 SUPPORT VECTOR MACHINES

Based on the results of statistical learning theory and as a next-generation classification method, SVM was introduced in 1992 by Boser, Guyon, and Vapnik.

SVMs are becoming increasingly popular in many areas and disciplines, from bioinformatics to science and technology, due to many attractive features, such as precision and efficiency in modeling and empirical performance [88–89]. SVMs replace NNs in a variety of areas, including engineering, information retrieval, and bioinformatics and belong to the general category of core methods [89].

According to [90], SVMs are defined as learning systems that use a hypothesis space of linear functions in a high-dimensional feature space. This learning strategy is a principled and very powerful method that in the few years since its introduction in the 1990s it has already outperformed most other systems in a large number of applications.

SVM can process data without losing prior knowledge. This property makes SVM suitable for online condition monitoring and fault diagnosis in real-time applications. Furthermore, due to improved computing power and the development of algorithms for rapid learning, it is now possible to train SVM in real applications [91].

SVMs have the disadvantage that they have black box settings in their performance, which do not give the user much information about why a particular prediction was made.

3.5.1 Fault Diagnosis using Support Vector Machine

The stator current signals are processed using the DWT characteristic extractor and the characteristics are calculated for all collected data sets. Different scenarios are taken into account. The healthy state of the motor characteristics, the stator fault condition characteristics, the rotor switch rod fault functions, the eccentric fault functions, and the combined fault functions are divided into classes and the set of complete data is divided into training and test data. Consequently, SVM with linear kernel function as classifier is applied to training a well test data set to maintain accuracy. The block diagram of the entire process is shown in Figure 3.8.

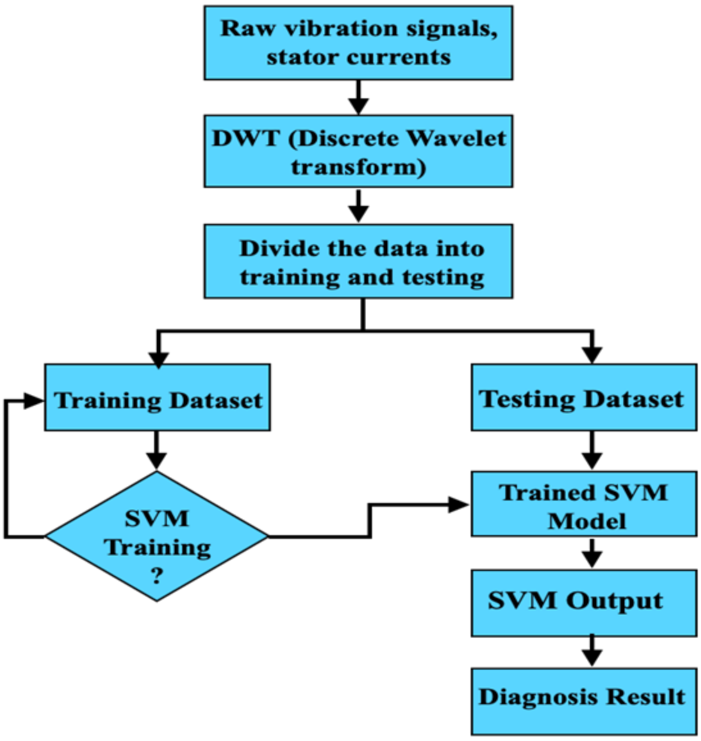

Figure 3.8: SVM based IM fault diagnosis block diagram

3.5.2 Principle of SVMs

SVM is considered a binary output classifier where the classification depends on separating the data under test into two main classes. The two data sets that can be separated with different linear hyperplanes are shown in Figure 3.9.

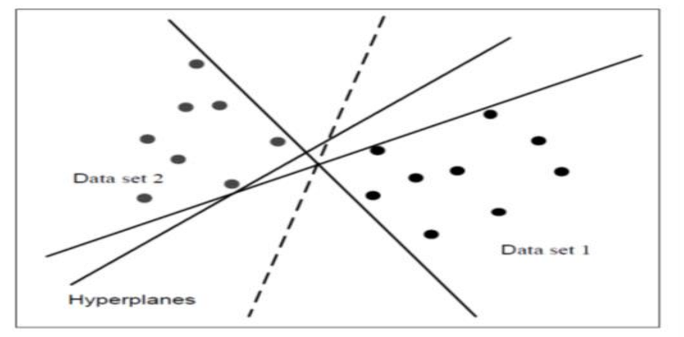

Figure 3.9: Two data sets with different hyper-planes [91]

Of the many hyperplanes that separate, only one (the dotted line) can offer the maximum margin of separation. Finding this hyperplane is the basic working principle of SVMs. Find the hyperplane that provides the maximum separation distance between the two data sets to be tested. The edge represents the distance between the next training point and the separation hyperplane. The classification task generally involves the use of two data sets, training and test data. The raw data is divided into two sets of test and training data. SVM decides which is the ideal hypertext division layer that provides the best information partition and then enforces the separation between these two classes [91].

Take the following vectors of the two classes and then expand the hole between them, accepting that they are directly isolated, as shown in Figure 3.9.

The elaboration of information consists of information designs that, regardless of its characteristics or its esteem as a brand, deliver an objective called a class identifier.

A definitive objective of the SVM calculation is to make a model that predicts the class name of the test information occasions when just the information properties are entered.

Given a training data set with n training examples, (xi, yi), i= 1, 2, …, n, where each example has d inputs i.e. each xi is a list of d real numbers; (xi ϵ Rd) and y=±1 , and yi are the labels or targets of the samples, (R) is real numbers. The hyper-planes are characterized by a vector (w), which is orthogonal to the hyper-plane, and a constant (b). The hyper-plane that separates the data is expressed by:

$$x + b = 0 \tag{3.8}$$

The canonical hyper-plane which separates the data from the hyper-plane expressed by equation (3.8) by a distance of at least 1 should satisfy the following conditions:

$$w.x + b \geq +1 \; when \; y_i = +1$$

$$w.x + b \leq -1 \; when \; y_i = -1$$

The preparation vectors are mapped into high dimensional space. A division hyper plane is discovered which boosts the edge between the two isolated classes. The procedure requires the arrangement of the accompanying enhancement issue

$$min_{w,b,z}\frac{1}{2}\|W\| + c\sum_{i=1}^{N}\alpha_i \qquad (3.9)$$

$$Subject\ to:\ y_i(w^T\emptyset(x_i) - b \geq 1 - \alpha_i, \alpha_i \geq 0$$

Where α is a coefficient related with each preparation test and known as the double portrayal of the choice limit in equation (3.9). The parameters α, b and w are gotten through the advancement procedure. (x) is the new example to be characterized.

3.5.3 SVM kernels

SVMs depend on the idea of SVM centers. The centering machines offer a separate system that can be adapted to different assignments and rooms by selecting the core capacity and basic calculation.

SVM uses centers to deal with learning disabilities. SVM uses several types of main capacitance centers, such as Direct, Polynomial, and Outspread (RBF). Non-straight center elements are used to mark information to an area with high readings in which the information can be directly distinguished. Choosing the best type of part is an integral part of the repair process. This is done tentatively by testing different parts and choosing the one that gives the best results.

SVMs are considered a phenomenal classifier for dual classes, but can be used to handle multiclass problems with multiclass extensions, where the multiclass problem is divided into a sequence of companies of two classes and this is known as multi-class. SVM can be moved up as a classifier for multiple classes.

Serviceability is critical to good SVM pooling. The selection of the correct part and the preliminary setting of the parameters have a direct effect on the final result. There are numerous accessible sub-works. These are three of the most used bits [91]:

1. Linear: *K(x,xi) = xT xi*
2. Polynomial: *K(x,xi) = (ᵞ xT xi+1)d, ᵞ>0*
3. Radial Basis Function (RBF): *K(x,xi) = exp (-ᵞ | |x- xi ||2), ᵞ>0*

Where: d is the degree of the polynomial and equals 1 for the linear kernel. The parameter ᵞ controls the width of the Gaussian and ||x|| is the norm of x.

3.5.4 SVM Testing

For testing, the following two methods are used. Leave-One-Out (LOO) and N-fold cross-validation. In N-fold cross-validation, the data sample set is divided into complementary N-subsets. The first subset is used for testing the model that trained on the remaining subsets N subsets. The analysis is performed upon one subset which called the training set. Validation analysis is performed on the other subset which is called the validation set or testing set. The process is repeated for next subset and so. To reduce variability, the above procedure is run for multiple iterations upon the different N partitions of the whole set, and the validation results are averaged over the rounds. This process is repeated for N rounds.

3.6 RANDOM FOREST

A Random Forest is a machine learning technique that's used to solve regression and classification problems. It utilizes ensemble learning , which is a technique that combines many classifiers to provide solutions to complex problems. A RF algorithm consists of many decision trees. Random Forest (RF), derived from the decision tree classifier, is a composite method. Grow trees to maximum size and without pruning using the CART method (Classification And Regression Trees). RF is used to implement the SCIM health monitoring system under various conditions of constant load and variable conditions over time.

3.6.1 Fault Diagnosis using Random Forest

RF can improve classification accuracy resulting from growing an ensemble of trees and making them vote for the most promising class. A convenient method to build the ensembles is by random vectors which are generated via random selection procedure from integrated training set. The constituent in this method is that one has to prepare k random vectors, Θk, which are independent of the past random vectors Θ1, Θ2, Θ3,…, Θk-1 but with the same distribution to build the trees among the RF. The corresponding individual classifier is noted by C (X, Θk) [92]. For example, in the bagging processing the random vector Θ as the N observations randomly draws out from entire training data proportionally where N is the number of observations of training data. And then they vote for the most popular class. Breiman names these procedures as RFs. Figure 3.10 depicts the block diagram of RF utilized for identifying the faults in IM. The collected dataset of various operating condition of IM like healthy, rotor bar faults, stator faults, eccentric faults and combined faults are divided into training and testing. Afterwards the training process is performed to train the RF model to detect and classify the faulty condition in the IM autonomously.

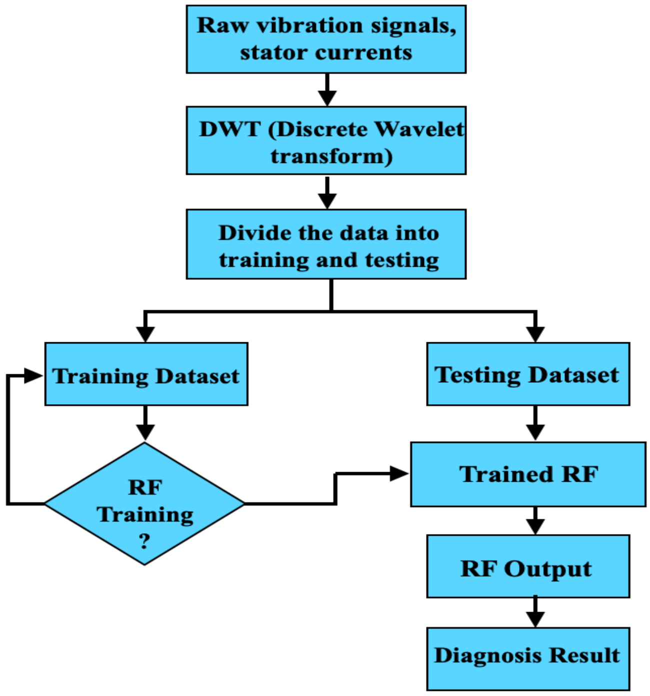

Figure 3.10: Block diagram of RF on fault diagnosis

3.6.2 Two Randomized Procedures in RF Tree Building

As mentioned above, RF significantly improves classification accuracy compared to the decision tree classifier. For this reason, RF uses two random methods when building trees. Each tree is structured in the following way. Assume that the number of cases in the training set is N and the number of variables in the classifier is M. Select the number of input variables that will be used to determine the decision at a node in the tree.

This number, m, should be much less than M (m<< M). Secondly, choose a training set by choosing N samples from the training set with replacement. And then, for each node of the tree randomly select m of the M variables on which to base the decision at that node. Calculate the best split based on these m variables in the training set. Finally, each tree is fully grown and not pruned. There are two different randomized procedures in the next four steps. That is, RF randomly draws a fixed amount from a training set or calls it the bagging process [92]. Each base classifier in the set is trained on a bootstrap of all the available data. However, each of these bootstrap replicates tends to omit about a third of the sample. Therefore, each classifier in the set is trained on approximately two-thirds of the original data. Consequently, each item in the sample of size n trains approximately (2/3) k of all classifiers in the set so that it can be used to validate the remaining k / 3. Figure 3.11 where n is the number of training data, k is the total number of individual tree classifiers. This part of the data is called non-included data to provide an unbiased estimate of the failure of the single tree test set. The rest of the data is used to build the single tree classifier.

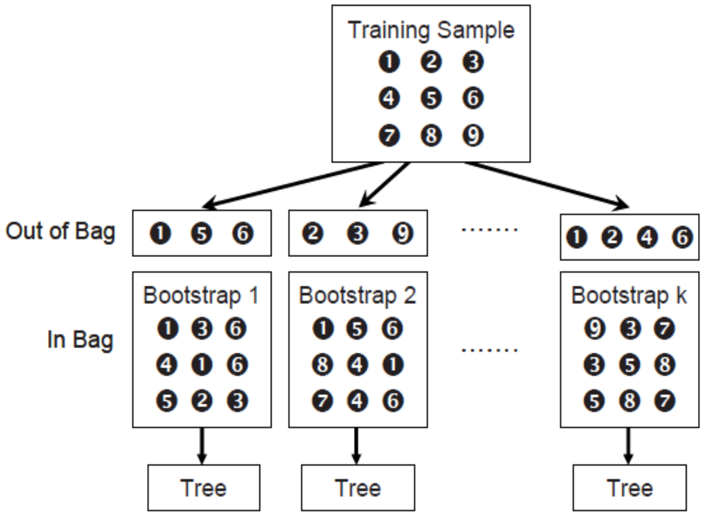

Figure 3.11: Schematic of bagging using the decision tree as the classifier [92]

After bagging processing, the other random procedure is displayed in node splitting during tree classifier creation. Unlike a normal CART-like algorithm for splitting the decision tree, CART only looks at n variables within the RF algorithm, which are a small number and are randomly drawn from all M variables rather than full variables. Breiman's research explains why these two random methods are effective in increasing classification accuracy: Improvements will occur in unstable methods, where a small change in the training set can result in a large change between the component classifiers and the classifiers trained by the entire training set. In RF, regardless of bagging processing or random selection of variables to split the node, it is the difference between individual trees and forests. Therefore, these two sources of randomness are the most important characteristics of RF.

3.6.3 Convergence of RF

RF adopts a set of decision trees and determines the categorical classes using a majority voting algorithm. Therefore, serious over-tuning consideration is required to test RF performance. It may restricted in very specific random features of the training data that are not causally related to the objective function. However, RF can completely prevent overfitting [92]. To confirm this point, a limit function is defined first. Given an ensemble of a series of classifiers C1 (X), C2 (X), …, Ck (X), and with the training set drawn at random from the distribution of the random vector Y X, define the margin function as shown in equation (3.10):

$$mg(X,Y) = av_k I(C_k(X) = Y) - max_{j \neq Y} av_k I(C_k(X) = j) \tag{3.10}$$

where X is input metric, avk is the normal number of votes at X, Y for the comparing class and I (•) is the marker work. The edge estimates the degree to which the normal number of votes at X, Y for the correct class surpasses the normal decision in favor of some other class. The bigger the edge, the more trust in the characterization.

According to this function, the generalization error is given by:

$$PE^* = P_{x,y}(mg(X,Y) < 0) \tag{3.11}$$

Where, $P_{X,Y}$ indicates the probability which is over the X, Y space in equation (3.11).

3.7 SUMMARY

Various types of IM faults like rotor bar faults, stator faults and eccentric faults occurrences and their causes are discussed in brief. Several fault diagnosis techniques like DWT and vibration analysis are also elaborated in terms of its benefits in selecting as features extraction in implementing health monitoring system for SCIM. Furthermore, the classification techniques of soft computing proposed in the research work are discussed in this chapter. Proposed model of SVM and RF for fault detection and diagnosis are elaborated and described in a flow chart. The deep learning method DBNN is explained briefly and its application in FD is described with a block diagram. DBNN analysis is done to achieve more robust accuracy in detecting the fault at the early stage which means detecting the occurrence of fault just in time to avoid any further damage to the industrial machine.

CHAPTER 4

BEHAVIORAL ANALYSIS OF INDUCTION MOTOR UNDER DIFFERENT FAULTS

4.1 INTRODUCTION

This chapter includes the different fault analysis using ANSYS RMxprt & Maxwell 2D and MATLAB in SCIM. The designed model is put under different faulty conditions like broken rotor bar fault , stator fault , eccentricity fault and combined faults and their effects on the motor behavior are analyzed under various load ranges closely on the basis of rotor speed, torque, stator current and power. The performance of motor under constant and time varying load is evaluated. Furthermore, the implementation model of MATLAB is used to apply the machine learning and deep learning algorithm to detect and classify the faults using DWT as a feature extractor.

4.2 INDUCTION MOTOR UNDER BROKEN ROTOR BAR FAULTY CONDITION

Rotor bar fault is an incipient fault and its effects on the system within the starting are nearly unnoticeable. Early identification of a wrecked rotor bar limits machine mischief leads to economical repair. Often, the wrecked bar condition begins with a break at the intersection between the rotor bar and furthermore the complete the process of ring as an aftereffects of warm and mechanical burdens. These anxieties are a great deal of crucial once starting engines with high-idleness hundreds. The bowing of a messed up bar in view of changes in temperature makes the bar intrude. When one bar breaks, the nearby bars convey flows bigger than their style esteems, causing a ton of damage if the messed up bar condition isn't quickly identified. Inter-bar flows that appear to be inferable from the messed up bar affect the development of the shortcoming inside the rotor, exacting mischief inside the covers of the rotor centre. These areas plan to consider totally various models of machine with one, two, and three broken bars to break down the symphonies substance of the stator loop flows for these operational conditions.

4.2.1 One Broken Rotor Bar Fault Analysis

The IM is experimented with one rotor bar fault generated in ANSYS RMxprt model and its various characteristics are observed to analyze the behavior under faulty condition. Designed IM model and its structural information are displayed in Figures 4.1, 4.2 and 4.3. Figure 4.1 displays the designed SCIM model using ANSYS RMxprt with one broken rotor bar marked with circle. The designed model is then fed to Maxwell 2D for FEM analysis. Figures 4.2 and 4.3 show the flux density and current density distribution of the designed motor under one broken fault condition respectively. From the graphs, it can be clearly seen that the distribution of the flux and current is not uniform as it was in healthy motor condition.

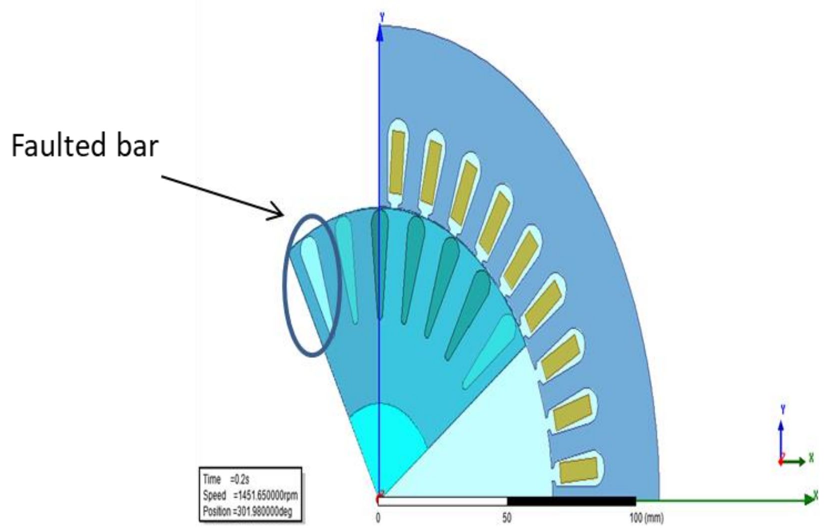

Figure 4.1: Model with one broken rotor bar

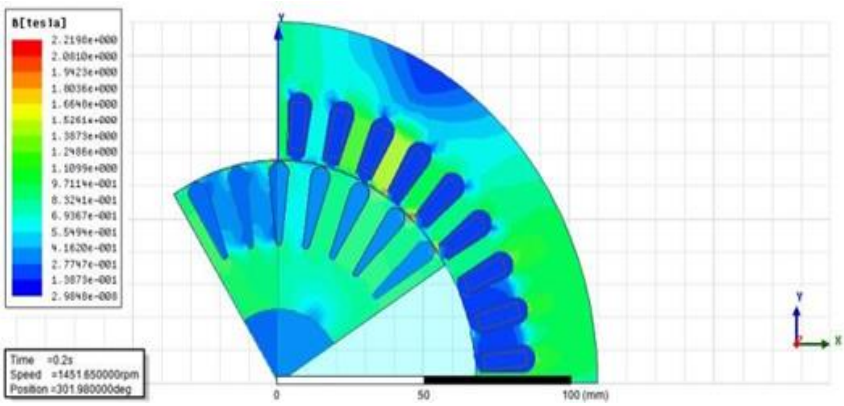

Figure 4.2: Induction Motor flux density distributions during fault condition with one broken rotor bar

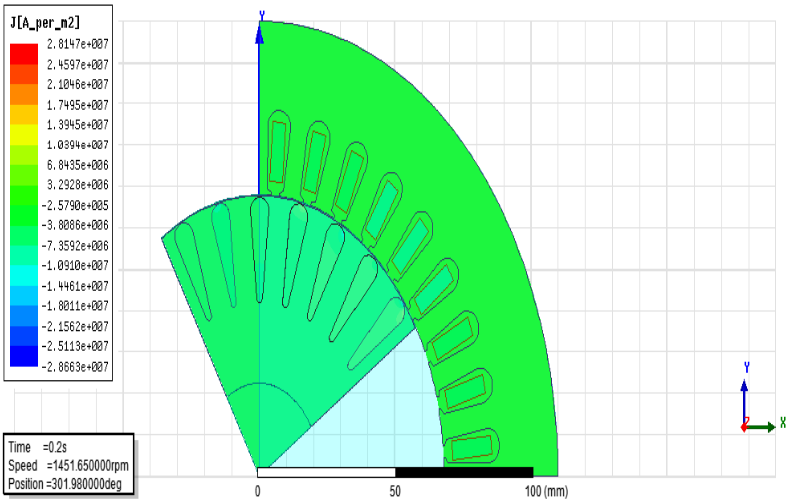

Figure 4.3: Current density plot of IM during fault condition with one broken rotor bar

From the distribution of magnetic flux density and current density in Figures 4.2 and 4.3, it is seen that because of the absence of prompted flows in the one broken bar, the attractive field becomes asymmetrical prompting immersion in the rotor and stator teeth close to the flawed bar. Accordingly the wrecked bar deficiencies affect the machine parameters, for example, torque and speed motions because of the impact of reverse attractive field part.

The IM machine with one broken rotor bar fault design operating characteristics are illustrated in Figures 4.4, 4.5, 4.6 and 4.7 in terms of torque, flux linkage, current and power respectively. Figures 4.4 and 4.5 display the torque and the flux linkage graphs obtained during the analysis respectively. The torque obtained is around 28.68 Nm and the flux is stable after 70 seconds of operating time.

Figure 4.6 illustrates the FEM IM model stator current response under one broken rotor bar faulty condition the three-phase current showing quite high oscillations and distortion due to the presence of one rotor bar fault. Figure 4.7 illustrates the average power in watts under one rotor bar faulty condition. The average power obtained is 4361.33 watt which is lower as compared to the normal operating condition. The motor performance under faulty condition deteriorates results in lower torque and power along with increase in the transients which results in vibration and wired sound in the motor while operation.

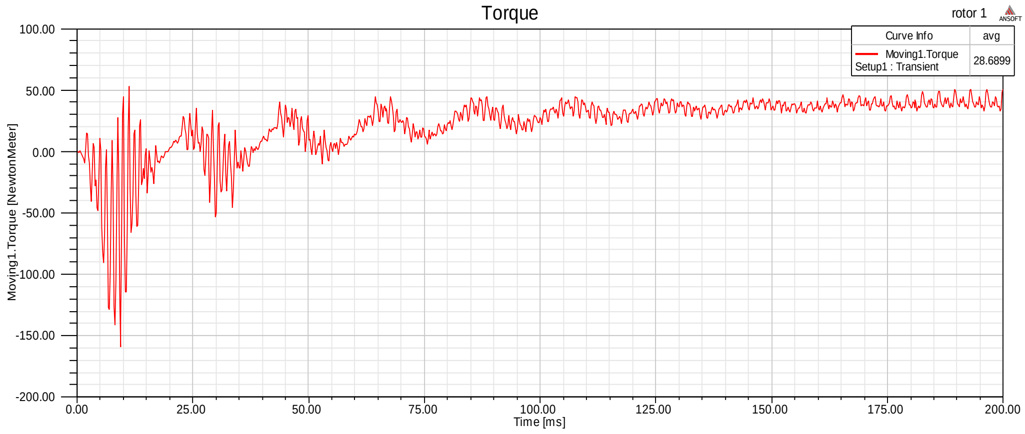

Figure 4.4: IM torque response over period of time during fault condition with one broken rotor bar

Figure 4.5: Flux linkage response of Induction motor during fault condition with 1 broken rotor bar

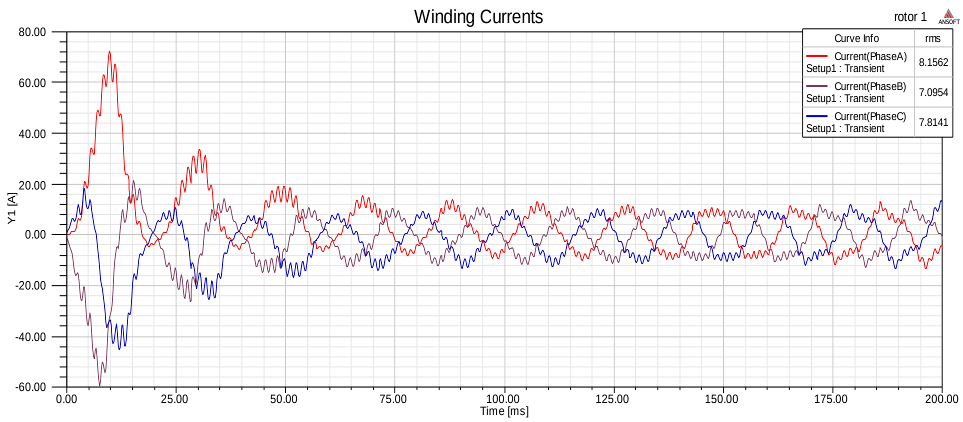

Figure 4.6: Induction Motor current response during fault condition with one broken rotor bar

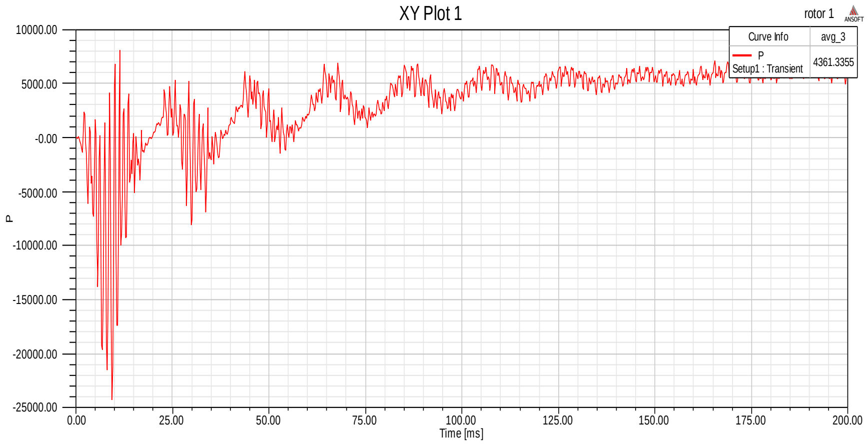

Figure 4.7: Induction Motor output power response during fault condition with one broken rotor bar

4.2.2 Two Broken Rotor Bars Fault

The FEM model is designed under rotor bar fault at two different locations and then its flux distribution and current, torque and powers are observed. IM designed model and its flux distribution are displayed in Figures 4.8, 4.9 and 4.10. Figure 4.8 displays the RMxprt designed SCIM model with two broken rotor bar marked with the circle. Figure 4.9 & 4.10 displays the SCIM flux density and current distribution of the two broken rotor bars model of SCIM. The uniformity of the flux and current distribution is disturbed and the distribution is no longer even.

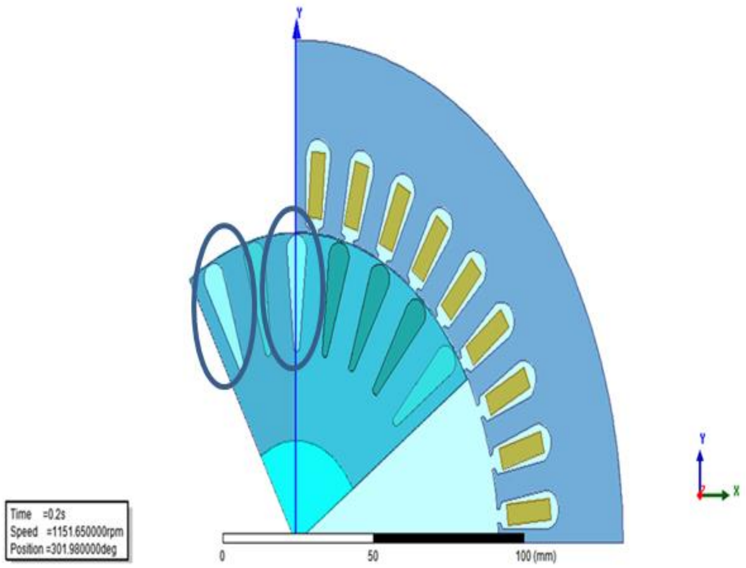

Figure 4.8: Model with two broken rotor bar

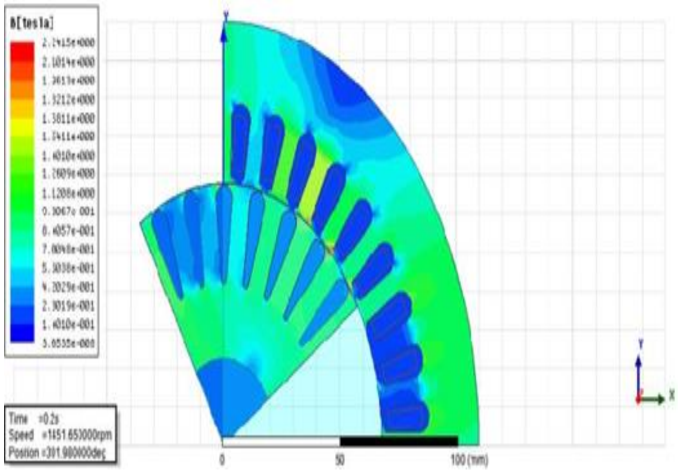

Figure 4.9: Induction Motor flux density distributions during fault condition with two broken rotor bars

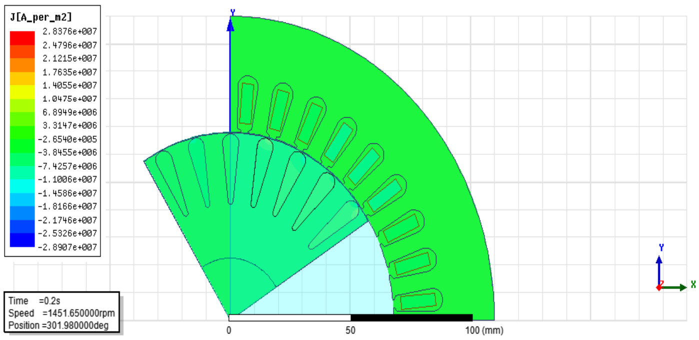

Figure 4.10: Current density plot of Induction Motor during fault condition with two broken rotor bars

The two broken rotor bar faulty IM motor characteristics are presented in Figures 4.11, 4.12, 4.13 and 4.14. Figures 4.11 and 4.12 displays the torque and flux produced in motor at two broken rotor bars fault, the transient in torque are higher as compared to motor with one or no faulty rotor bar. Figure 4.13 illustrates the FEM IM model stator current response under healthy operating condition the three-phase current displaying high oscillations and distortion due to the presence of two broken rotor bar faults. The starting current peaks are very high and gets stable at around 75 sec of time. The severity of the oscillation increases as the number of broken rotor bar increases. Figure 4.14 illustrates the average power in watts under two broken rotor bar faulty condition. The average power obtained is 3981.21watt which is quite lower as compared to the normal operating condition. The power is reduced as the faulty broken bar numbers increases to two.

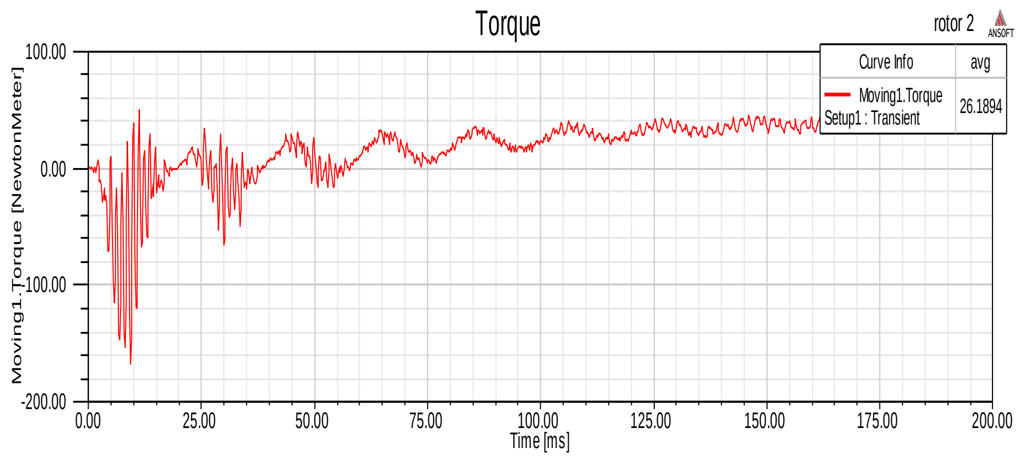

Figure 4.11: Induction Motor torque response over period of time during fault condition with two broken rotor bars

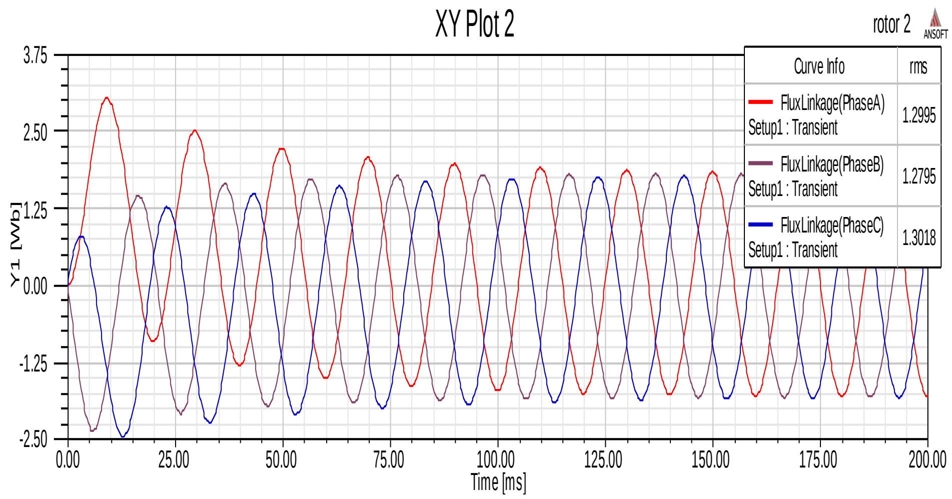

Figure 4.12: Flux linkage response of Induction Motor during fault condition with 2 broken rotor bars

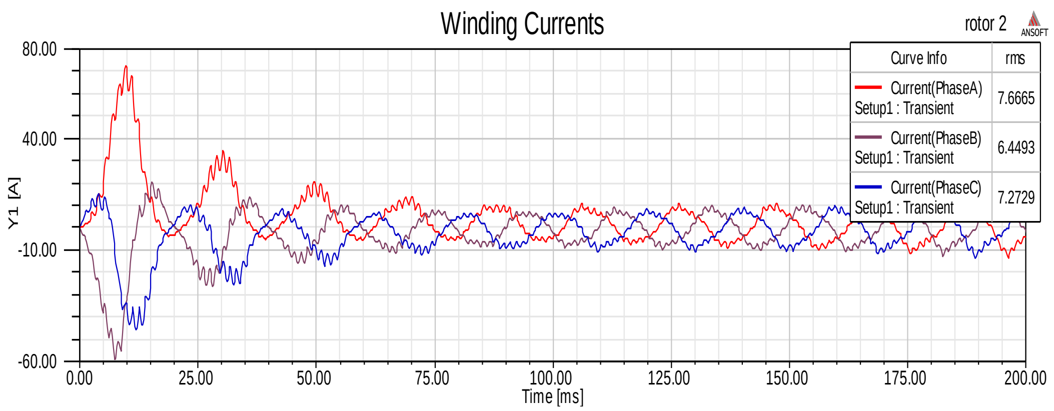

Figure 4.13: Induction Motor current response during fault condition with two broken rotor bars

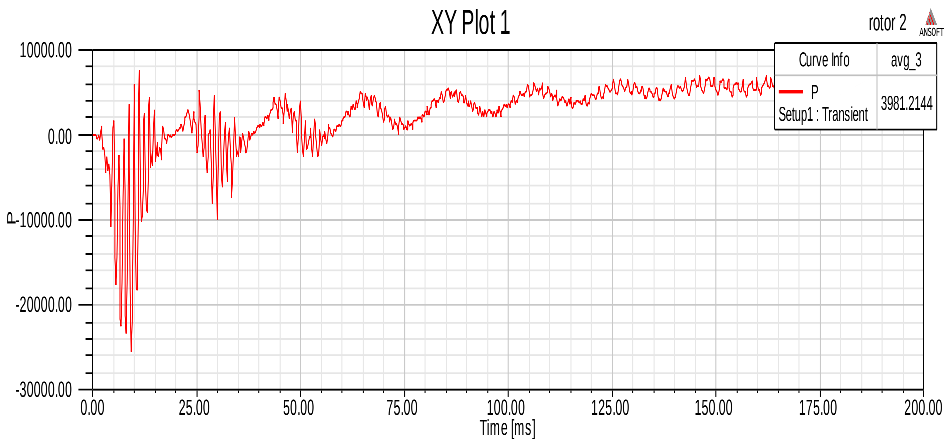

Figure 4.14: Induction Motor output power response during fault condition with two broken rotor bars

4.2.3 Three Broken Rotor Bars Fault

The FEM model is put under rotor bar fault at three different locations and then its flux distribution, current, torque and powers are analyzed. Figure 4.15 shows the motor model with three broken rotor bar encircled. From the distribution of magnetic flux density and current density plot as shown in Figures 4.16 and 4.17, it is seen that due to the lack of induced currents in the three broken bar, the magnetic field becomes more asymmetrical leading to saturation in the rotor and stator teeth near the faulty bars resulting in broken bar faults have an impact on the machine parameters such as torque and speed oscillations due to the influence of inverse magnetic field component.

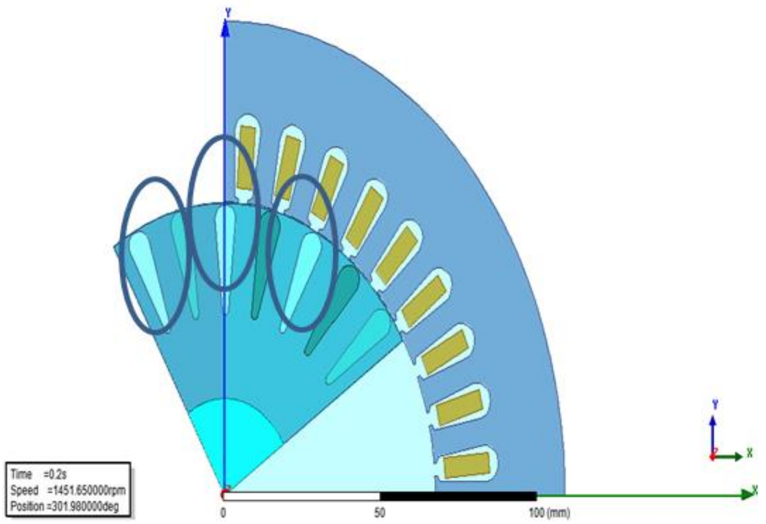

Figure 4.15: Model with three broken rotor bar

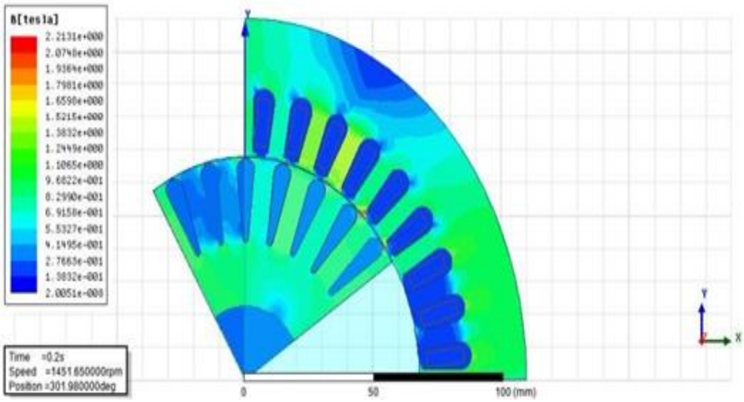

Figure 4.16: Induction Motor flux density distributions during fault condition with three broken rotor bars

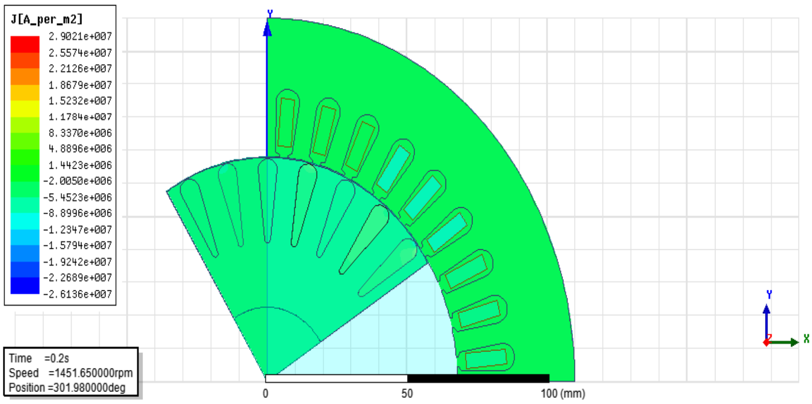

Figure 4.17: Current density plot of Induction Motor during fault condition with three broken rotor bars

The motor performance characteristics under three broken rotor bar faults are analyzed and depicted in Figures 4.18, 4.19, 4.20 and 4.21. Figures 4.18 and 4.19 displays the torque and flux linkage response of the motor during three broken rotor bars. The torque produced is 24.67 Nm and the flux oscillations stabilize at around 78 seconds. Figure 4.20 illustrates the FEM SCIM model stator current response under three broken rotor bar faulty condition. Due to the faulty condition the current showing high oscillations and higher distortion levels. The initial current overshoots are high and it gets stabilizes at around 78 sec simulation time. Figure 4.21 illustrates the average power in watts under three rotor bar faulty conditions. The average power obtained is 3750.34watt which is lower as compared to the healthy operating condition of the SCIM. The motor faulty condition deteriorates the performance of the motor.

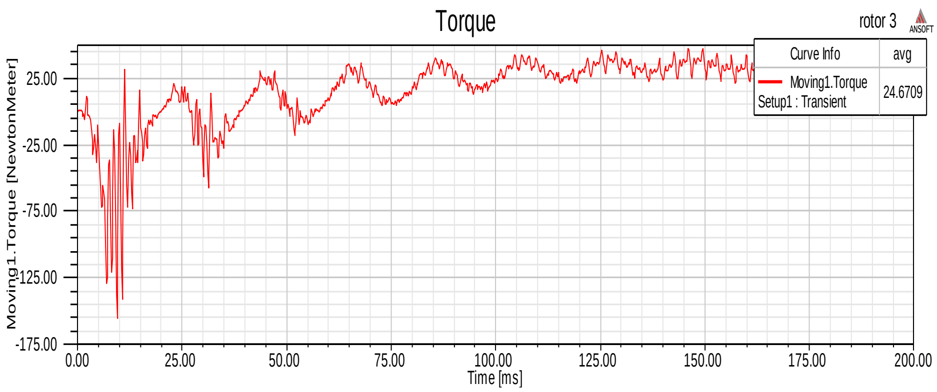

Figure 4.18: Induction Motor torque response over period of time during fault condition with three broken rotor bars

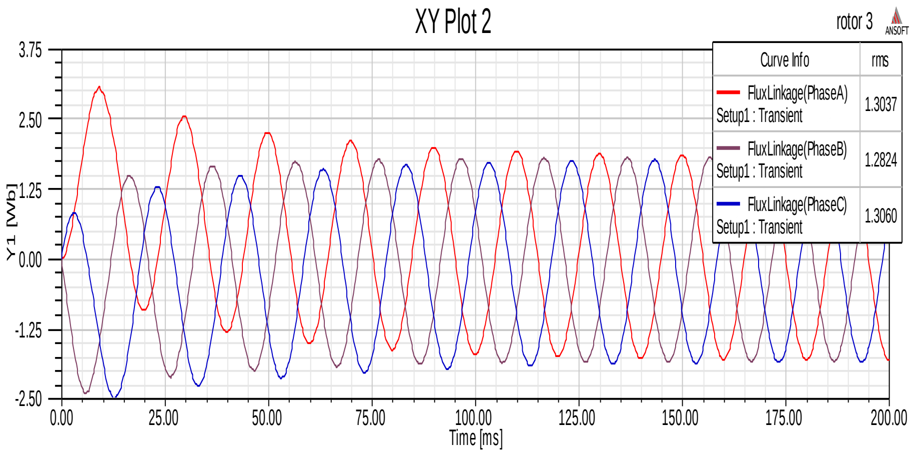

Figure 4.19: Flux linkage response of Induction Motor during fault condition with three broken rotor bars

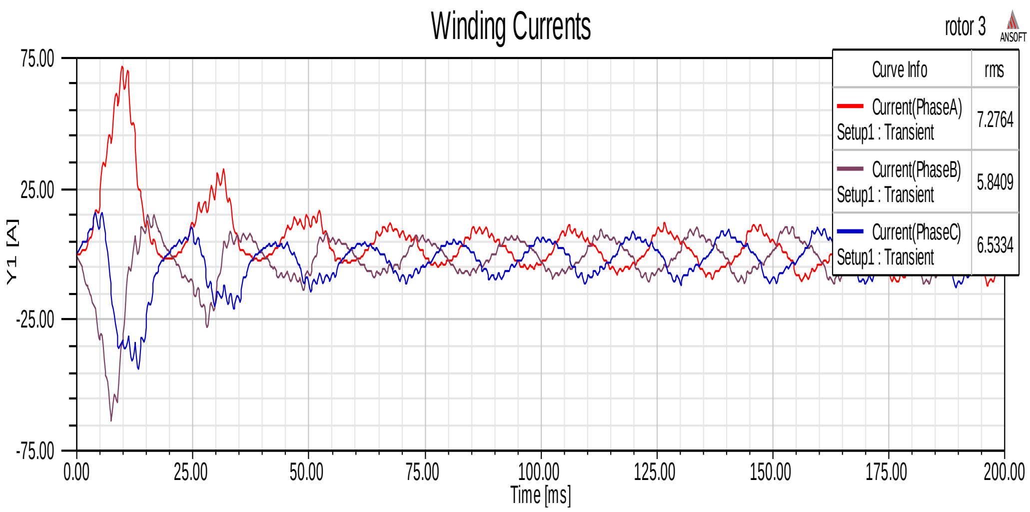

Figure 4.20: Induction Motor current response during fault condition with three broken rotor bars

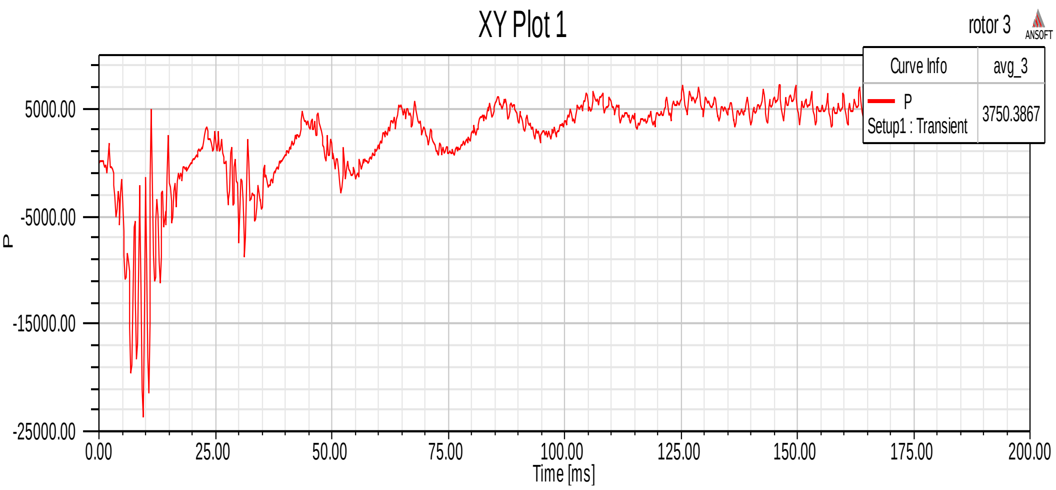

Figure 4.21: Induction Motor output power response during fault condition with three broken rotor bars

4.3 RESULTS AND DISCUSSION OF FEM ANALYSIS

The outcome of induction machine under different faulty conditions are determined and analysed in the table underneath where Table 4.1 looks at average magnetic torque at 1451.65rpm speed. The torque reduces as the fault level increases in the rotor bars of the SCIM. The torque value from 33.4175Nm in case of healthy operating condition reduced down to 24.6709Nm in case of three broken rotor bars.

Table 4.1: Average magnetic torque during three different broken bar faulty conditions

S. No.	Conditions	Average magnetic torque (Nm)
1	Healthy motor	33.4175
2	one broken rotor bar	28.6899
3	two broken rotor bar	26.1894
4	three broken rotor bar	24.6709

Here below in Table 4.2, it compares stator current at 1451.65rpm speed. The current reduction experiences from 8.9257A to 7.27A moving from healthy condition to three broken bar faulty condition respectively.

Table 4.2: Stator current with three broken rotor bar faulty conditions

S. No.	Conditions	Stator current A (rms)
1	Healthy motor	8.9257
2	one broken rotor bar	8.1562
3	two broken rotor bar	7.66651
4	three broken rotor bar	7.2764

Here below in Table 4.3, it compares average mechanical power at 1451.65rpm rated speed. The average power obtained also experienced the reduction as moving from healthy to severe faulty condition. The experimentation of running IM at different broken rotor bars faults have been conducted and from Tables 4.1, 4.2 and 4.3 it has been concluded that the motor performance deteriorated when subjected to broken rotor bar faults.

Table 4.3: Average mechanical power during fault condition with three broken rotor bar

S. No.	Conditions	Average output power (W)
1	Healthy motor	5080.01
2	one broken rotor bar	4361.33
3	two broken rotor bar	3981.21
4	three broken rotor bar	3750.38

4.4 MATLAB IMPLEMENTATION MODEL

The MATLAB model of SCIM is designed to investigate the motor performance under various loading operating conditions and under various fault condition specially broken rotor bar. The designed MATLAB model with broken rotor bar is displayed in

Figure 4.22 which is modeled in free body diagram programming environment of MATLAB.

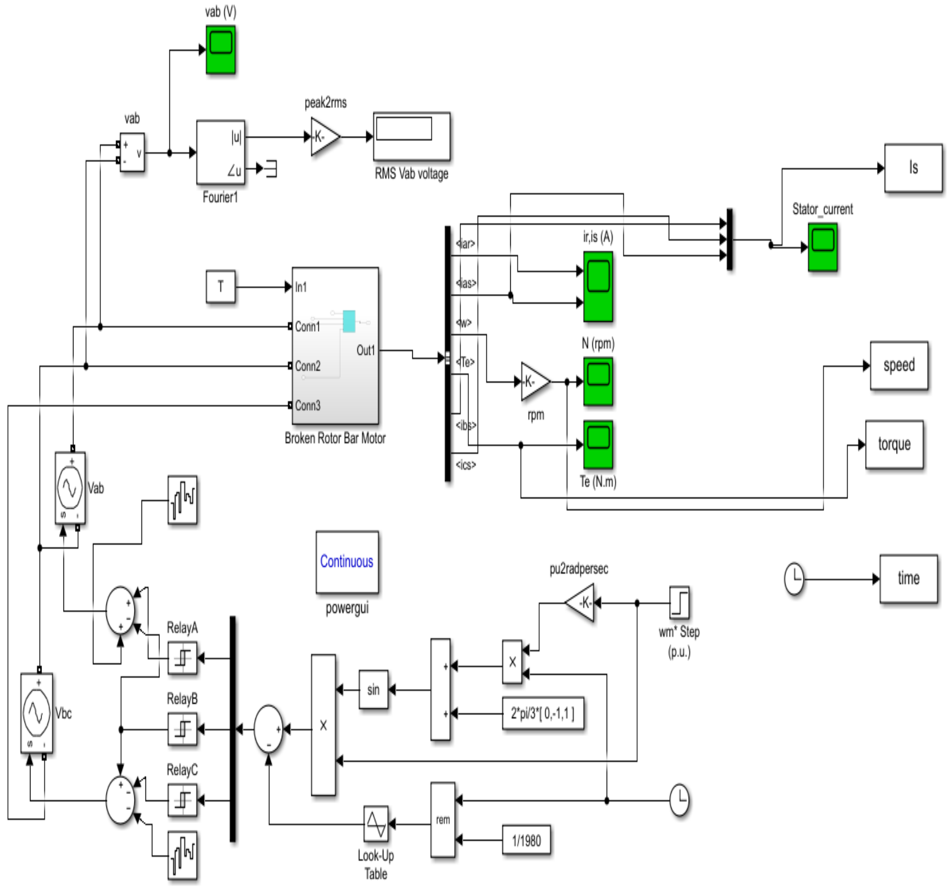

Figure 4.22: MATLAB implementation model for broken rotor bar

4.4.1 Motor Implementation with One Broken Rotor Bar Faulty Condition

For the implementation and experimentation SCIM (5Hp, 400Volts and 50Hz) is considered. Motor is subjected to one broken rotor bar fault and the performance is analyzed on the basis of speed, torque, stator & rotor current and power. Figure 4.23 (a, b, c and d) displays the speed (rpm) at different constant loads here it can be concluded that the speed obtained is around 1250 (rpm) and there are bit of prominent oscillations in synchronous region also as compared with the healthy motor speed. Oscillation results in vibration and disturbing sound generation in motor which increases as the severity of the fault increases. Figure 4.23 (a, b, c and d) displays the torque obtained during one broken rotor bar fault at different constant loads. The oscillations are quite high and deviation of the torque from stable condition is on the higher side suppressing the motor performance. The magnitude of the torque is around 23.59Nm with high ripples indicating the lag and vibration on the movement of the motor. Figure 4.24 (a, b, c and d) displays the stator and rotor current during one broken rotor fault. The initial oscillations are higher as normal but the oscillations are experienced at stable state also i.e. after achieving the synchronous speed the motor experiencing the oscillations due to the broken bar presence.

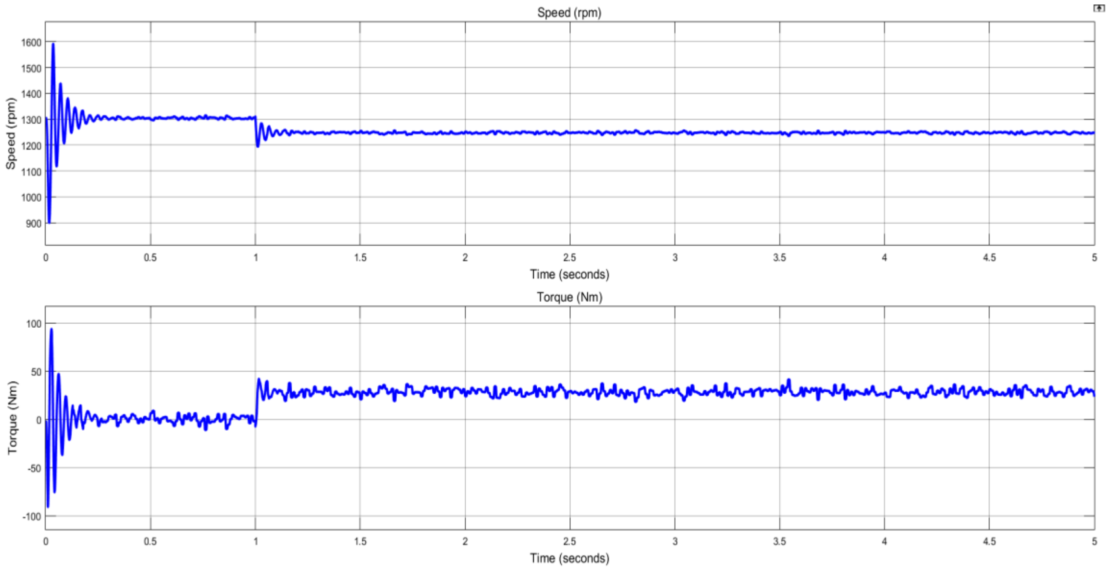

(a) One broken bar torque and speed at full load condition

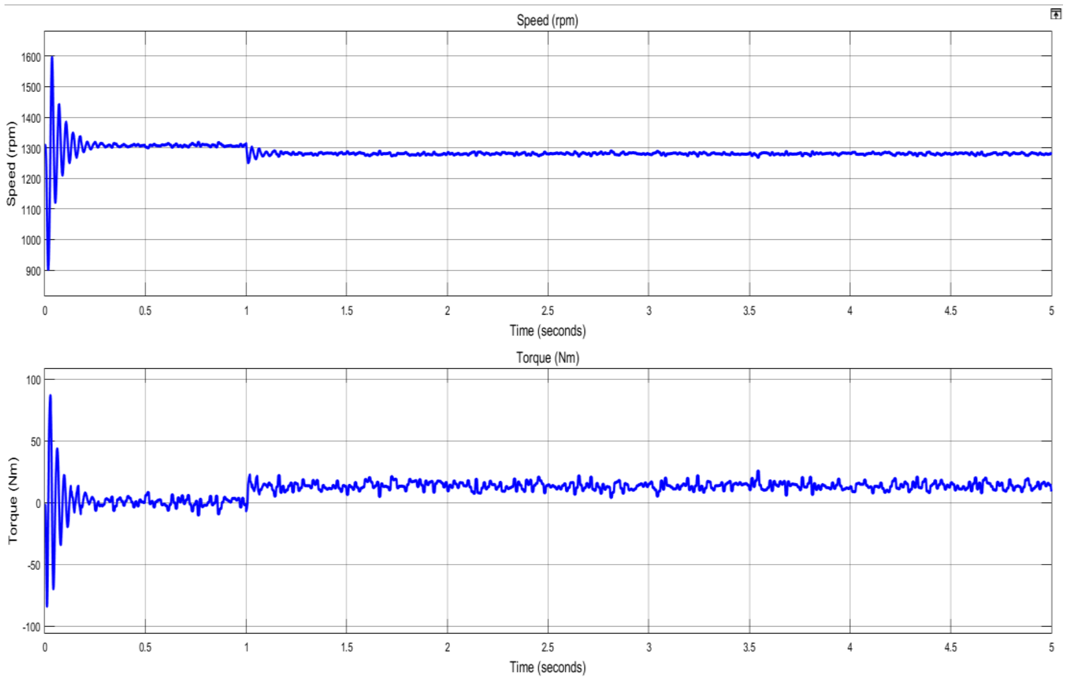

(b) One broken bar torque and speed at half load condition

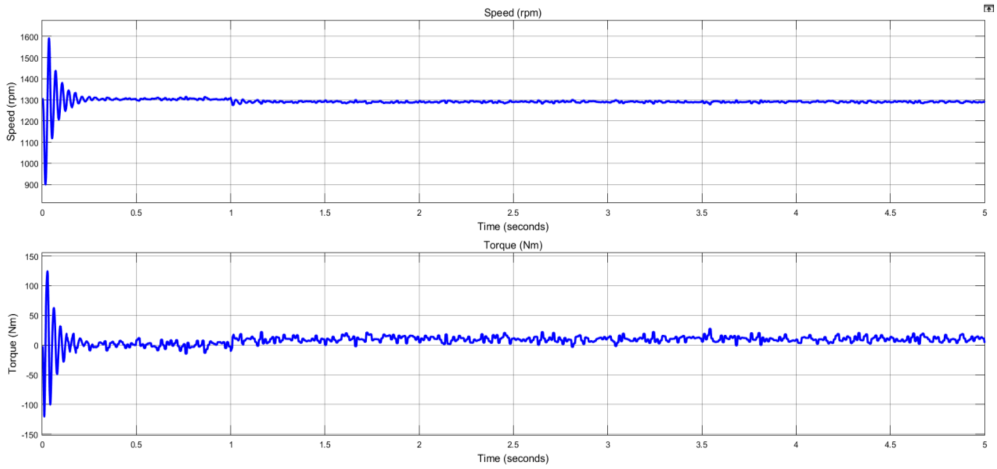

(c) One broken bar torque and speed at quarter load condition

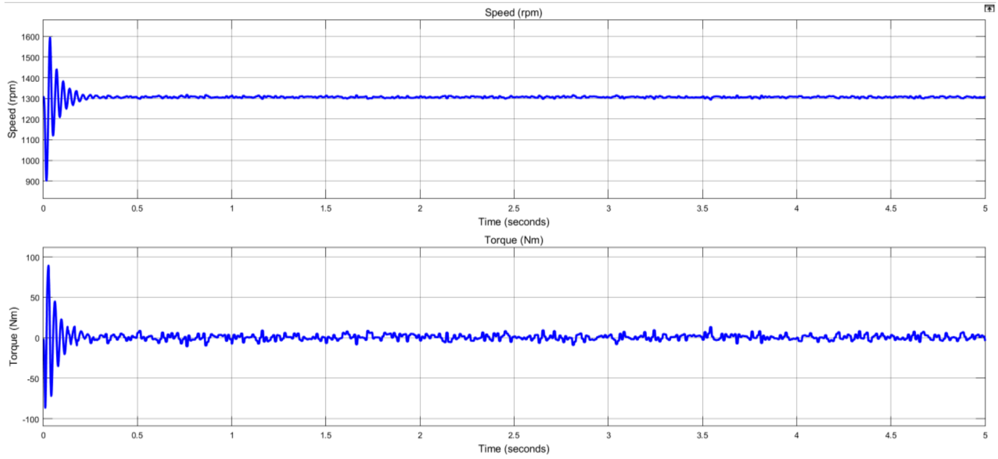

(d) One broken bar torque and speed at no load condition

Figure 4.23: (a, b, c & d) IM speed (rpm) and torque (Nm) response during fault at 100%, 50%, 25% and no loading conditions with one broken rotor bar

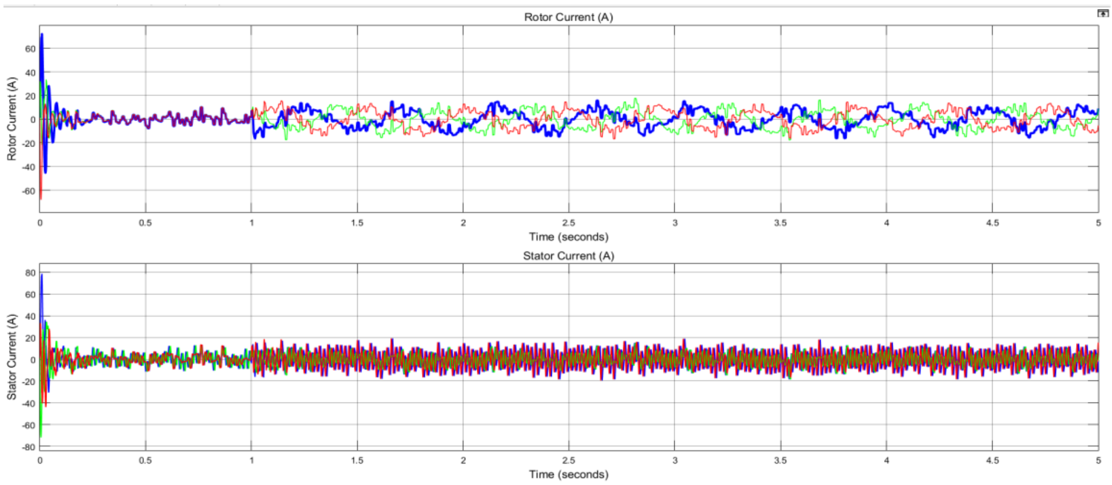

(a) One broken bar rotor and stator at full load condition

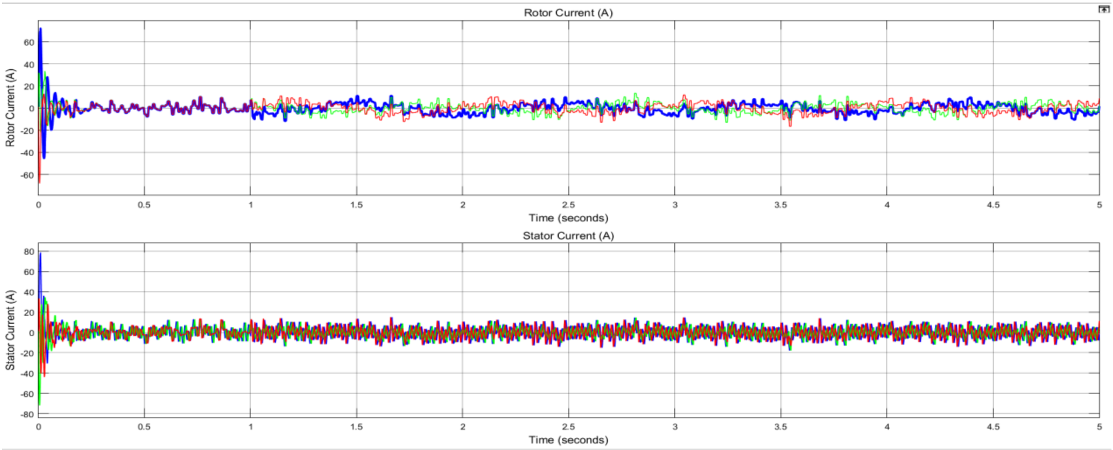

(b) One broken bar rotor and stator at half load condition

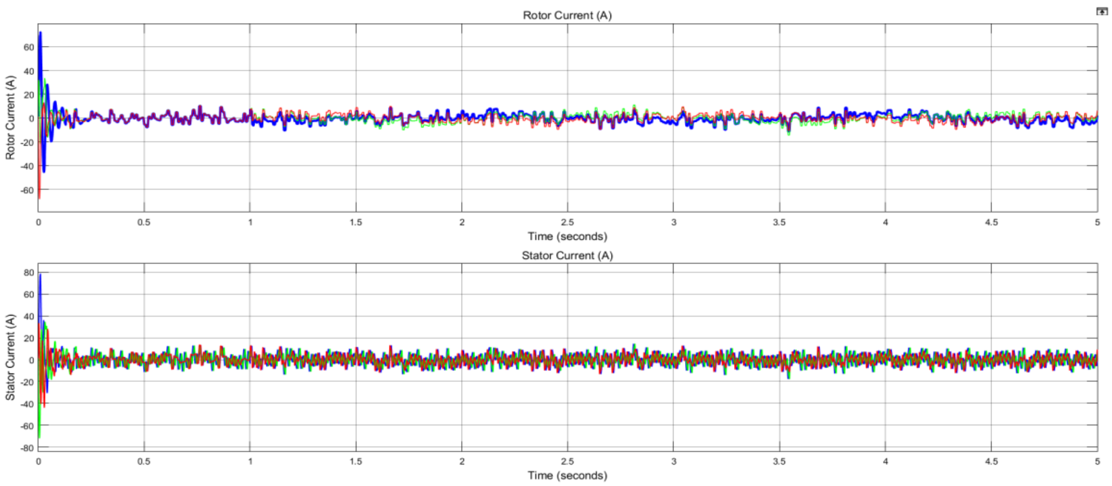

(c) One broken bar rotor and stator at quarter load condition

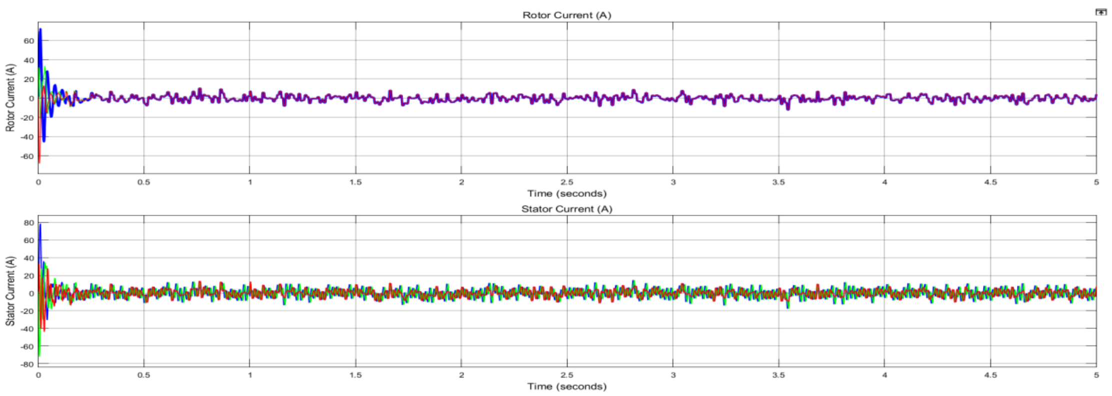

(d) One broken bar rotor and stator at no load condition

Figure 4.24: (a, b, c, and d) IM rotor and stator current (A) response during fault at 100%, 50%, 25% and no loading conditions with one broken rotor bar

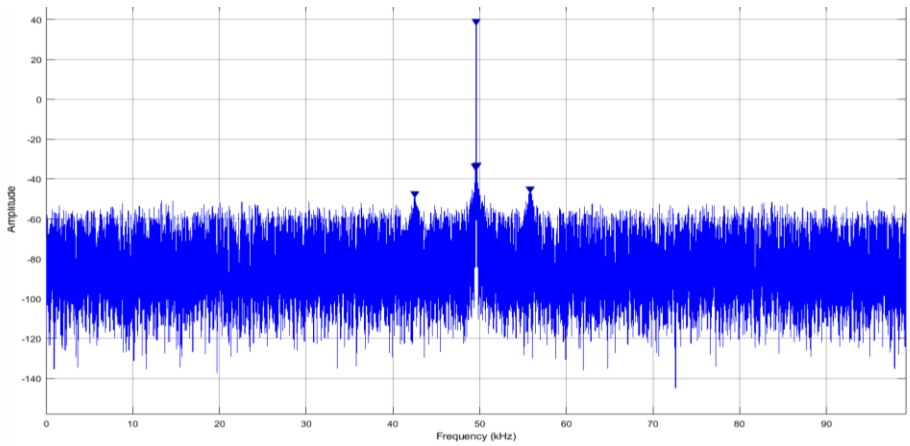

Figure 4.25: Power spectrum of motor stator current with one broken rotor bar faulty condition

Power spectrum signature of the motor under one broken bar is observed in Figure 4.25 which depicts the motor current power spectrum signature with the sidebands peaks of faulty frequencies which shows the presence of the faulty condition in motor while operation. The side band on the left side is at 44Hz $f_{br} = (1 - 2s)f_s$ and on the right side is at 56Hz $f_{br} = (1 + 2s)f_s$. The frequency spectrum is obtained after spectral analysis of the stator current of the IM.

4.4.2 Motor Implementation with Two Broken Rotor Bars Faulty Condition

In second scenario, the motor is subjected to two broken rotor bars fault and the performance is analyzed on the basis of speed, torque, stator and rotor current displayed in Figures 4.26 and 4.27 in comparison with the motor characteristics obtained during healthy operating condition. Figure 4.26 (a, b, c and d) displays the speed (rpm) at different constant loads here it can be clearly seen that the speed obtained is around 1231 rpm which is lower as compared to speed 1435 rpm obtained at healthy operating condition and highly prominent oscillations at stable state are also experienced. Figure 4.26 (a, b, c and d) other part displays the torque of IM under two broken rotor bar faulty condition at different constant loads. On encounter with faulty condition the motor providing the oscillatory torque. The torque is not stable and average torque experienced is about 22.24 Nm which is lesser as compared with 27.17 Nm torque at healthy operating condition.

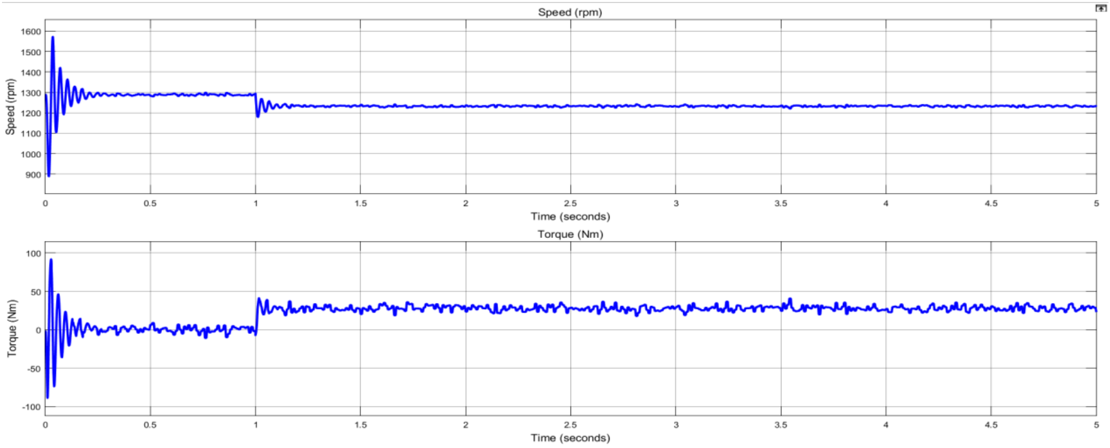

(a) Two broken bar torque and speed at full load condition

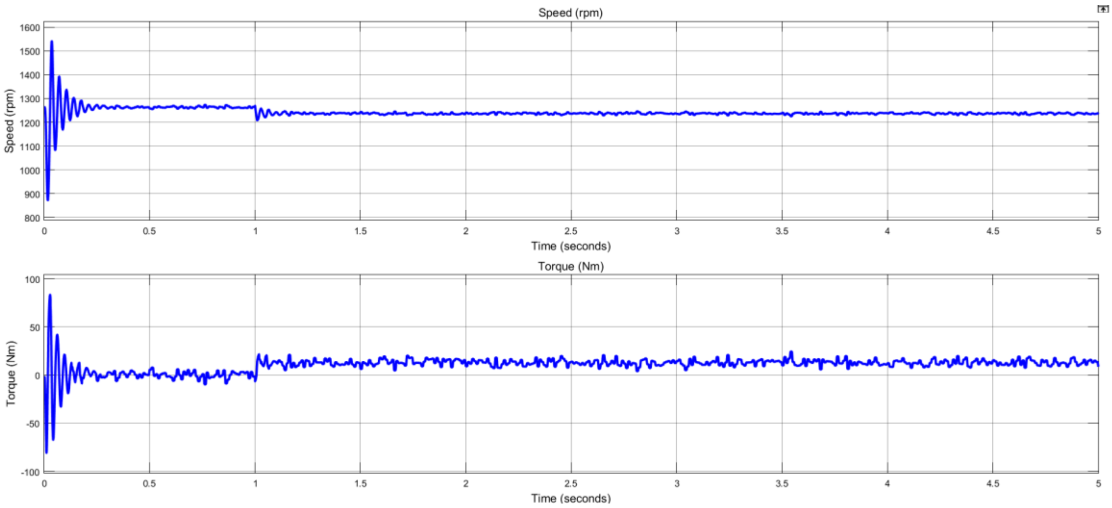

(b) Two broken bar torque and speed at half load condition

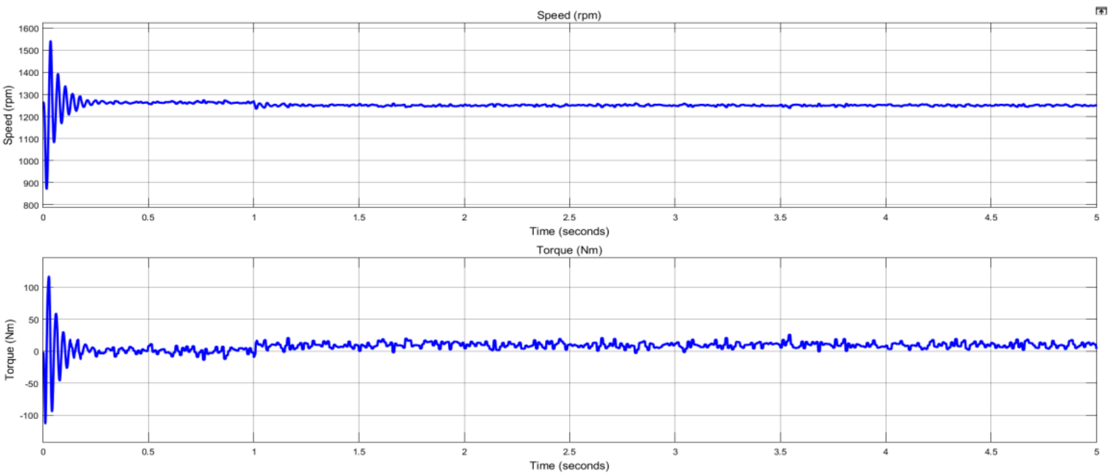

(c) Two broken bar torque and speed at quarter load condition

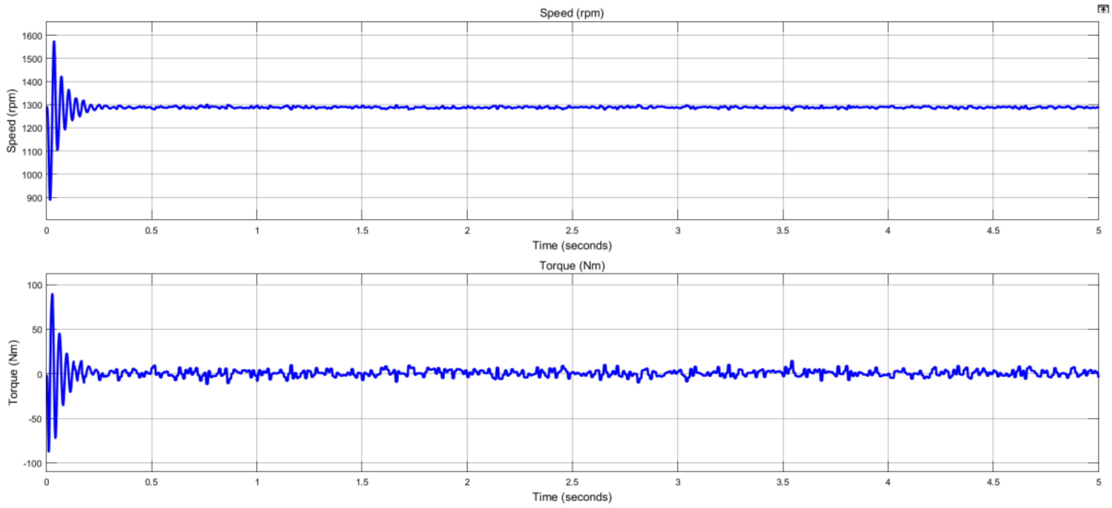

(d) Two broken bar torque and speed at no load condition

Figure 4.26: (a, b, c, and d) IM speed (rpm) and torque (Nm) response during fault at 100%, 50%, 25% and no load conditions with one broken rotor bars

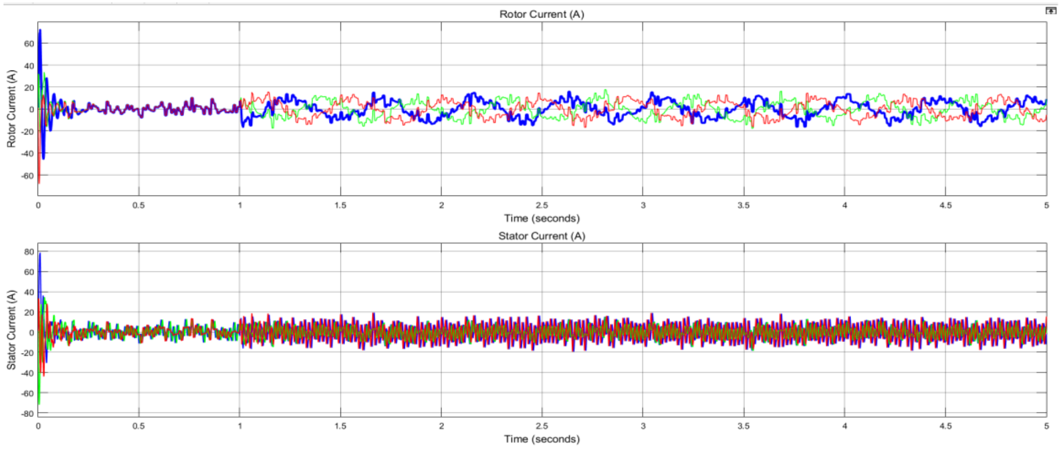

(a) Two broken bar rotor and stator at full load condition

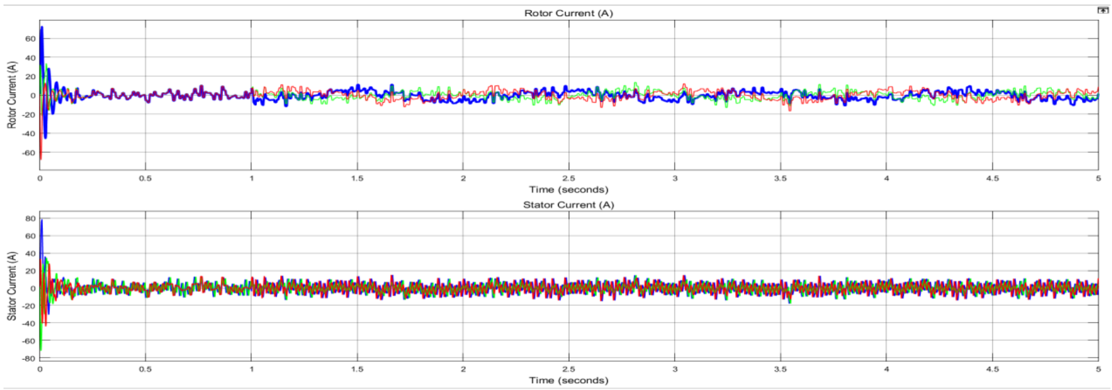

(b) Two broken bar rotor and stator at half load condition

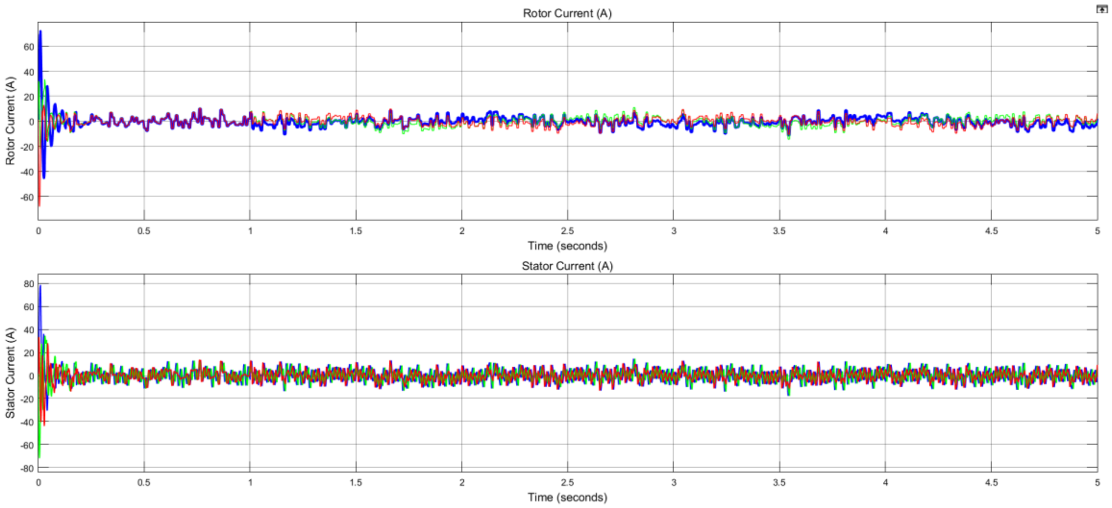

(c) Two broken bar rotor and stator at quarter load condition

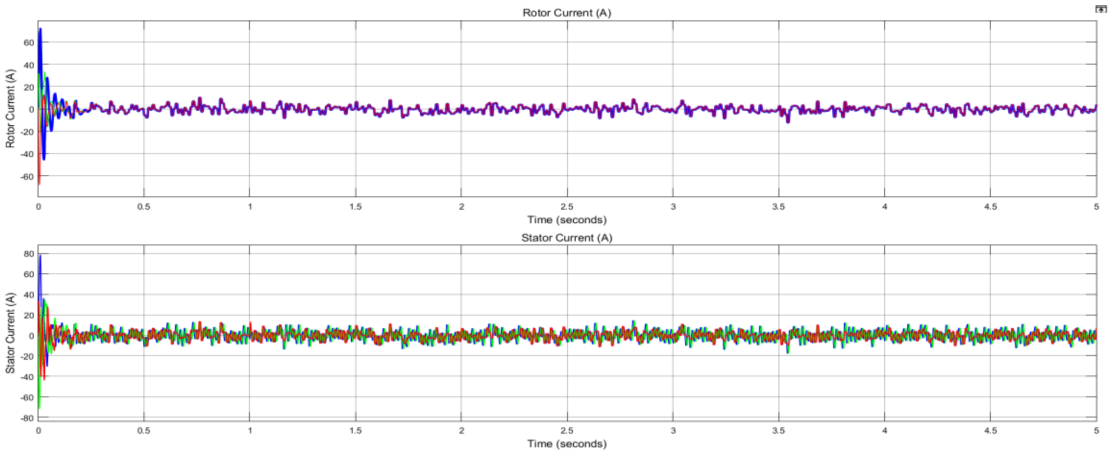

(d) Two broken bar rotor and stator at no load condition

Figure 4.27: (a, b, c, and d) IM rotor and stator current (A) response during fault at 100%, 50%, 25% and no load conditions with two broken rotor bars

The rotor current experiences high distortion and unstable phase magnitudes of currents shown in Figure 4.27. The oscillations are higher at the stable state and suppressing the motor performance by making the current synchronization unstable. Rotor current vibrations are prominent and peaks are continuous indicating the stress on the motor which is degrading the performance of the motor. Figure 4.28 illustrates the motor current power spectrum signature with the sidebands peaks. Here the sidebands are quite prominent and are there in various frequency range. The presence of severe faulty condition is felt in motor while operation. The side band on the left side is at 44Hz and on the right side is at 56Hz and some others also experienced at 30Hz and 60Hz.

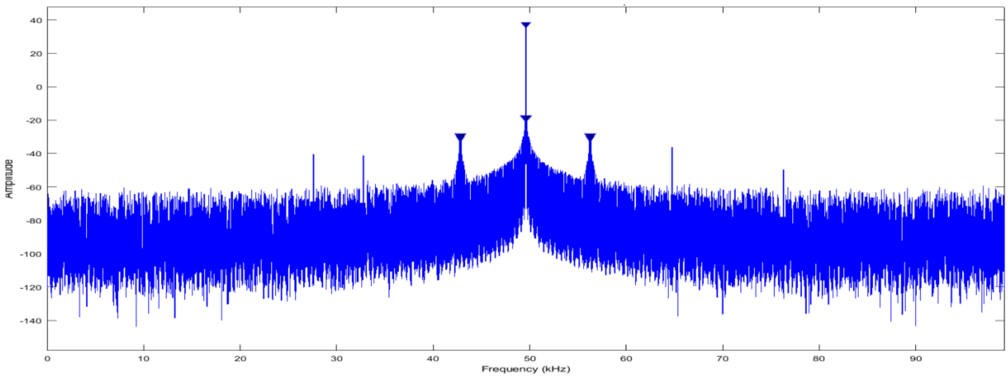

Figure 4.28: Power spectrum of motor stator current with two broken rotor bars faulty condition

4.4.3 Motor Simulation with Three Broken Rotor Bars Faulty Condition

In third scenario, the motor is subjected to three broken rotor bars fault and the performance is observed on the basis of speed, torque, stator and rotor current depicted in Figures 4.29, 4.30. Figure 4.29 (a, b, c and d) displays the speed (rpm) under three broken rotor bar modelling in MATLAB at different constant load conditions. From the figure, it is clear that the speed reduces with a high rate as the degradation in the motor increases with three broken bar faults in the IM. Figure 4.29 other part displays the torque of IM under three broken rotor bar faulty condition. The motor torque magnitude reduces with high oscillation due to the presences of the high faults in bars of the rotor. Figure 4.30 (a, b, c, and d) two parts illustrates the rotor current and stator current respectively under three broken rotor bar condition at different constant load conditions. The stator and rotor current become highly unstable under the three broken bar condition. The distortion in the stator and rotor current are very high quite visible in both the parts of the Figure 4.30. Figure 4.31 illustrates the motor current power spectrum signature with the sidebands peaks. Here the sidebands are quite prominent and are there in various frequency ranges. The side band on the left side is at 44Hz and on the right side is at 56Hz, the magnitude of the side bands have increased as compared to the magnitude in healthy, one and two broken rotor bar.

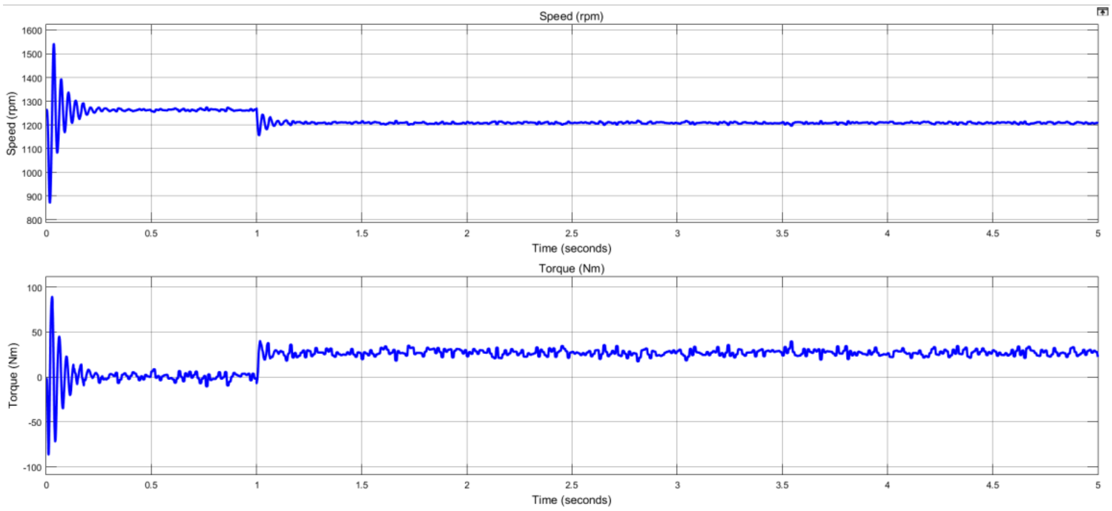

(a) Three broken bar speed and torque at full load condition

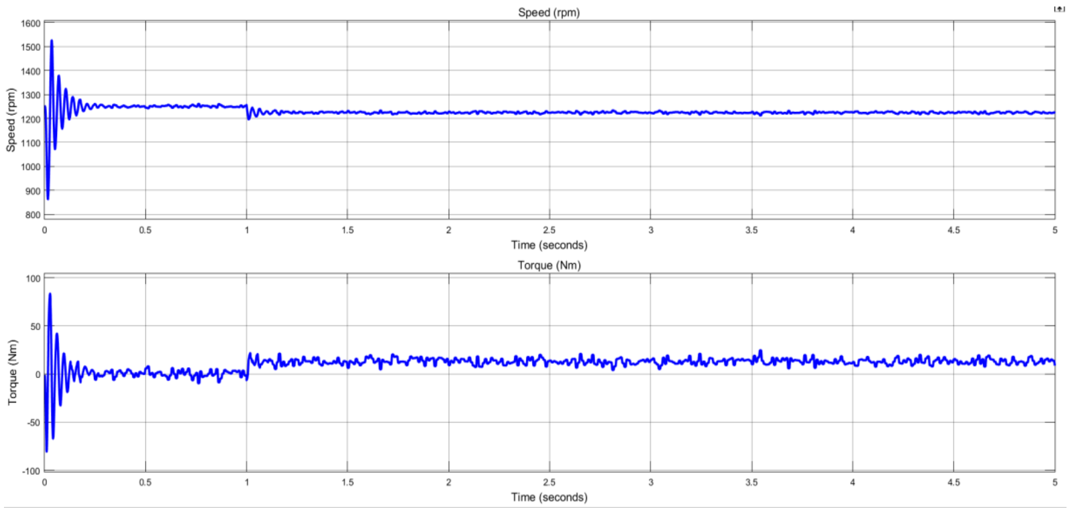

(b) Three broken bar speed and torque at half load condition

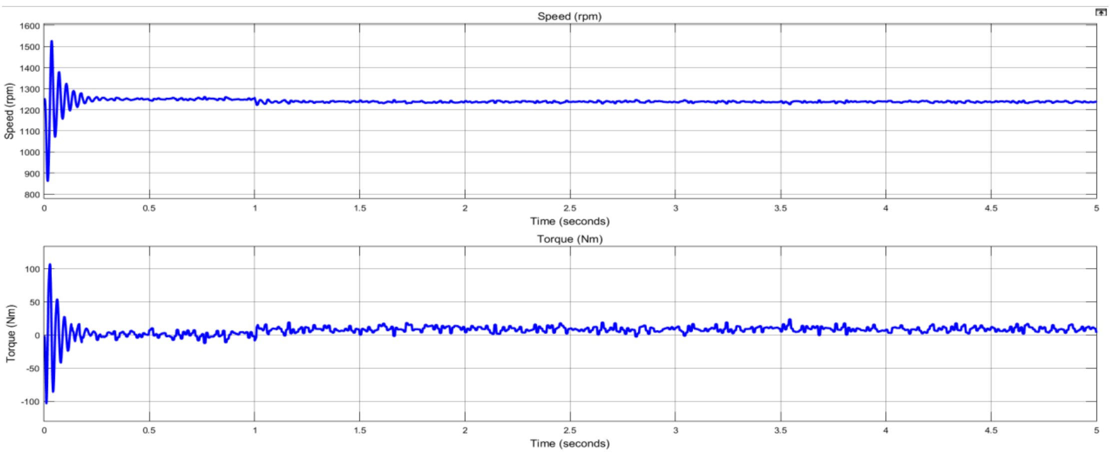

(c) Three broken bar speed and torque at quarter load condition

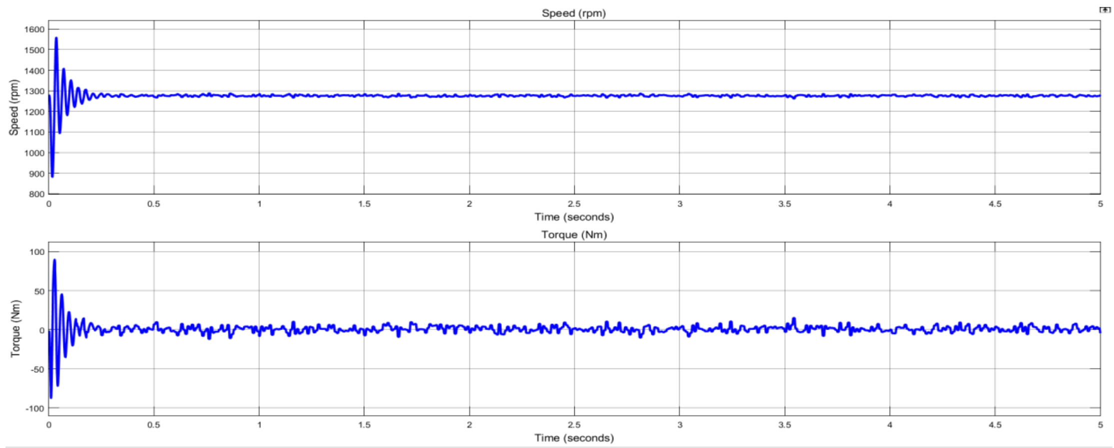

(d) Three broken bar speed and torque at no load condition

Figure 4.29: (a, b, c and d) IM speed (rpm) an torque (Nm) response during fault at 100%, 50%, 25% and no load conditions with three broken rotor bars

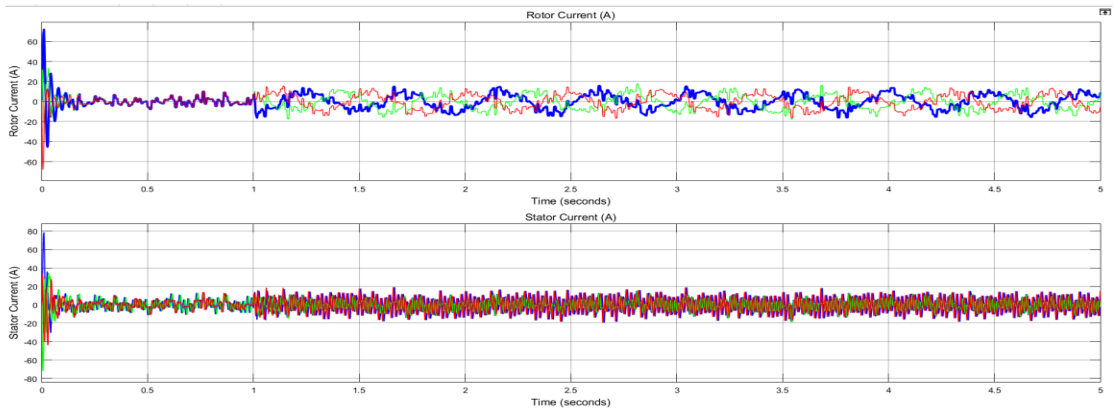

(a) Three broken bar rotor and stator at full load condition

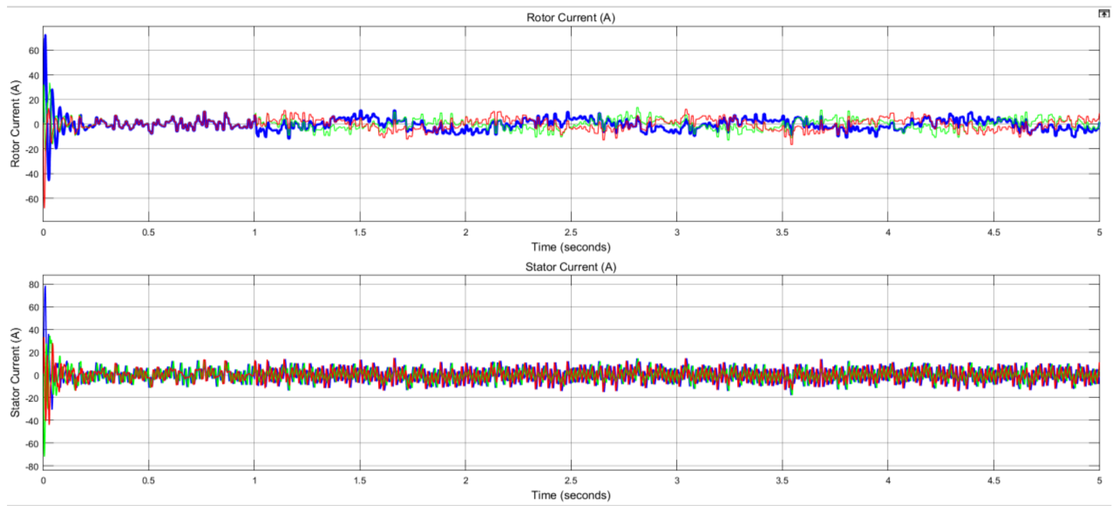

(b) Three broken bar rotor and stator at half load condition

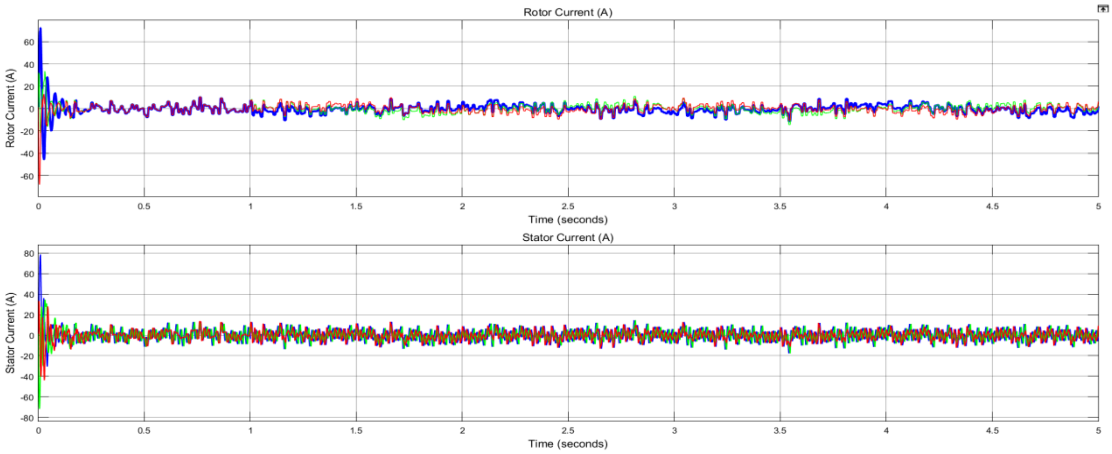

(c) Three broken bar rotor and stator at quarter load condition

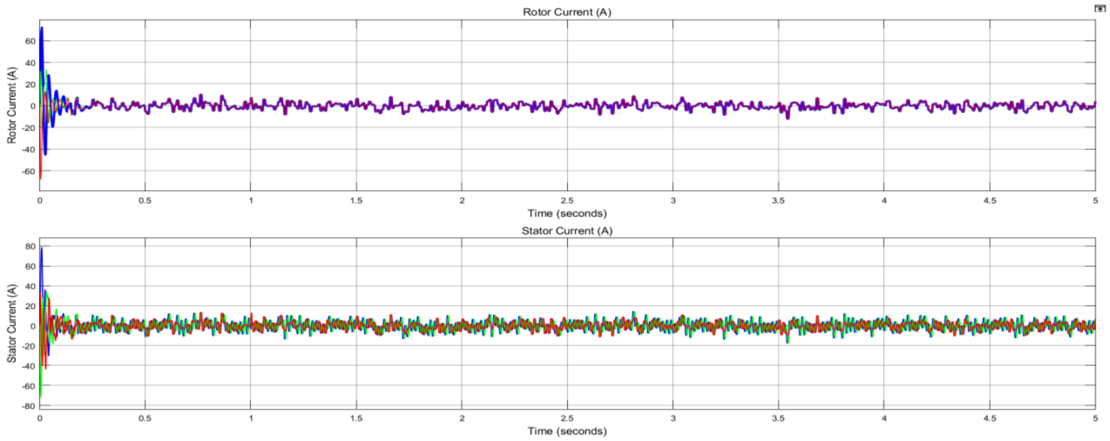

(d) Three broken bar rotor and stator at no load condition

Figure 4.30: (a, b, c and d) IM rotor and stator current (A) response during fault at 100%, 50%, 25% and no load conditions with three broken rotor bars

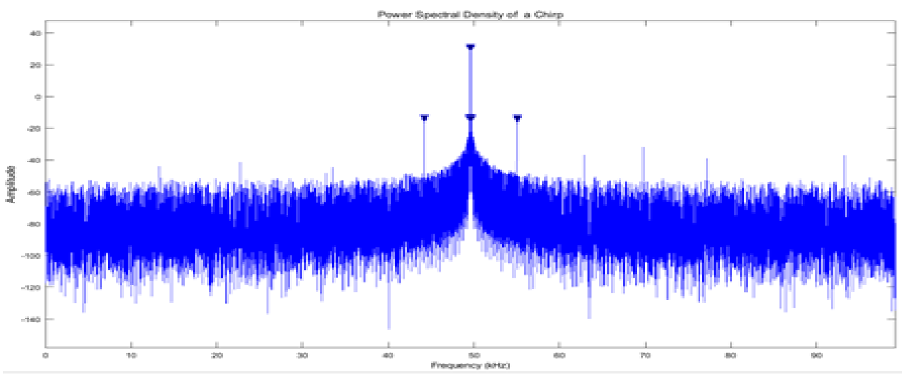

Figure 4.31: Power spectrum of motor stator current with three broken rotor bar faulty condition

SCIM characteristics responses at different rotor bar faulty conditions are illustrated in Tables 4.4 and 4.5. From the Table 4.4 it can be clearly seen that the speed tends to reduce as the number of rotor bar fault increases. At full load the speed is 1251 rpm on 1 broken bar of rotor fault which reduces to 1211 in case of 3 broken bars of rotor. So, the speed is highly impacted on encounter of the fault. Similarly, the torque behavior is illustrated in Table 4.5 where the effects of 1 broken bar to 3 broken bar of rotor are presented and the reduction of torque is visible. At full load the torque from 23.59 Nm at 1 broken bar reduced to 22.12 Nm at 3 broken bar fault. The designed model with broken bar rotor fault has been executed successfully under different constant loading conditions and its characteristics parameters have been analyzed in comparison with healthy state results given in chapter 2 and shown in Table 2.2.

Table 4.4: (1, 2 and 3) broken rotor bar faulty SCIM motor speed at different loading conditions

Loading conditions	Speed (rpm) (1-brb)	Speed (rpm) (2-brb)	Speed (rpm) (3-brb)
Full Load	1251	1231	1211
Half Load	1281	1241	1224
Quarter load	1294	1254	1242

Table 4.5: (1, 2 and 3) broken rotor bar faulty SCIM motor torque at different loading conditions

Loading Conditions	Torque (Nm) (1-brb)	Torque (Nm) (2-brb)	Torque (Nm) (3-brb)
Full Load	23.59	22.24	22.12
Half Load	9.05	8.92	8.72
Quarter load	3.76	3.48	3.14

The motor performance deteriorated when analyzed under various broken rotor bar faulty conditions (i.e. 1, 2 and 3 broken rotor bar), it has been observed that the motor torque and speed reduced considerably as the severity of the fault increases

4.4.4 Effect of Time Varying Load on the Motor under Broken Rotor Bar Faulty Condition

The Induction Motor is put under various load variations in continuous operation for the 15 seconds, the load torque is varied during runtime from 0-3 seconds the motor is at no load, 3-5 seconds the motor is at full load, 5-8 seconds the motor is half load, 8-11 seconds the motor is quarter load and 11-15 seconds the motor is at no load. The characteristics obtained during the time varying scenarios are analyzed and depicted in Figures 4.32, 4.33, 4.34 and 4.35. Figure 4.32 displays the speed and torque of the healthy motor at time varying loading conditions and Figure 4.33 displays the speed and torque curve produced at broken rotor bar faulty condition under time varying loading conditions. From both 4.32 and 4.33, it can be clearly seen that the magnitude of the torque and speed are lower at faulty in Figure 4.33 as compared to the healthy in Figure 4.32.

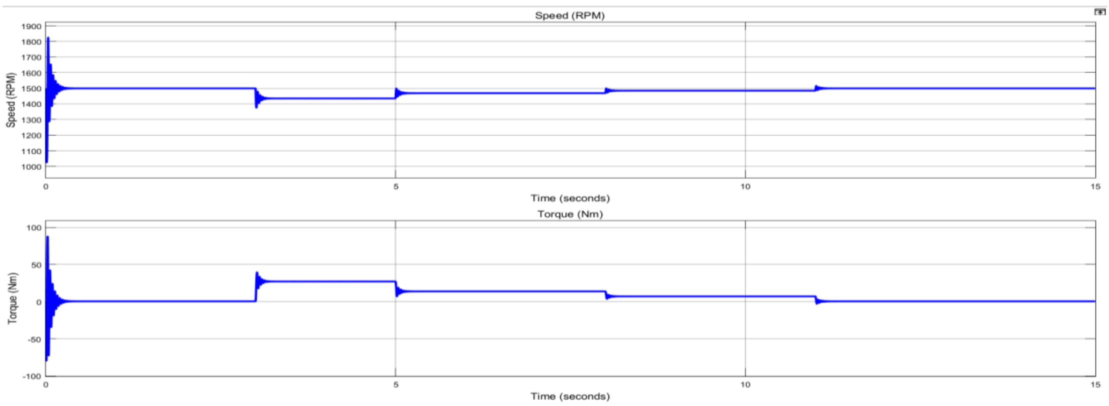

Figure 4.32: IM Speed (rpm) and torque (Nm) of healthy operating condition at time varying loading conditions

The variation of speed can be seen in Figure 4.32 as the load varies the speed tends to change and tries to achieve the stability and it can be seen that there is not much of the oscillation during run time apart from initial overshoot that shows the implemented model obtained is stable. The torque varies as per the demand varies can be seen significantly in Figures 4.32 and 4.33. The stator current and rotor current also got affected with dynamic variation of the load shown in Figures 4.34 and 4.35 for comparison with healthy one. The stability of the implemented model is visible as there is no abrupt variation in power while there is a changeover of the demand load.

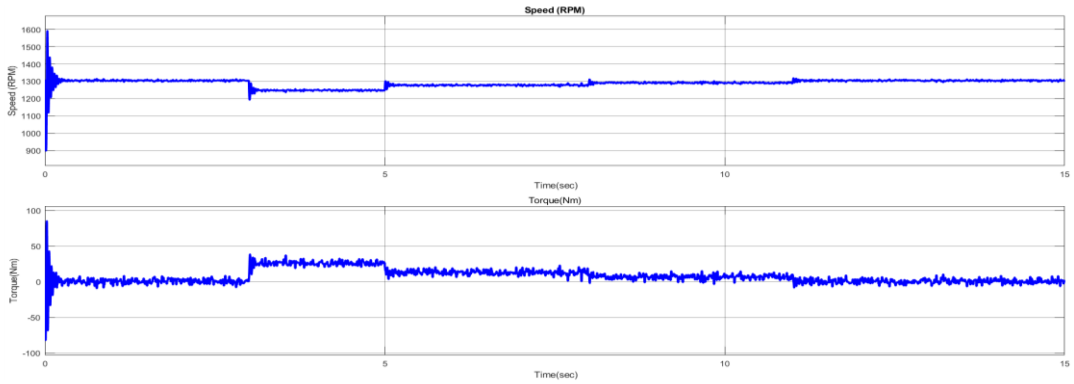

Figure 4.33: IM Speed (rpm) and torque (Nm) under broken rotor bar faulty condition at time varying loading conditions

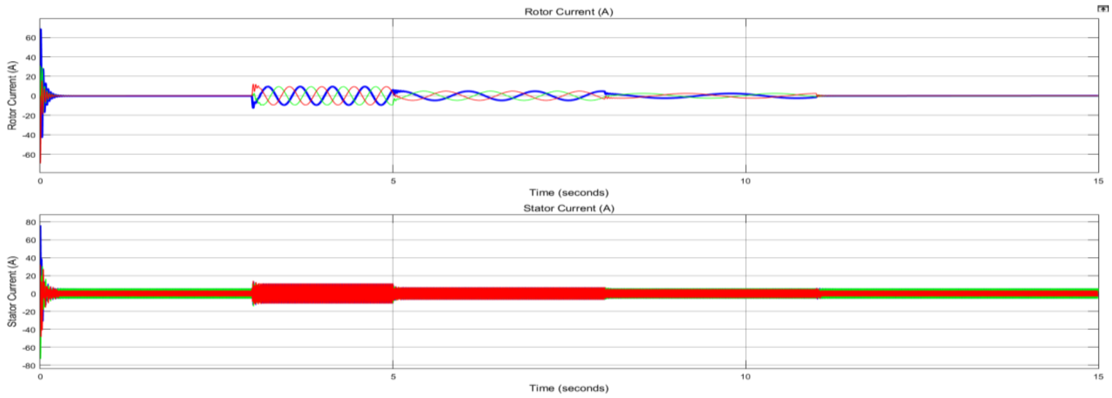

Figure 4.34: IM rotor and stator current (A) of healthy operating condition at time varying loading conditions

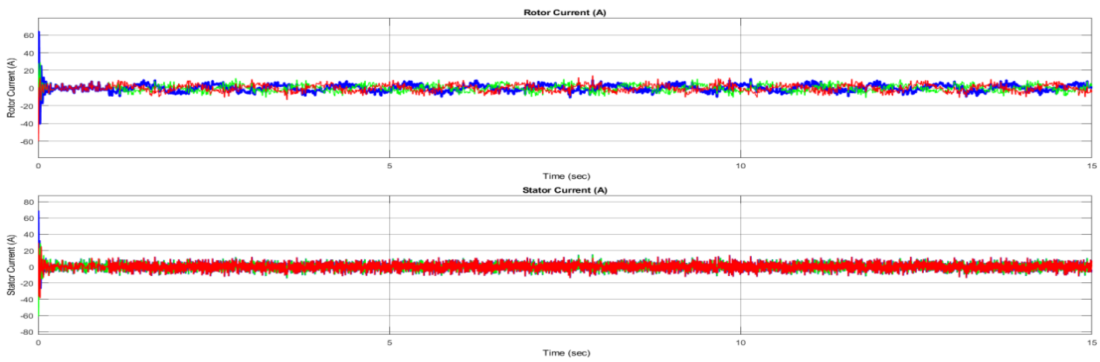

Figure 4.35: IM rotor and stator current (A) under broken rotor bar faulty condition at time varying loading conditions

4.5 INDUCTION MOTOR UNDER STATOR WINDING FAULTY CONDITIONS

Overheating is one of the main causes of stator winding insulation deterioration and even failure of it. The insulation degrading or failure is mainly caused by poor ventilation, problem in cooling circuit or overload condition, contamination in air and/or humidity etc. These erroneous conditions are possibly causing shorted turns, shorted coils (same phase, it is the most common fault), phase to phase, phase or coil to ground and single phasing. Such failures cause stator electrical imbalance as well as variations in the current harmonic content. Mechanical problems can also occur in the stator such as loosen edges, but this is statistically less frequent.

4.5.1 Faulty Condition in Induction Motor having One Coil Open of Stator Winding

The designed FEM model of SCIM is tweaked by opening one coil of phase A of stator winding to analyze the harmonic content of the motor at 1451.65 rpm. FEM structural design model with flux density maps are shown in Figures 4.36 and 4.37. Figure 4.36 shows the IM FEM model with one coil of phase (A) open of stator winding. From the distribution of magnetic flux density in Figure 4.37, it is seen that due to the lack of induced currents sue to the open coil fault, the magnetic field becomes asymmetrical leading to saturation in the rotor and stator teeth near the faulty location.

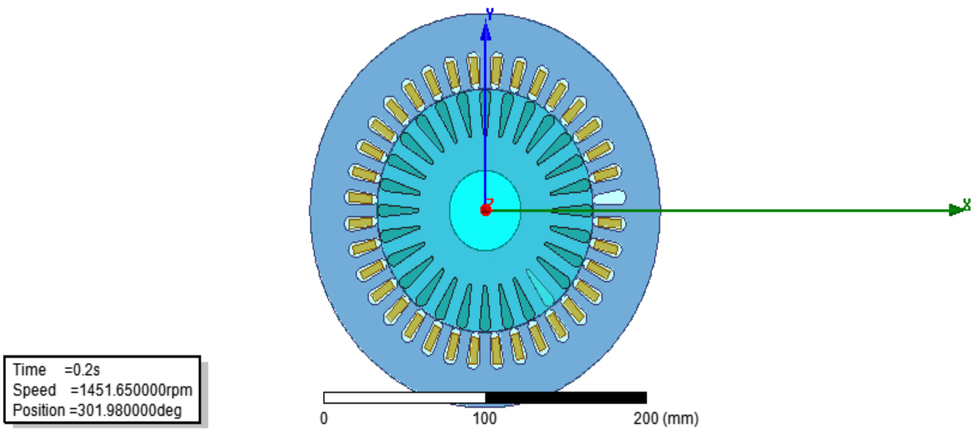

Figure 4.36: Model of Induction Motor with one coil of phase (A) open of stator winding

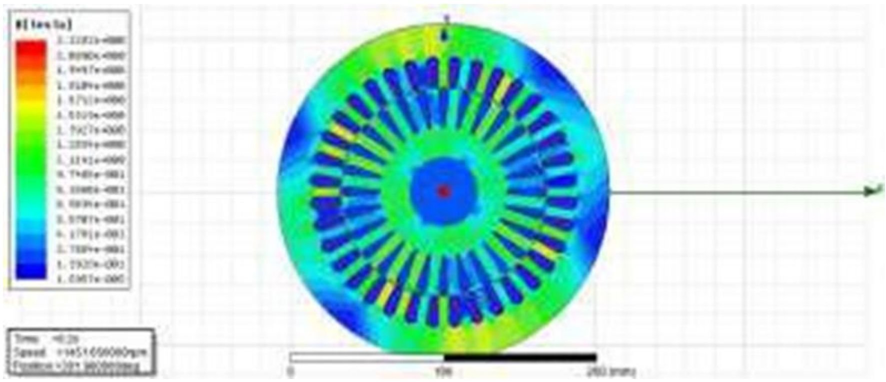

Figure 4.37: Flux density distribution of Induction Motor during fault condition with one coil open of stator winding

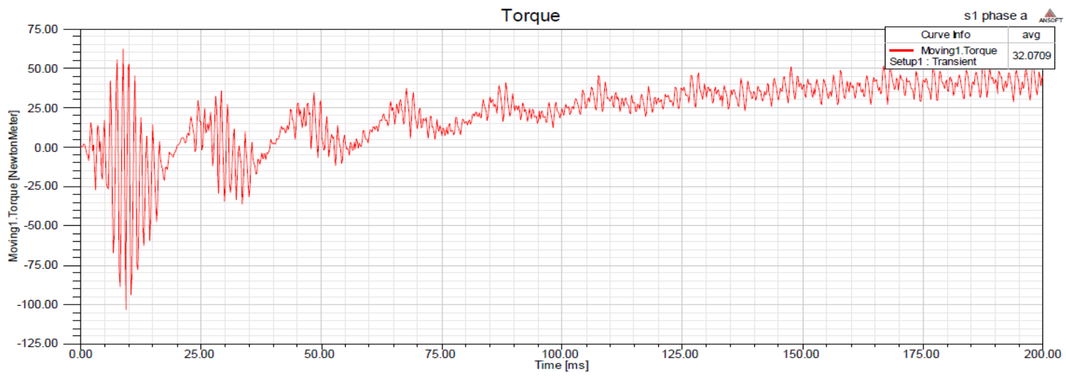

Figure 4.38: Torque response of Induction Motor over period of time during fault condition with one coil open of stator winding

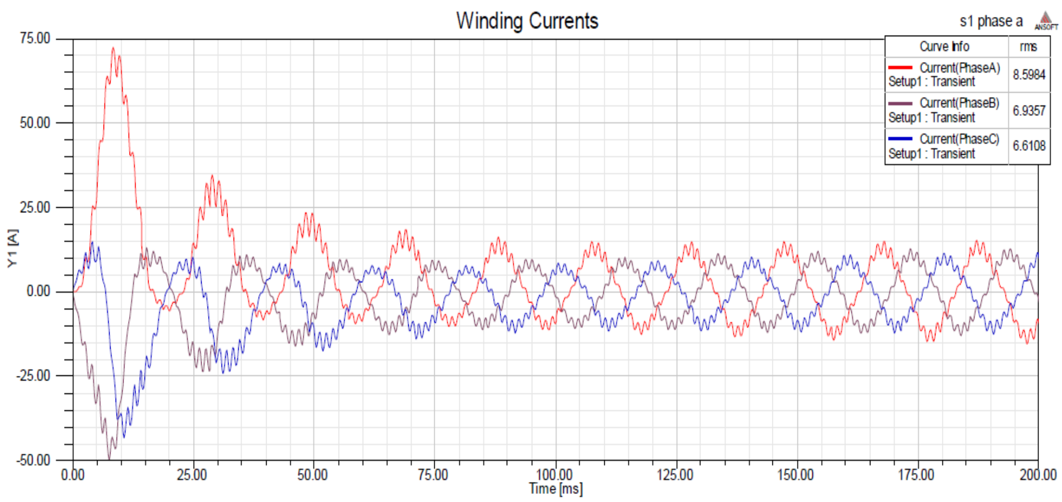

Figure 4.39: Current response of Induction Motor during fault condition with one coil open of stator winding

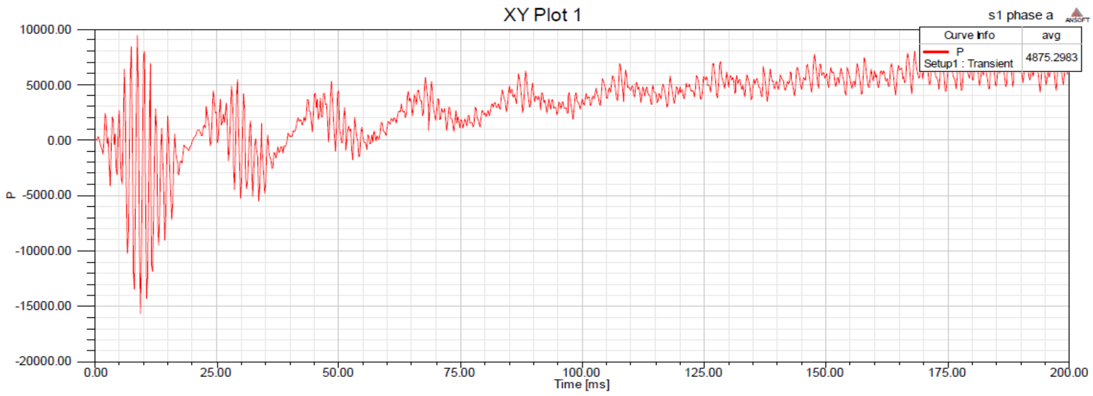

Figure 4.40: Output power response of Induction Motor during fault condition with one coil open of stator winding

As a result the stator winding faults have an impact on the machine parameters such as torque and speed oscillations due to the influence of inverse magnetic field component. The 3-phase current tends to have high oscillation when put under open coil faulty state, motor characteristics are depicted in Figures 4.38, 4.39 and 4.40.

4.5.2 Faulty Condition in Induction Motor having Two Coils Open of Stator Winding

The FEM designed model is modified to generate stator winding fault with two coil open of stator winding and then its structural model performance in terms of flux distribution, current, torque and powers are analyzed presented in Figures 4.41 and 4.42. Figure 4.41 displays the FEM model with two open coils which are marked with two arrows in the model. Figure 4.42 displays the distribution of magnetic flux density where the magnetic field is more asymmetrical due to the presence of two open coils in stator which in turns lead to saturation in the rotor and stator teeth near the faulty coil location.

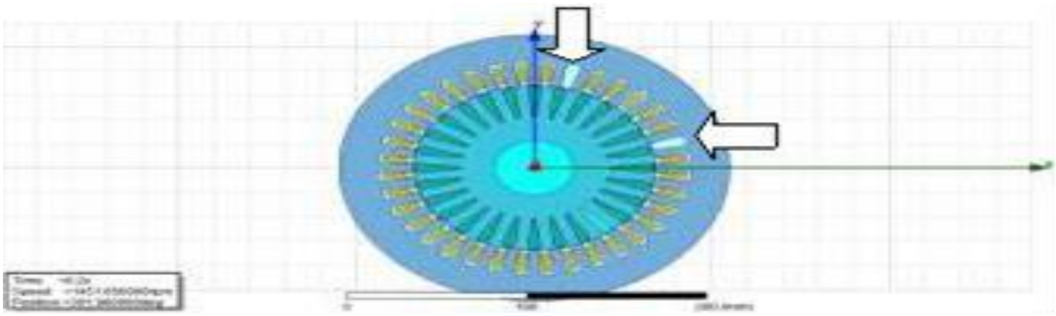

Figure 4.41: Model of Induction Motor with two coils open of stator winding

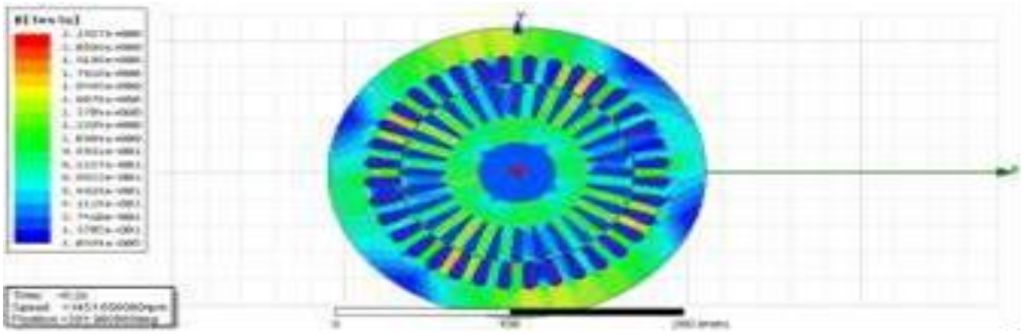

Figure 4.42: Flux density distribution of Induction Motor during fault condition with two coils open of stator winding

The impact of two open coils at stator windings on torque current and power is analysed and graphs obtained are shown in Figures 4.43, 4.44 and 4.45.

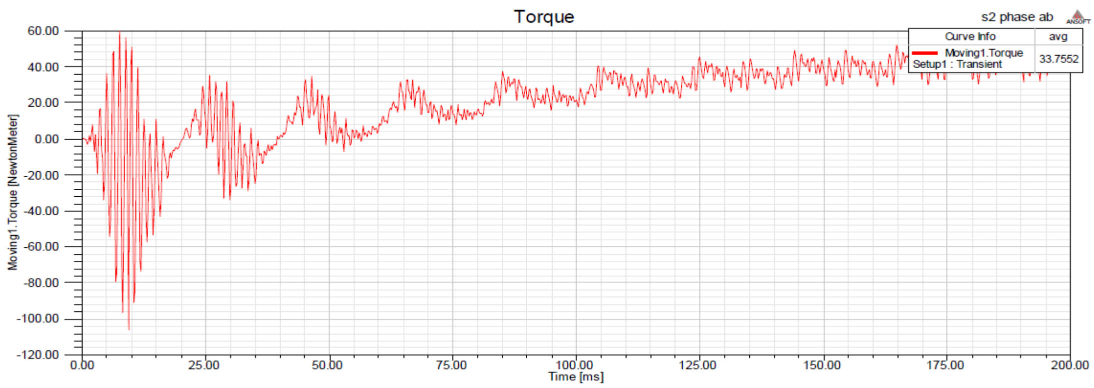

Figure 4.43: Torque response of Induction Motor over period of time during fault condition with two coils open of stator winding

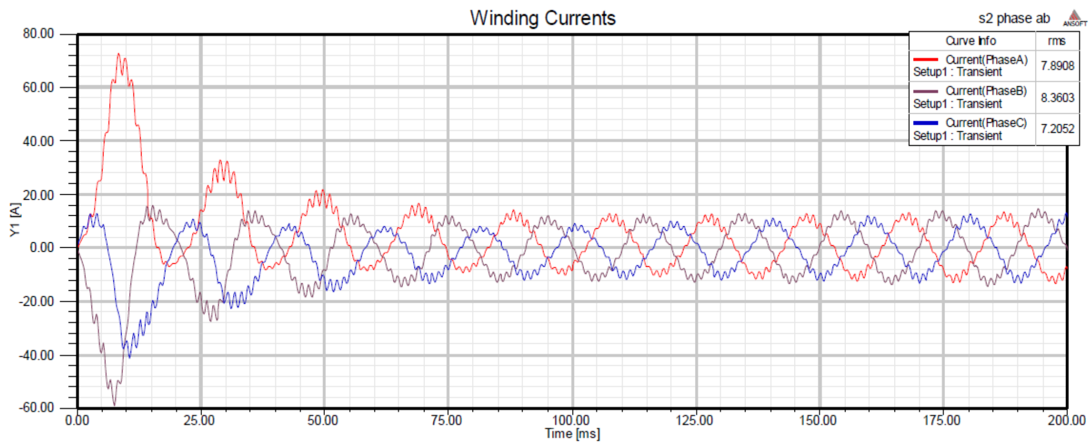

Figure 4.44: Current response of Induction Motor during fault condition with two coils open of stator winding

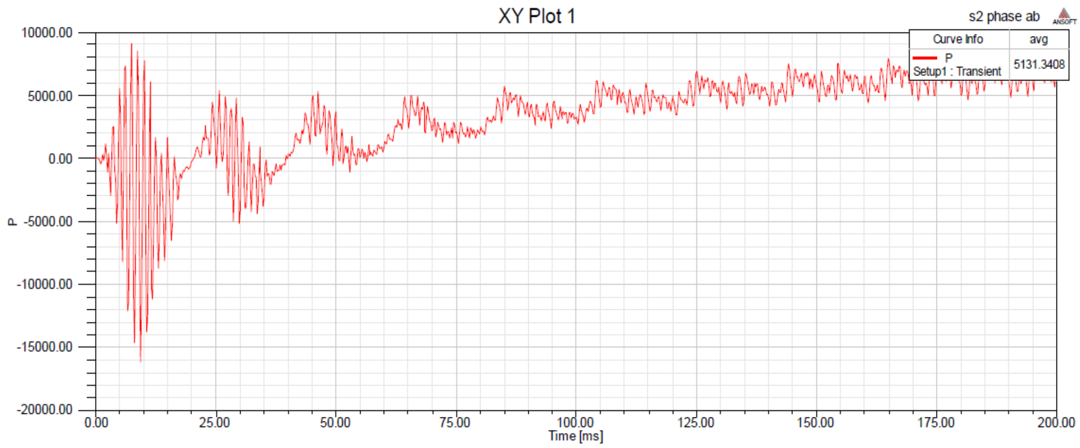

Figure 4.45: Output power response of Induction Motor during fault condition with two coils open of stator winding

4.5.3 Faulty Condition in Induction Motor having Three Coil Open of Stator Winding

In third experimentation, the FEM designed model is modified to generate more severe stator fault i.e. with three open coil windings. FEM modified model with its flux density map is displayed in Figures 4.46 and 4.47. Figure 4.46 shows the motor model with three coils open of stator winding marked with three arrows. Figure 4.47 depicts the magnetic flux density at three open coil stator fault; from the magnetic flux density map it is clear that the flux distribution is highly asymmetric as compared to healthy, one and two stator fault conditions.

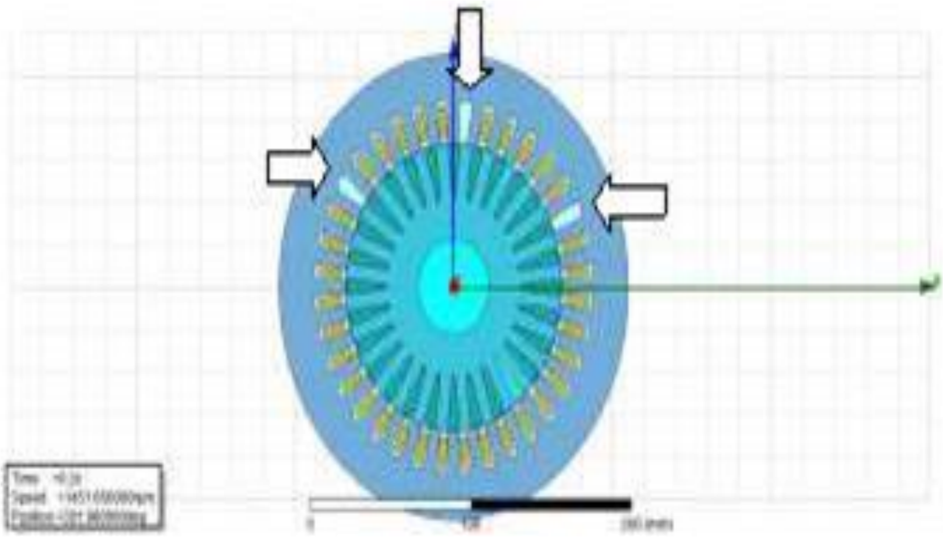

Figure 4.46: Model of Induction Motor with three coils open of stator winding

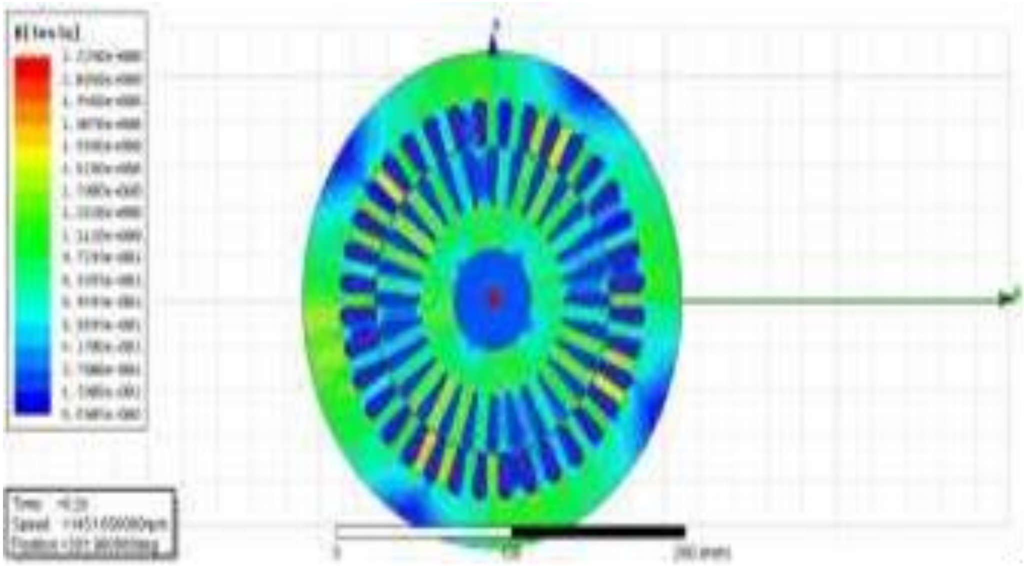

Figure 4.47: Flux density distribution of Induction Motor during fault condition with three coils open of stator winding

The effect of asymmetric magnetic flux and three open coil stator fault on characteristics parameter of the motor in terms of torque, currents and power are displayed in Figures 4.48, 4.49 and 4.50.

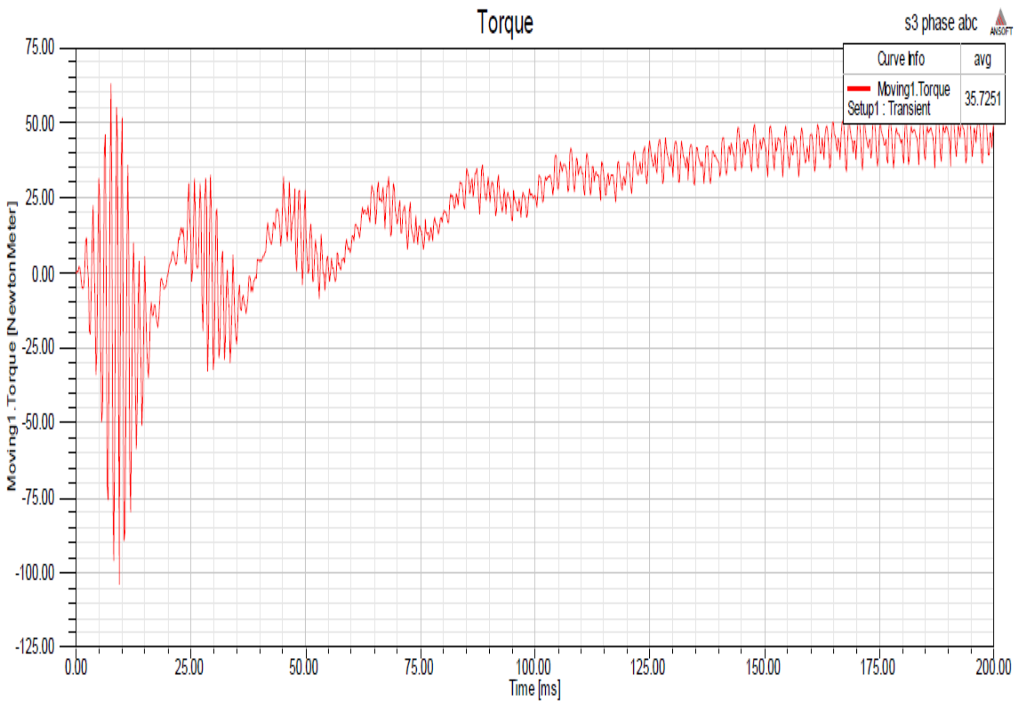

Figure 4.48: Torque response of Induction Motor over period of time during fault condition with three coils open of stator winding

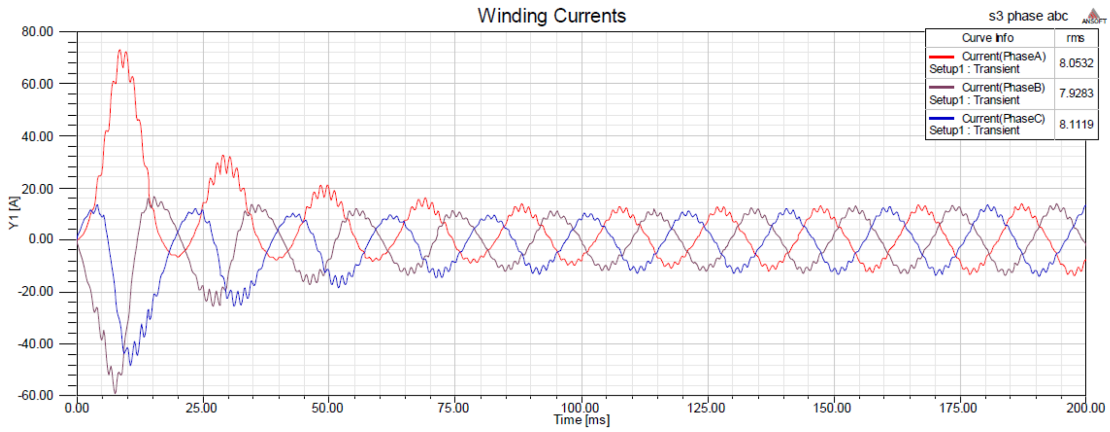

Figure 4.49: Current response of Induction Motor during fault condition with three coils open of stator winding

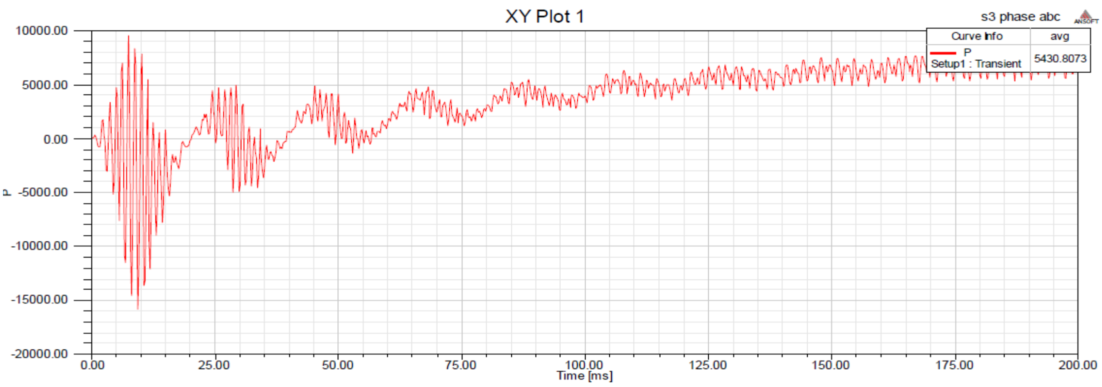

Figure 4.50: Output power response of Induction Motor during fault condition with three coils open of stator winding

4.6 RESULTS AND CONCLUSION OF FEM ANALYSIS

The FEM model of IM is analyzed for three different stator faulty conditions one, two and three open coils stator windings. The deigned model is modified to generated stator open winding faults and its characteristics parameters have been observed. The obtained parameters have been verified and effect of stator fault results in poor performance of motor due to which the motor become unsuitable for the any process industry operation. Thus the need of fault monitoring and diagnosis is very higher as the downtime in industry should be avoidable to keep the production. These abrupt behaviors of motor parameters as utilized to extract the features and those features are furthermore used to detect and classify the fault and its type using machine learning and deep learning algorithms.

4.7 MATLAB IMPLEMENTATION MODEL

The MATLAB model of SCIM is designed to investigate the motor performance under stator short circuit faulty operating condition. The motor is put under stator short circuited winding fault and its characteristics behavior is analyzed which are used for detection and diagnose of the fault using deep learning method. Figure 4.51 displays the MATLAB working model of SCIM with stator winding fault.

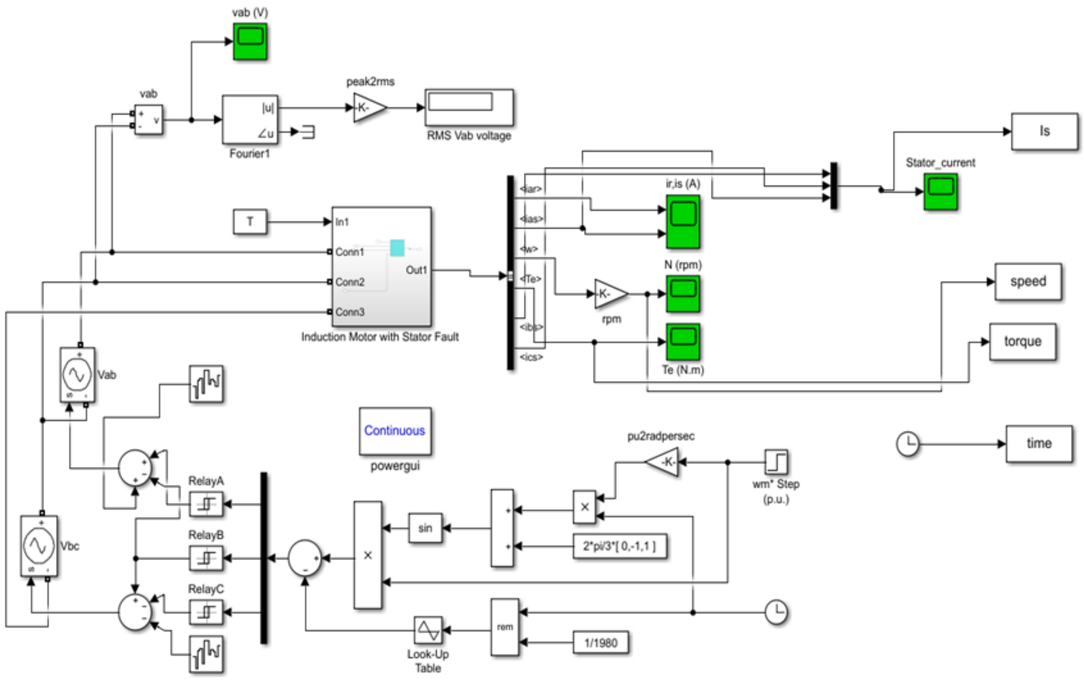

Figure 4.51: Induction motor model with stator fault condition

4.7.1 Implementation Model of Stator Winding Faulty SCIM at Full Load

The second type of fault in SCIM considered is stator short circuit fault. The stator winding faulty motor model is operated under time varying loading condition and characteristics obtained at full load are illustrated in Figure 4.52 and 4.53. Figure 4.52 shows the rotor & stator current and Figure 4.53 shows the torque & speed at the full load. Under the stator winding fault the motor distortion in stator current are extensive and rotor current shows the distortion on peaks of its waveforms.

The torque & speed is distorted and the sped reduces at full load as compared to the healthy condition. The effect of the short circuit winding at the stator side results in lower speed and distorted magnitude of the torque.

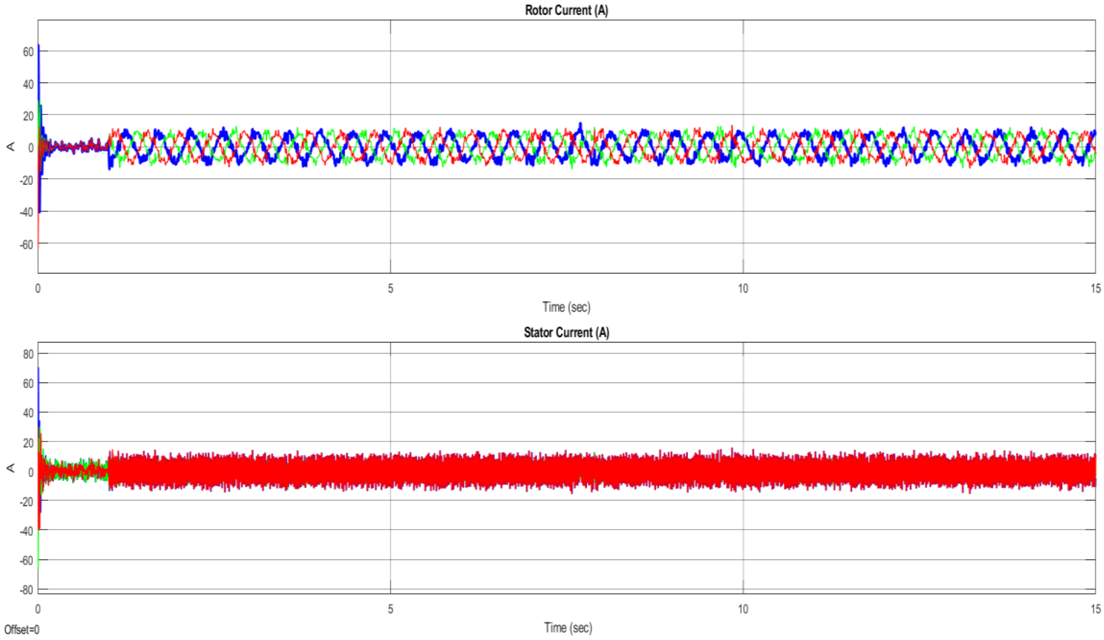

Figure 4.52: Rotor and stator current of stator winding fault SCIM at full loading condition

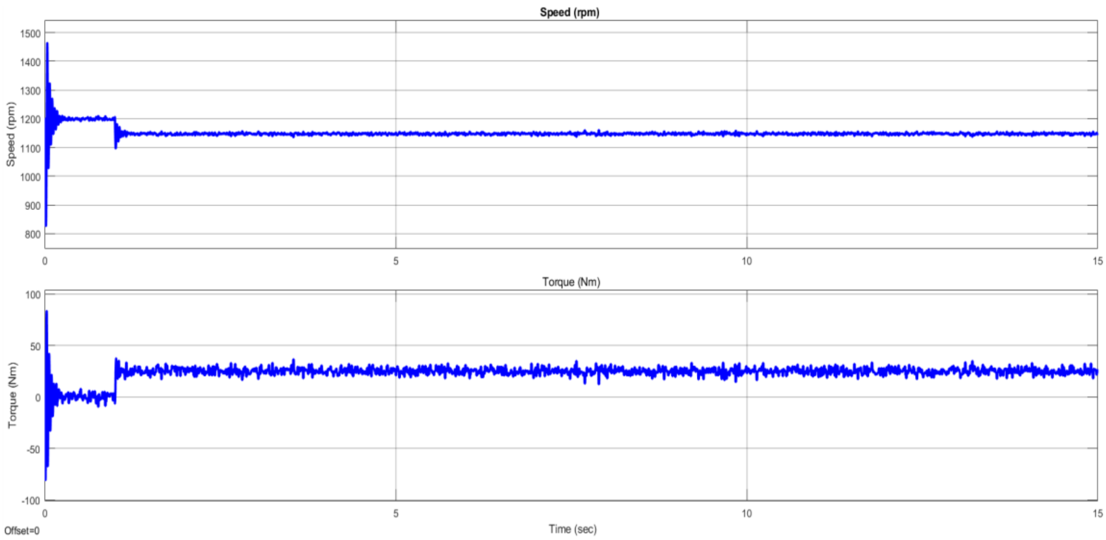

Figure 4.53: Speed and torque of stator winding fault SCIM at Full loading condition

4.7.2 Implementation Model of Stator Winding Faulty SCIM at 50% Load

The MATLAB model is operated under varied loading conditions, here the motor is put at 50% loading condition to extract the features and analyze the effect of its variation. The stator winding faulty MATLAB model characteristics parameters are obtained at 50% load are illustrated in Figure 4.54 and Figure 4.55.

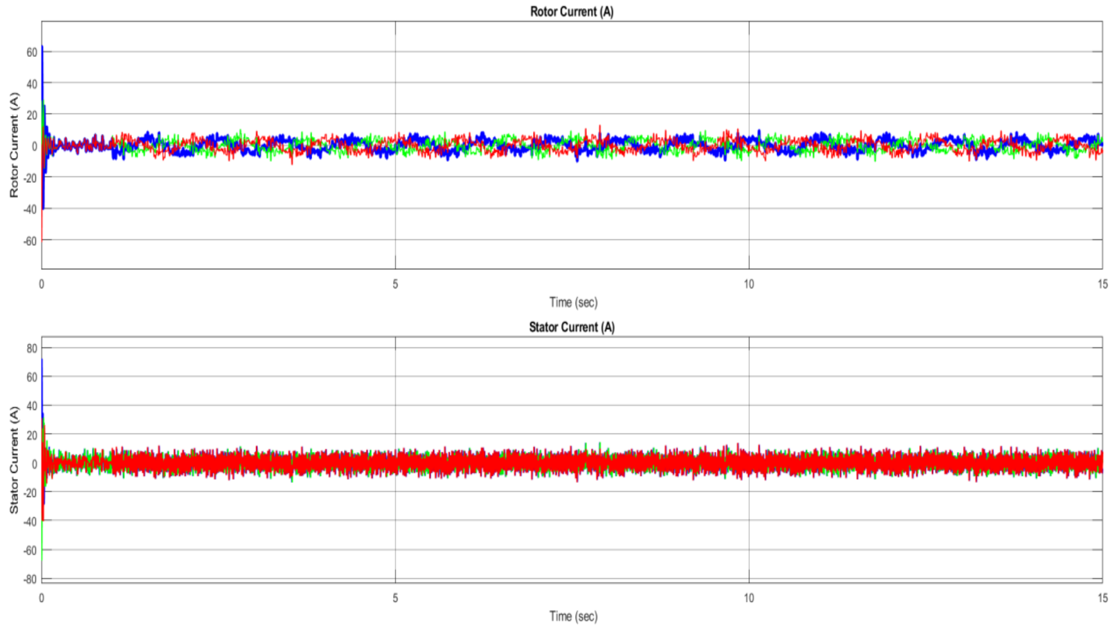

Figure 4.54: Rotor and stator current of stator winding fault SCIM at 50% loading

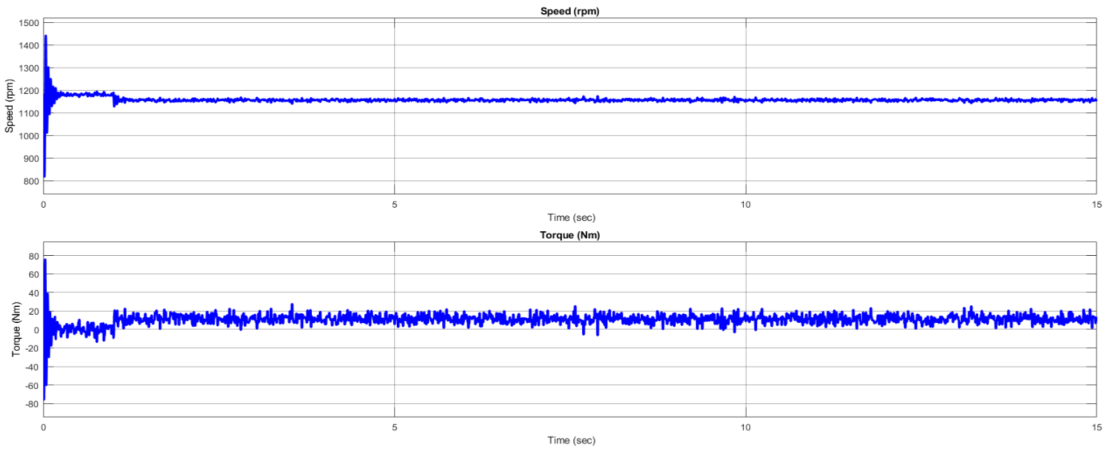

Figure 4.55: Speed and torque of stator winding fault SCIM at 50% loading

4.7.3 Implementation Model of Stator Winding Faulty SCIM at 25% Load

Here, the motor is operated at 25% loading condition under short circuit stator winding faulty condition. The characteristics of the motor as displayed in Figures 4.56 and 4.57. Figure 4.56 depicts the stator and rotor currents whereas Figure 4.57 displays the speed and the torque of the motor. The torque and speed is 1189 rpm and 4.24 Nm respectively which is quite lower as compared to healthy state values 1484 rpm and 7.14 Nm. Distortion in current and oscillations in torque and speed leads to degraded performance of motor under short circuit faulty condition.

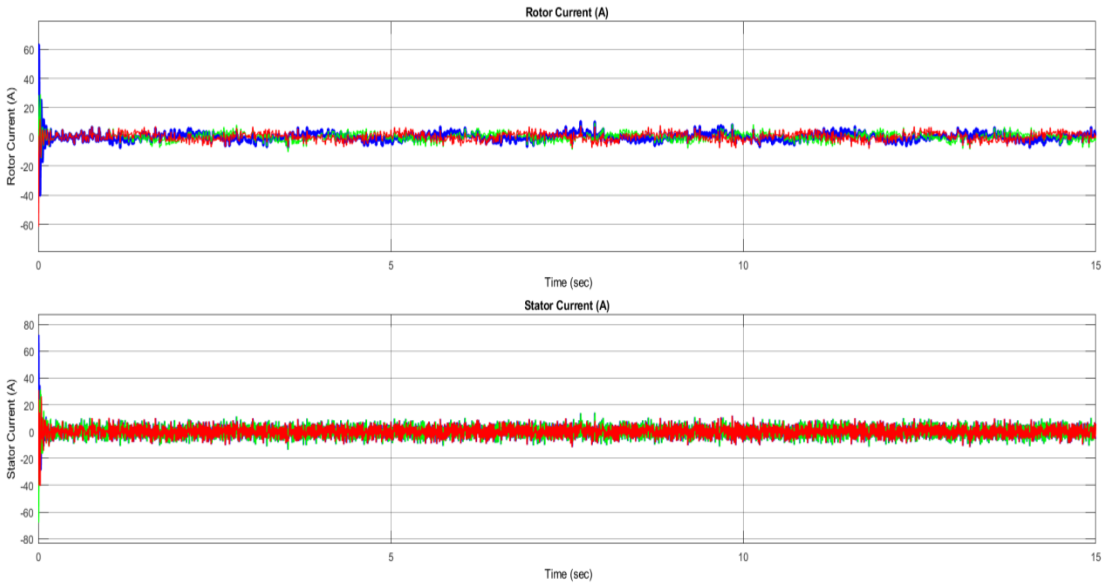

Figure 4.56: Rotor and stator current of stator winding fault SCIM at 25% loading

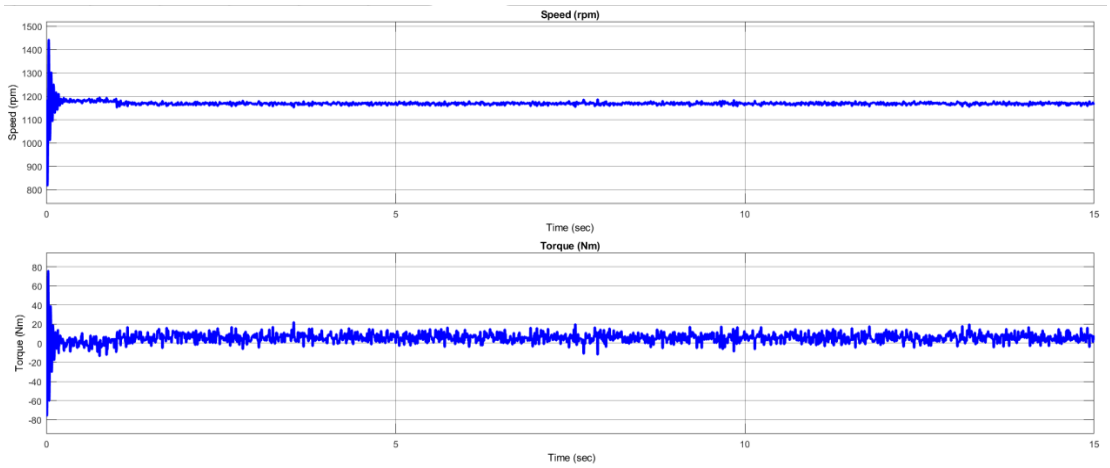

Figure 4.57: Speed and torque of stator winding fault SCIM at 25% loading

4.7.4 Implementation Model of Stator Winding Faulty SCIM at No Load

Here, the motor is operated at 25% loading condition under short circuit stator winding faulty condition. The characteristics of the motor as displayed in Figure 4.58 and 4.59. Figure 4.58 depicts the stator and rotor current whereas 4.59 displays the speed and the torque of the motor. The torque and speed graph is compared with healthy state torque and speed, it is found that the distortion occurred due to the fault in current and oscillations in torque and speed leads to degraded performance of motor under short circuit faulty condition.

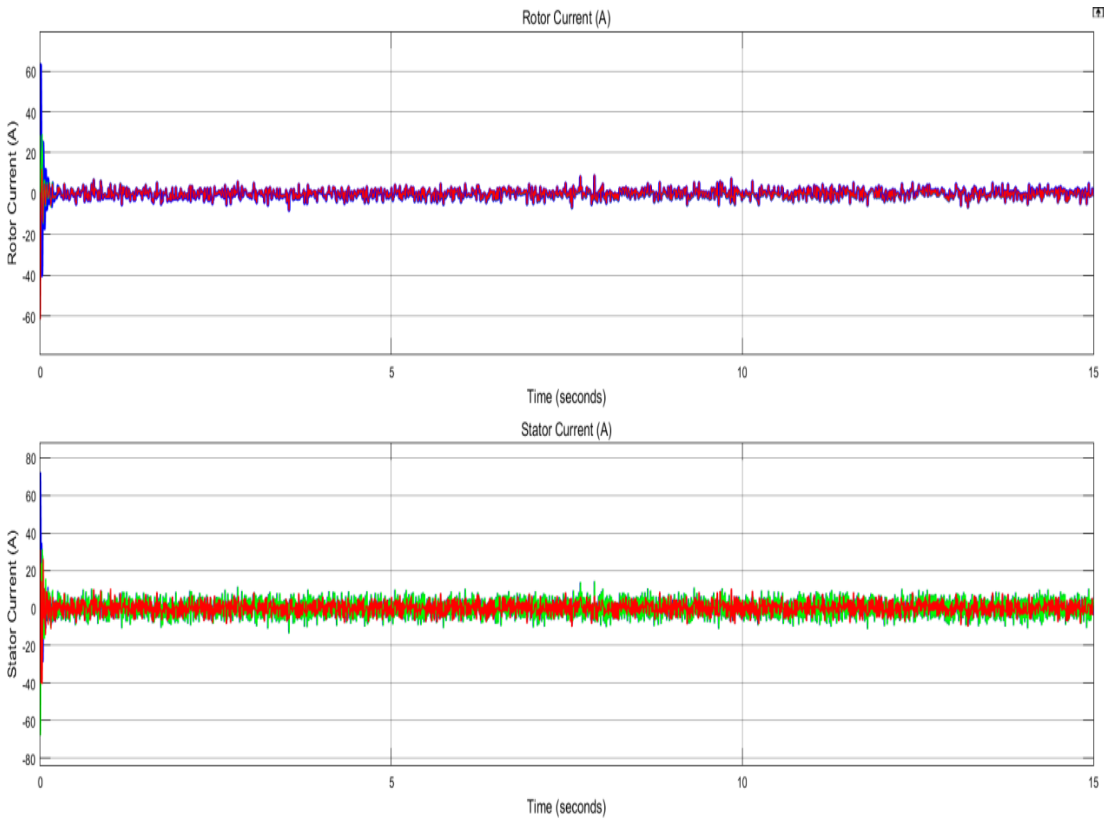

Figure 4.58: Rotor and stator current of stator winding fault SCIM at no load

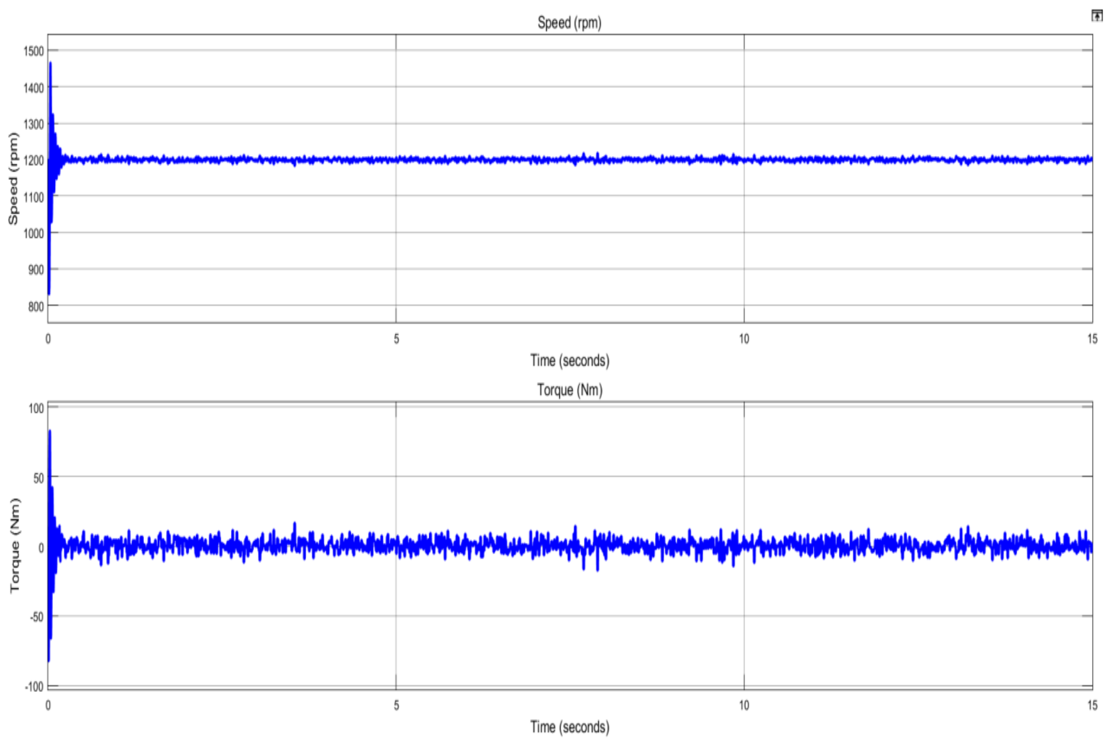

Figure 4.59: Speed and torque of stator winding fault SCIM at no load

Table 4.6 summarizes the short winding stator fault motor behavioral characteristics. The torque produced at full load is 20.31 Nm which is low and the speed is 1149 rpm. The motor performance is degraded under the stator fault conditions as compared to healthy state stated in Table 2.2 in chapter 2. The torque and speed have deviated largely from its healthy state, which leads to the damage of the motor if the problems persist for longer period of time. The need of detecting these types of faults as early as possible is the utmost requirement. The stator short circuit faulty state experiments have been effectively performed and speed, torque and stator current parameters have been obtained as per requirement in order to process these findings for feature extraction and ultimately utilized for automatic fault detection and diagnosis.

Table 4.6: Stator short circuit winding fault SCIM motor speed and torque at different loading conditions

Loading conditions	Torque (Nm)	Speed (rpm)
Full Load	20.31	1149
Half Load	8.76	1179
Quarter Load	4.24	1189

4.7.5 Effects of Time Varying Load on the Motor under Stator Short Circuit Winding Faulty Condition

The time varying effects of healthy motors are displayed in Figure 4.60 for the comparison of the oscillations and distortions with faulty condition. The IM under stator short circuit winding fault is experimented under various time varying loading conditions in continuous operation for the operation of 15 seconds where 0-3 seconds at no load, 3-5 seconds at full load, 5-8 seconds at half load, 8-11 seconds at quarter load and 11-15 seconds at no load conditions are used, the load torque and speed are varied and the effects of that variation are analyzed and depicted in Figure 4.61.

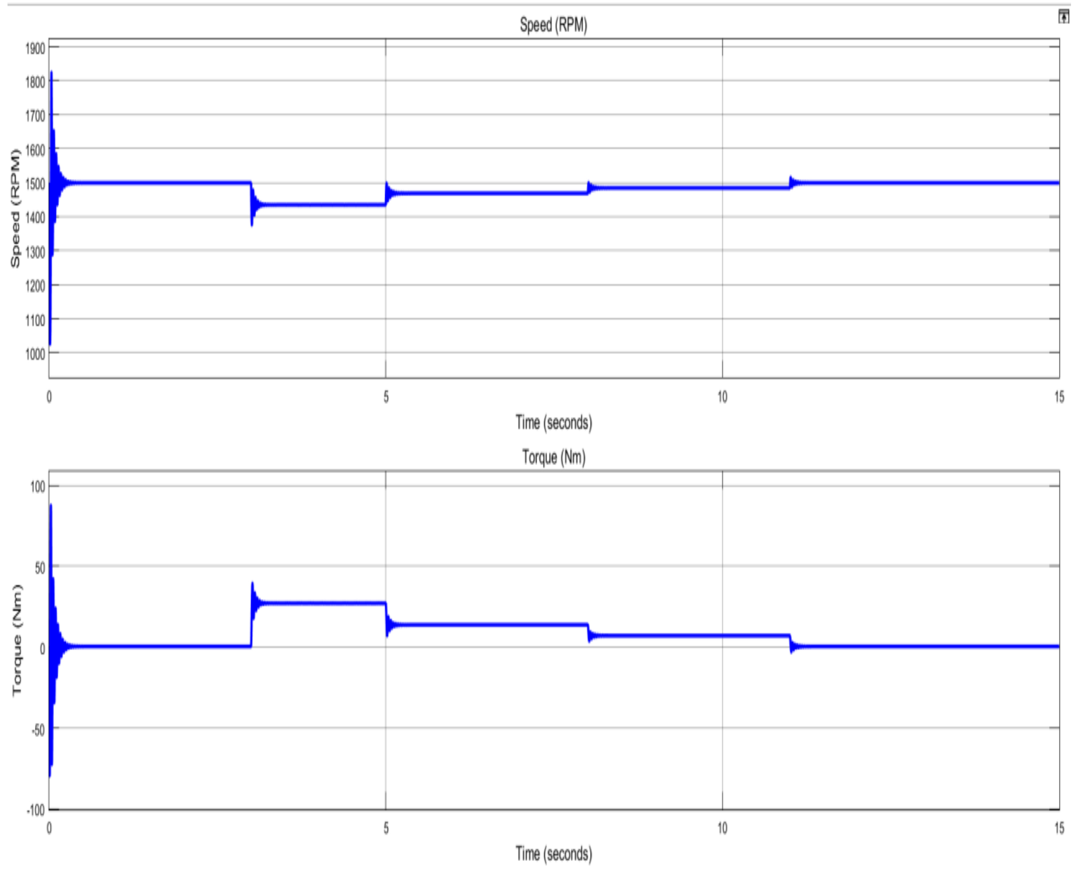

Figure 4.60: IM speed (rpm) and torque (Nm) of healthy operating condition at time varying loading conditions

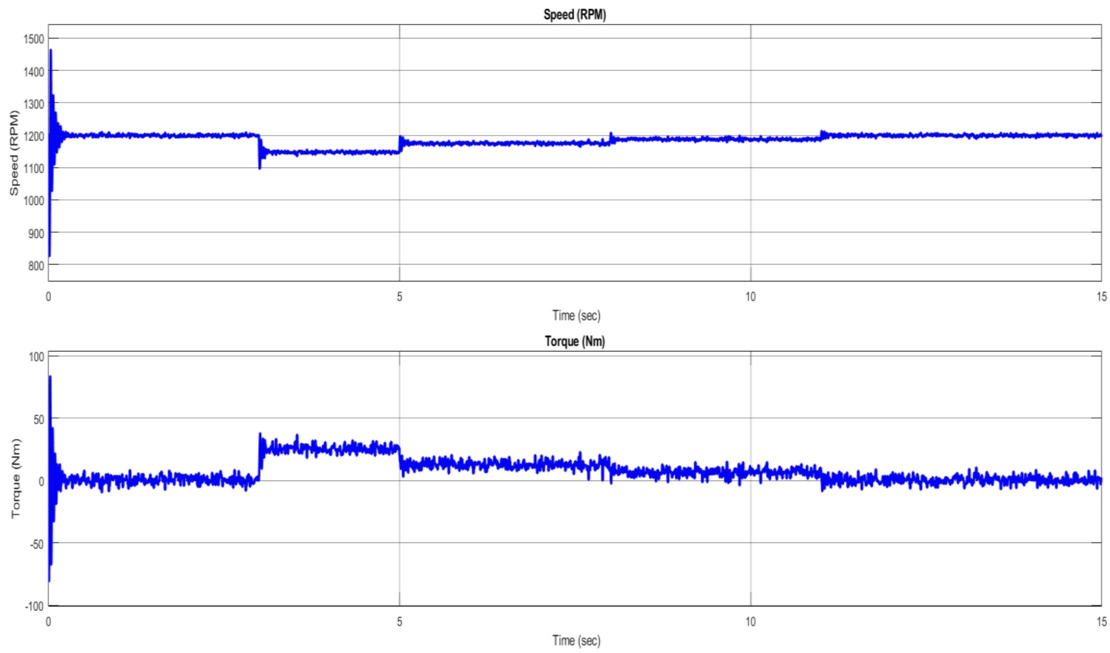

Figure 4.61: IM torque(Nm) and speed (rpm) under time varying loading conditions at stator short circuit faulty condition

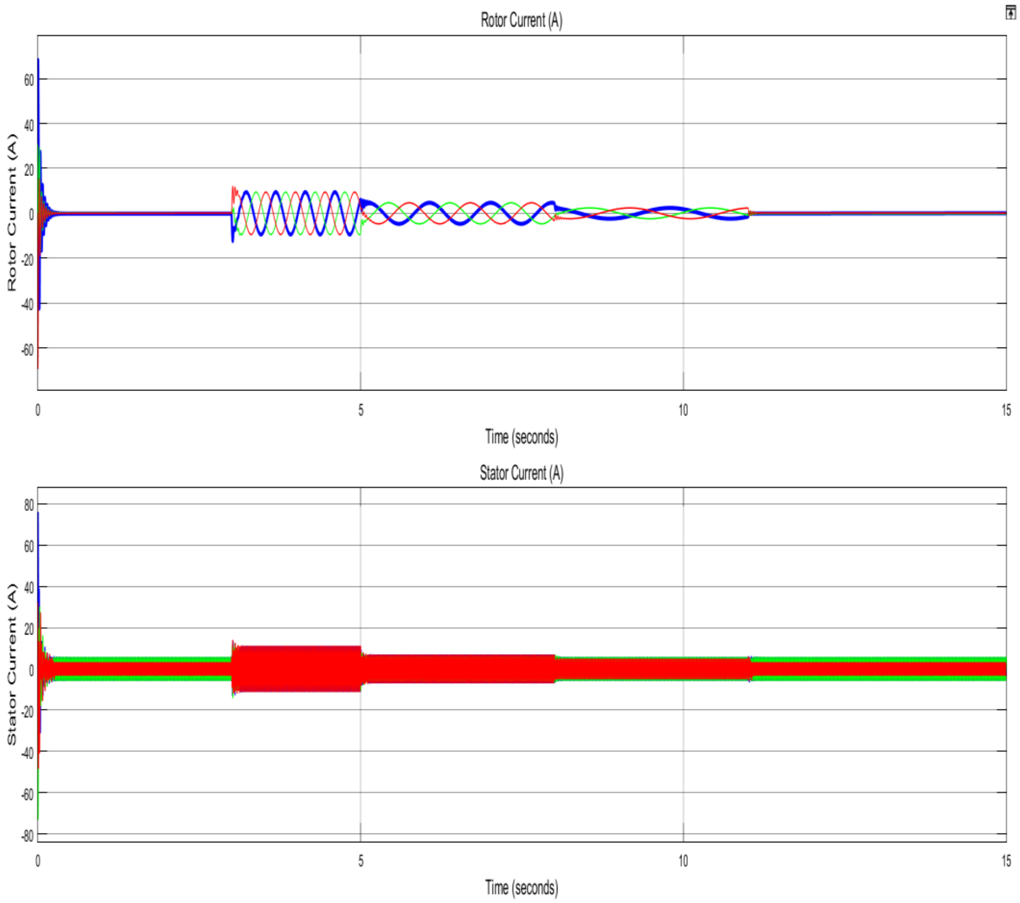

Figure 4.62: IM rotor and stator current (A) under time varying loading conditions at healthy state

The variation of speed can be seen in Figure 4.60 for healthy and 4.61 for faulty state, as the load varies the speed tends to change and tries to achieve the stability and it can be seen that there is not much of the oscillation during run time apart from initial overshoot that shows the operating system obtained is stable. The torque varies as per the demand varies can be seen significantly in Figure 4.61. Figure 4.62 shows the stator current and rotor current for healthy state and Figure 4.63 for faulty state which are also got affected with dynamic variation of the load. The experimentation of time varying loading effects has been conducted successfully and all the outputs achieved have been compared with respect to healthy state. After comparison of healthy with faulty graphs, faults can be easily identified.

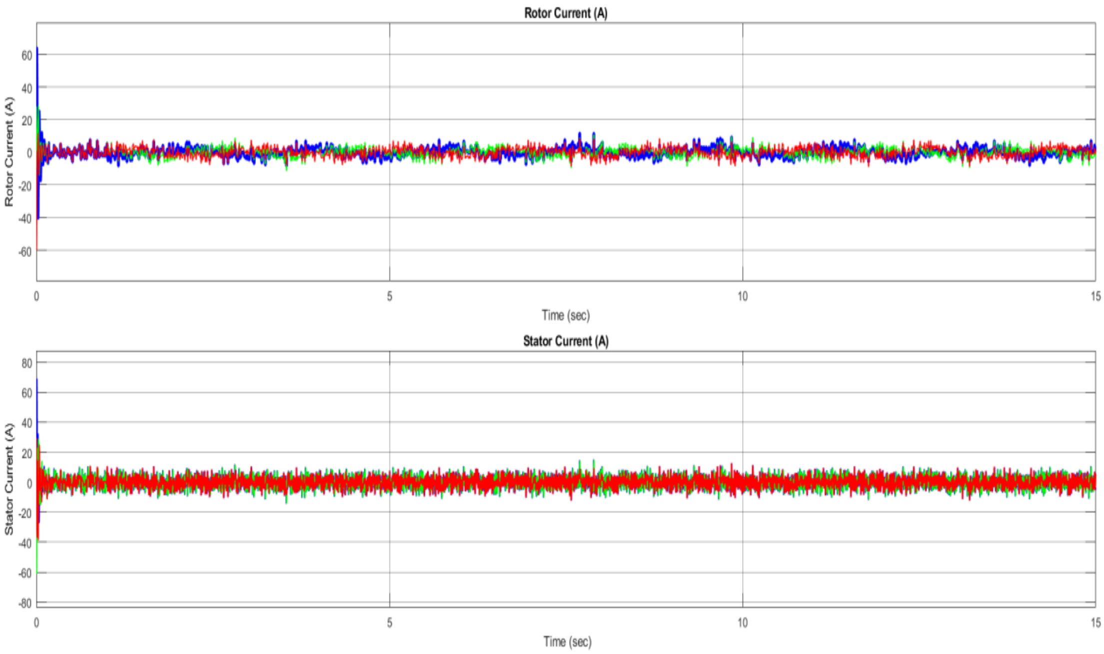

Figure 4.63: IM rotor & stator current (A) under time varying loading conditions at stator short circuit faulty condition

4.8 ECCENTRICITY FAULTS

Eccentricity is common mechanical fault in electrical machine. Approximately, 80% of the mechanical faults lead to the eccentricity. Eccentricity fault may occur during manufacturing and assembling process. Eccentricity exits when there is a non-uniform distance between the rotor and stator in the air-gap. Figure 4.64 represents healthy IM without eccentric fault.

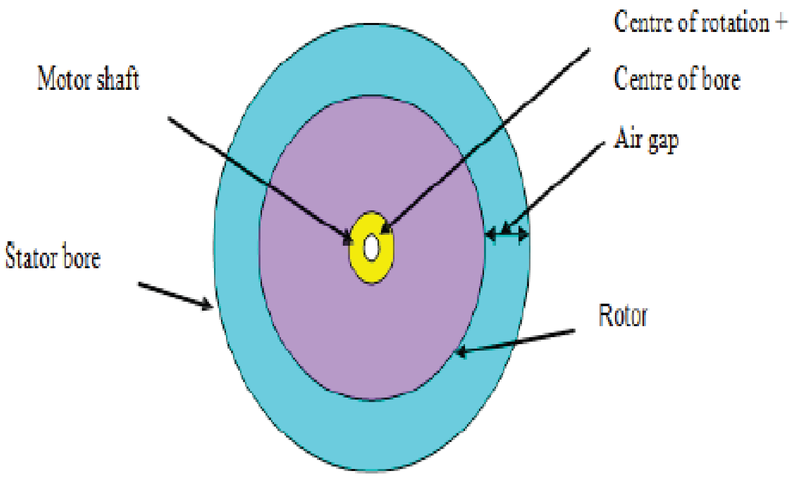

Figure 4.64: Healthy Induction Motor

There are two types of eccentricity faults: Static Eccentricity and Dynamic Eccentricity and combination of both are mixed eccentricity.

In the SE, the symmetrical axis of rotor coincides with the rotational axis of the rotor, but it is displaced from stator symmetrical axis as depicted in Figure 4.65(a). In this case, air-gap distribution is non-uniform around the rotor but the minimum air-gap angular position is fixed. SE fault is created by shifting the stator geometry. However, static eccentricity may cause dynamic eccentricity, too. Assuming that the rotor shaft assembly is sufficient stiff, the level of static eccentricity does not change. Due to the air gap asymmetry, the stator currents will contain well defined components, and these can be detected.

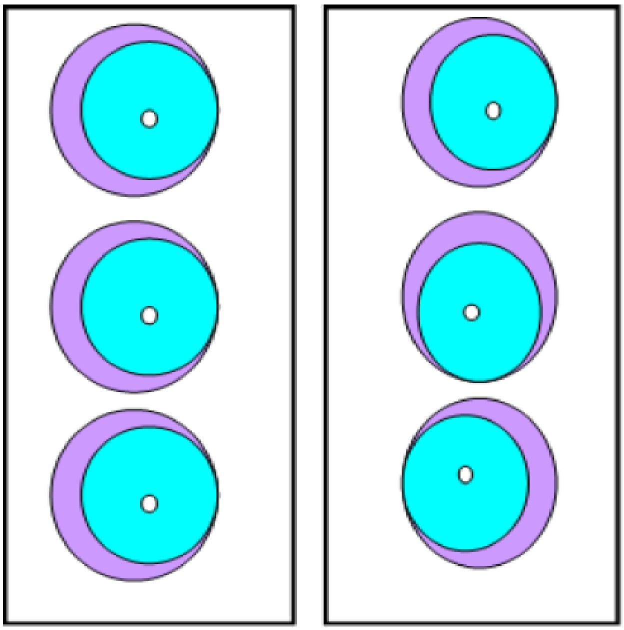

Figure 4.65: (a) Static Eccentricity (b) Dynamic Eccentricity

DE means that the rotor is rotating on the stator bore axis but not on its own axis. The off-center axis of rotation spin along a circular path with the same speed as the rotor does as depicted in Figure 4.65(b). This kind of eccentricity may be caused by a bent shaft, mechanical resonances, bearing wear or movement, and even static eccentric. Therefore, the non-uniform air-gap of a certain spatial position is sinusoidally modulated, and results in an asymmetric magnetic field gives rise to revolving unbalance magnetic pull. Due to dynamic eccentricity, side band components appear around the slot harmonics in the stator line current frequency spectra.

4.9 ANALYZING BEHAVIOUR OF IM UNDER ECCENTRIC FAULTY CONDITION

The modeling work was conducted on a three phase IM having specifications given in chapter 2 Table 2.1, is designed using RMxprt and Maxwell 2D is used for FEM analysis. The proposed model of IM is shown in Figure 4.66.

Here, a 3 phase IM is operated under various conditions of Static and Dynamic Eccentricity, and the results are shown.

- Fault condition with 34.48% Dynamic Eccentricity
- Fault condition with 27.58% Dynamic Eccentricity
- Fault condition with 34.48% Static Eccentricity
- Fault condition with 27.58% Static Eccentricity

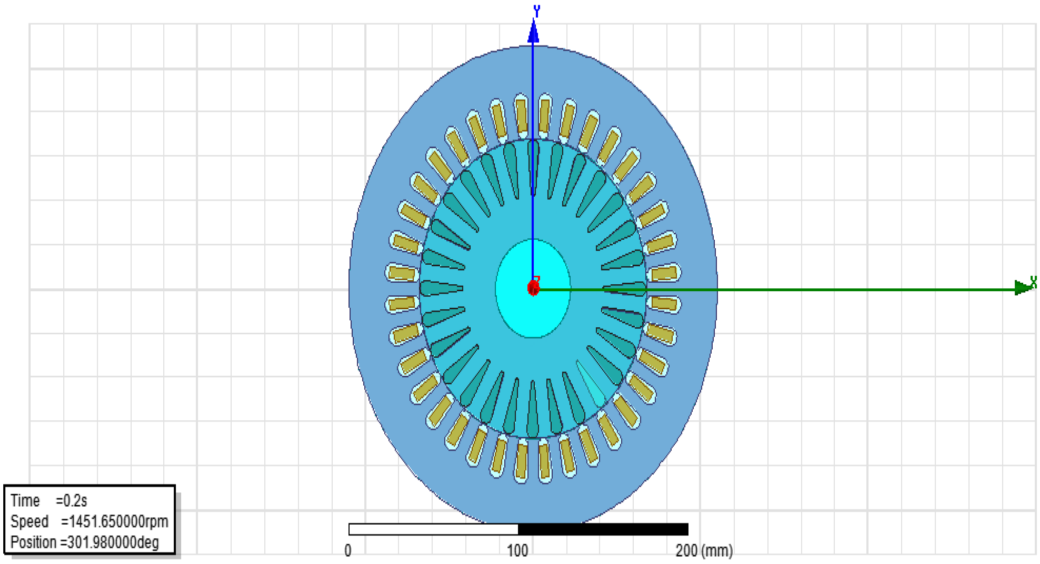

Figure 4.66: Induction Motor FEM model

4.9.1 Induction Motor having Fault Condition with 34.48% Dynamic Eccentricity

The FEM designed model is put under DE faulty condition and its magnetic flux density map is analyzed. Figure 4.67 displays the flux density distribution with 34.48 % DE.

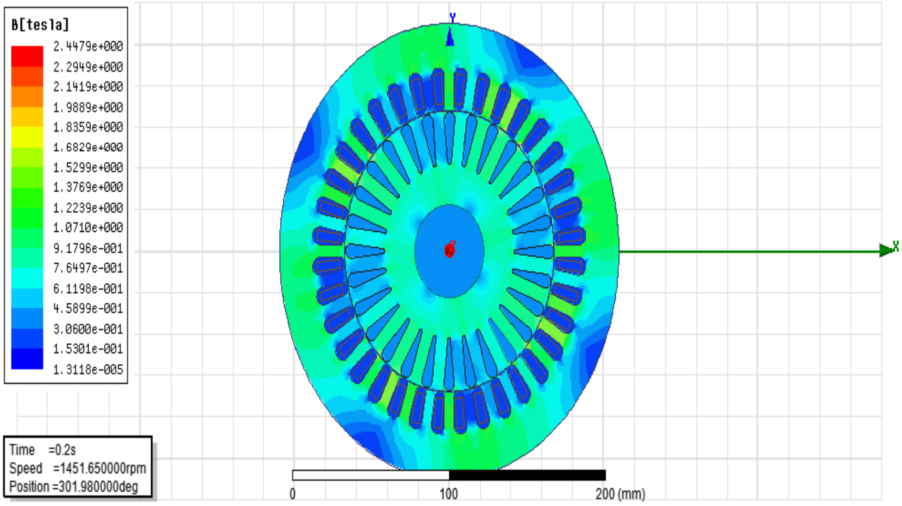

Figure 4.67: Flux density distribution with 34.48% DE

The nominal air gap in designed motor is 0.29. So, for creating 34.48 dynamic eccentricities along x-axis required shift distance is 0.1mm. Figure 4.68 depicts the current density distribution at 34.48 % DE faulty condition.

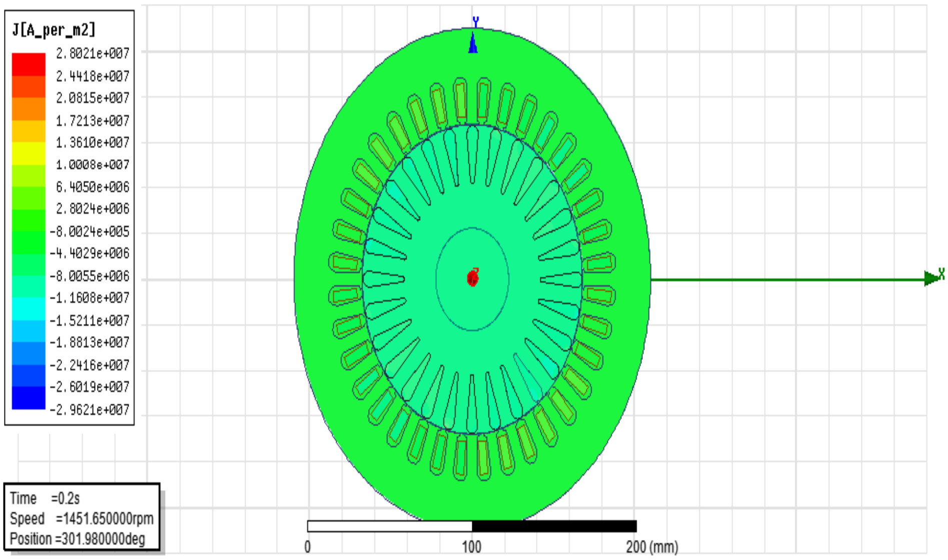

Figure 4.68: Current density distribution with 34.48% DE

The effects of DE fault on FEM model are analyzed by obtaining characteristics parameter of the IM model shown in Figures 4.69, 4.70 and 4.71. Figure 4.69 displays the torque obtained 25.7804Nm with high level of visible distortion. Figure 4.70 shows the stator current 8.1635A with high distortions at the beginning of the running condition. The power obtained at DE fault is shown in Figure 4.71 and its magnitude is 3919.05W.

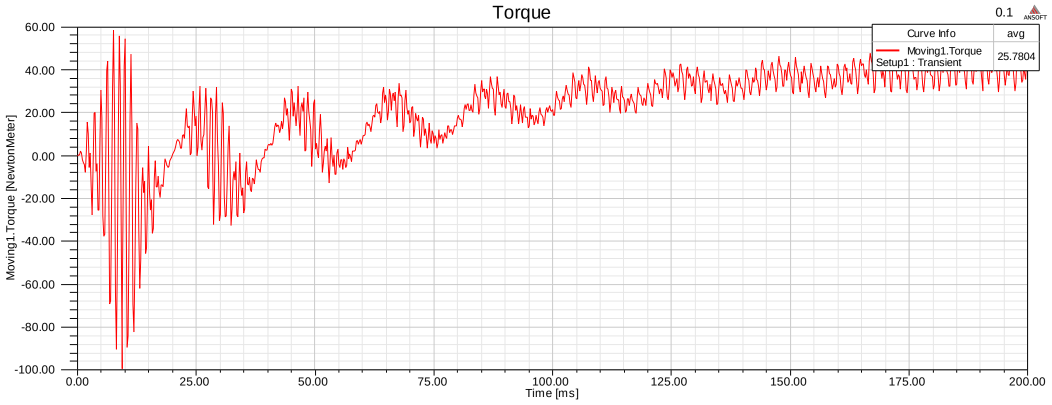

Figure 4.69: Torque response of Induction Motor with 34.48% DE

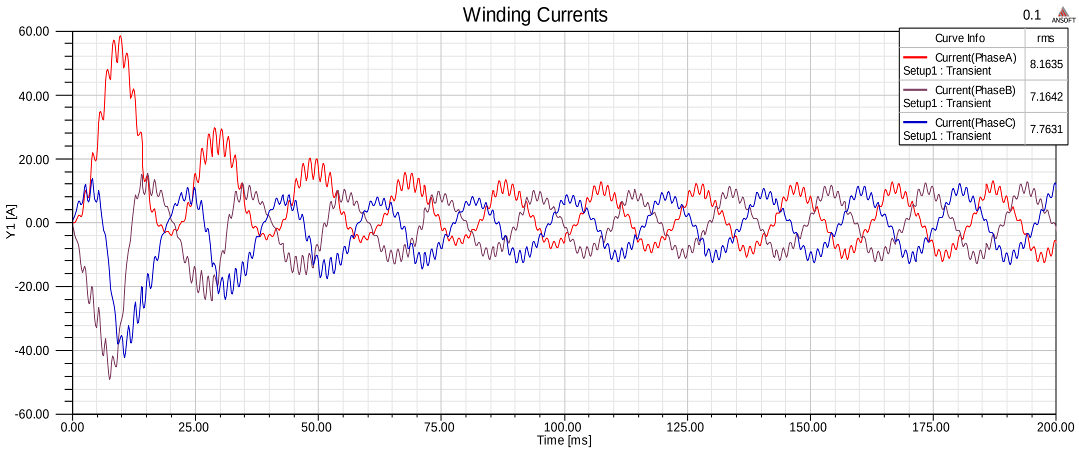

Figure 4.70: Current response of Induction Motor with 34.48% DE

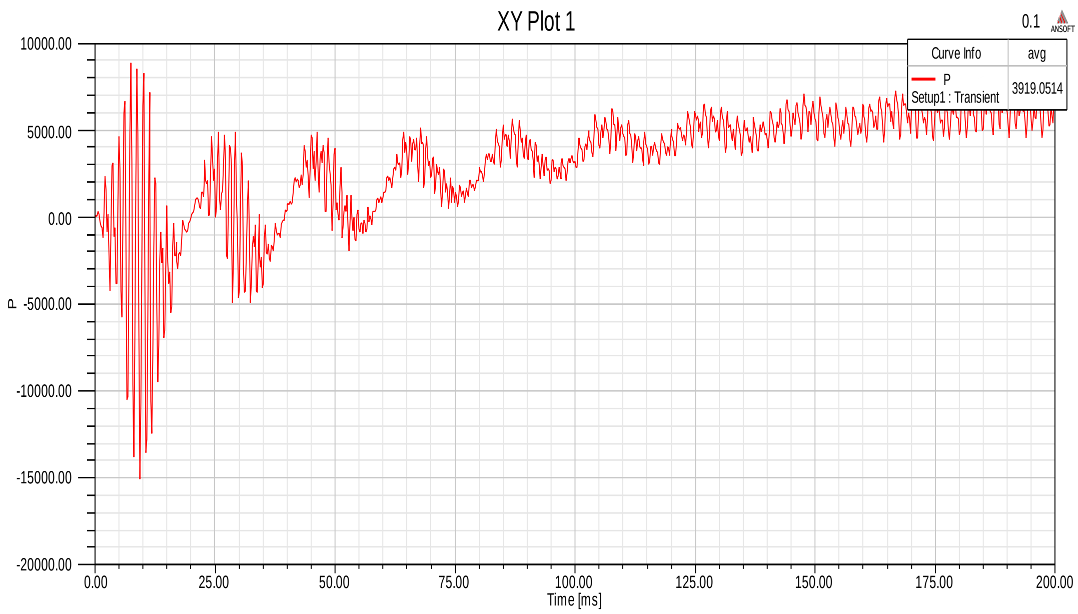

Figure 4.71: Output power response of Induction Motor with 34.48% DE

4.9.2 Induction Motor having Fault Condition with 27.58% Dynamic Eccentricity

In the second eccentric faulty experimentation, the FEM designed model is put under 27.58% DE fault. The model current and magnetic flux densities are shown in Figures 4.72 and 4.73. The nominal air gap in designed motor is 0.29.So, for creating 27.58% dynamic eccentricity along x-axis required shift distance is 0.08mm.

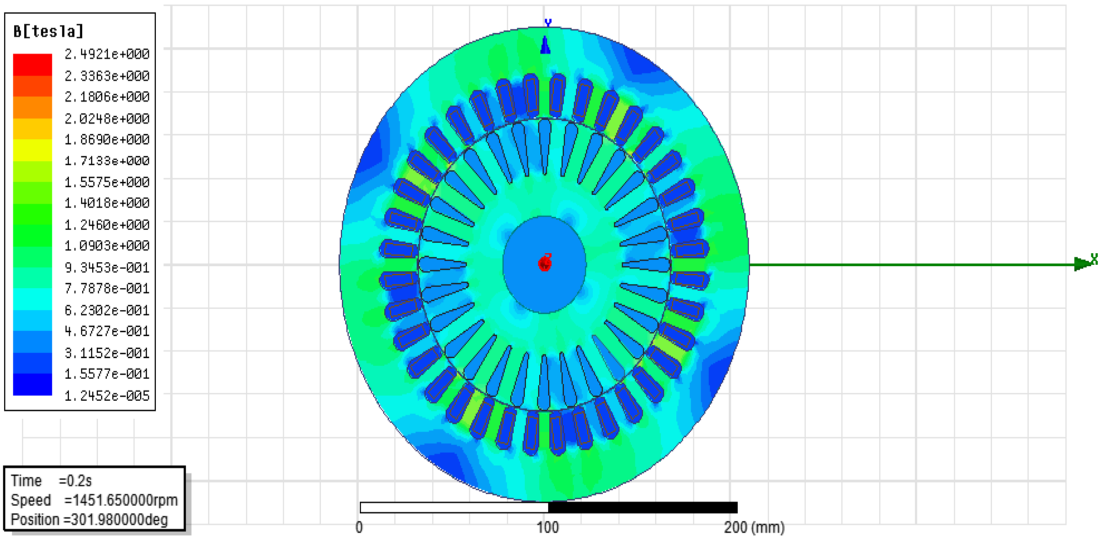

Figure 4.72: Flux density distributions with 27.58% DE

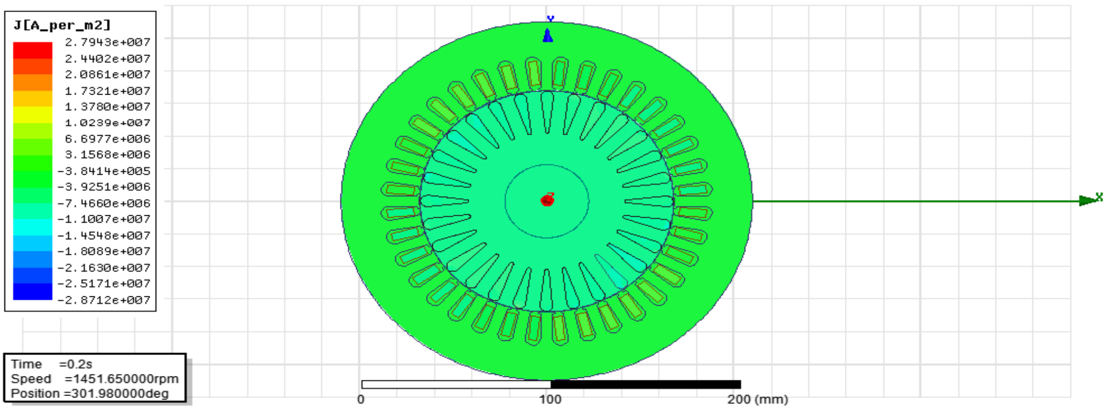

Figure 4.73: Current density distribution with 27.58% DE

The effects of 27.58% DE fault on machine characteristics parameters such as torque, stator current and power are analyzed and are shown in Figures 4.74, 4.75 and 4.76. Figure 4.74 displays the torque produced during 27.58% DE fault. The magnitude of the torque is 25.79Nm. Figure 4.75 illustrates the FEM induction motor model stator current response under normal condition the 3-phase current showing high oscillations and distortion due to the presence of 27.58% DE fault. Figure 4.76 illustrates the average power in watts under 27.58% DE faulty condition. The average power obtained is 3921.89W which is quite lower as compared to the normal operating condition.

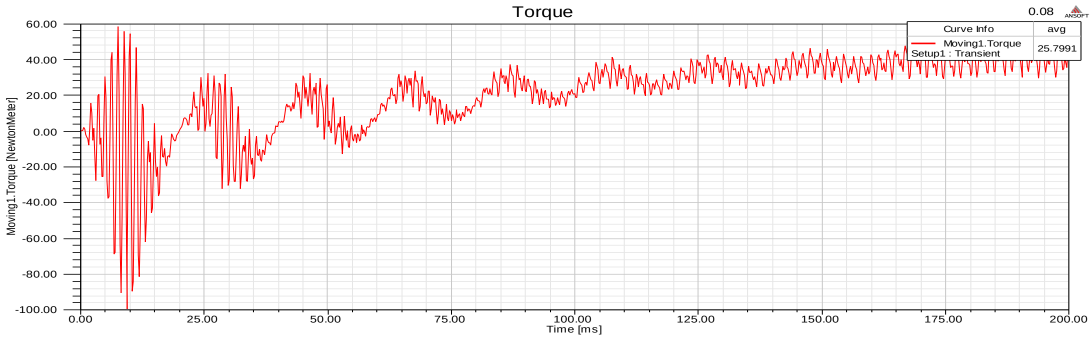

Figure 4.74: Torque response of induction motor with 27.58% DE

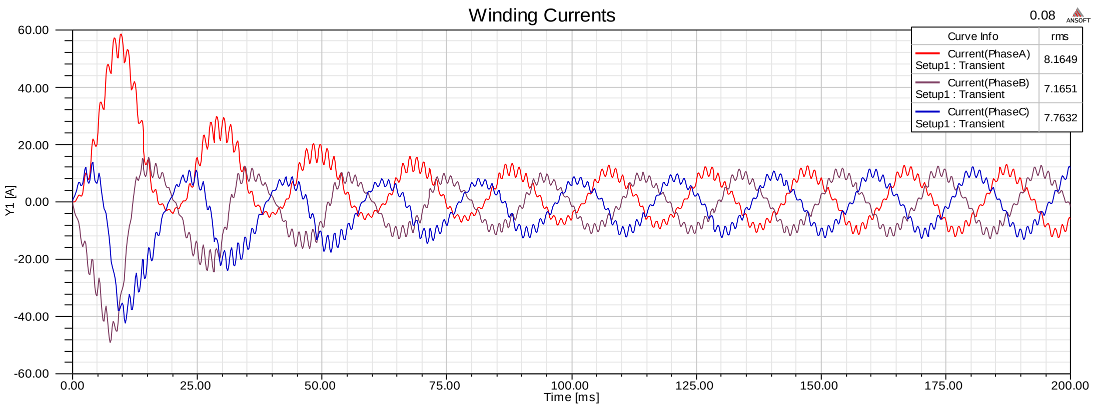

Figure 4.75: Current response of Induction Motor with 27.58% DE

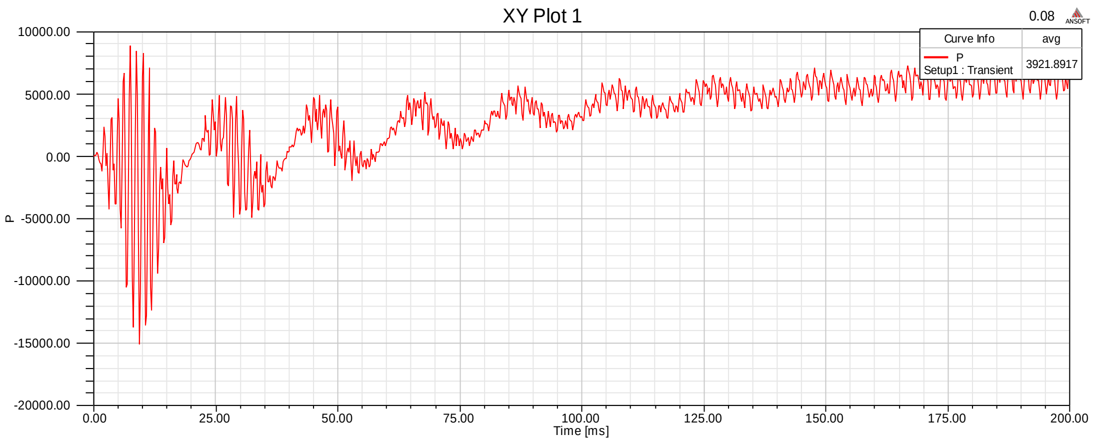

Figure 4.76: Output power response of Induction Motor with 27.58% DE

4.9.3 Induction Motor having Fault Condition with 34.48% Static Eccentricity

The third experimentation is the static eccentric fault generation and its behavior observation. The FEM model is tweaked for 34.48% SE fault, its flux and current density distribution maps are shown in Figures 4.77 and 4.78.

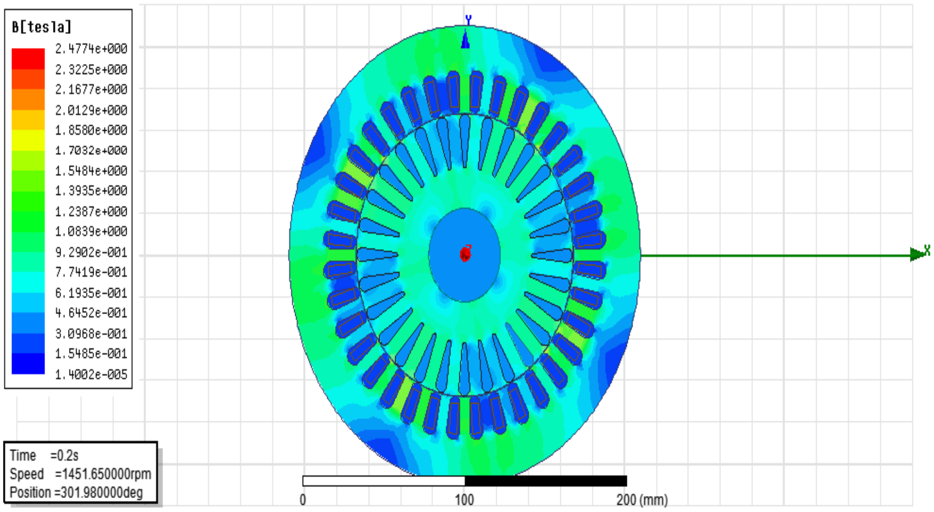

Figure 4.77: Flux density distribution with 34.48% SE

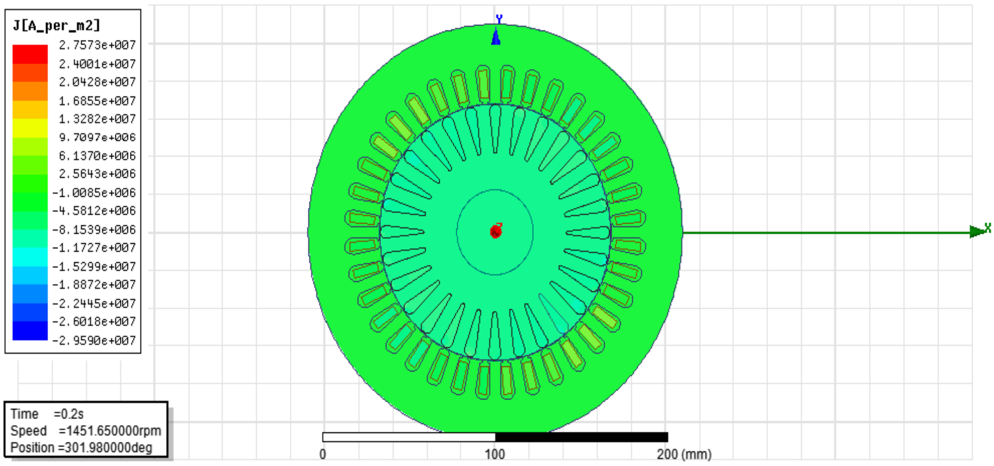

Figure 4.78: Current density distribution with 34.48% SE

The effects of SE fault with 34.48% on the different characteristics parameters of motor are observed are and elaborated in Figures 4.79, 4.80 and 4.81. Figure 4.79 displays the torque developed which is 25.8117 Nm with ripples while in operation. Figure 4.80 displays the distorted current obtained with 8.1660A. Figure 4.81 depicts the power produced which is 3923.7994W which is lower as compared to healthy state power 3927.9849W.

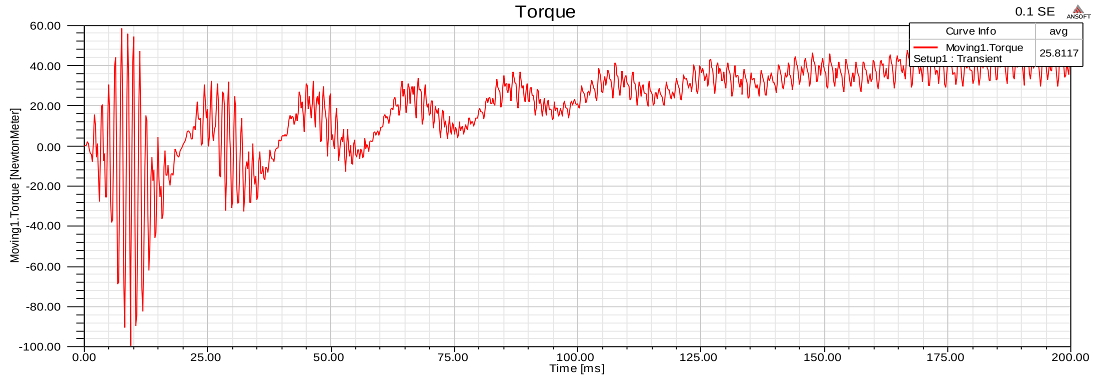

Figure 4.79: Torque response of Induction Motor with 34.48% SE

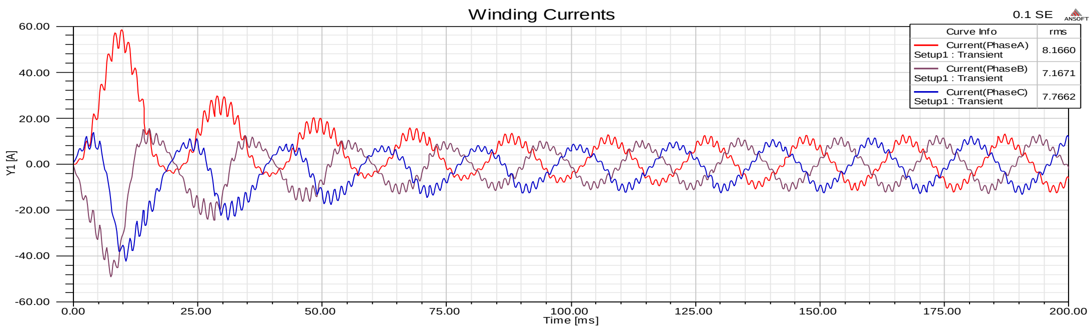

Figure 4.80: Current response of Induction Motor with 34.48%SE

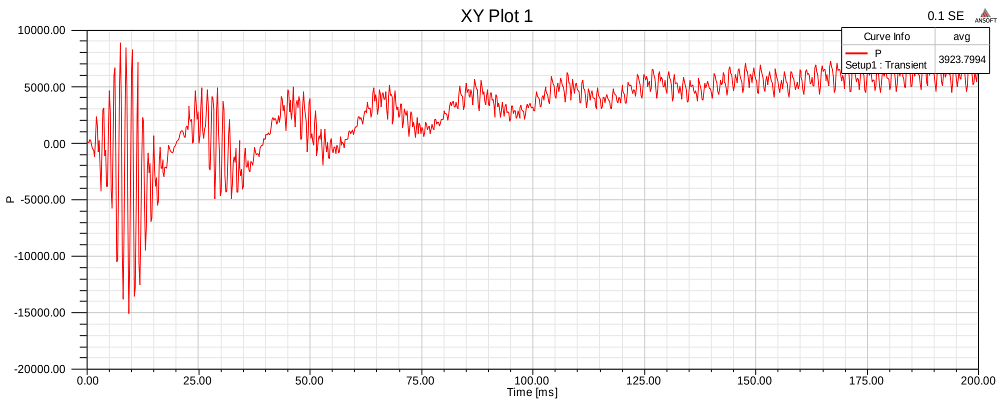

Figure 4.81: Output power response of Induction Motor with 34.48% SE

4.9.4 Induction Motor having Fault Condition with 27.58% Static Eccentricity

The fourth experimentation is the static eccentric fault generation and its behavior observation. The FEM model is tweaked for 27.58% SE fault, its flux and current density distribution maps are shown in Figures 4.82 and 4.83. The flux density graph in Figure 4.82 displays the non-uniformity of the flux in the IM results in wear and tear of the motor.

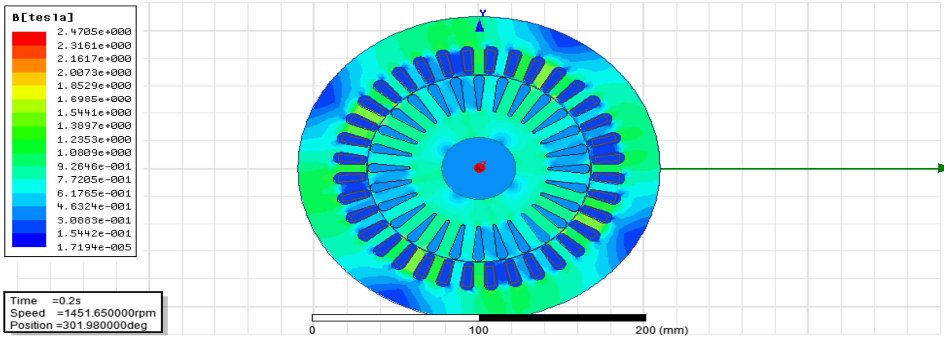

Figure 4.82: Flux density distribution with 27.58% SE

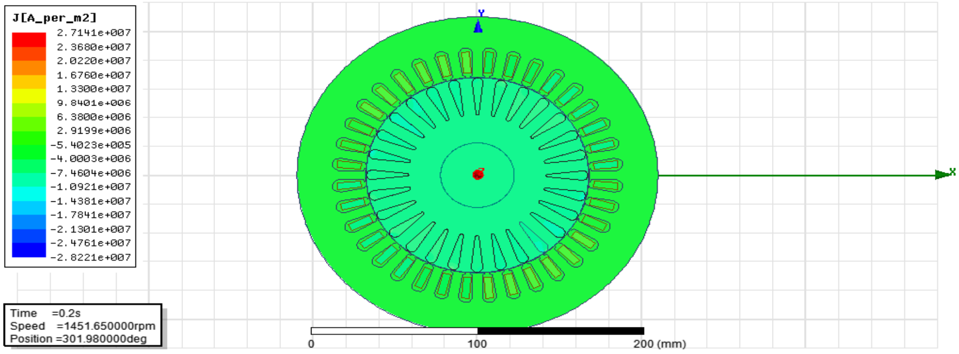

Figure 4.83: Current density distribution with 27.58% SE

The effects of SE fault with 27.58% on the different characteristics parameters of motor are observed are and elaborated in Figures 4.84, 4.85 and 4.86. Figure 4.84 displays the torque developed which is 25.82 Nm with ripples while in operation. Figure 4.85 displays the distorted current obtained with 8.1670 A. Figure 4.86 depicts the power produced which is 3925.65W which is lower as compared to healthy state power 3927.9849W.

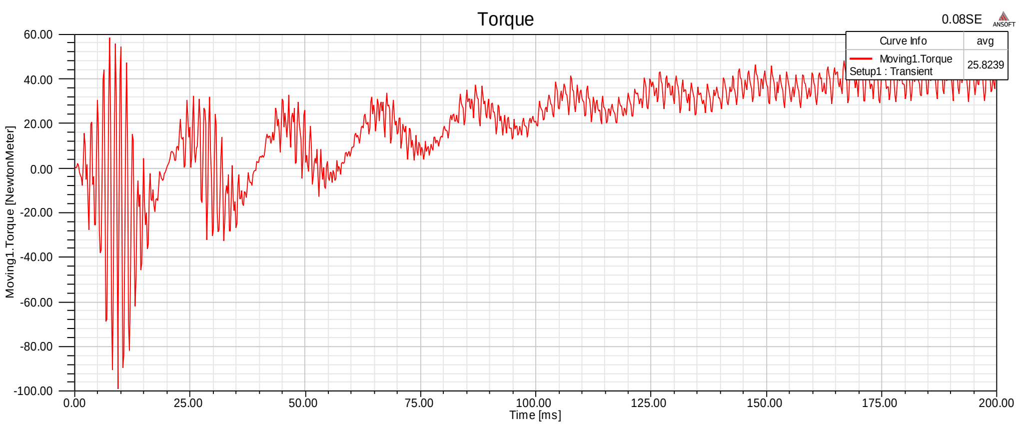

Figure 4.84: Torque response of Induction Motor with 27.58% SE

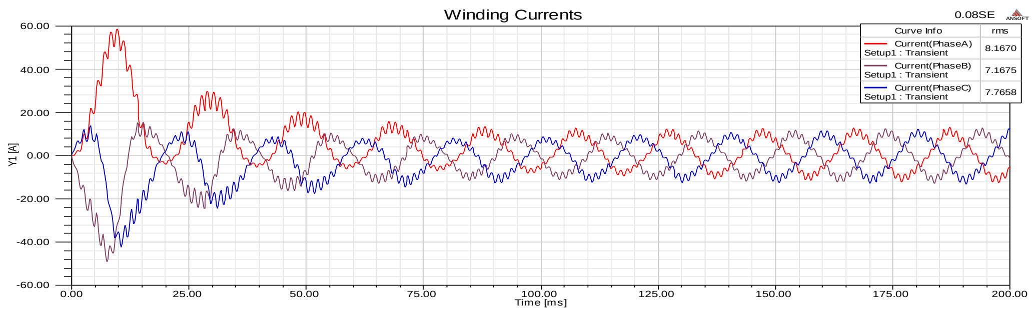

Figure 4.85: Current response of Induction Motor with 27.58%SE

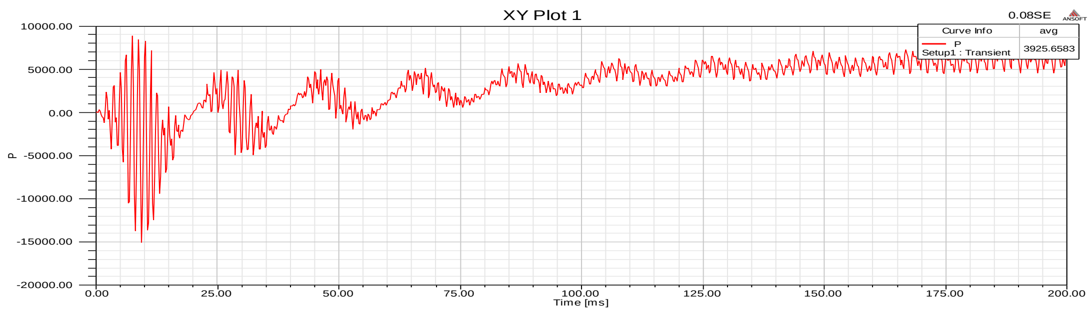

Figure 4.86: Output power response of Induction Motor with 27.58% SE

4.10 RESULTS AND CONCLUSION

The results of IM under different eccentric fault conditions are calculated and compared in the table below where Table 4.7 compares the IM under normal conditions with the two different DE situations and Table 4.8 compares the IM under normal conditions with the two different SE situations. The analysis of above results show that due to non-uniform air gap, flux distortion will occur that causes distortion in torque, flux, voltage and power in terms of fluctuations and mechanical vibrations.

Table 4.7: Comparison table between normal DE conditions with 34.48% and 27.58% variation

Conditions	Normal Conditions	Faulty Conditions	
Parameters	Healthy	34.48% DE	27.58% DE
Magnetic torque Nm (Average)	25.8392	25.7804	25.7991
Stator current A(rms)	8.1644	8.1635	8.1649
Power W (Average)	3927.9849	3919.0514	3921.8917

Table 4.8: Comparison table between normal and SE conditions with 34.48% and 27.58% variation

Conditions	Normal Conditions	Faulty Conditions	
Parameters	Healthy	34.48% SE	27.58% SE
Magnetic torque Nm(Average)	25.8392	25.8117	25.8239
Stator current A (rms)	8.1644	8.1660	8.1670
Power W (Average)	3927.9849	3923.7994	3925.6583

4.11 ECCENTRIC FAULT GENERATION IN MATLAB

The MATLAB model of SCIM as shown in Figure 4.87 is designed to investigate the motor performance under Eccentric fault condition and different combined faults combinations (rotor-stator, stator-eccentric and rotor-eccentric). To extract the features from its stator waveform behavior and apply the deep learning method to detect these faults as soon as they appear in the motor.

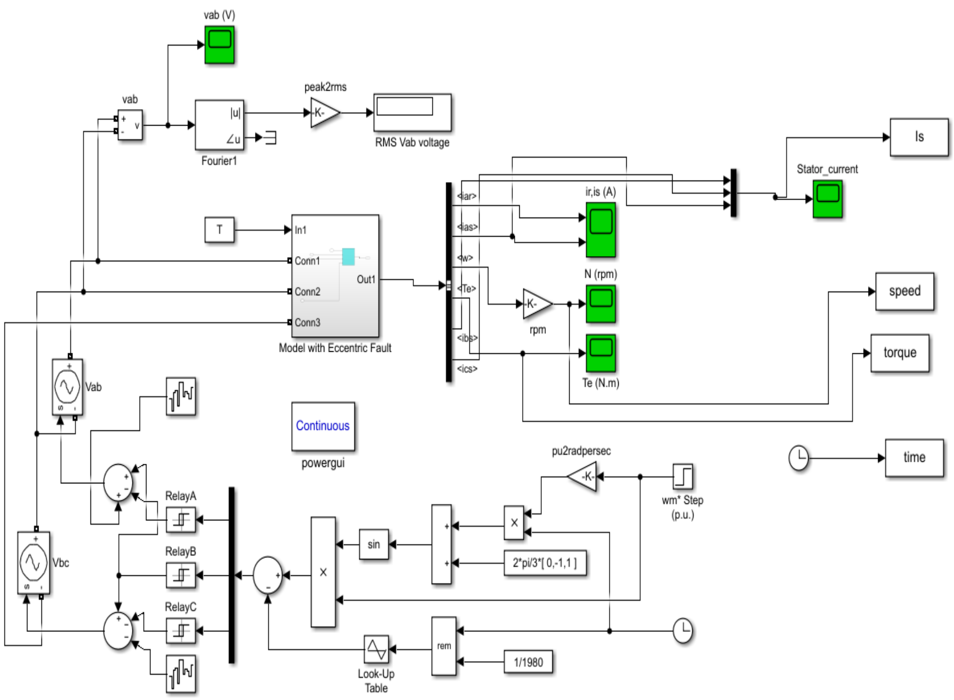

Figure 4.87: Induction motor implementation model with eccentric fault condition

- **Implementation Model of Static Eccentric Fault in SCIM at Full Load**

The MATLAB model with static eccentric fault in SCIM is operated under various loading conditions. The motor characteristics obtained at full load are illustrated in Figure 4.88 and Figure 4.89. Figure 4.88 shows the rotor and stator current and Figure 4.89 shows the torque and speed at the full load torque obtained is 23.04 Nm and speed attained at full load is 1197 rpm.

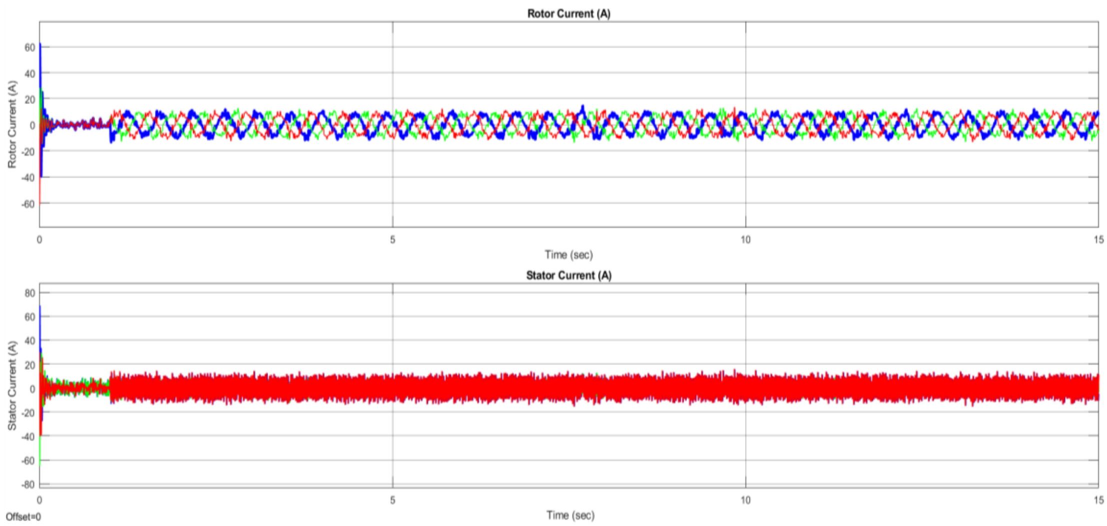

Figure 4.88: Rotor and stator current of static eccentric fault in SCIM at Full load

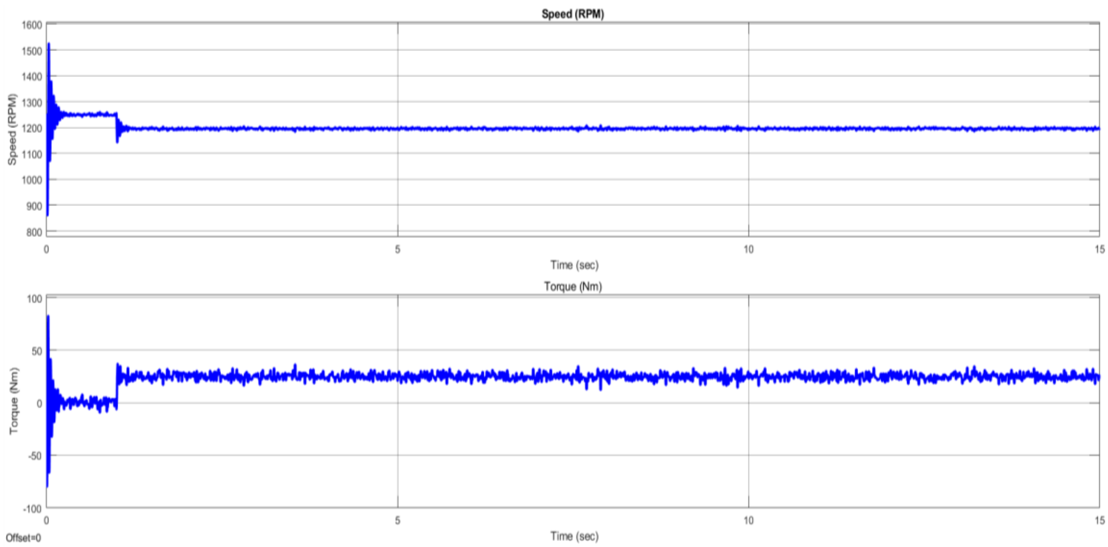

Figure 4.89: Speed and torque of static eccentric fault SCIM at Full load

- **Implementation Model of Static Eccentric Fault in SCIM at 50% Load**

The motor is now set at 50% loading condition and its characteristics obtained briefly illustrated in Figure 4.90 and Figure 4.91. Figure 4.90 shows the rotor and stator current and Figure 4.91 shows the torque and speed at the 50% load. The torque obtained is 10.90 Nm and the speed developed in motor is 1225 rpm. The static eccentric fault degraded the performance of the motor at all loading conditions.

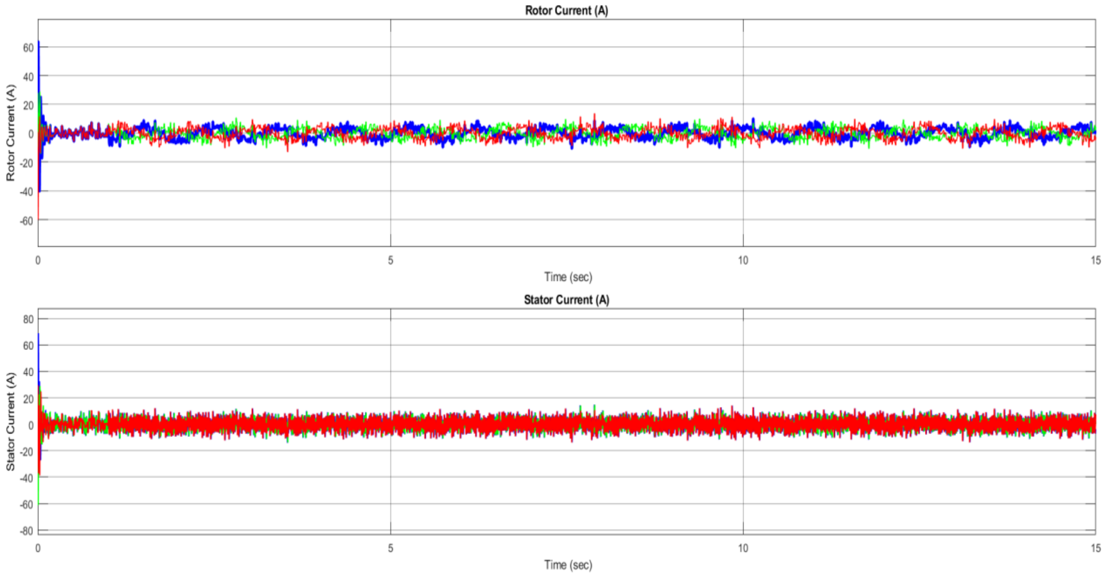

Figure 4.90: Rotor and stator current of static eccentric fault in SCIM at 50% loading

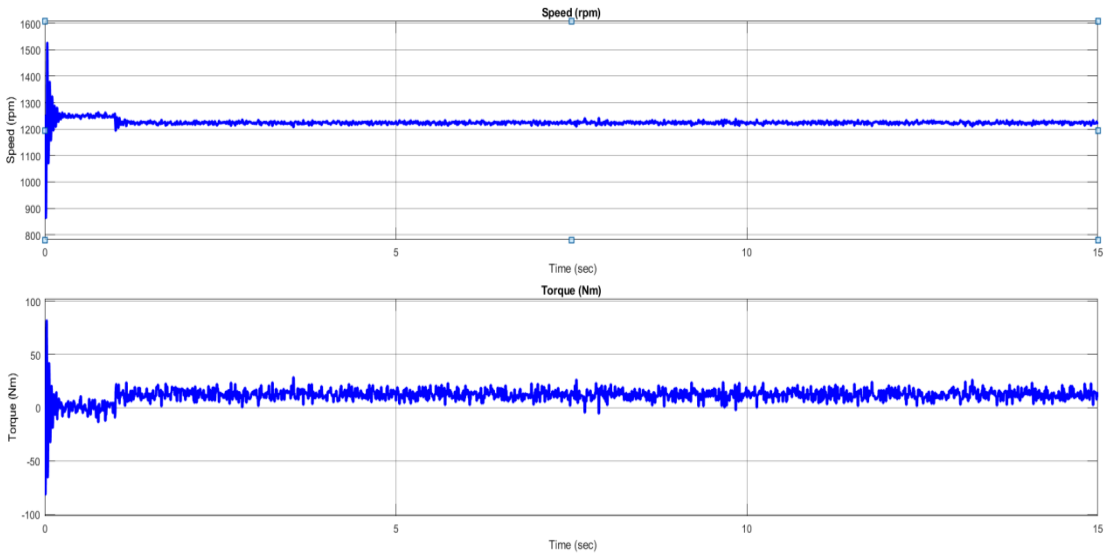

Figure 4.91: Speed and torque of static eccentric fault in SCIM at 50% loading

- **Implementation Model of Static Eccentric Fault in SCIM at 25% Load**

The eccentric faulty MATLAB model of the motor is put at 25% loading condition. Its characteristics obtained at 25% load are illustrated in Figure 4.92 and Figure 4.93. Figure 4.92 shows the rotor and stator current and Figure 4.93 shows the torque and speed. The magnitude of the torque is 4.82 Nm and speed is 1238 rpm. The magnitude of the torque decreases as per the demand load percentage and speed increase due to the decrement of the loading percentage.

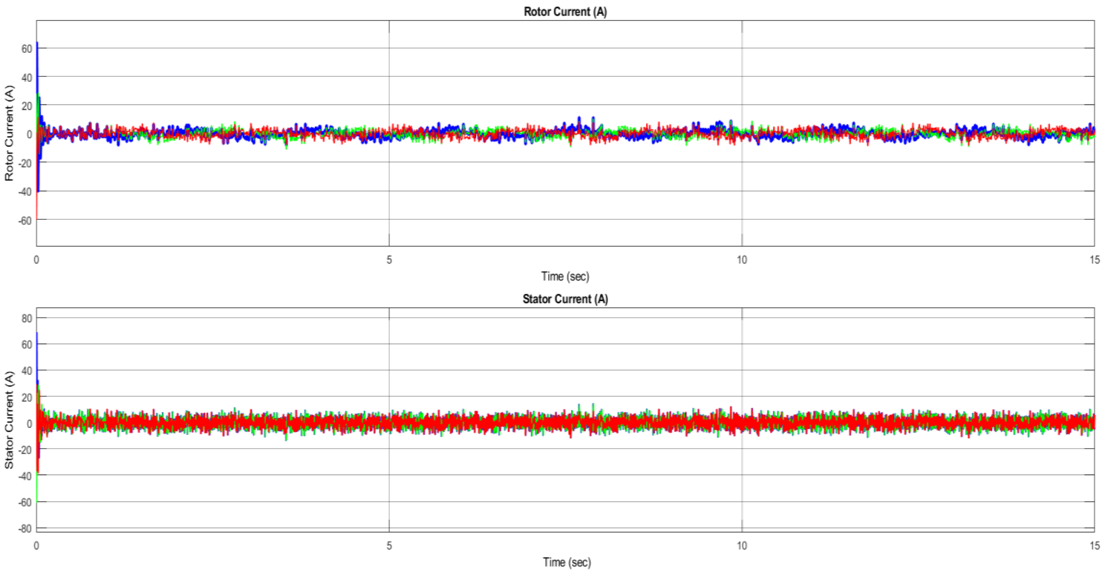

Figure 4.92: Rotor and stator current of static eccentric fault in SCIM at 25% loading

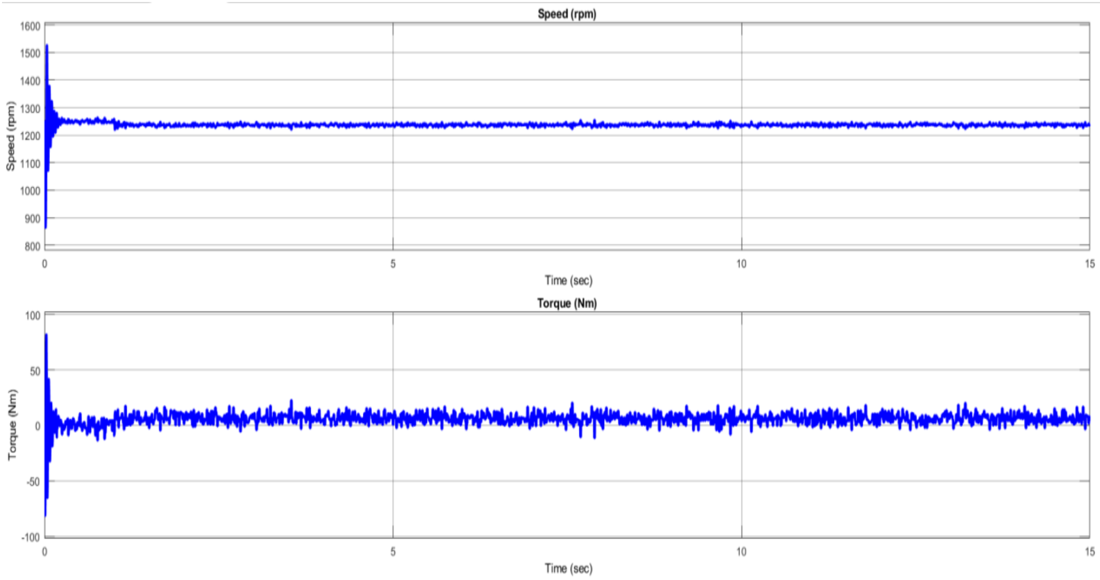

Figure 4.93: Speed and torque of static eccentric fault in SCIM at 25% loading

- **Implementation Model of Static Eccentric Fault in SCIM at No Load**

The eccentric faulty MATLAB model of the motor is put at no load condition. Its characteristics obtained at no load are illustrated in Figure 4.94 and Figure 4.95. Figure 4.94 shows the rotor and stator current and Figure 4.95 shows the torque and speed. The magnitude of the torque is 4.82 Nm and speed is 1238 rpm. The magnitude of the torque decreases as per the demand load percentage and speed increase due to the decrement of the loading percentage.

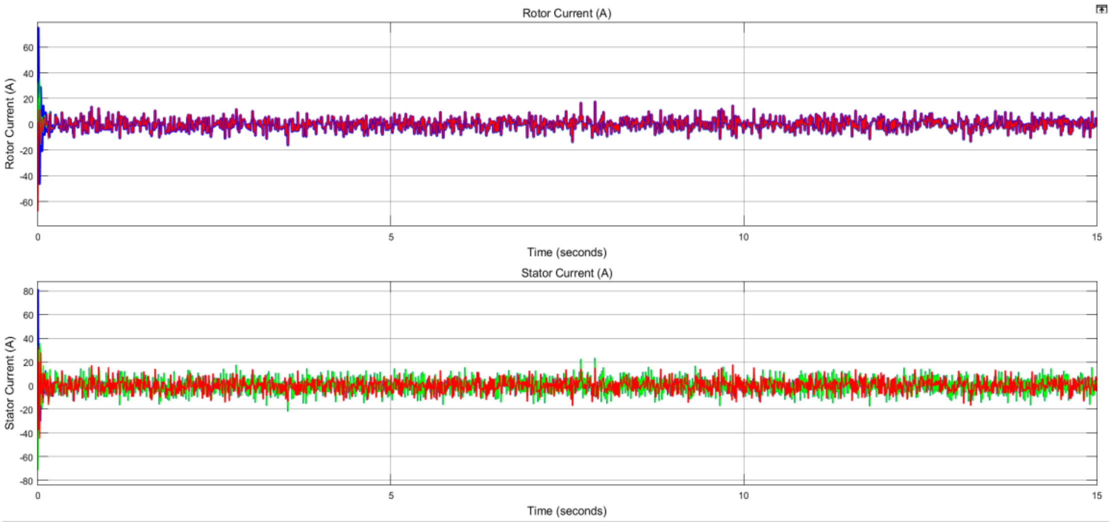

Figure 4.94: Rotor and stator current of static eccentric in fault SCIM at no load

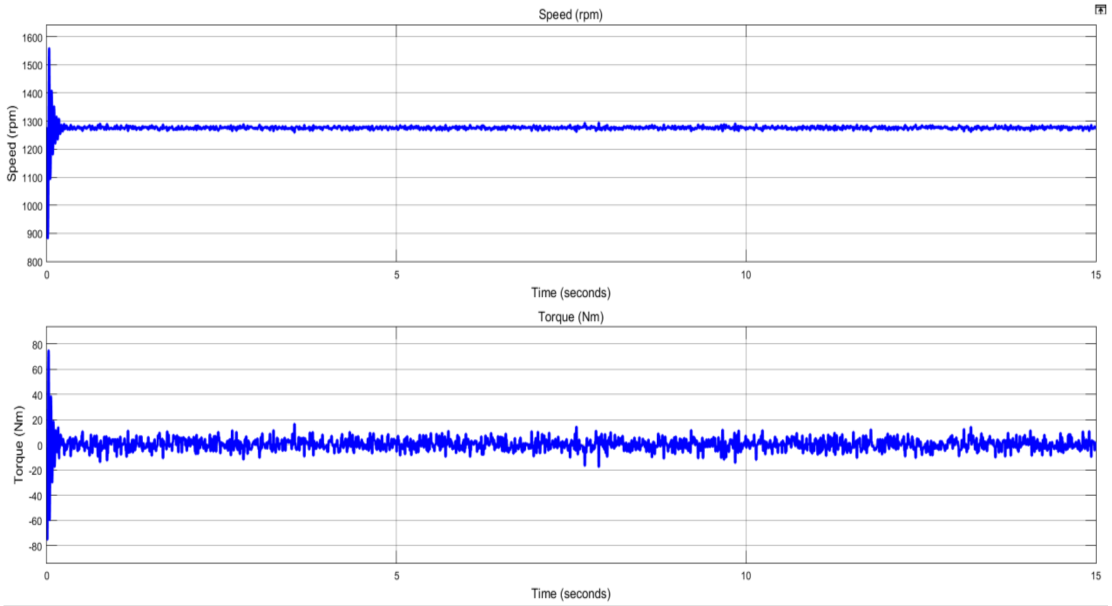

Figure 4.95: Speed and torque of static eccentric fault in SCIM at no load

Table 4.9 summarizes the static eccentric fault motor behavioral characteristics. The torque produced at full load is 23.04 Nm which is lesser as compared to healthy condition output and the speed is 1197 rpm at full load. The designed motor is put under varied loading condition to generate the data for the classification at later stage and to analyze the behavior which will be further utilized to classify the fault type.

Table 4.9: Static eccentric fault SCIM motor speed and torque at different loading conditions

Loading conditions	Torque (Nm)	Speed (rpm)
Full Load	23.04	1197
Half Load	10.90	1225
Quarter Load	4.82	1238

4.12 EFFECTS OF TIME VARYING LOAD ON THE MOTOR UNDER STATIC ECCENTRIC FAULTY CONDITION

The IM was subjected to multiple load variations in continuous operation for 15 seconds, the loads varied are as 0-3 seconds at no load, 3-5 seconds at full load, 5-:8 seconds at 50% load, 8-11 seconds at 25% load, 11-15 seconds at no load

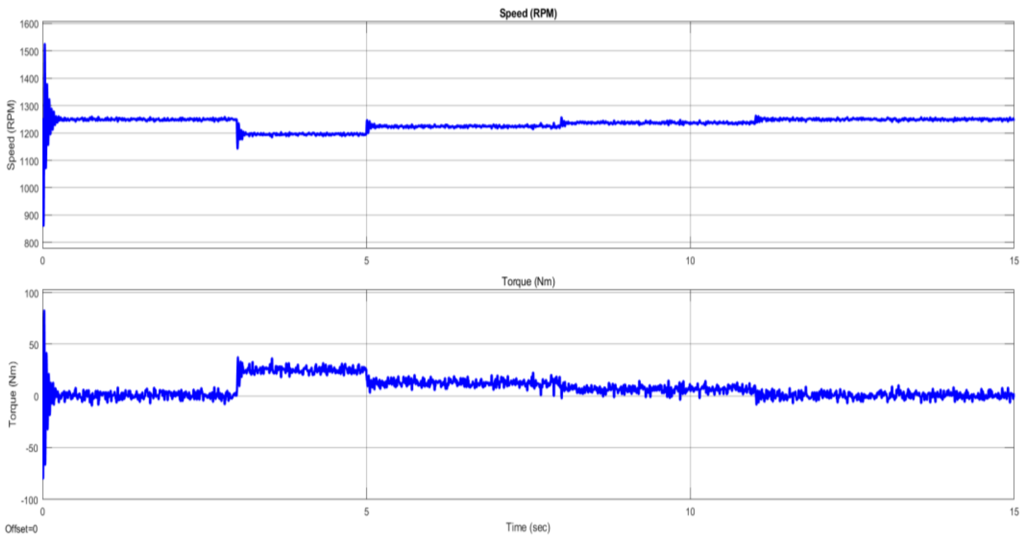

Figure 4.96: IM Torque (Nm) and speed (rpm) of static eccentric condition under time varying loading conditions

The results are presented in Figures 4.96 and 4.97. The variation of speed is shown in Figure 4.96 as the load varies the speed appears to change and striving to reach stability and it can be seen that there is not much of the oscillation during run time apart from initial overshoot that shows the implementation system obtained is stable. The torque varies as per the demand varies can be seen significantly in Figure 4.96 and the stator current and rotor current also got affected with dynamic variation of the load shown in Figure 4.97.

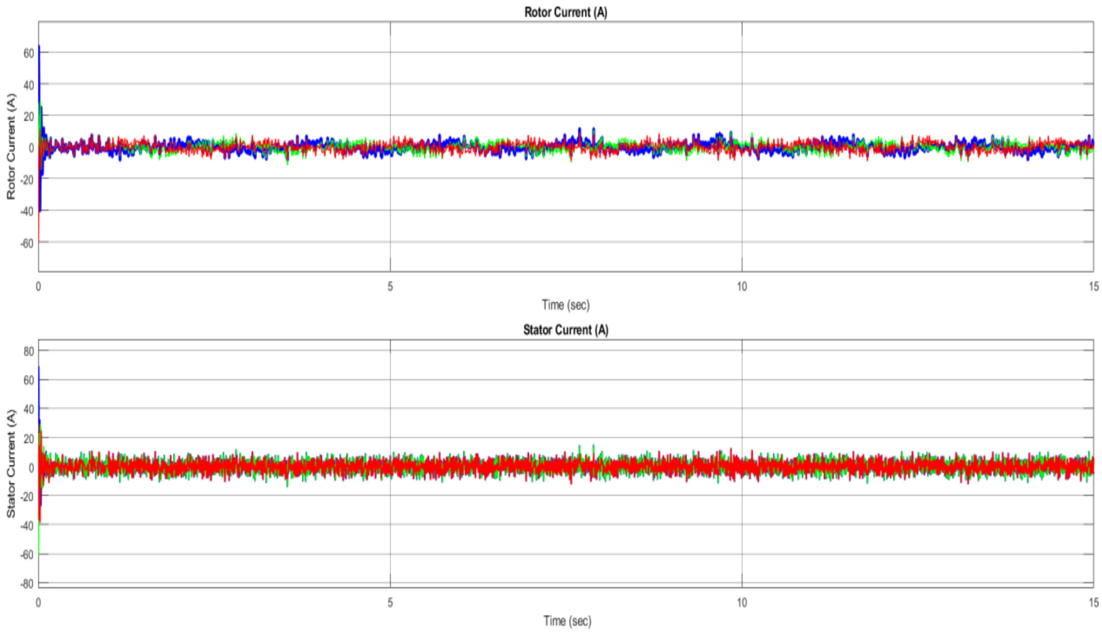

Figure 4.97: IM rotor and stator current (A) of static eccentric condition under time varying loading conditions

4.13 COMBINED FAULT ANALYSIS

In this section, IM is analyzed under various multiple faults conditions. Different combinations of faults are produced in MATLAB model and then their characteristics behaviors are noted and features are calculated under different loading conditions and on the basis of distortion of stator current. The combinations of faults considered are as follows:

- Rotor-Stator combined fault

- Stator-Eccentric combined fault
- Rotor-Eccentric combined fault

4.13.1 Rotor-Stator Combined Fault at Different Loading Conditions

The combined fault in motor is analyzed under varied loading conditions each type of combined fault combination is put under different loading conditions in order to obtain its performance characteristics which will further be utilized as data to extract features for fault detection and classification.

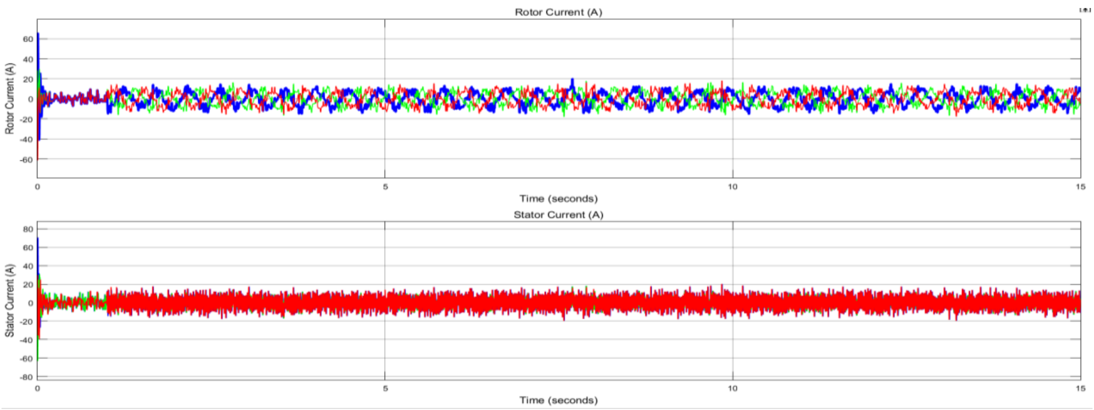

Figure 4.98: IM rotor and stator current (A) under rotor-stator combined fault at 100% loading condition

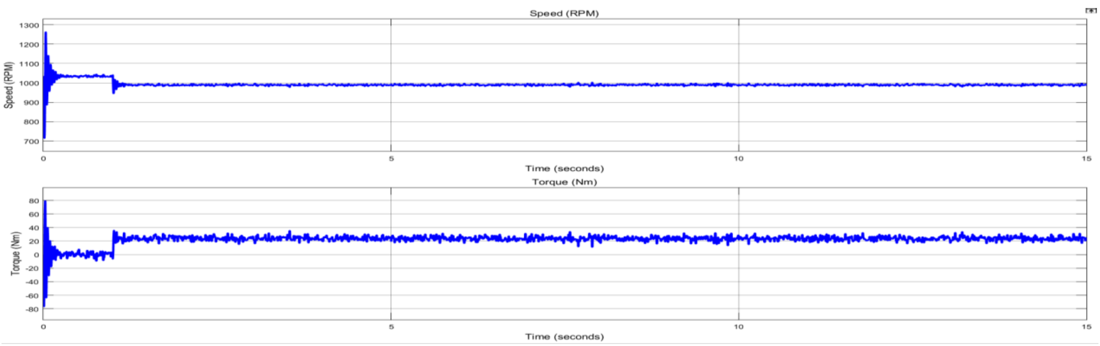

Figure 4.99: IM torque (Nm) and speed (rpm) under rotor-stator combined fault at 100% loading condition

The full load motor parameters are shown in Figures 4.98 and 4.99. Figure 4.98 shows the stator and rotor current at combined fault where the oscillations of the waveforms are at a highest level and it is deviating from being a pure sinusoidal current waveform. The distortion can also be seen in Figure 4.99 depicting the motor torque and speed, this distortion results in the vibration of the motor while running and deteriorating its performance.

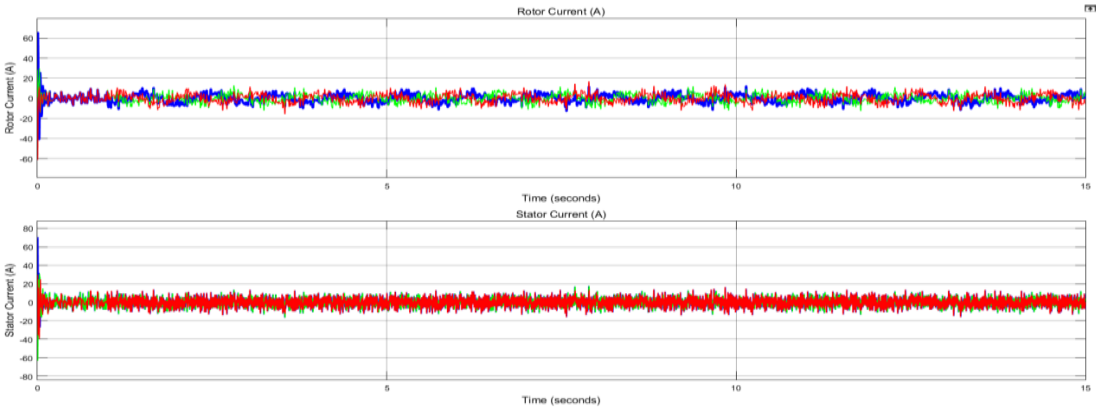

Figure 4.100: IM rotor and stator current (A) under rotor-stator combined fault at 50% loading condition

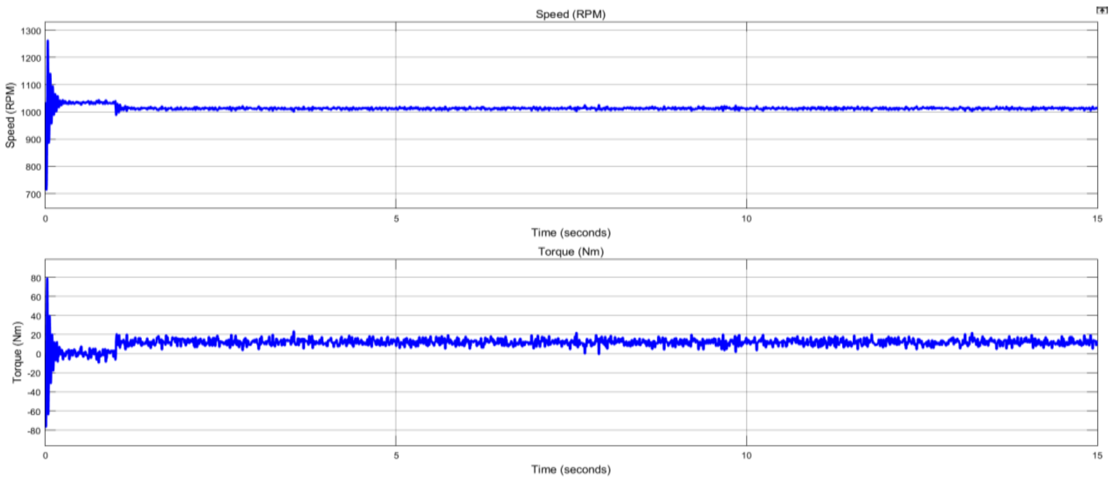

Figure 4.101: IM torque (Nm) and speed (rpm) under rotor-stator combined fault at 50% loading condition

The motor behavior at 50% loading condition is depicted in Figures 4.100 and 4.101. From the Figures, it can be clearly seen that at the combined fault condition the motor is at a peak stress level and not able to move without jerks. The magnitude of torque lower and speed is higher as compared to the full load condition which is justified as per the demand load this varies accordingly. Figures 4.102 and 4.103 depicts the stator and rotor currents, speed and torque respectively at 25 % loading condition. Here, in these the torque 3.98 Nm which is lower as compare to 50% and 100% loading condition and speed is 1025 rpm which is higher as compared to 50% loading speed 1014 and 100 % loading speed 991 rpm. Figures 4.104 and 4.105 represent behavior of motor at no loading condition same as per expected results under no load condition.

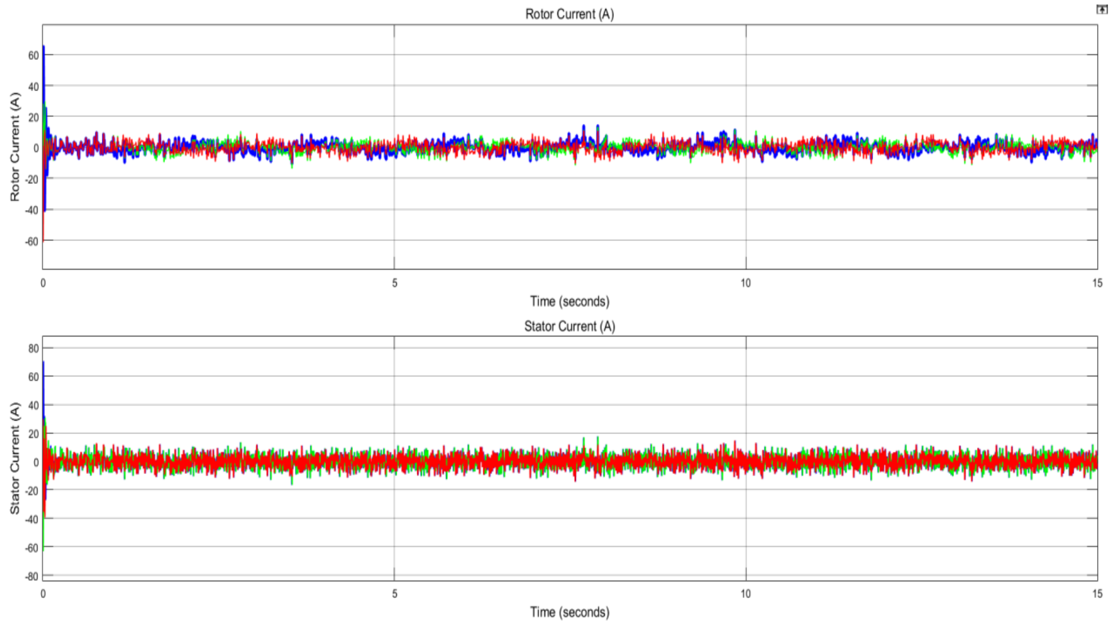

Figure 4.102: IM rotor and stator current (A) under rotor-stator combined fault at 25% loading condition

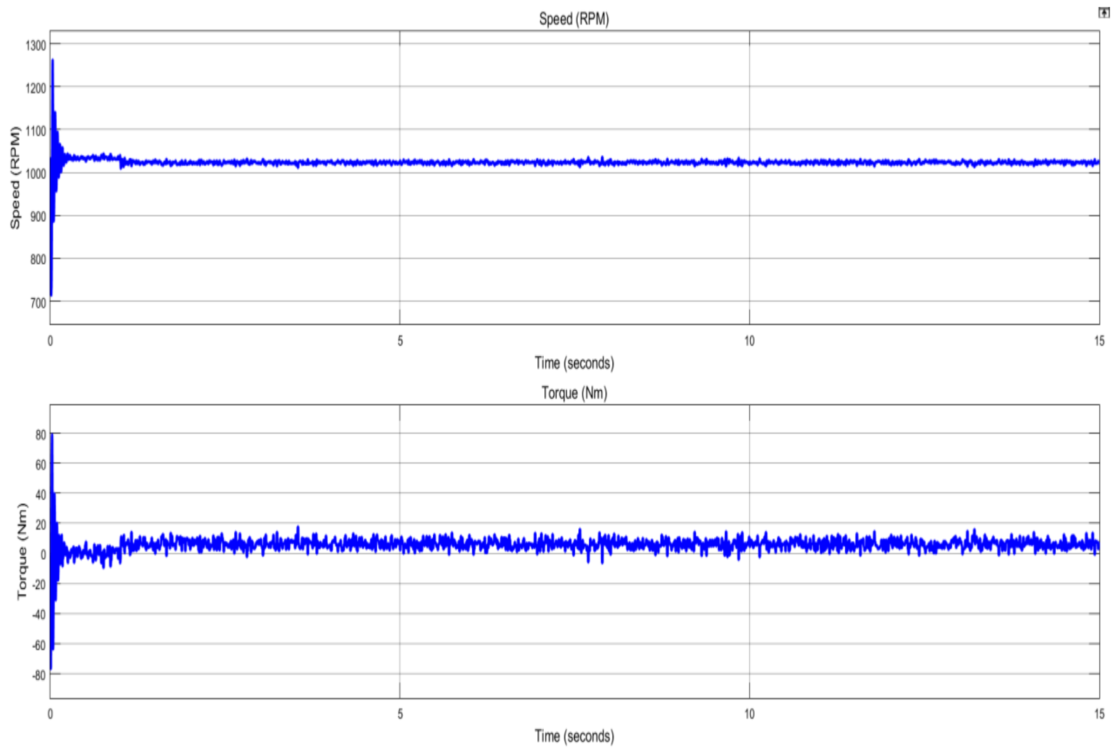

Figure 4.103: IM torque (Nm) and speed (rpm) under rotor-stator combined fault at 25% loading condition

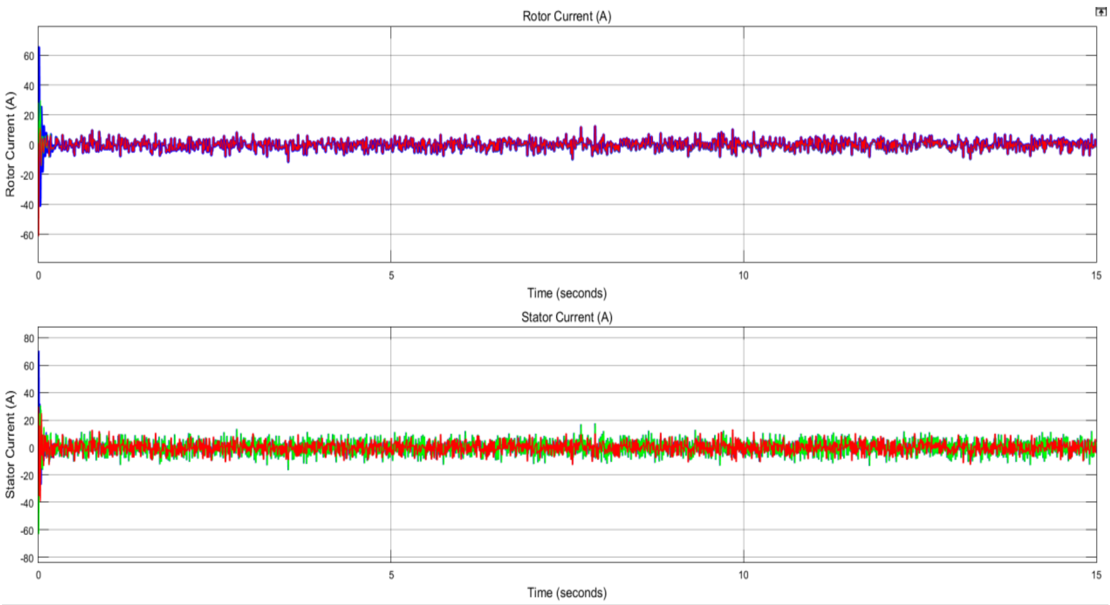

Figure 4.104: IM rotor and stator current (A) under rotor-stator combined fault at no loading condition

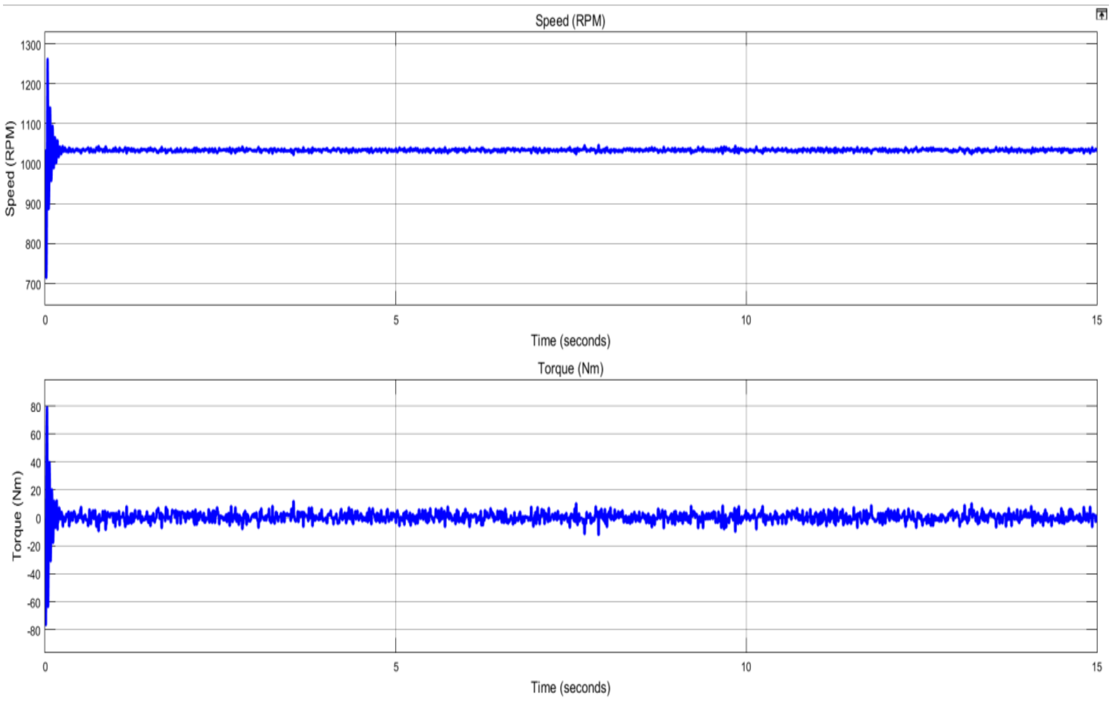

Figure 4.105: IM torque (Nm) and speed (rpm) under rotor-stator combined fault at no loading condition

Table 4.10 illustrating the complete performance of the motor at rotor-stator combined faults, the variation of the speed and torque can be seen and due to the vibration and stress the negative torque is also experienced. The combined fault of rotor-stator has been successfully generated and its characteristics have been obtained. The motor model have shown considerable good results at different constant loading condition validating the model by getting the results as per the theoretical desired values of torque, speed and currents.

Table 4.10: Rotor-stator combined fault SCIM motor speed and torque at different loading conditions

Loading conditions	Torque (Nm)	Speed (rpm)
Full Load	**21.8**	**991**
Half Load	**9.92**	**1014**
Quarter Load	**3.98**	**1025**

4.13.2 Stator-Eccentric Combined Fault at Different Loading Conditions

The IM is put under combined fault combination which is stator-eccentric and its performance under different loading conditions is analyzed. Stator current, rotor current, speed and torque are the parameters on which motor performance is evaluated. Figures 4.106 and 4.107 show the behavior of the IM motor under stator – eccentric combined faulty condition at 100% loading. At 100% loading condition the speed 927.8 rpm which is lowered as compare to rotor-stator combined faulty condition speed 991 rpm. So, the stator-eccentric fault tends to deteriorate the performance more extensively.

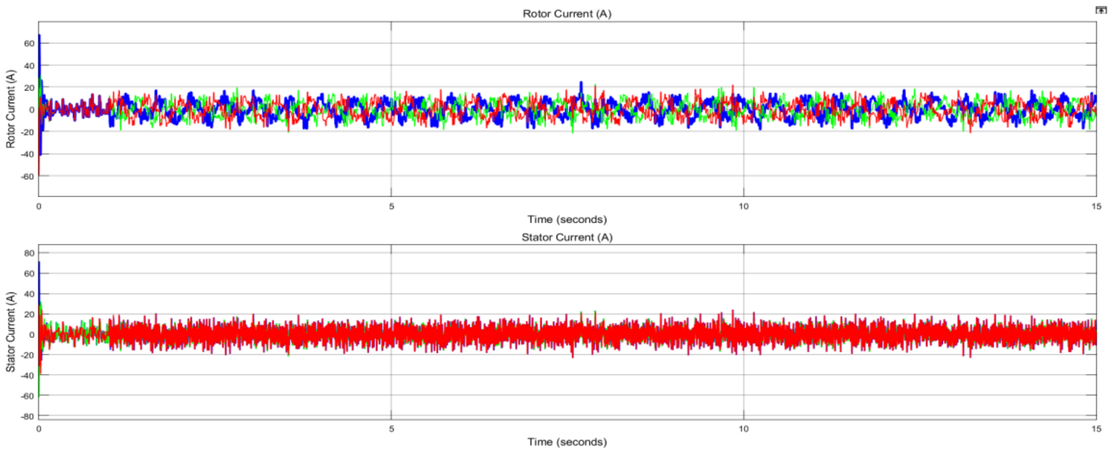

Figure 4.106: IM rotor and stator current (A) under stator- eccentric combined fault at 100% loading condition

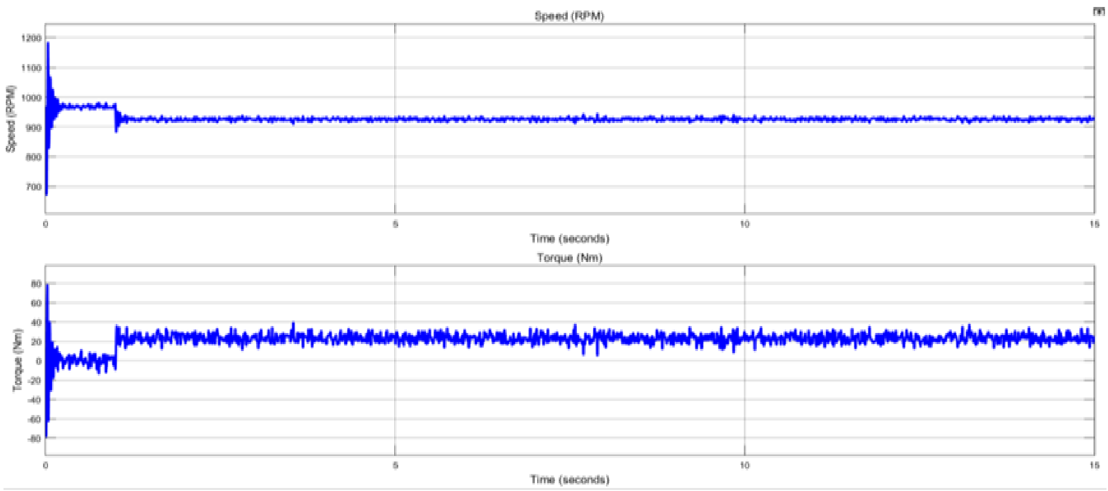

Figure 4.107: IM torque (Nm) and speed (rpm) under stator- eccentric combined fault at 100% loading condition

Figures 4.108 and 4.109 show the behavior of the IM motor under stator – eccentric combined faulty condition at 50% loading. Figure 4.108 displays the rotor and stator currents and Figure 4.109 depicts the speed and torque. Figures 4.110 and 4.111 show the behavior of the IM motor under stator – eccentric combined faulty condition at 25% loading. Figure 4.110 shows rotor and stator at no load and Figure 4.111 depicts the torque and speed no load performance of the motor. Figures 4.112 and 4.113 represent behavior of motor at no loading condition same as per expected results under no load condition.

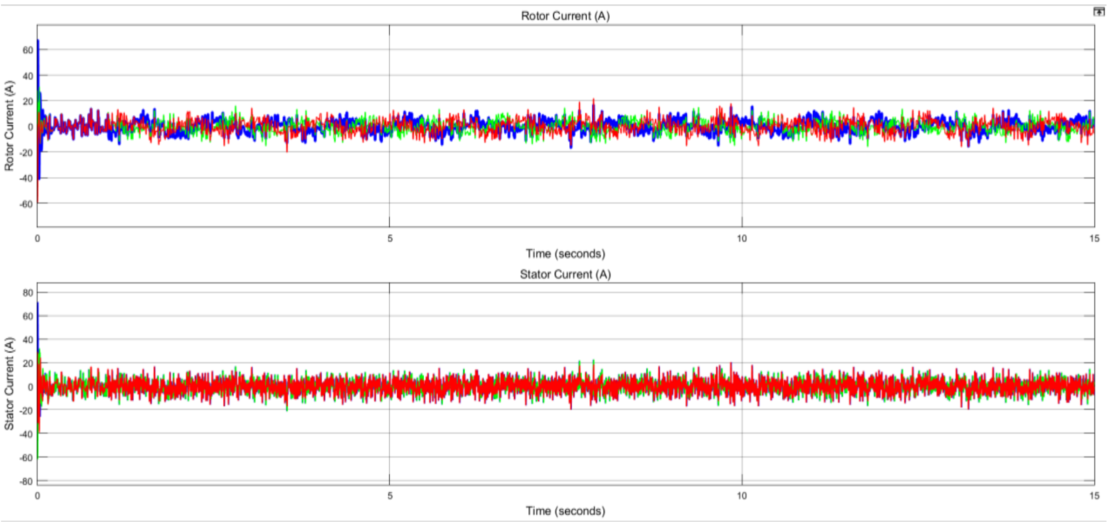

Figure 4.108: IM rotor and stator current (A) under stator- eccentric combined fault at 50% loading condition

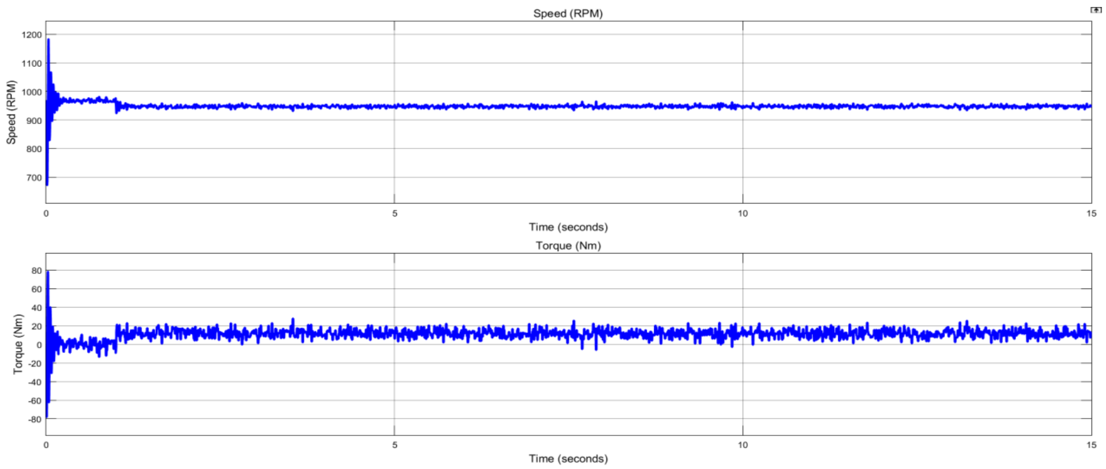

Figure 4.109: IM torque (Nm) and speed (rpm) under stator- eccentric combined fault at 50% loading condition

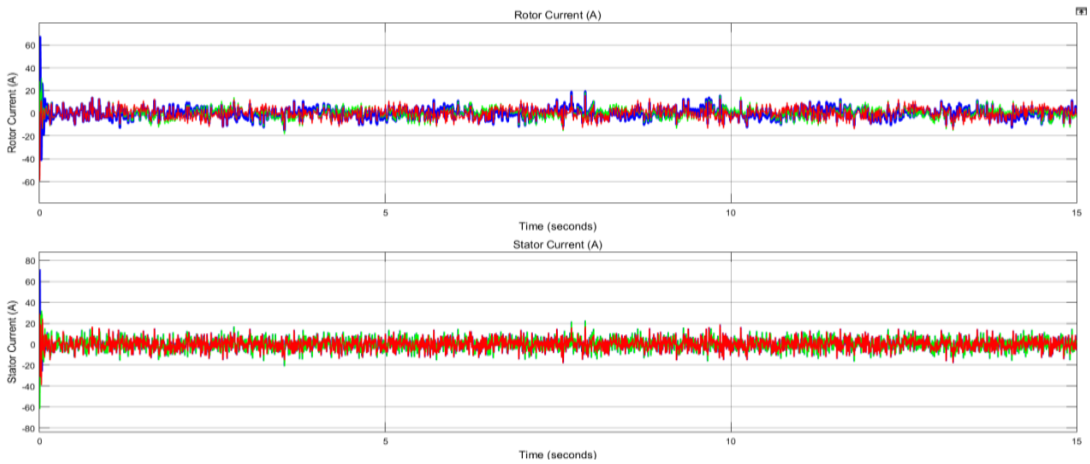

Figure 4.110: IM rotor and stator current (A) under stator- eccentric combined fault at 25% loading condition

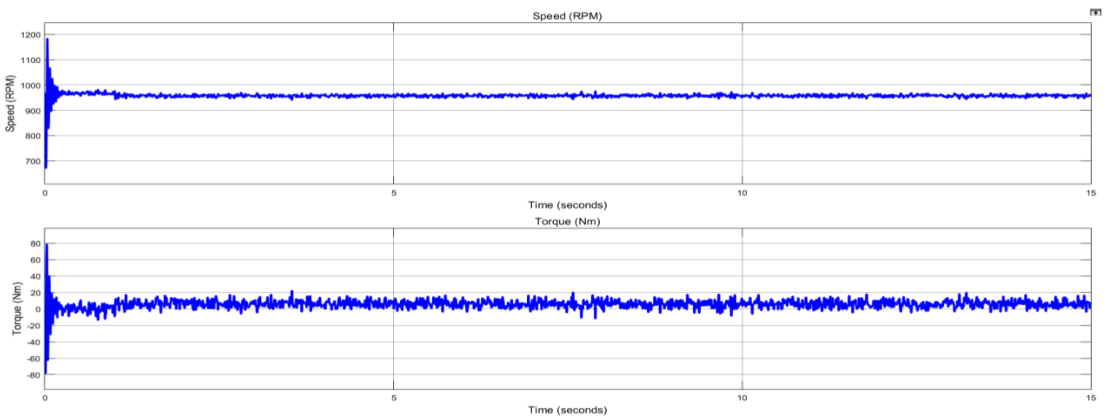

Figure 4.111: IM torque (Nm) and speed (rpm) under stator-eccentric combined fault at 25% loading condition

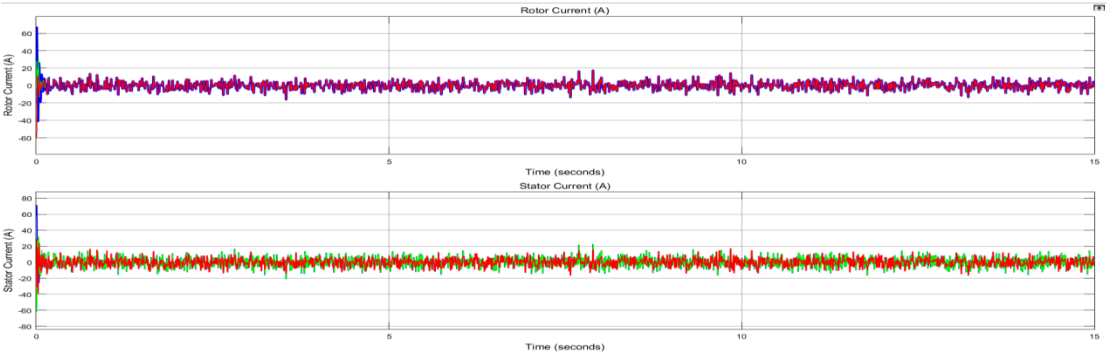

Figure 4.112: IM rotor and stator current (A) under stator- eccentric combined fault at no load condition

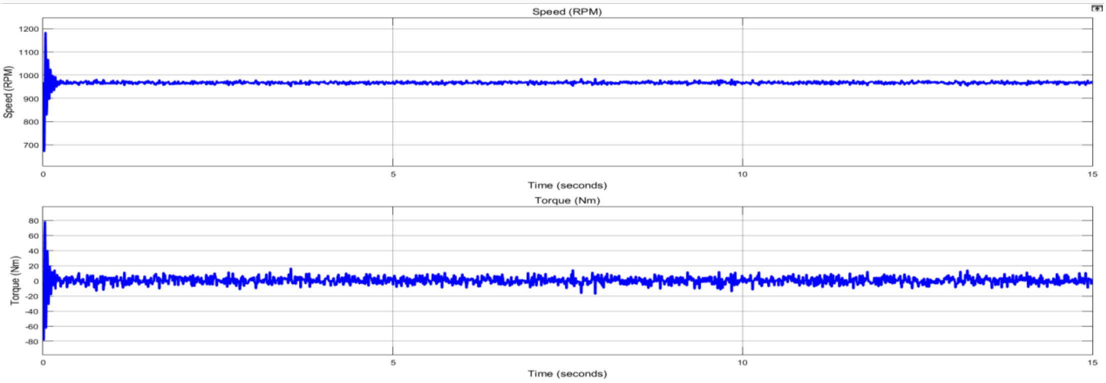

Figure 4.113: IM torque (Nm) and speed (rpm) under stator-eccentric combined fault at no load condition

The IM model have been successfully experimented with another combined fault i.e. stator-eccentric at different constant loading conditions and all of its parameters like speed and torque have been obtained at full, half, and quarter load are shown in Table 4.11.

Table 4.11: Stator-eccentric combined fault SCIM motor speed and torque at different loading conditions

Loading conditions	Torque (Nm)	Speed (rpm)
Full Load	**20.71**	**927.8**
Half Load	**9.37**	**948.7**
Quarter Load	**3.69**	**958.8**

4.13.3 Rotor-Eccentric Combined Fault at Different Loading Conditions

Third experimentation is done with rotor-eccentric combination of fault, where motor is put under both the faults at the same time in the implementation model of MATLAB. Figures 4.114 and 4.115 shows the behavior of the IM motor under rotor – eccentric combined faulty condition at 100% loading. Figures 4.116 and 4.117 show the behavior of the IM motor under rotor – eccentric combined faulty condition at 50% loading. Figures 4.118 and 4.119 display the effect on parameters at 25 % loading whereas Figures 4.120 and 4.121 show the results of motor parameters at no load condition.

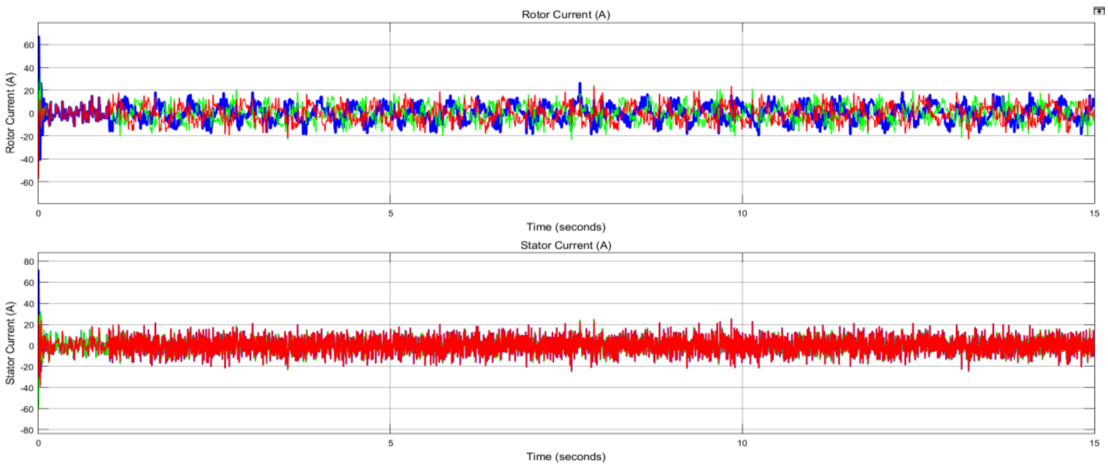

Figure 4.114: IM rotor and stator current (A) under rotor- eccentric combined fault at 100% loading condition

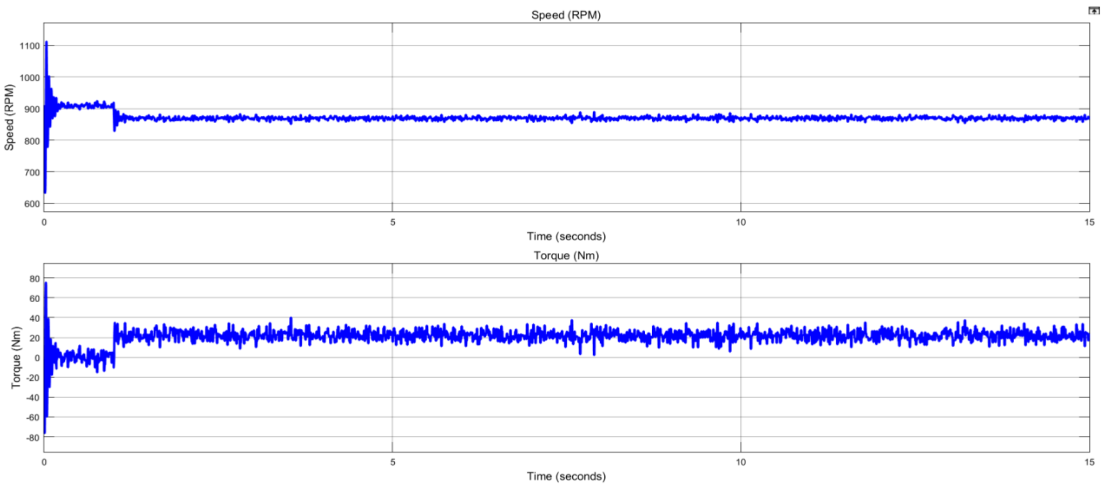

Figure 4.115: IM torque (Nm) and speed (rpm) under rotor- eccentric combined fault at 100% loading condition

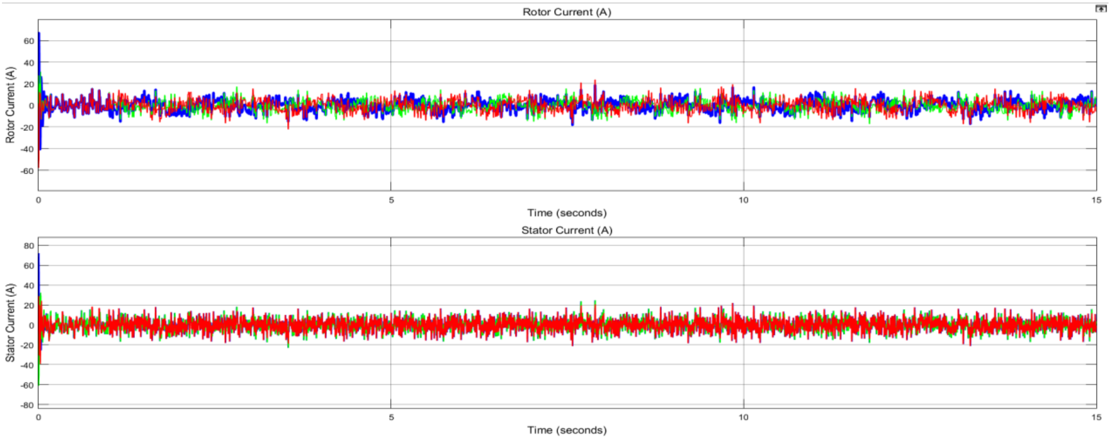

Figure 4.116: IM rotor and stator current (A) under rotor- eccentric combined fault at 50% loading condition

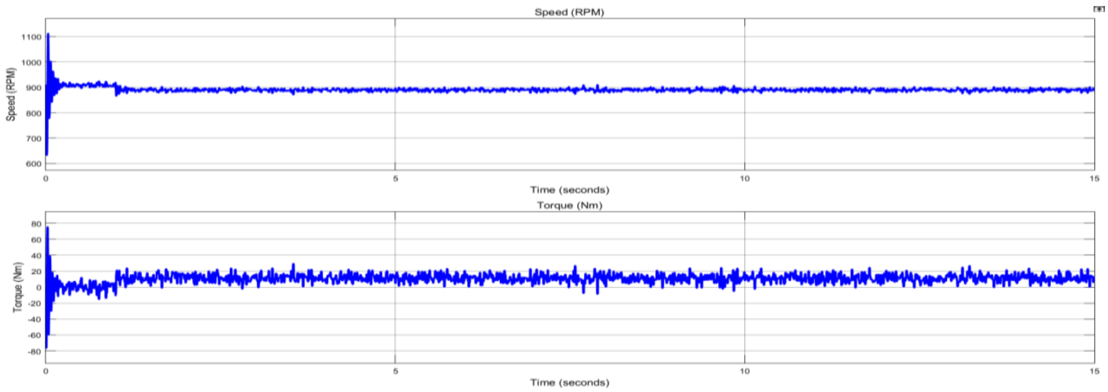

Figure 4.117: IM torque (Nm) and speed (rpm) under rotor- eccentric combined fault at 50% loading condition

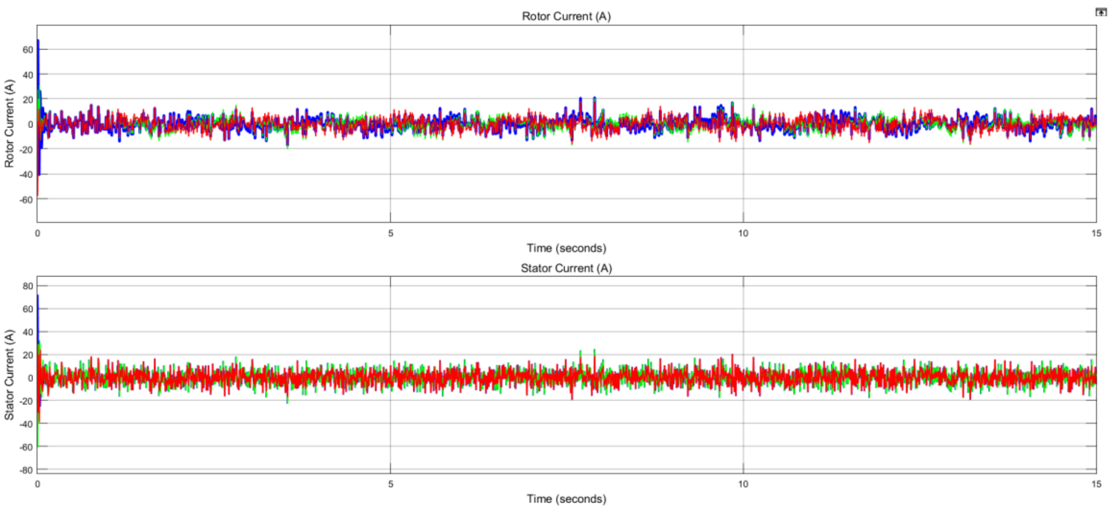

Figure 4.118: IM rotor and stator current (A) under rotor- eccentric combined fault at 25% loading condition

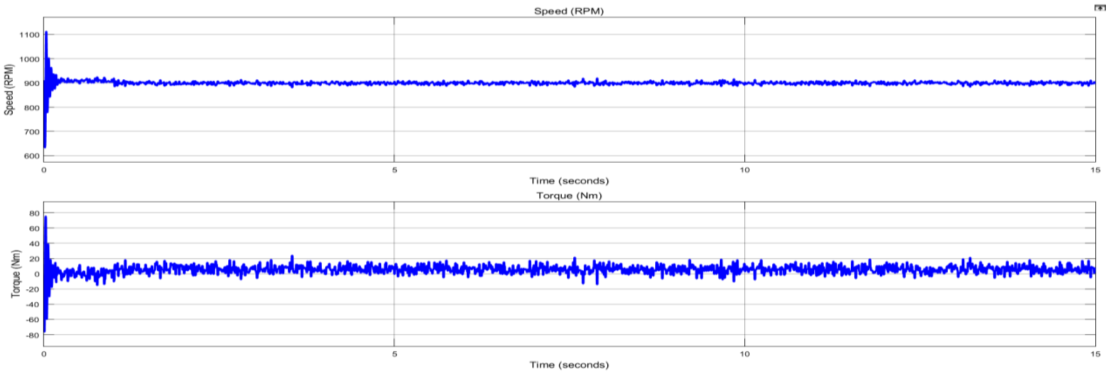

Figure 4.119: IM torque (Nm) and speed (rpm) under rotor-eccentric combined fault at 25% loading condition

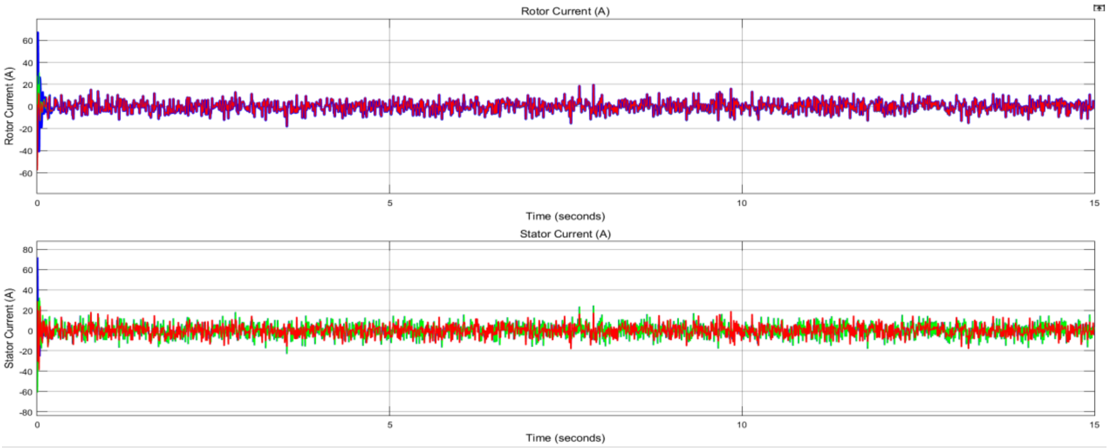

Figure 4.120: IM rotor and stator current (A) under rotor- eccentric combined fault at no load condition

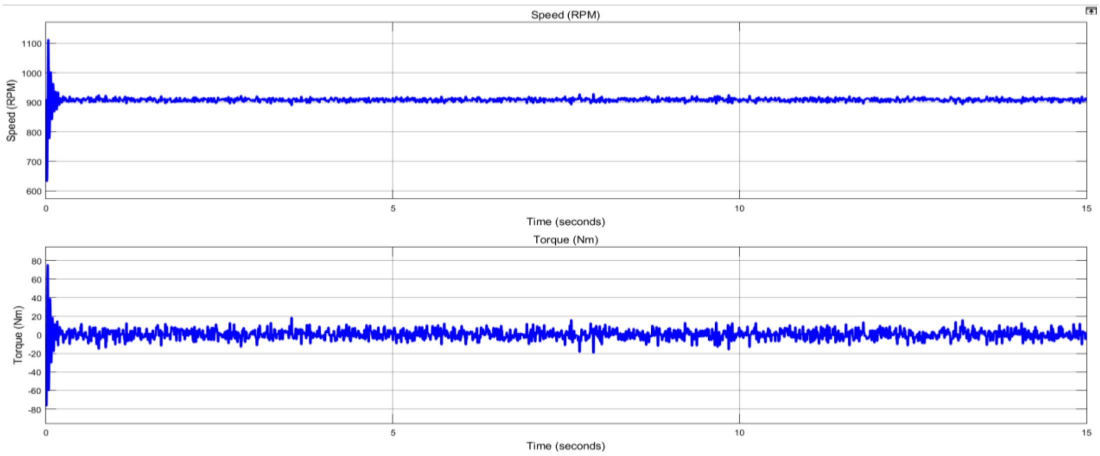

Figure 4.121: IM torque (Nm) and speed (rpm) under rotor-eccentric combined fault at no load condition

The combined faults have been easily identified in the MATLAB implemented model and the results obtained should further be used for the feature extraction process that would further be utilized to implement the automated detection of combined faulty condition in the motor at runtime.

Table 4..12: Rotor-eccentric combined fault SCIM motor speed and torque at different loading conditions

Loading conditions	Torque (Nm)	Speed (rpm)
Full Load	**19.35**	**872**
Half Load	**8.54**	**892.5**
Quarter Load	**3.13**	**902**

Table 4.12 illustrates the rotor-eccentric combined fault SCIM motor speed and torque at different loading conditions. The motor speed reduced down to 872 rpm at full load condition. The combined fault affected the motor performance as the normal speed is quite low as compared to the normal healthy condition performance of the motor. Furthermore, occurrence of fault identification with classification of its type using deep learning and machine learning techniques with its type would be implemented which was not done earlier, this research work occupying this research gap considering the combined fault for the detection and classification.

4.13.4 Combined Fault under Time Varying Loading Condition

The experimentation of time varying loading effect on different combined faulty motor has been performed in MATLAB and its characteristics parameters have been identified. For the investigation the motor is operated for 15 seconds and after every 3 seconds interval the demand load is varied as follows 0-3 seconds it’s no load, 3-5 seconds its 100 % load, 8-11 seconds its 50% load and 11-13 seconds its 25% load and for 13-15 seconds it’s no load. The stability of the motor can be observed from the Figures 4.122 , 4.123, 4.124 and 4.125 which depict the healthy and combined faults torque and speed variations of rotor-stator, stator-eccentric and rotor-eccentric respectively. As the load demands increases torque tends to increase and speed tends to decrease due to the stress on the motor, this conventional behavior of motor is completely depicted in the entire time varying Figures 4.122, 4.123, 4.124 and 4.125.

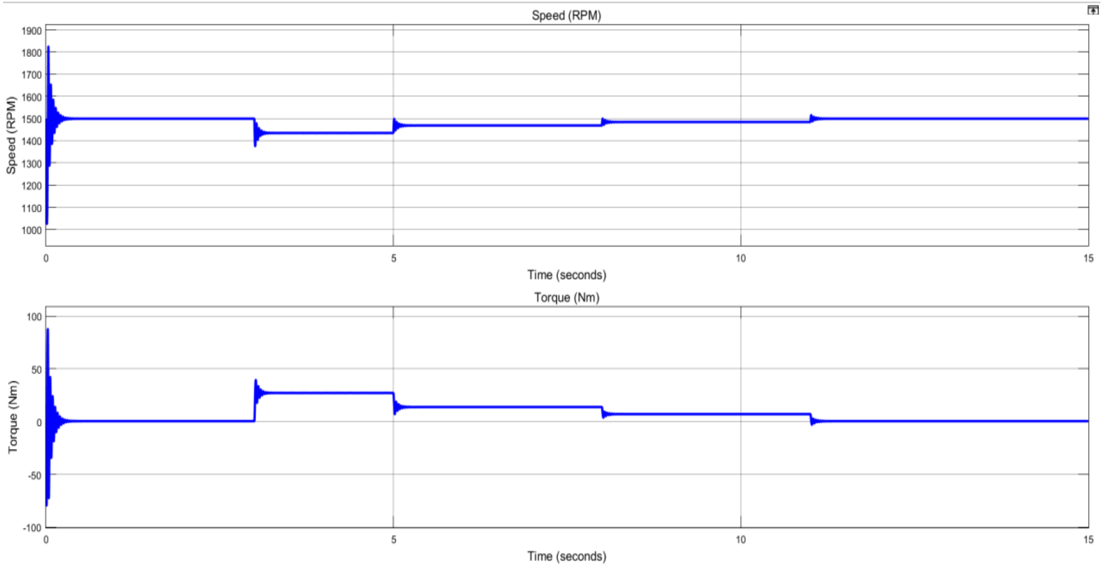

Figure 4.122: IM torque (Nm) and speed (rpm) at normal healthy condition under time varying loading condition

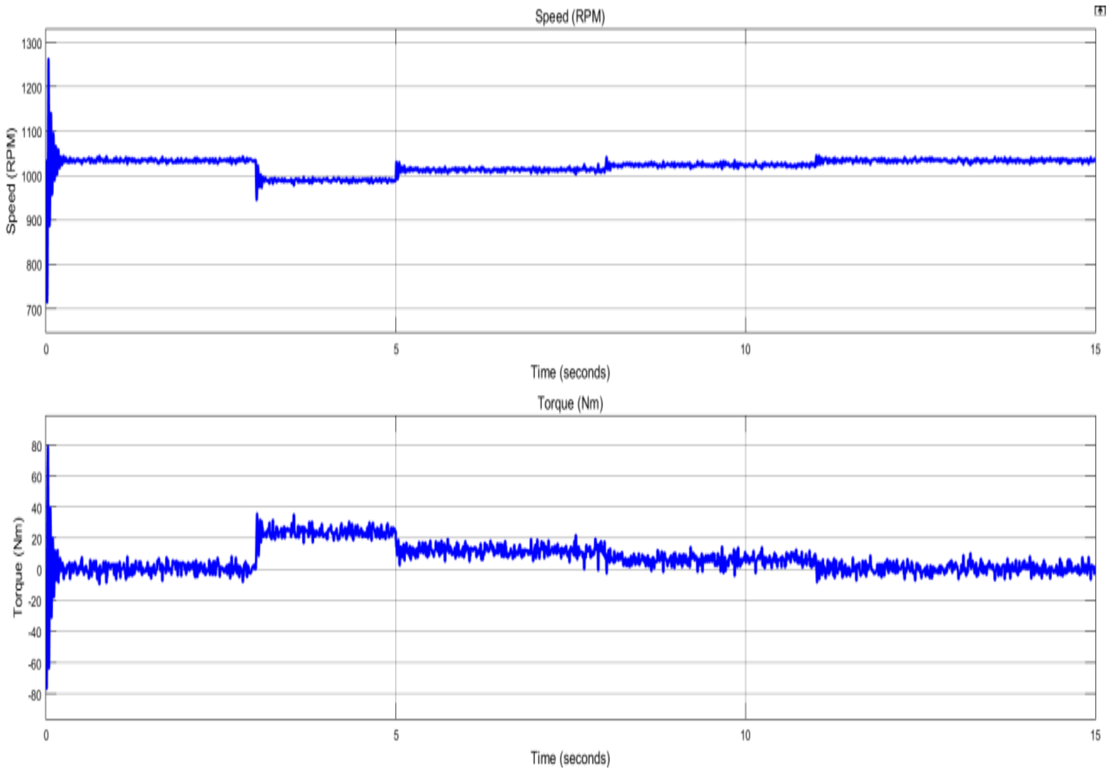

Figure 4.123: IM torque (Nm) and speed (rpm) at rotor-stator combined fault under time varying loading condition

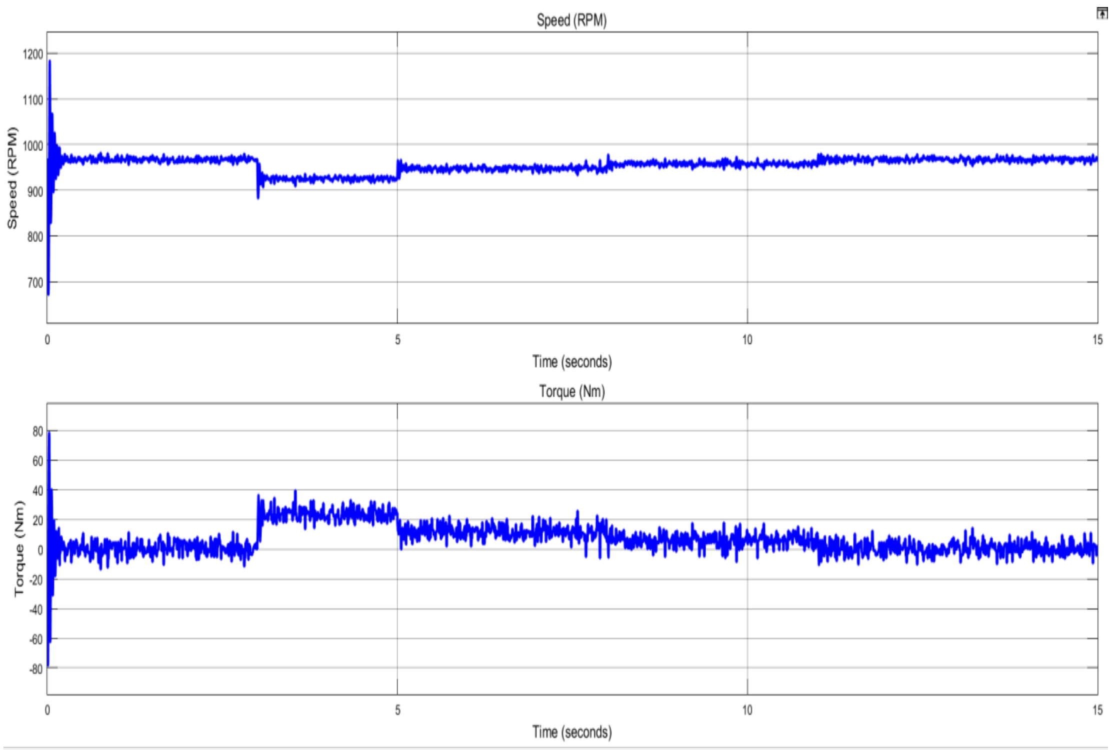

Figure 4.124: IM torque (Nm) and speed (rpm) at stator-eccentric combined fault under time varying loading condition

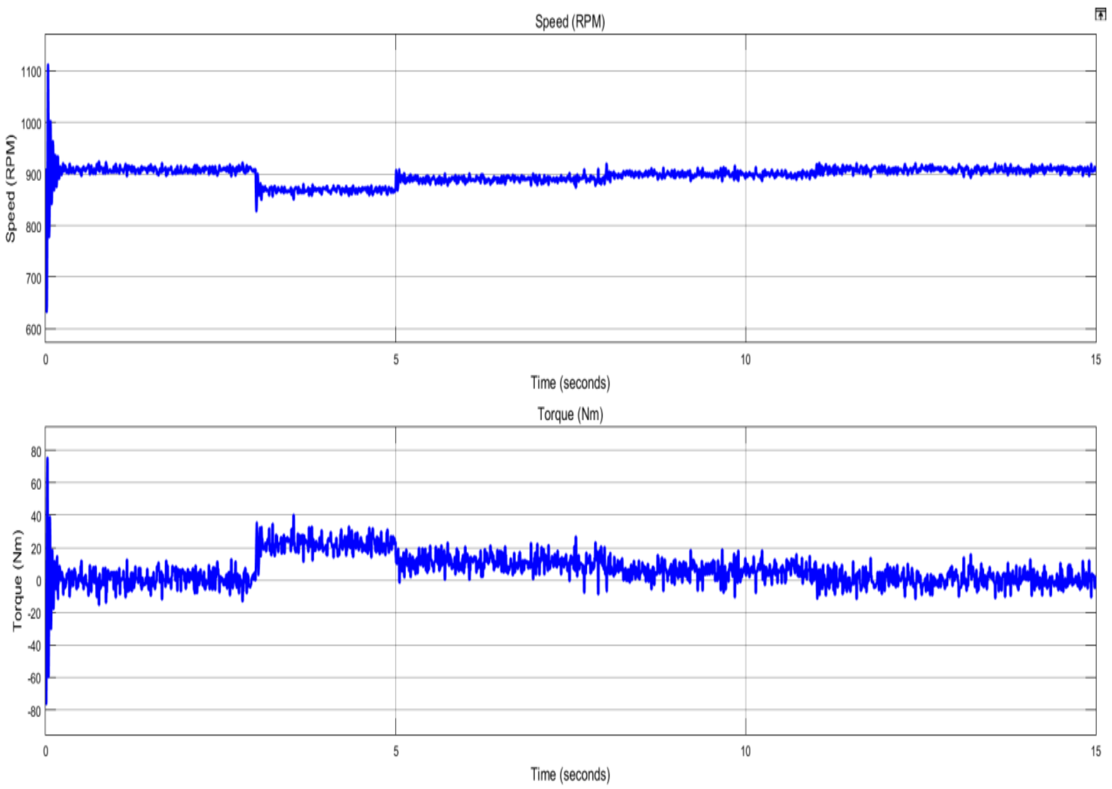

Figure 4.125: IM torque (Nm) and speed (rpm) at rotor-eccentric combined fault under time varying loading condition

4.14 SUMMARY

The main objective of the chapter is to address the conduct of the 3 phased induction machines under different faults like broken rotor bar, stator fault, eccentricity fault and combined faults (rotor –stator, rotor- eccentric and stator - eccentric) at different constant and time varying loading conditions. A 5kW SCIM is considered for the analysis and faults are generated in motor and its behavior is investigated. The motor characteristics parameters like rotor speed, stator current and its torque is evaluated and closely analyzed.

From the analysis of the broken rotor bar results, it is concluded that as the severity of fault increases with increases the number of broken rotor bar due to the variations in magnitudes of the fault frequency sideband components, fluctuations in the magnetic torque and stator current increases. The stator current is continuously decreasing with the increase in number of broken rotor bars at the different loading levels.

Under MATLAB model operation the motor is put at various varied loading conditions to get its maximum performance analysis along with different faults. Loading considered are 100%, 50%, 25% and no load. The performance is evaluated on the basis of its speed, torque, rotor, stator current and power spectrum.

The SCIM performance under time varying loading conditions is analyzed and its stability in terms of variation of torque produced and speed variation are observed in both healthy and broken rotor bar faulty environment.

The three-phase IM model have been successfully operated under stator and eccentric faulty conditions at different constant and time varying loading conditions and its characteristics parameters are noted and their variations are being used to extract features in the further stages of the health monitoring system implementation. All experimentations have been executed effectively and the stator and eccentric faults effects have been achieved as per the requirement.

The experimentation on IM model with stator faults (open winding and short circuit) and eccentric faulty conditions have been conducted successfully and obtained all the desired parameters for the feature extraction process.

The effect of time varying loading conditions have also been considerably observed by operating motor at different load demands at different times during the runtime. The motor remained stable at loading variation during runtime stating the model robustness and stability.

In this chapter, the introduction of combined faults (i.e. presence of more than one fault at the time of execution) of the motor is done which is used to evaluate the robustness of the proposed algorithm of classification and detection of faults. The combined faults are more severe and parameter obtained are more degraded which are considered as features and used for feature extraction. Combined faults considered are rotor-stator, stator-eccentric and rotor-eccentric all are investigated and the performance of the motor is evaluated under various combination of combined fault at different constant and time varying loading conditions. This research work have considered the left-out more severe faults which are combined faults and designed models have easily operated and performance characteristics have been obtained successfully for further processing in the stage where automatic detection and classification of the faults would be done using deep learning techniques.

CHAPTER 5

MACHINE LEARNING ALGORITHM BASED FAULT DIAGNOSIS EXPERIMENTATION

5.1 INTRODUCTION

The fault detection and its classification are discussed in brief in this chapter. IM characteristics in terms of vibrations and stator currents are converted into DWT features. For the dataset creation the total 4000 samples are taken into consideration, out of which 1000 samples are of healthy state, 500 samples each class of rotor fault, stator fault, eccentric faults, rotor-stator combined faults, rotor-eccentric faults and stator-eccentric faults. The data of all 7 classes is divided into training and testing to train the proposed machine learning and deep learning framework stated in chapter 4 using DBNN, SVM and RF. The accuracy in detecting and classifying the different types of possible faults is compared within the proposed algorithms in order to get the most robust framework. Furthermore, the comparison with previous work is done to validate the accuracy obtained with proposed algorithm. Firstly, feature extraction using DWT is discussed followed by DBNN method then SVM method and finally RF method is described.

The classification algorithms performances metrics used are as follows:

1. **Confusion matrix:** A confusion matrix is a summary of prediction results on a classification problem. The number of correct and incorrect predictions are summarized with count values and broken down by each class.
2. **Accuracy:** It is the fraction of relevant instances among the total instances

   A = (TP+ TN)/ (TN + TP+ FN + FP) * 100 (5.1)

3. **Precision:** It is the fraction of relevant instances among the retrieved instances.

   P = TP/ (TP + FN) *100% (5.2)

4. **Recall:** It is the fraction of relevant instances that were retrieved

   R = TN/ (FP + TN) *100% (5.3)

Where,

- **True Positive (TP):** Number of correctly identified positive examples as positive.
- **True Negative (TN):** Number of correctly identified negative examples as negative.
- **False Positive (FP):** Number of incorrectly identified positive examples as negative.
- **False Negative (FN):** Number of incorrectly identified negative examples as positive.

5.2 INDUCTION MOTOR VIBRATION SIGNALS

The IM vibration analysis is done for various operating condition like healthy and faulty conditions. Vibrations generally develop during the oscillations of the mechanical parts while in operating conditions. The oscillation becomes severe if any electrical and mechanical fault exists in the motor. This oscillatory motion and stator current analysis are important factor to detect the presence of fault in the motor.

The IM vibration graphs are depicted in Figures 5.1 to 5.8. In Figure 5.1, the healthy operating condition of the motor is displayed at different constant loading conditions, from the Figures it can be seen clearly that the vibration signals are very smooth and there is a good uniformity in the signal.

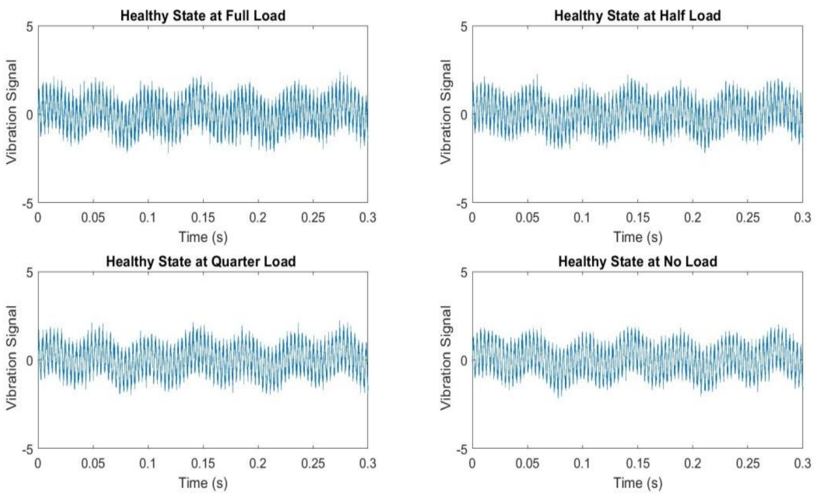

Figure 5.1: Healthy state vibration signals of IM at full, half, quarter and no loads

In Figure 5.2, the broken rotor faulty condition vibration signals are displayed at different loading conditions in which the oscillations of the signals are quite prominent as compared to the healthy operating condition. Similarly, the stator fault and eccentric faulty conditions are shown in Figure 5.3 and 5.4 in which both have shown the prominent oscillations.

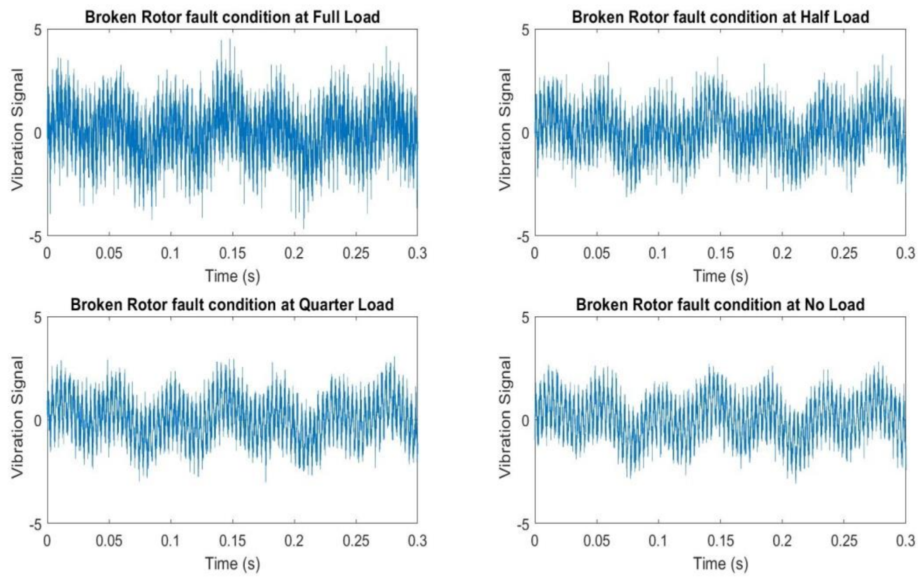

Figure 5.2: Broken rotor bar vibration signals of IM at full, half, quarter and no loads

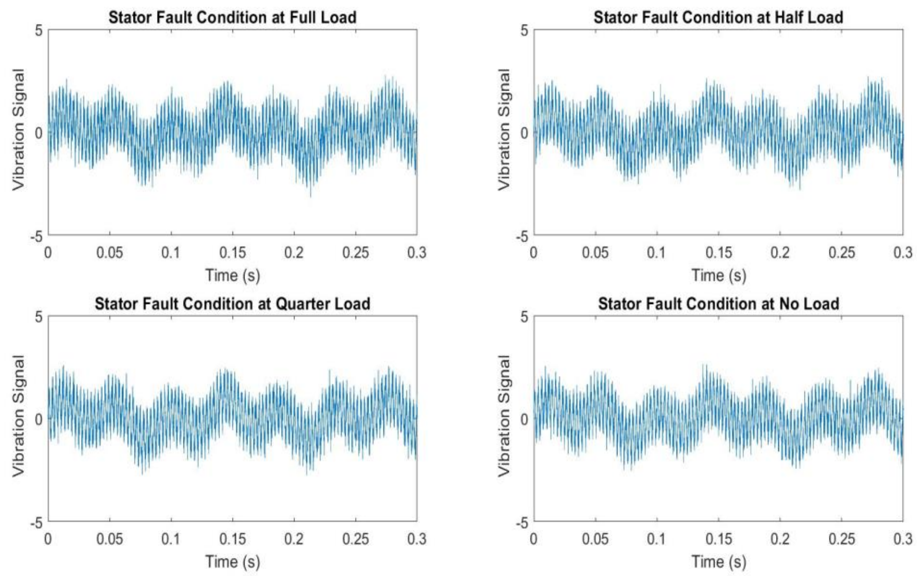

Figure 5.3: Stator fault vibration signals of IM at full, half, quarter and no loads

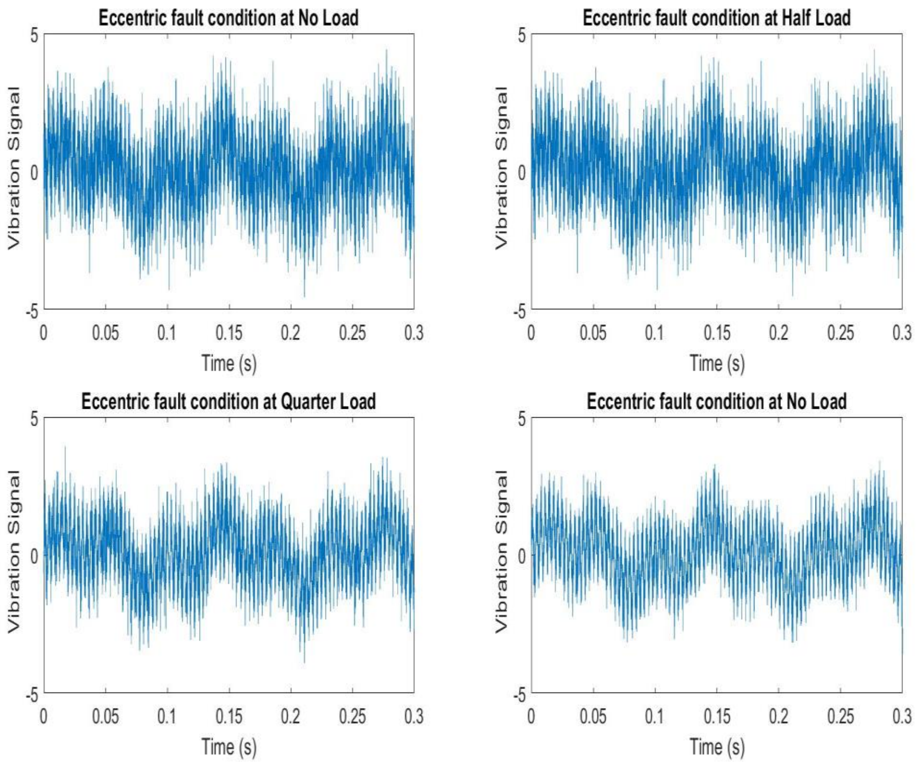

Figure 5.4: Eccentric fault vibration signals of IM at full, half, quarter and no loads

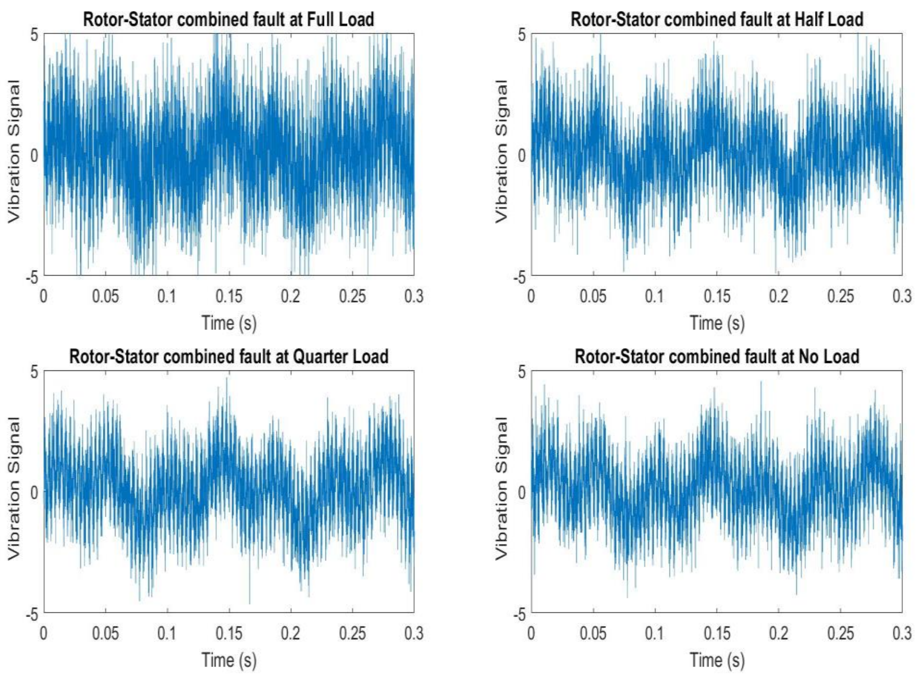

Figure 5.5: Rotor-stator combined fault vibration signals of IM at full, half, quarter and no loads

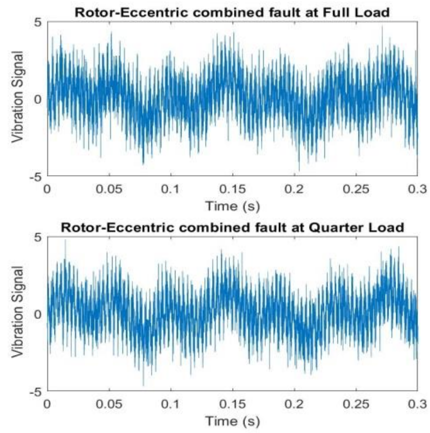

Figure 5.6: Rotor-eccentric combined fault vibration signals of IM at full, half, quarter and no loads

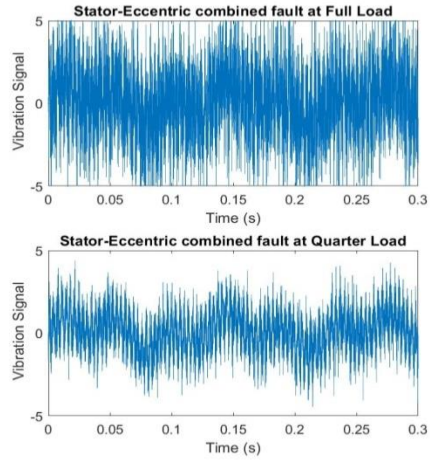

Figure 5.7: Stator-eccentric combined fault vibration signals of IM at full, half, quarter and no loads

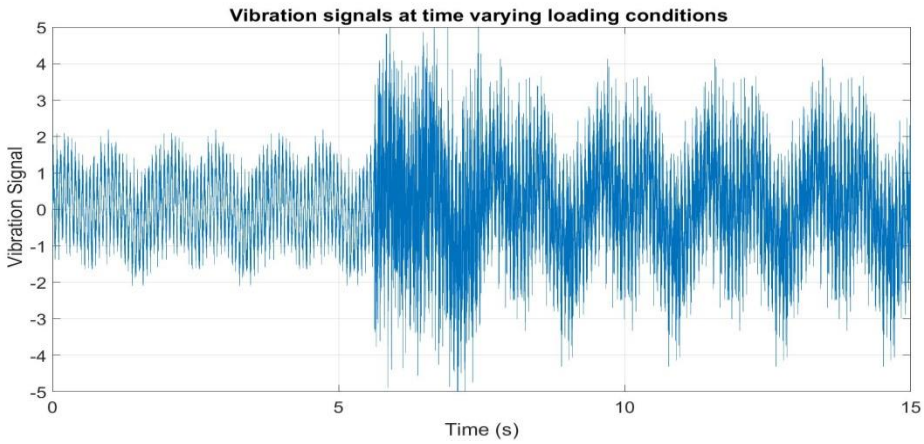

Figure 5.8: Vibration signals of IM at time varying loading condition

Figures 5.1-5.4 shows the healthy and single faults (rotor, stator and eccentric) vibration signals analysis at different constant loading conditions whereas Figures 5.5, 5.6 and 5.7 show the rotor-stator, rotor-eccentric and stator-eccentric combination of the faults at different constant loading conditions respectively. Figure 5.8 displayed the vibration signals at time varying loading condition. From these Figures, it can be analyzed that the peaks of the magnitude of the vibrations are quite high as compared to single faults. Vibration signals as per the requirement have been obtained successfully under all conditions of constant and time varying loading.

5.3 DWT FEATURE EXTRACTION OF STATOR CURRENT

The Discrete Wavelet Transform is utilized for the feature extraction of the IM current variations. The motor stator current is taken as input and 2 level DWT is performed with ‘db4’ as the wavelet. The low frequency components of the wavelet is selected from the 1st level and computed 2nd level DWT which finally taken as features. Figure 5.9 to 5.15 depicts the samples of DWT features on healthy and different faulty conditions at various constant loading conditions. Figure 5.16 shows the DWT features at time varying loading condition to classify the fault and its type.

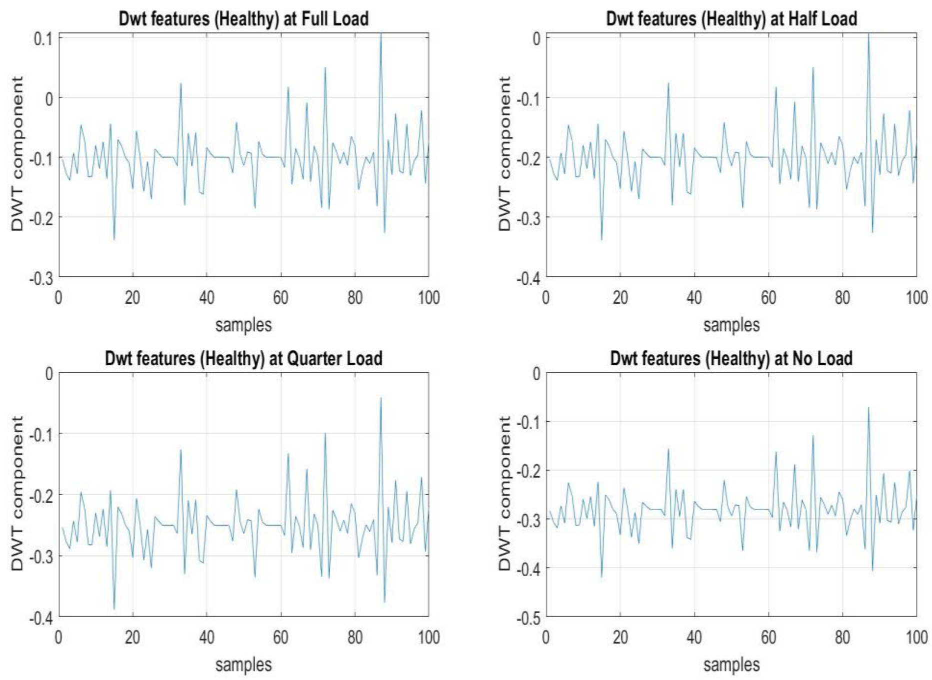

Figure 5.9: DWT features extracted in healthy operating condition at full, half, quarter and no loads

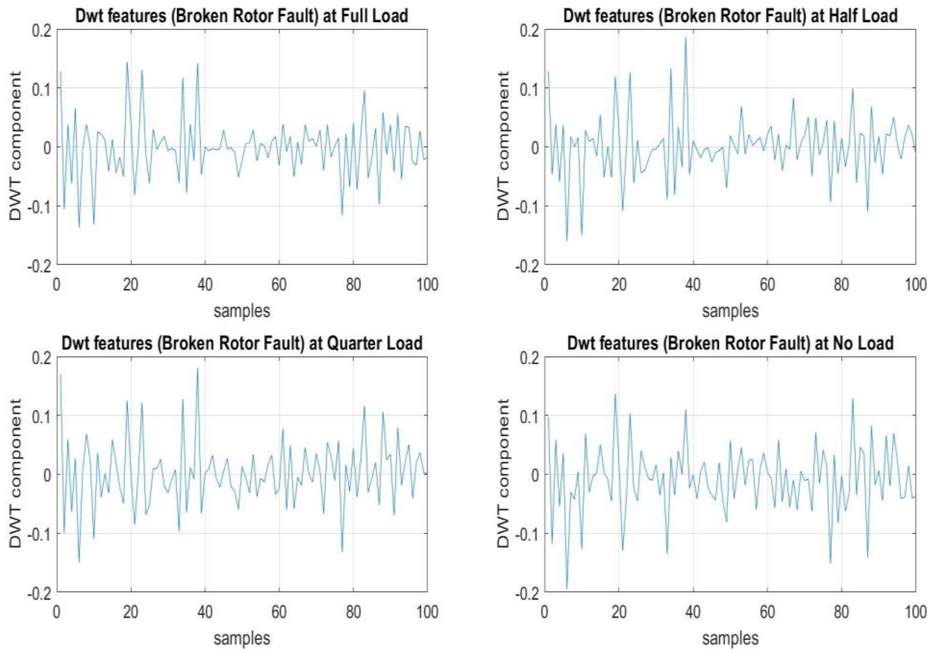

Figure 5.10: DWT features extracted in broken rotor faulty operating condition at full, half, quarter and no loads

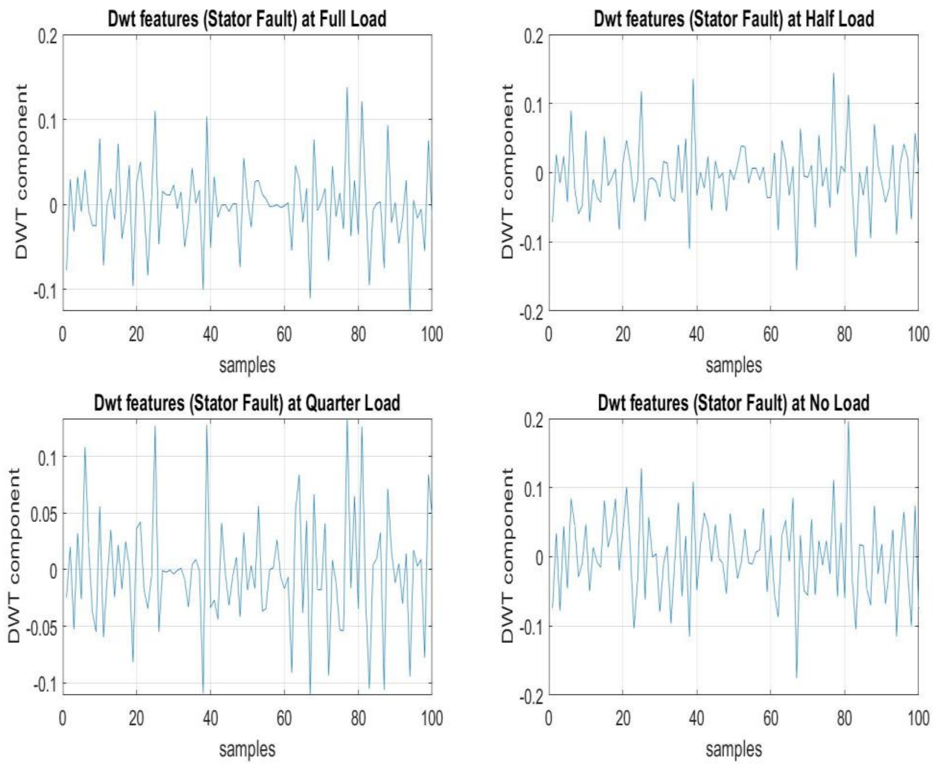

Figure 5.11: DWT features extracted in stator faulty operating condition at full, half, quarter and no loads

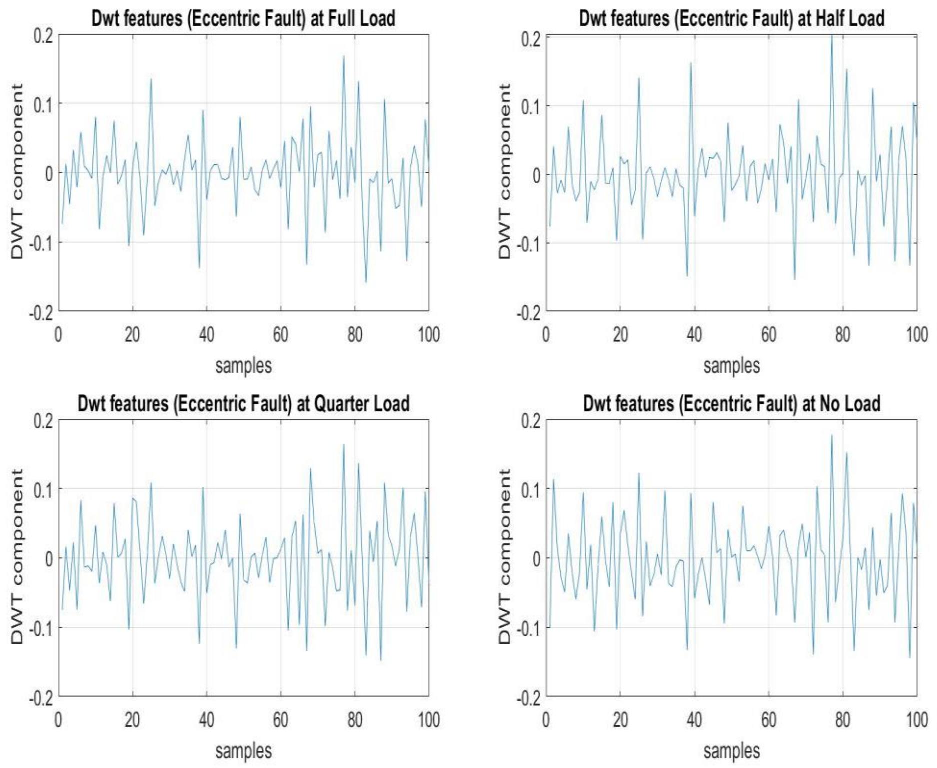

Figure 5.12: DWT features extracted in eccentric faulty operating condition at full, half, quarter and no loads

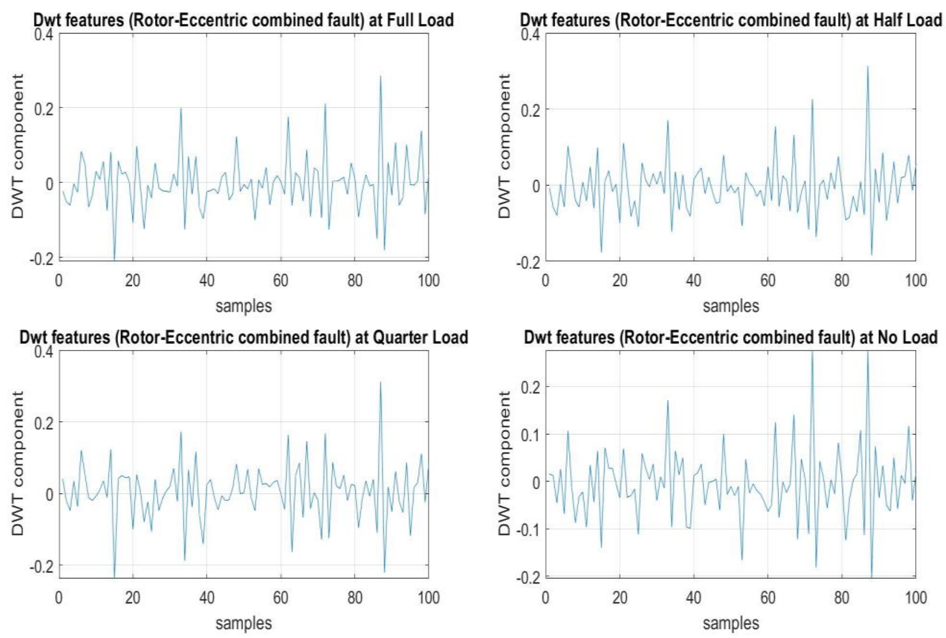

Figure 5.13: DWT features extracted in rotor-eccentric combined faulty operating condition at full, half, quarter and no loads

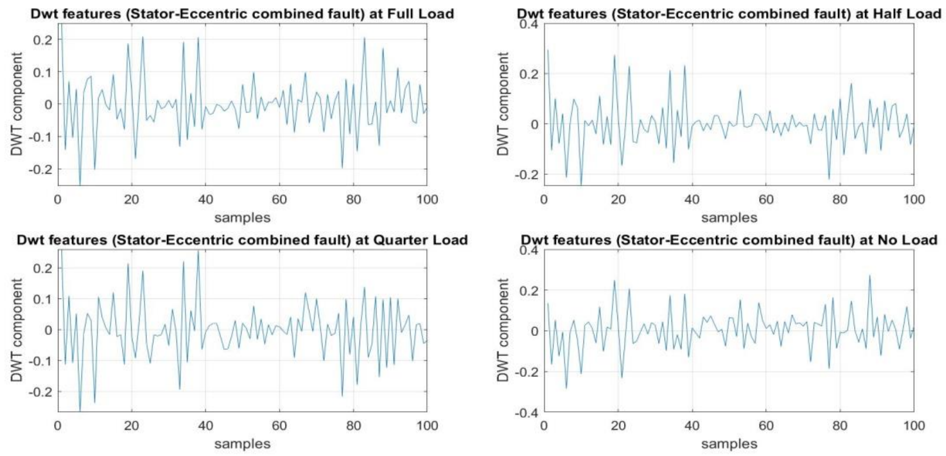

Figure 5.14: DWT features extracted in stator-eccentric combined faulty condition at full, half, quarter and no loads

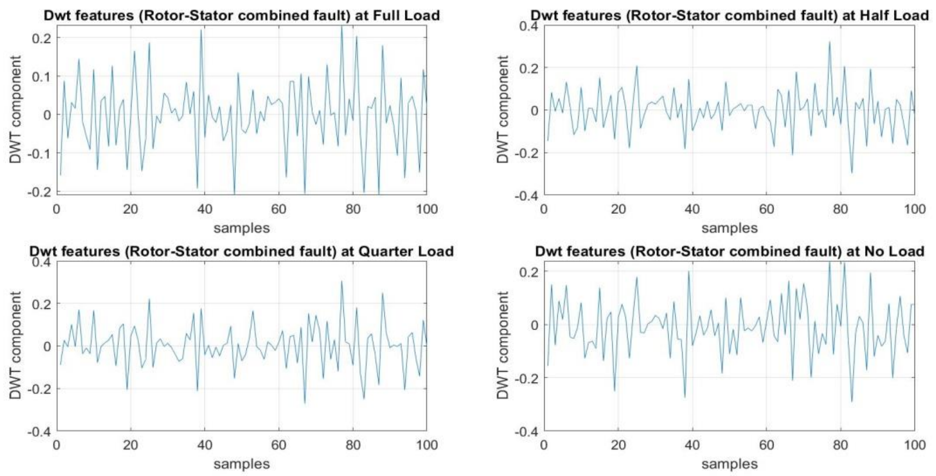

Figure 5.15: DWT features extracted in rotor-stator combined faulty operating condition at full, half, quarter and no loads

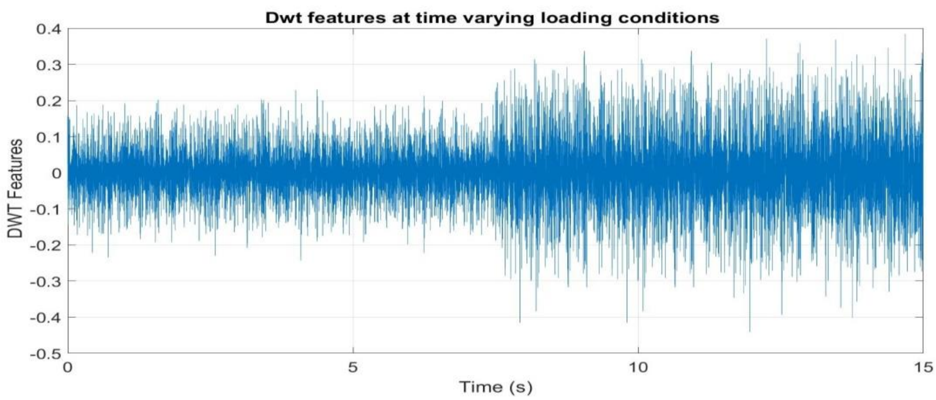

Figure 5.16: DWT features extracted in time varying loading conditions

DWT extracted features of 4000 samples are collected few of those are shown in Figures 5.9-5.15. 1000 samples of healthy operating condition and 500 each of all possible combination of single and combined faults are taken into consideration.

5.4 DBNN TRAINING FOR FAULT CLASSIFICATION

The total 4000 collected samples are divided into training and testing set, 70% of the data is divided into training and 30% data is divided into testing. The analysis of classification is done till 10-fold cross validation to assure the accuracy. Three layer DBNN architecture is used for the classification with RBM layers. In which, 800-set optimal data is used to make the backward fine-tuning learning from the classification layer to low layers and 800-set test data is used to investigate the recognition rate of DBN classifier. Additionally, it is found in this work that the main factors affecting the recognition rate are three aspects: different units in second layer of DBN classifier, the number of layers and training data.

The DBNN training is performed using scale conjugate gradient method for training with Mean Square Error (MSE) as a performance measurement calculation. Total numbers of epochs considered are 200 and performance achieved is 0.00262. The performance of the training process is illustrated in the Figures 5.17 and 5.18. Figure 5.17 shows the convergence graph of the MSE, from the graph it is clear that the training error loss is up to 10e-3 which is quite near to 0 within 200 training epochs.

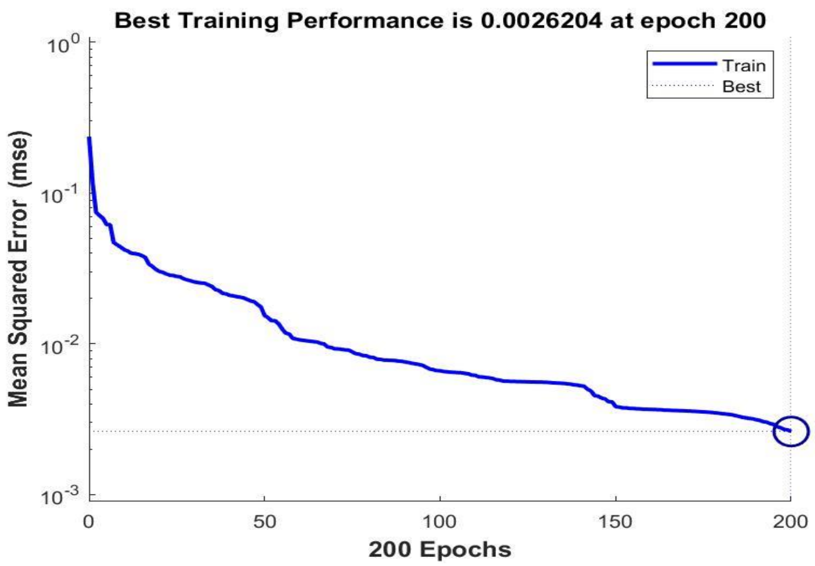

Figure 5.17: DBNN training performance parameters

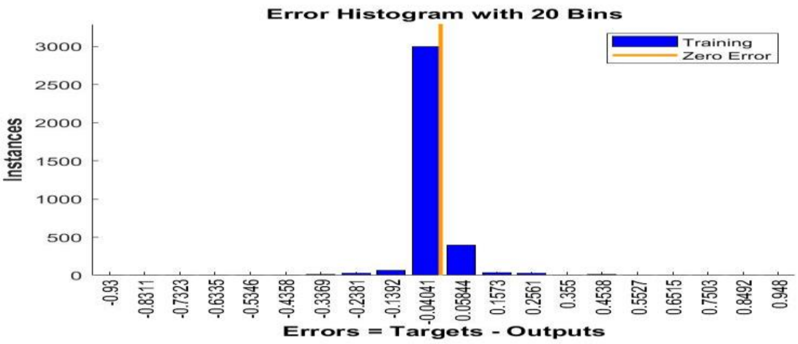

Figure 5.18: DBNN training error histogram

Figure 5.18 shows the error histogram is displayed where also it can be seen that the histogram bin is accumulated at center where the minimum of value is there. Both Figures 5.17 and 5.18 depict the robustness of the training phase.

Tables 5.1-5.4 describe the performance of the proposed DBNN architecture via confusion matrix at different loading conditions of IM. The confusion matrices rows depict the actual 7 classes and columns depict the predicted 7 classes. The diagonal elements of the matrix show the correct predicted numbers. Therefore the sum of total diagonal elements divided by total number of samples measures the accuracy. Table 5.1 shows the confusion matrix at 100% loading with accuracy of 99.83 (i.e. obtained using 1198/1200). At 50% loading condition the accuracy obtained is 1190/1200 i.e. 99.16% shown in Table 5.2. At 25% loading condition the accuracy is 99.08% and at no load conditions it is 98.99% as shown in Tables 5.3 and 5.4 respectively. Here, it can be clearly seen that at lesser severity at no load condition, the proposed method obtained the 98.99% accuracy validates the capability of the system to detect the diminished faults at an incipient stage.

Table 5.1 Confusion matrix at 100% loading condition using DBNN as classifier

Healthy	300	0	0	0	0	0	0
Rotor	0	150	0	0	0	0	0
Stator	0	0	150	0	0	0	1
Eccentric	0	0	0	150	1	0	0
Rotor-Eccentric	0	0	0	0	149	0	0
Stator-Eccentric	0	0	0	0	0	150	0
Rotor-Stator	0	0	0	0	0	0	149
	Healthy	Rotor	Stator	Eccentric	Rotor-Eccentric	Stator-Eccentric	Rotor-Stator

Table 5.2 Confusion matrix at 50%loading condition using DBNN as classifier

	Healthy	Rotor	Stator	Eccentric	Rotor-Eccentric	Stator-Eccentric	Rotot-Stator
Healthy	300	0	0	0	0	1	0
Rotor	0	147	0	0	0	0	0
Stator	0	0	150	0	0	0	4
Eccentric	0	0	0	150	2	0	0
Rotor-Eccentric	0	0	0	0	148	0	0
Stator-Eccentric	0	3	0	0	0	149	0
Rotor-Stator	0	0	0	0	0	0	146

Table 5.3 Confusion matrix at 25%loading condition using DBNN as classifier

	Healthy	Rotor	Stator	Eccentric	Rotor-Eccentric	Stator-Eccentric	Rotot-Stator
Healthy	299	0	0	0	0	1	0
Rotor	0	147	0	0	1	1	0
Stator	0	0	150	0	0	0	4
Eccentric	0	1	0	150	1	0	0
Rotor-Eccentric	1	0	0	0	148	0	0
Stator-Eccentric	0	1	0	0	0	148	0
Rotor-Stator	0	0	0	0	0	0	146

Table 5.4 Confusion matrix at no load condition using DBNN as classifier

	Healthy	Rotor	Stator	Eccentric	Rotor-Eccentric	Stator-Eccentric	Rotot-Stator
Healthy	299	1	0	0	0	1	0
Rotor	0	147	0	0	1	0	0
Stator	1	0	150	0	0	0	3
Eccentric	0	0	0	150	1	0	0
Rotor-Eccentric	0	0	0	0	148	1	0
Stator-Eccentric	0	1	0	0	0	146	0
Rotor-Stator	0	0	0	0	0	2	147

5.5 SUPPORT VECTOR MACHINE CLASSIFIER ON DWT FEATURE

The SVM classifier is one of the versatile classifier of the machine learning domain which has been applied on several applications using its different kernel function. The

SVM Radial Bias Function (RBF) kernel function is utilized to accomplish the fault diagnosis problem in SCIM. The training of the SVM is done on the training dataset kept common for all the classifier used. The training loss function graph is shown in Figure 5.19, from the figure it can be seen that the convergence of the loss is at the lowest possible point which is around 0.04.

The loss is minimized to the lowest possible extent. And the accuracy, precision and recall are calculated using the testing data confusion matrix at all different constant loading conditions which are elaborated in Table 5.5-5.8. The overall accuracy of the system is 1170/1200 = 97.5%. Precision of the SVM is 0.97 and recall is 0.97.

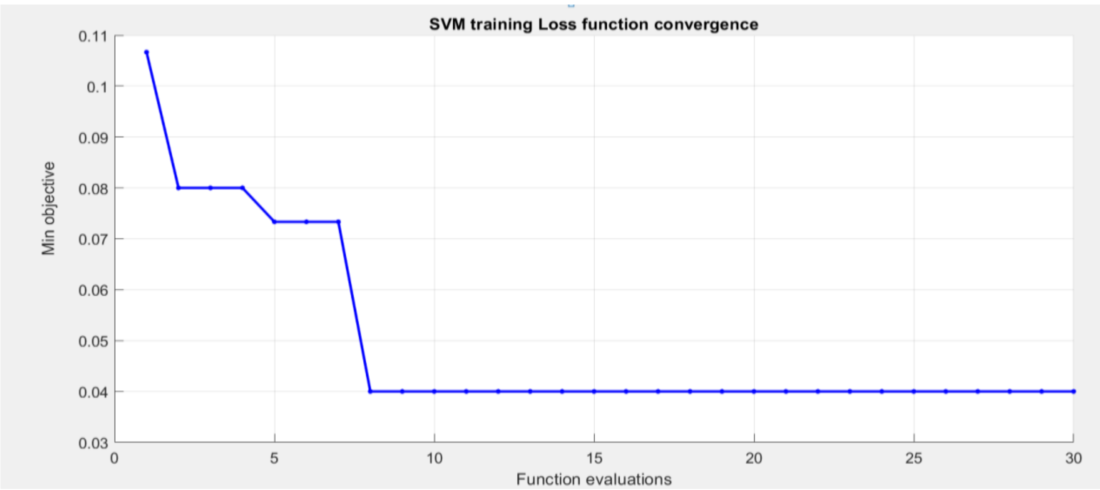

Figure 5.19: SVM training loss function graph

Table 5.5 Confusion matrix at 100% loading condition using SVM as classifier

Healthy	290	0	1	0	0	0	0
Rotor	0	150	0	2	0	0	0
Stator	2	0	148	0	0	3	1
Eccentric	0	0	0	145	2	2	0
Rotor-Eccentric	5	0	1	1	147	0	3
Stator-Eccentric	3	0	0	0	0	145	0
Rotor-Stator	0	0	0	2	1	0	146
	Healthy	**Rotor**	**Stator**	**Eccentric**	**Rotor-Eccentric**	**Stator-Eccentric**	**Rotor-Stator**

Table 5.6 Confusion matrix at 50% loading condition using SVM as classifier

Healthy	290	0	1	0	0	0	0
Rotor	0	147	0	2	0	0	0
Stator	2	1	145	0	0	3	1
Eccentric	0	0	0	145	2	2	0
Rotor-Eccentric	5	1	2	1	147	0	3
Stator-Eccentric	3	1	1	0	0	145	0
Rotor-Stator	0	0	1	2	1	0	146
	Healthy	Rotor	Stator	Eccentric	Rotor-Eccentric	Stator-Eccentric	Rotor-Stator

Table 5.7 Confusion matrix at 25% loading condition using SVM as classifier

Healthy	290	0	1	1	0	0	0
Rotor	0	147	1	3	1	0	0
Stator	2	1	144	1	1	3	1
Eccentric	0	0	0	142	2	2	0
Rotor-Eccentric	5	1	2	1	145	0	3
Stator-Eccentric	3	1	1	0	0	144	1
Rotor-Stator	0	0	1	2	1	1	145
	Healthy	Rotor	Stator	Eccentric	Rotor-Eccentric	Stator-Eccentric	Rotor-Stator

Table 5.8 Confusion matrix at no load condition using SVM as classifier

Healthy	285	0	1	1	0	0	0
Rotor	0	146	1	3	1	0	0
Stator	5	2	144	2	2	3	1
Eccentric	2	0	0	141	2	2	0
Rotor-Eccentric	5	1	2	1	144	1	3
Stator-Eccentric	3	1	1	0	0	143	1
Rotor-Stator	0	0	1	2	1	1	145
	Healthy	Rotor	Stator	Eccentric	Rotor-Eccentric	Stator-Eccentric	Rotor-Stator

5.6 RANDOM FOREST CLASSIFIER ON DWT FEATURES

The RF is one of the ensembles learning process of the machine learning algorithms where the collection of decision trees is used to reach to the best solution. The 10-fold cross validation process is used to train and test the dataset of 4000 samples. The compete misclassification process graph is shown in Figure 5.20 where the minimum value achieved is 0.06.

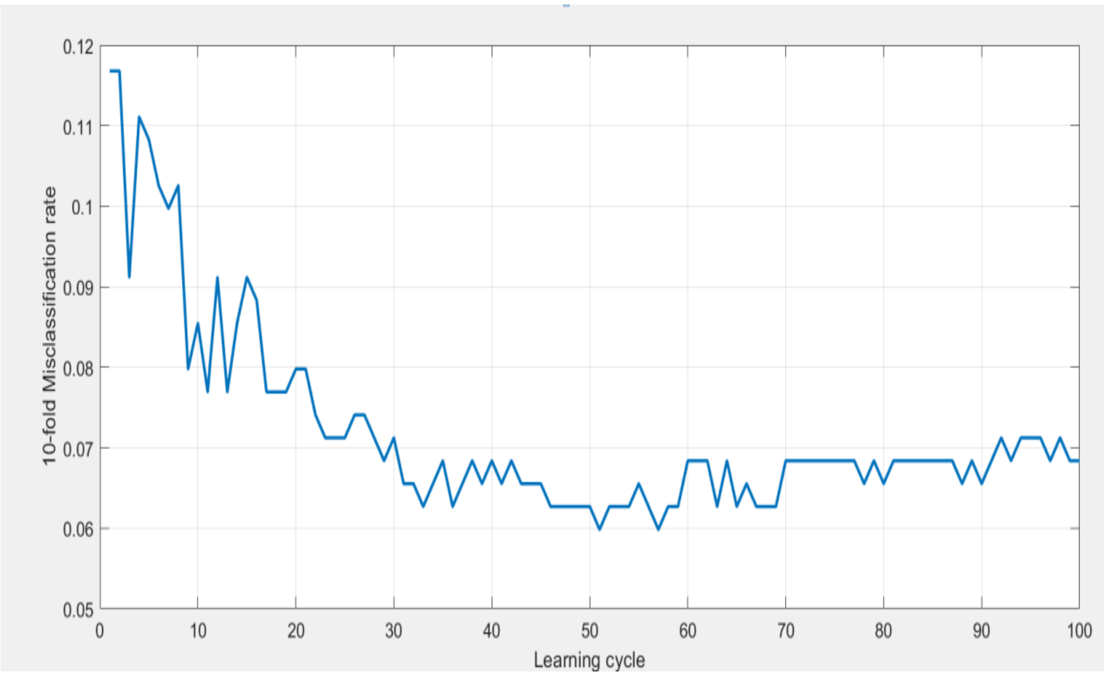

Figure 5.20: RF training misclassification graph

Table 5.9 Confusion matrix at 100%loading condition using RF as classifier

Healthy	285	1	1	0	0	0	0
Rotor	1	147	1	2	0	0	0
Stator	2	0	147	1	0	3	1
Eccentric	2	2	0	144	2	2	0
Rotor-Eccentric	5	0	1	1	146	1	3
Stator-Eccentric	3	0	0	0	1	144	1
Rotor-Stator	2	0	0	2	1	0	145
	Healthy	Rotor	Stator	Eccentric	Rotor-Eccentric	Stator-Eccentric	Rotor-Stator

Table 5.10 Confusion matrix at 50%loading condition using RF as classifier

Healthy	285	1	1	0	0	0	0
Rotor	1	143	2	2	0	0	0
Stator	2	2	146	1	0	3	1
Eccentric	2	2	0	143	2	2	1
Rotor-Eccentric	5	1	1	1	145	1	3
Stator-Eccentric	3	1	0	1	1	143	1
Rotor-Stator	2	0	0	2	2	1	144
	Healthy	Rotor	Stator	Eccentric	Rotor-Eccentric	Stator-Eccentric	Rotor-Stator

Table 5.11 Confusion matrix at 25%loading condition using RF as classifier

Healthy	284	2	1	0	0	0	0
Rotor	1	142	2	2	0	0	0
Stator	2	2	145	1	0	3	1
Eccentric	2	2	0	140	2	2	1
Rotor-Eccentric	5	1	1	1	145	2	3
Stator-Eccentric	4	1	0	2	1	142	2
Rotor-Stator	2	0	1	4	2	1	143
	Healthy	Rotor	Stator	Eccentric	Rotor-Eccentric	Stator-Eccentric	Rotor-Stator

Table 5.12 Confusion matrix at no load condition using RF as classifier

Healthy	283	2	1	2	0	0	0
Rotor	2	142	2	2	0	0	0
Stator	2	2	145	1	1	3	1
Eccentric	2	2	0	138	2	2	1
Rotor-Eccentric	5	1	1	1	144	4	3
Stator-Eccentric	4	1	0	2	1	140	2
Rotor-Stator	2	0	1	4	2	1	143
	Healthy	Rotor	Stator	Eccentric	Rotor-Eccentric	Stator-Eccentric	Rotor-Stator

Tables 5.9-5.12 illustrate the confusion matrix of all the healthy and faulty samples accuracies at 100%, 50%, 25% and no load conditions. All confusion matrices have been obtained successfully and FD detection at all conditions have been stated. The healthy samples are recognized with 100 % accuracy. In faulty states like rotor and stator the accuracy is almost 100% in rest there is a downfall in accurate detection of the fault which leads to the overall accuracy of 96.5%. So, the average overall accuracy of the system is 1159/1200 = 96.5%. Precision is 0.983 and recall is 0.97.

5.7 COMPARISON OF MACHINE AND DEEP LEARNING ALGORITHM FOR FAULT DIAGNOSIS OF INDUCTION MOTOR

The three algorithms are compared on the basis of the accuracy, precision and recall illustrated in Tables 5.13-5.16 under different constant loading conditions. Deep learning algorithm like DBNN train machines by learning . Deep learning is a subset of machine learning, which is essentially a neural network with three or more layers. A large dataset of input and output pairs help it to minimize the difference between its prediction and expected output. A Deep learning methods are very popular now a days in the field of fault diagnosis as they can learn feature extraction well and successfully handle big data for detection and classification task in case of fault occurrence. DBNN a class of deep neural network, composed of multiple layers of hidden units, with connection between the layers but not between units with each other. From Tables 5.13-5.16, it can be seen that the deep learning method DBNN has given 99.83% accuracy whereas RF and SVM have given 96.5% and 97.5% accuracies. The precision and recall of deep learning method DBNN also is on the higher side. The accuracy, precision and recall have successfully been obtained at all different loading conditions with significant high correctness. The overall performance of the DBNN is better in terms of detection and classification of fault. The obtained accuracy in DBNN proves that in almost 100% of time the DBNN detect the fault correctly and classify its type with a good precision. Furthermore, this can be utilized in proper maintenance steps that could be taken if the type of fault is precisely detected. So, DBNN adds a good value to the SCIM maintenance where the problem of monitoring and detecting the faults consumes lots of time. So, the downtime can be drastically reduced and machine can be made intelligent.

Table 5.13 Machine learning and deep learning algorithms performance comparison chart at 100% loading

Algorithm	Accuracy (%)	Precision (p)	Recall (r)
Deep learning method DBNN	99.83	0.99	0.99
Random Forest	96.5	0.98	0.97
Support Vector Machine	97.5	0.97	0.97

Table 5.14 Machine learning and deep learning algorithms performance comparison chart at 50% loading

Algorithm	Accuracy (%)	Precision (p)	Recall (r)
Deep learning method DBNN	99.16	0.99	0.99
Random Forest	95.75	0.98	0.97
Support Vector Machine	97.08	0.97	0.97

Table 5.15 Machine learning and deep learning algorithms performance comparison chart at 25% loading

Algorithm	Accuracy (%)	Precision (p)	Recall (r)
Deep Learning method DBNN	99.08	0.99	0.98
Random Forest	95.08	0.95	0.96
Support Vector Machine	96.41	0.96	0.97

Table 5.16 Machine learning and deep learning algorithms performance comparison chart at no load

Algorithm	Accuracy (%)	Precision (p)	Recall (r)
Deep Learning Method DBNN	98.99	0.98	0.97
Random Forest	94.58	0.95	0.94
Support Vector Machine	95.66	0.95	0.95

Figure 5.21, 5.22 and 5.23 are showing the comparison of all the three methods used for FD in terms of accuracy, precision and recall comparison at different constant loading conditions respectively. In all the three graphs the DBNN performance is profound as compared to the machine learning algorithms SVM and RF. The RF classifier is based on ensemble learning where bunch of decision trees altogether tends to get the best accuracy out of the sample provided to it while training, in the fault detection case the accuracy obtained from collection of decision trees creating random forest is 96.5%.

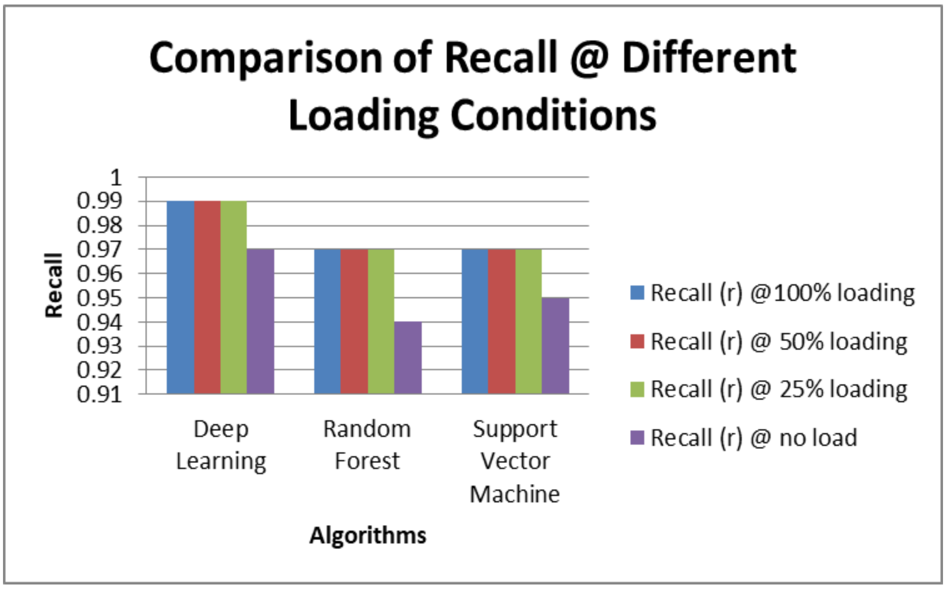

Figure 5.21: Recall bar graph comparisons at different loading conditions

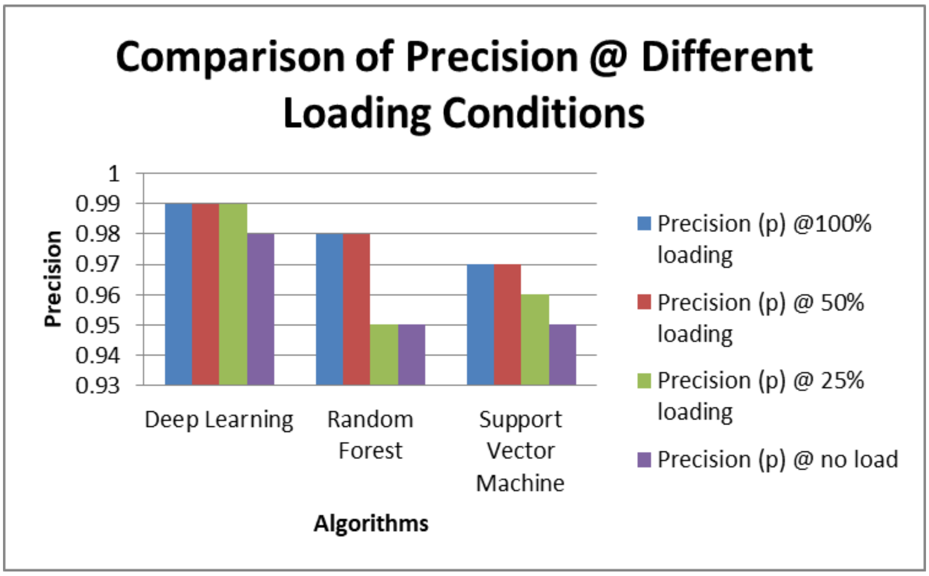

Figure 5.22: Precision bar graph comparisons at different loading conditions

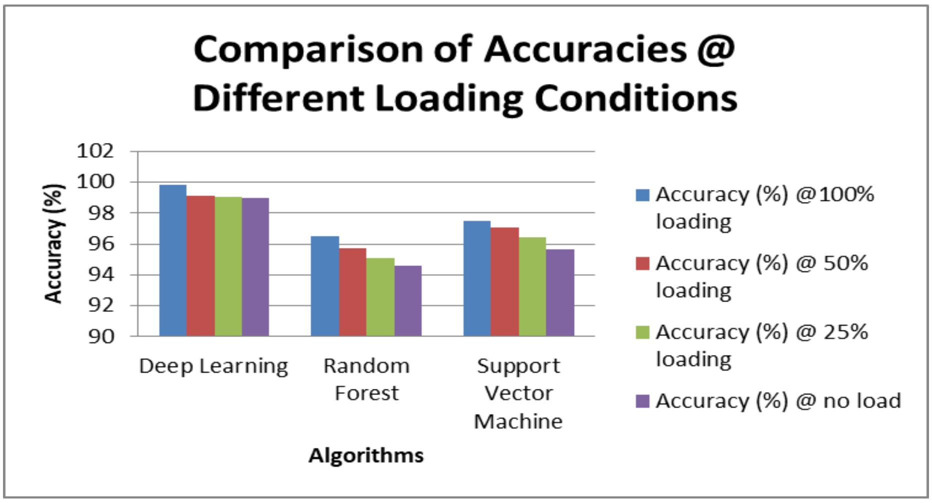

Figure 5.23: Accuracy bar graph comparisons at different loading conditions

On the other side, SVM with RBF kernel function extract the 97.5 % accuracy for 7 classes fault classification problem it is due to the fact that RBF kernel function handles the non-linearity of the system effectively while performing the convergence during the training process. So, overall performance comparison is like the performance of DBNN is greater than SVM and the performance of SVM is greater than RF in terms of precision, recall and accuracy.

5.8 FAULT DETECTION AT TIME VARYING LOAD CONDITION

The experimentation of fault detection and classification under time varying loading condition is conducted on all three FD methods SVM, RF and DBNN displayed in Figures 5.24, 5.25 and 5.26. The motor is subjected to faults seven times during runtime (Rotor Fault, Rotor fault, Rotor-Eccentric fault, Rotor-Stator fault, Stator Fault, Rotor-Eccentric Fault, Eccentric fault).

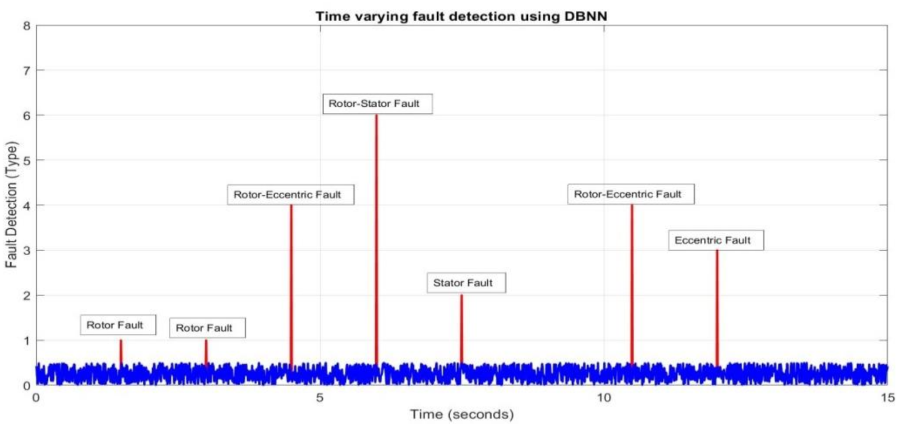

Figure 5.24: Time varying fault detection using DBNN

Figure 5.24 depicts the fault detection and classification using proposed DBNN technique under time varying load condition. All the seven faults have been successfully detected using DBNN framework. Figure 5.25 shows the detection of fault during runtime using SVM algorithm, from the figure it can be seen that the rotor fault is misinterpreted as stator fault and rest all other faults are correctly detected and classified. Figure 5.26 display the performance of RF algorithm under time varying loading condition. RF algorithms have incorrectly classified multiple faults Rotor fault classified as stator fault and rotor-stator fault is classified as stator-eccentric. Here, it is concluded that all three approaches have detected the faults successfully and in classification the DBNN have shown the better performance as compared to SVM and RF.

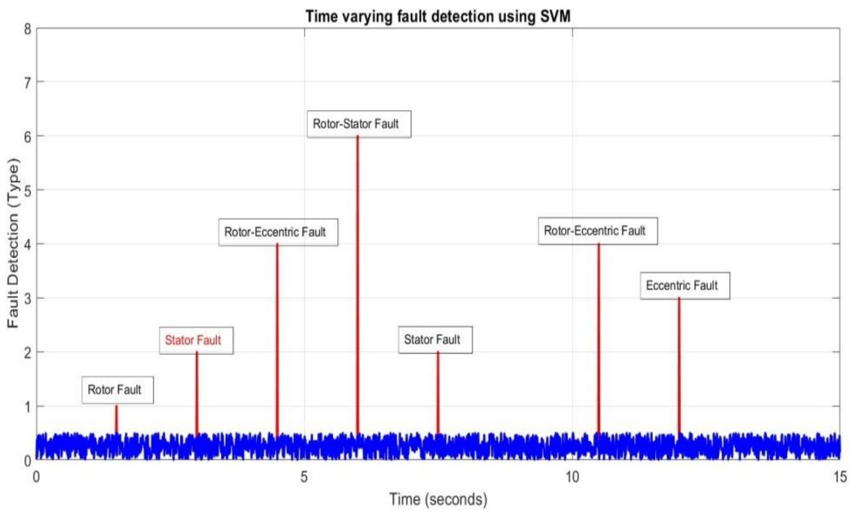

Figure 5.25: Time varying fault detection using SVM

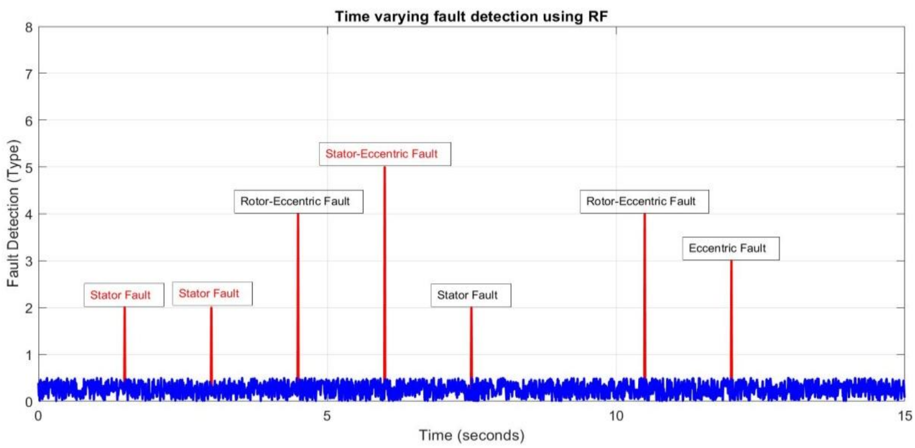

Figure 5.26: Time varying fault detection using RF

The runtime fault detection have been the part of the research since so many past years. This research work have introduced the detection as well as classification of the fault at the same time i.e. which type of fault occur at the time of fault so that the downtime due to the repair of the motor could be reduced and can be valuable in increasing the productivity in the industry. In this research work the novel approach is used for the online fault detection and classification is done considering various more severe combined faults under constant and time varying loading conditions.

5.9 SUMMARY

In this chapter, the fault diagnosis methods are applied to diagnose the faults in motor with its classification. The feature extraction is done using DWT using stator current and the vibration signals. Identification of the faults is done using machine learning and deep learning methods mainly SVM, RF and DBNN. Overall the performance of all the algorithms is good. The DWT feature extractor segregates the vibration and current signals into electrical signals in an efficient way and database created for all the possible faults occurrences in SCIM motor for example rotor faults, stator faults, eccentric faults and combined faults. Dataset is then utilized for supervised learning process divided into training and testing with 10-k fold cross validation approach for SVM, RF and DBNN. The analyses of three algorithms are done on the basis of different loading conditions and time varying load to increase the data set and authenticate the performances of the proposed architecture. Features are extracted and divided in different sets at 100%, 50%, 25% and no load condition to analyze the performance of algorithms at different severity level of the fault. Subsequently, the detection and classification of the faults under all loading conditions is performed with high accuracies. During the investigation of the classification algorithm, it is found that DBNN has performed well and obtained a 99.83% accuracy of classification of fault. SVM with RBF kernel extracted 97.5 % and RF the ensemble classification machine learning algorithms have shown 96.5% accuracy.

CHAPTER 6

CONCLUSIONS, CONTRIBUTIONS AND FUTURE WORK

6.1 INTRODUCTION

The present research work contributes to the field of fault detection and diagnosis in Induction Motor by applying advanced algorithms of machine learning and deep learning. The IMs are the backbone of industrial processes such as power, automotive, machine tools plant processes. Due to the increased use of IM, the need for fault detection and classification has increased significantly. Therefore, the classification of faults of induction motors such as rotor faults, stator faults, eccentric faults, and various combined faults (rotor-stator, stator-eccentric, and rotor-eccentric) are the focus of this research.

6.2 CONCLUSIONS

The common types of faults in Induction Motor are analyzed in the research work. Various condition monitoring methods and fault diagnosis methods have been discussed and reviewed. The present research work is divided into three parts: first part is to design and implement the IM model in RMxprt and Maxwell 2D software tool to analyze the effects of load variations and faulty conditions in the motor. Second part is to design the mathematical modeling of IM in MATLAB software tool. Explicitly the effects of rotor bar faults (one bar, two bars and three bars), (Stator open winding & short circuit faults), eccentric faults and combined faults (one or more faults at the same time) on the motor have been extensively experimentally analyzed.

Third part, is the IM fault diagnosis using DWT analysis of stator current which identify the patterns caused during the different operating conditions of the motor (healthy or faulty) and furthermore, the classification of the faults is done using various machine learning algorithms like RF, SVM and DBNN. The training dataset used is built from stator current envelope i.e. spectral analysis and its feature extraction at each level under different motor operating conditions. Several implementation executions have been performed on the IM (squirrel-cage) setting the motor under different loading conditions constant & time varying under different faults like rotor, stator, eccentric and combined faulty operating conditions. The implementation showed that the condition of any fault causes vibrations in the stator current, torque and speed. It can be seen that these oscillations are proportional to the type of fault. The fault generation and the motor behavior at different range of load condition is executed using Maxwell 2D with FEM technique. Machine learning and deep learning algorithms with DWT are applied on MATLAB model to detect and classify the faults.

The conclusions of the research work are summarized as follows:

1. Literature survey in the field of IM fault diagnosis techniques have been performed which is further categorize in three sections model based methods, signal processing based methods and soft computing algorithm based techniques.

2. Healthy SCIM characteristics have been experimentally obtained with the help of ANSYS RMxprt tool and MATLAB software.

3. Broken rotor bar faults generation and detection have been successfully performed:

- Broken rotor bar faults are generated using FEM analysis in ANSYS RMxprt and Maxwell 2D. The vibration in stator, current and speed have been observed by experimenting motor at one, two and three broken rotor bars and it's been analyzed that the vibration tends to increase and distortion magnitude increases as broken rotor bar faults.
- The effects of rotor faults have been observed in comparison to healthy motor behavior under constant loading condition.
- MATLAB implemented SCIM model has proficiently generated the broken rotor bar faults and motor parameters are obtained.
- The experimentations of effects of constant loads variation (100%, 50%, 25% and no load) on broken bar faulty motor in comparison to healthy motors for fault diagnosis have been successfully presented.

- Power spectrum of generated faulty conditions has been investigated which concludes the behaviour of motor as the magnitudes of the sidebands increases on the increment of severity of the faults.
- The effect of time varying loading condition during runtime has been executed conclusively, stating the robustness of the implemented SCIM model.
- The characteristics obtained from different constant loading condition were further used for feature extraction for automatic detection and classification of broken rotor bars.

4. Stator open and short circuit winding faults detection and classification experimentation was performed:

- Open winding faults have been effectively generated in RMxprt model and its characteristics were obtained using FEM analysis using Maxwell 2D.
- The experimentation on short circuit stator winding fault has been performed using MATLAB implemented model. The effects of different constant load (100%, 50%, 25% and no load) on faulty SCIM motor have been successfully analysed and compared with healthy motor.
- Time varying loading condition experiment has been performed on short circuited stator winding faulty motor and its effect has been observed.
- Obtained characteristics at the time of stator faulty condition have been further utilised to extract features for classification of fault types.

5. Designed SCIM has been analysed on the presence of eccentric faulty condition both dynamic and static:

- Static and dynamic faults have been successfully generated using Rmxprt designed model and its characteristics behaviour has been observed at constant load condition using Maxwell 2D and also compare with healthy one.
- Static eccentric fault has been successfully implemented using MATLAB software and its effect under different loading conditions (100%, 50%, 25% and no load) have been presented in this research work.
- The faulty motor has been positioned under time varying loading condition and the stability performance analysis has been successfully performed.

6. Considering the gap in research work where the combined faults based research were hard to find, an experimentation on combined faults has been efficiently conducted:

- The distortion of the characteristics of the motor has been analysed on various combined faulty conditions (rotor-stator, stator-eccentric and rotor-eccentric).
- The effect of combined faulty conditions on the different (100%, 50%, 25% and no load) constant loading conditions has been presented effectively and the implemented model stability has been observed from the characteristics obtained.
- The experimentation on the effect of time varying loading condition on different set of combined faults has been conducted positively and all the characteristics have been obtained and presented.
- The characteristics obtained were further more utilised to obtain features for classification process.

7. The proposed DBNN model framework has been developed successfully to detect and classify the type of fault during the runtime:

- DWT features have been comprehensively extracted using stator current signature at different faulty conditions (rotor, stator, eccentric, and combination of combined faults) under constant and time varying loading conditions.
- Machine learning algorithms SVM and RF have also been used for detection and classification of fault along with proposed DBNN framework. The results of proposed method has been compared with other machine learning algorithm, the proposed method has outperformed the others existing ones.
- Combined faults have been detected and classified successfully from the proposed DBNN framework.

6.3 CONTRIBUTIONS OF THE RESEARCH WORK

The vital prominence of this research work based on the methods which effectively detects faults in IM under different constant and time varying loading conditions prior to the system failure.

- From the research work, it is concluded that the motor performance varies drastically when put at different constant and time varying loading conditions and it adversely affect its wear and tear which makes motor prone to get faulty.

  - **In order to observe all these effects,** in this research work fifty six experiments have been conducted using two different machine learning algorithm and one deep learning algorithm to detect and classify faults like rotor, stator and eccentric and their combinations (rotor-stator, stator-eccentric and eccentric-rotor) at different constant loading conditions and time varying load.

- The data driven method/technique deep learning is applied in the present work for intelligent fault detection and classification of a particular fault under all situations.

  - **The implemented DBNN method** performance outcomes obtained in terms of accuracy has been proved to be effective and outstanding under change of constant loading conditions like the motor at 100% loading condition tends to deteriorate more and its effect on its characteristics parameters are higher due to which the extracted features of the motor at 100% loading helps classification algorithm to detect and classify the type of faults precisely and same for other loading effects even at no load where small effect of faults occur.
  - **Also fault detection methods** have shown great performance under severe conditions when combined faults occur .

- The supervised machine learning algorithms such as SVM and RF have performed well in the field of detection of different type of faults at different constant loading conditions and during time varying load in this research work.

  - **Comparing all the algorithms (DBNN, SVM and RF)** on the basis of accuracy, precision and recall, it is found that SVM gives better results than RF but as the deep learning algorithms utilize the supervised and unsupervised concepts to attain the maximum accuracy for the classification processes due to this reason the DBNN algorithm has achieved higher accuracy as compared to RF and SVM in all different loading conditions for different types of faults.

- The proposed method DBNN with DWT is adopted to design hybrid approach DBNN-DWT for fault detection and classification of single and combined fault under different constant and time varying loading conditions.

  - **The present research work** outperformed the other existing ones which is only possible due to robust feature extraction using unsupervised learning of features of advance deep learning method to classify the faults more precisely.

6.4 FUTURE WORK

- In future, the high rating motor should be considered for the experimentation to robustness of the proposed algorithms.

- Online motor fault diagnosis using deep learning methods should be performed to detect the fault as early as possible and avoid the harm to the motor.

- The diagnosis of power quality problems, which are related to motor power supply, may be incorporated in the system.

- Based on this research, a real-time system can be developed in which the IM data can be captured and entered into an intelligent system at the same time. The intelligent system would process the condition of the IM and issue the suitable command accordingly.

REFERENCES

[1] I. M. Culbert and W. Rhodes, "Notice of violation of IEEE publication principles: using current signature analysis technology to reliably detect cage winding defects in squirrel-cage induction motors", *in IEEE Transactions on Industry Applications,* Vol. 43, No. 2, pp. 422-428, March 2007.

[2] N. Bessous, "Reliability surveys of fault distributions in rotating electrical machines, case study of fault detections in IMs", *1st International Conference on Communications, Control Systems and Signal Processing (CCSSP),* EL OUED, Algeria, pp. 535-543, 2020.

[3] S. Bindu and V. V. Thomas, "Diagnoses of internal faults of three phase squirrel cage induction motor - A review", *International Conference on Advances in Energy Conversion Technologies (ICAECT), Manipal*, pp. 48-54, 2014.

[4] D. Kim, D. Hong, J. Choi, Y. Chun, B. Woo and D. Koo, "An analytical approach for a high speed and high efficiency induction motor considering magnetic and mechanical problems", *in IEEE Transactions on Magnetics,* Vol. 49, No. 5, pp. 2319-2322, May 2013.

[5] A. Siddique, G. S. Yadava and B. Singh, "A review of stator fault monitoring techniques of induction motors", *in IEEE Transactions on Energy Conversion*, Vol. 20, No. 1, pp. 106-114, March 2005.

[6] A. M. Knight and S. P. Bertani, "Mechanical fault detection in a medium-sized induction motor using stator current monitoring," *in IEEE Transactions on Energy Conversion*, Vol. 20, No. 4, pp. 753-760, December 2005.

[7] S. Altug, Mo-Yuen Chen and H. J. Trussell, "Fuzzy inference systems implemented on neural architectures for motor fault detection and diagnosis", *in IEEE Transactions on Industrial Electronics*, Vol. 46, No. 6, pp. 1069-1079, December 1999.

[8] S. Pharne and A. Patil, "Fault diagnosis of motor using fuzzy logic technique", *International Conference on Energy, Communication, Data Analytics and Soft Computing (ICECDS),* Chennai, pp. 3110-3115, 2017.

[9] J. F. Martins, V. Ferno Pires and A. J. Pires, "Unsupervised neural-network-based algorithm for an on-line diagnosis of three-phase induction motor stator fault”, *in IEEE Transactions on Industrial Electronics*, Vol. 54, No. 1, pp. 259-264, February, 2007.

[10] H. D. L. Rações, F. J. T. E. Ferreira, J. M. Pires and C. V. Damásio, "Application of different machine learning strategies for current and vibration based motor bearing fault detection in induction motors”, *IECON 2019 - 45th Annual Conference of the IEEE Industrial Electronics Society, Lisbon, Portugal*, pp. 68-73, 2019.

[11] D. Basak, A. Tiwari and S. P. Das, "Fault diagnosis and condition monitoring of electrical machines - *A Review*”, *IEEE International Conference on Industrial Technology, Mumbai*, pp. 3061-3066, 2006.

[12] X. Liang and K. Edomwandekhoe, "Condition monitoring techniques for induction motors”, *IEEE Industry Applications Society Annual Meeting, Cincinnati, OH*, pp. 1-10, 2017.

[13] M. J. Castelli, J. P. Fossati and M. T. Andrade, "New methodology to faults detection in induction motors via MCSA”, *IEEE/PES Transmission and Distribution Conference and Exposition: Latin America, Bogota*, pp. 1-6, 2008.

[14] Nandi and H. A. Toliyat, “Condition Monitoring and Fault Diagnosis of Electrical Machines – A Review”, *in Proc. 34th Annual Meeting of the IEEE Industry Applications*, pp. 197-204, 1999.

[15] Balamurugan S., Arumugam R., Paramasivam S., Malaiappan M. ,“Transient Analysis of induction motor using finite element analysis”, *IEEE Industrial Electronics Society, 30th annual conference IECON*, pp. 1526-1529, 2004.

[16] J. F. Bangura and N. A. Demerdash, "Diagnosis and characterization of effects of broken bars and connectors in squirrel-cage induction motors by a time-stepping coupled finite element-state space modeling approach," in *IEEE Transactions on Energy Conversion*, Vol. 14, pp. 1167-1176, December 1999.

[17] K. N. Gyftakis, D. V. Spyropoulos, J. C. Kappatou and E. D. Mitronikas, "A

Novel Approach for Broken Bar Fault Diagnosis in Induction Motors Through Torque Monitoring," in *IEEE Transactions on Energy Conversion*, Vol. 28, pp. 267-277, June 2013.

[18] Martinez, Javier, Anouar Belahcen, and Antero Arkkio, "Combined FE and two dimensional spectral analyses of broken cage faults in induction motors", *IECON 39th Annual conference of the IEEE Industrial Electronics Society*, 2013.

[19] Sandarangani and Martinez, C., "Electrical machines–design and analysis of induction and permanent magnet motors", *Royal Institute of Technology, Stockhol*, 2000.

[20] Bentounsi A. and Nicolas A., "On line diagnosis of defaults on squirrel cage motor using FEM", *IEEE Transactions on Magnetics*., Vol. 34, No. 5, pp. 3511-3574, 1998.

[21] John F. Watson, Neil C. Paterson, David G. Dorrell, "The use of finite element methods to improve techniques for the early detection of faults in 3- phase induction motors", *IEEE Transactions on energy conversion*, Vol. 14, No. 3, pp. 655-660, 1999.

[22] Martin Blödt, Jérémi Regnier, and Jean Faucher, "Distinguishing load torque oscillations and eccentricity faults in induction motors using stator current wigner distributions", *IEEE Transactions on Industry Applications*, Vol. 45, No. 6, 2009.

[23] Aileen Christina. J, Nagarajan. S and S. Rama Reddy. "Detection of broken Bars in three phase squirrel cage induction motor using finite element method", *International Conference on Emerging Trends in Electrical and Computer Technology*, pp. 249-254, 2011.

[24] Vaseghi B., Takorabet N., Meibody-Tabar F., "Modeling of 1M with stator winding inter-turn fault validated by FEM", *Proceedings of the International Conference on Electrical Machines*, 2008.

[25] Preston T. W., Reece A. B. J., Sangha P. S., "Induction motor analysis by time-stepping techniques", *IEEE Transactions on Magnetics*, Vol. 24, No. 1, pp. 471-

474. Jan 1988.

[26] Ali Ebadi, Mohammad Mirzaie and Sayyed, “Employing finite element method to analyze performance of three-phase squirrel cage induction motor under voltage harmonics”, *Research Journal of Applied Sciences, Engineering and Technology,* Vol 3, pp. 1209-1213, 2011.

[27] P. Lombard, G. Meunier, “A general method for electric and magnetic coupled problem in 2D magneto dynamic domain”, *IEEE Transactions on Magnetics,* Vol. 28, No. 2, pp. 1291-1294, March 1992.

[28] J. Grieger, R. Supangat, N.Ertugrul, W.L. Soong, D. A. Gray, C. Hansen, “Estimation of static eccentricity severity in induction motors for online condition monitoring”, Proceedings of the 41st *IEEE IAS Annual Meeting Industry Applications Conference,* pp. 2312-2319, October, 2006.

[29] V. Fireteanu and P.Taras, “Diagnosis of induction motor rotor faults based on finite element evaluation of voltage harmonics of coil sensors”, *IEEE Sensors Applications Symposium (SAS),* pp.1-5, February, 2012.

[30] N. Halem, S. E. Zouzou, K. Srairi, S. Guedidi and F. A. Abbood, “Static eecentricity fault diagnosis using signature analysis of stator current and air gap magnetic flux by finite element method saturated induction motors”, Vol.4, No.2, pp.118-128, June 2013.

[31] Yazidi, H. Henao, G. A. Capolino, M. Artioli, F. Filippetti, and D. Casadei, “Flux signature analysis: An alternative method for the fault diagnosis of induction machines”, in Proceedings *IEEE Power Tech, St. Petersburg, Russia,* pp. 1–6, 2005.

[32] Randy R. Schoen, Brian K. Lin, Thomas G. Habetler, Jay H. Schlag, and Samir Farag, “An unsupervised, on-line system for induction motor fault detection using stator current monitoring”, *IEEE Transaction on Industry Applications,* Vol. 31, No. 6, pp. 1280-1286, 1995.

[33] Rolf Isermann, “Model based fault detection and diagnosis status and applications,” *Annual Reviews in Control,* Vol. 29, No. 1, pp. 71–85, 2005.

[34] M. Arkan, D.K. Perović, P. Unsworth, "Online stator fault diagnosis in induction motors", *IEEE proceedings Electric Power Applications*, Vol. 148, pp. 537 – 547, November 2001.

[35] M. Sahraoui, A. Ghoggal, S. E. Zouzou A. Aboubou and H. Razik, "Modelling and detection of inter-turn short circuits in stator windings of induction motor", *IEEE Transactions on Energy Conversion*, Vol. 1, No. 1, pp. 4981-4986, 2006.

[36] S. Bachir, S. Tnani, J. C. Trigeassou, and G. Champenois, "Diagnosis by parameter estimation of stator and rotor faults occurring in induction machines", *IEEE Transactions on Industrial Electron*ics, Vol. 53, No. 3, pp. 963–973, 2006.

[37] F. L. Stanislaw, A .H. M. Sadrul Ula, A. M. Trzynadlowski, "Instantanious power as a medium for the signature analysis of induction motors", *IEEE Transactions on Industrial Applications,* Vol. 32, No. 4, pp. 904-909, 1996.

[38] G. G. Yen, K. C. Lin, "Wavelet packet feature extraction for vibration monitoring", *IEEE Transactions on Industrial Electronics*, Vol. 47, No. 3, pp. 650–667, 2000.

[39] Marques M., Martins J., Pires V.F., Jorge R.D., Mendes L.F., " Fault detection and diagnosis in induction machines: A case study ", *IFIP Advances in Information and Communication Technology*, Vol. 394. Springer, Berlin, Heidelberg, 2013.

[40] K. Kim, A. G. Parlos, and R. M. Bharadwaj, "Sensorless fault diagnosis of induction motors", *IEEE Transactions on Industrial Electronics*, Vol. 50, No. 5, pp. 1038– 1051, 2003.

[41] H. Douglas, P. Pillay, and A.K Ziarani, "A new algorithm for transient motor current signature analysis using wavelets," *IEEE on Transactions Industrial Applications,* Vol. 40, No. 5, pp. 1361–1368, 2004.

[42] T. Yang, H. Pen, Z. Wang and C. S. Chang, "Feature knowledge based fault detection of induction motors through the analysis of stator current data", IEEE Transactions on Instrumentation and Measurement, Vol. 65, No. 3, pp. 549-558, March 2016.

[43] A. M. da Silva, R. J. Povinelli and N. A. O. Demerdash, "Induction machine broken bar and stator short-circuit fault diagnostics based on three-phase stator current envelopes", IEEE Transactions on Industrial Electronics, Vol. 55, No. 3, pp. 1310-1318, March, 2008.

[44] M. Riera- Guasp, J. A. Antonino Daviu, M. Pineda-Sanchez, R. Puche Panadero and J. Perez-Cruz, "A general approach for the transient detection of slip dependent fault components based on the discrete wavelet transform", *IEEE Transactions on Industrial Electronics,* Vol. 55, No. 12, pp. 4167–4180, 2008.

[45] H. Nejjari and M. H. Benbouzid, "Monitoring and diagnosis of induction motors electrical faults using a current park's vector pattern learning approach", *IEEE Transactions on Industrial Applications,* Vol. 36, No. 3, 2000.

[46] F. Filippetti, G. Franceschini, and C. Tassoni, "Recent developments of induction motor drives fault diagnosis using artificial intelligence techniques", *IEEE Transactions on Industrial Electronics,* Vol. 47, No.5, pp. 994–1003, 2000.

[47] M. A. Awadallah, and Mon. M. Morcos, "ANFIS- based diagnosis and location of stator inter-turn faults in PM brushless DC Motors," *IEEE Transactions on Energy Conversions,* Vol. 19, No. 4, pp. 795-796, 2004.

[48] W. W. Tan and H. Huo, " A generic neuro-fuzzy model-based approach for detecting faults in induction motors," *IEEE Transactions on Industrial Electron*ics, Vol. 52, No. 5, pp. 1420-1427, 2005.

[49] M. S. Ballal, Z. J. Khan, H. M. Suryawanshi, R. L. Sonolikar, "Adaptive neural fuzzy inference system for the detection of inter-turn insulation and bearing wear faults in induction motor," *IEEE Transactions on Industrial Electron*ics, Vol. 54, No. 1, pp. 250–258, 2007.

[50] Pedro Vicente Jover Rodríguez, Antero Arkkio, "Detection of stator winding fault in induction motor using fuzzy logic," *Applied Soft Computing Journal,* Vol. 8, No. 2, pp. 1112–1120, 2008.

[51] R. H. Abiyev, O. Kaynak, "Fuzzy wavelet neural networks for identification and

control of dynamic plants- A novel structure and a comparative study," *IEEE Transactions on Industrial Electron*ics, Vol. 55, No. 8, pp. 3133–3140, 2008.

[52] M. B. K. Bouzid, G. Champenois, N. M. Bellaaj, L. Signac, and K. Jelassi, "An effective neural approach for the automatic location of stator inter-turn faults in induction motor," *IEEE Transactions on Industrial Electron*ics, Vol. 55, No. 12, pp. 4277-4289, 2008.

[53] J. Kurek and S. Osowski, "Support vector machine fault diagnosis of the broken rotor bars of squirrel-cage induction motor," *Neural Computing & Applications Journal,* Vol. 19, pp. 557-564, 2010.

[54] Feng Jia, Yaguo Lei, Jing Lin, Xin Zhou, Na Lu, "Deep neural networks A promising tool for fault characteristic mining and intelligent diagnosis of rotating machinery with massive data." *Mechanical Systems and Signal Processing Journal*, Vol 72, pp. 303–315, 2016.

[55] Zhang W, Peng G, Li C, Chen Yand Zhang Z. "A new deep learning model for fault diagnosis with good anti-noise and domain adaptation ability on raw vibration signals". *Sensors (Basel).*17(2):425, February 2017.

[56] X Yang, R Yan, R X Gao., "Induction motor fault diagnosis using multiple class feature selection". Proceedings of 2015 *IEEE International Instrumentation and Measurement Technology Conference (IIMTC), Pisa, Italy,* pp. 256–260, May 11-15, 2015.

[57] T. dos Santos, F. J. T. E. Ferreira, J. M. Pires and C. Damásio, "Stator winding short-circuit fault diagnosis in induction motors using random forest," *IEEE International Electric Machines and Drives Conference (IEMDC),* Miami, FL, , pp. 1-8, 2017.

[58] Aydin, Ilhan & Karakose, Mehmet & Akin, Erhan. "A new method for early fault detection and diagnosis of broken rotor bars," *Energy Conversion and Management Journal* , pp :1790-1799, 2011.

[59] Jagadanand, G., Lalgy Gopi, S. George and J. Jacob. "Inter-turn fault detection in induction motor using stator current wavelet decomposition", *International*

Journal of Electrical Engineering and Technology, Vol. 3, pp. 103-122, 2012.

[60] Fang R, "Induction machine rotor diagnosis using support vector machines and rough set". Lecture Notes in Computer Science, Springer, Berlin, Heidelberg, Vol. 4114, pp. 631–636, June 2006.

[61] Fatima Husari and Jeevanand Seshadrinath, "Sensitive inter-tum fault identification in induction motors using deep learning based methods", *IEEE International Conference on Power Electronics, Smart Grid and Renewable Energy* (PESGRE2020), 2020.

[62] E. Pandarakone, M. Masuko, Y. Mizuno and H. Nakamura, "Deep neural network based bearing fault diagnosis of induction motor using fast fourier transform analysis," *IEEE Energy Conversion Congress and Exposition (ECCE)*, Portland, OR, pp. 3214-3221, 2018.

[63] Heydarzadeh, Mehrdad & Hedayati Kia, Shahin & Nourani, Mehrdad & Henao, Humberto & Andr´, G & Capolino, Gérard-André., "Feature learning using deep neural networks for fault diagnosis in electromechanical systems", *ASME Dynamic Systems and Control Conference,* November 2019.

[64] John Grezman, Jianjing Zhang, Peng Wang, Kenneth A. Loparo and Robert X. Gao, "Interpretable convolutional neural network through layer-wise relevance propagation for machine fault diagnosis" IEEE Sensors Journal Vol. 20 , No. 6 , March15, 2020.

[65] Mohammad Zawad Ali, Md Nasmus Sakib Khan Shabbir, Xiaodong Liang, Yu Zhang and Ting Hu, "Machine learning-based fault diagnosis for single- and multi-faults in induction motors using measured stator currents and vibration signals", *IEEE Transactions on Industry Applications,* Vol. 55, No. , pp: 2378 – 2391, May 2019.

[66] Tarannum Khan , Pyla Alekhya and Jeevanand Seshadrinath, "Incipient Inter-turn Fault Diagnosis in Induction motors using CNN and LSTM based Methods", *IEEE Industry Applications Society Annual Meeting (IAS),* 2018.

[67] P.O. Donnell et al, "Report of Large Motor Reliability Survey of Industrial and

Commercial Installations, Part I," in IEEE Transactions on Industry Applications, Vol. IA-21, No. 4, pp. 853-864, July 1985.

[68] Neale, M. J. “The benefit of condition monitoring: Condition monitoring of machinery and plant,” Mechanical Engineering Publications Ltd., The Institution of Engineers, London, pp. 25-30, 1985.

[69] V. Wowk, “Machinery Monitoring. Machinery Vibration- Measurement and Analysis,” New York: McGraw-Hill Inc., pp. 17-18, 1991.

[70] P. C.Krause, O. Wasynczuk and S. D. Sudhoff, Analysis of electric machinery New York: IEEE Press, 1996.

[71] S. Wang, V. Dinavahi, and J. Xiao, “Multi-rate real-time model-based parameter estimation and state identification for induction motors,” *IET Electric Power Applications Journal*, Vol. 7, No. 1, pp. 77–86, 2013.

[72] S. Bachir, S. Tnani, J. Trigeassou, and G. Champenois, “Diagnosis by parameter estimation of stator and rotor faults occurring in induction machines,” *IEEE Transactions on Industrial Electronics*, Vol. 53, No. 3, pp. 963–973, 2006.

[73] Mei-shan Jin; A-lin Hou; Chang-li Qiu; Da-chuan Chen, “A maxwell 2D emulated analysis in the performance of linear introduction motor,” *International Conference on Computer, Mechatronics, Control and Electronic Engineering (CMCE)* , Vol.4, pp. 348-351, August 2010.

[74] Qiu Changli; Cheng Jihang; Li Jingquan, “Simulation analysis of the performance of linear introduction motor in maxwell 2D”, IEEE Symposium on Electrical & Electronics Engineering (EEESYM), pp.360-363, June 2012.

[75] Anagha Soman, Nupur Lokhande, D.G. Bhardwaj, “Performance and analysis of 3 phase Induction motor using ANSYS Maxwell”, International journal of pure and applied mathematics, Vol. 118, pp. 269-281, October 2018.

[76] Benoît Robyns, Bruno Francois, Philippe Degobert, and Jean Paul Hautier, “Vector control of induction machines: desensitisation and optimisation through fuzzy logic,” *Springer-Verlag London,* 2012.

[77] A. Trzynadlowski, The field orientation principle in control of induction motors, *Kluwer Academic Publishers*, Boston, Ch. 1, 1994.

[78] Mohammed, O.A., Abed, N.Y. and Ganu, S., "Modeling and characterization of induction motor internal faults using finite element and discrete wavelet transforms," *IEEE Transactions on Magnetics,* Vol.42, No.10, pp. 3434-3436, October 2006.

[79] P.F. Albrecht, J.C. Appiarius, R.M. McCoy, E.L. Owen, D.K. Sharma, "Assessment of the reliability of motors in utility applications – updated," *IEEE Transactions on Energy Conversion*, Vol.: EC-1, No. 1, pp.39-46, March 1986.

[80] J. Faiz and M. Ojaghi, "Instantaneous-Power Harmonics as Indexes for Mixed Eccentricity Fault in Mains-Fed and Open/Closed-Loop Drive-Connected Squirrel-Cage Induction Motors," in *IEEE Transactions on Industrial Electronics*, Vol. 56, pp. 4718-4726, November 2009.

[81] A. H. Bonnett, G. C. Soukup, "Cause and analysis of stator and rotor failures in three-phase squirrel-cage induction motors*," IEEE Transactions on Industrial Applications,* Vol. 28, No. 4, pp. 921–937, 1992.

[82] S. Rajakarunakaran, P. Venkumar, K. Devaraj, and K. S. P. Rao, "Artificial neural network approach for fault detection in rotary system," *Applied Soft Computing Journal,* Vol. 8, No. 1, pp. 740–748, 2008.

[83] J. Ramirez-Nino, A. Pascacio, "Detecting interturn short circuits in rotor windings," *IEEE Computer Applications in Power,* Vol. 14, No.4, pp. 39 - 42, 2001.

[84] Peter Vas, "Parameter estimation, condition monitoring, and diagnosis of electrical machines', *Clarendon Press, Oxford University Press Oxford, New York*, 1993.

[85] V T Tran, F Althobiani, A Ball., "An approach to fault diagnosis of reciprocating compressor valves using teager–kaiser energy operator and deep belief networks", *Expert Systems with Applications*, Vol. 41, No. 9, pp. 4113–4122, July, 2014.

[86] J Guo, X Xie, R Bie, et al., “Structural health monitoring by using a sparse coding-based deep learning algorithm with wireless sensor networks”, *Personal and Ubiquitous Computing*, Vol. 18, No.8, pp: 1977–1987, 2014.

[87] G E Hinton, S Osindero, Y W Teh. “A fast learning algorithm for deep belief nets”, *Neural Computation*, Vol. 18, No.7, pp: 1527–1554, 2006.

[88] I. Aydin, M. Karakose and E. Akin, "Artificial immune based support vector machine algorithm for fault diagnosis of induction motors," *International Aegean Conference on Electrical Machines and Power Electronics, Bodrum*, pp. 217-221, 2007.

[89] N. A. Mohsun, "Broken rotor bar fault classification for induction motor based on support vector machine-SVM," *International Conference on Engineering & MIS (ICEMIS*), Monastir, pp. 1-6, 2017.

[90] M. Gordi Armaki and R. Roshanfekr, “A new approach for fault detection of broken rotor bars in induction motor based on support vector machine,” *18th Iranian Conference on Electrical Engineering,* Isfahan, pp. 732-738, 2010.

[91] Z. Li, “New fault detection method for sliding bearings using empirical mode decomposition, genetic algorithm and support vector machine,” *Fifth International Conference on Intelligent Computation Technology and Automation*, Zhangjiajie, Hunan, pp. 225-228, 2012.

[92] X. Yang, R. Yan and R. X. Gao, “Induction motor fault diagnosis based on ensemble classifiers”, *IEEE International Instrumentation and Measurement Technology Conference Proceedings,* Taipei, pp. 1-5, 2016.

[93] Sm, Shashidhara & Raju, Dr.P., “Stator winding fault diagnosis of three-phase induction motor by park's vector approach”, *International Journal of Advanced Research in Electrical, Electronics and Instrumentation Engineering*, Vol. 2, pp. 2901-2906, 2013.

[94] Jie Tao, Yilun Liu, Dalian Yang, "Bearing Fault Diagnosis Based on Deep Belief Network and Multisensor Information Fusion", *Shock and Vibration Hindawi Publishing Corporation,* Vol. 2016, 2016.

[95] Yu-Min Hsueh, Veeresh Ramesh Ittangihal, Wei-Bin Wu, Hong-Chan Chang and Cheng-Chien Kuo, “Fault diagnosis system for induction motors by CNN

using empirical wavelet transform”, *Symmetry Journal on MDPI*, 2019.

[96] J. A. Corral-Hernandez and J. A. Antonino-Daviu, "Thorough validation of a rotor fault diagnosis methodology in laboratory and field soft-started induction motors," in *Chinese Journal of Electrical Engineering*, Vol. 4, pp. 66-72, September 2018.

[97] A. Guerra de Araujo Cruz, R. Delgado Gomes, F. Antonio Belo and A. Cavalcante Lima Filho, "A Hybrid System Based on Fuzzy Logic to Failure Diagnosis in Induction Motors," in *IEEE Latin America Transactions*, Vol. 15, , pp. 1480-1489, 2017.

[98] S. Shao, R. Yan, Y. Lu, P. Wang and R. X. Gao, "DCNN-Based Multi-Signal Induction Motor Fault Diagnosis," in *IEEE Transactions on Instrumentation and Measurement*, Vol. 69, pp. 2658-2669, June 2020.

[99] I. Kao, W. Wang, Y. Lai and J. Perng, "Analysis of Permanent Magnet Synchronous Motor Fault Diagnosis Based on Learning," in *IEEE Transactions on Instrumentation and Measurement*, Vol. 68, pp. 310-324, February 2019.

[100] A. Hajary, R. Kianinezhad, S. G. Seifossadat, S. S. Mortazavi and A. Saffarian, "Detection and Localization of Open-Phase Fault in Three-Phase Induction Motor Drives Using Second Order Rotational Park Transformation," in *IEEE Transactions on Power Electronics*, Vol. 34, pp. 11241-11252, November 2019.

[101] B. Gou, Y. Xu, Y. Xia, G. Wilson and S. Liu, "An Intelligent Time-Adaptive Data-Driven Method for Sensor Fault Diagnosis in Induction Motor Drive System," in *IEEE Transactions on Industrial Electronics*, Vol. 66, pp. 9817-9827, December 2019.

[102] S. Lu, Q. He, T. Yuan and F. Kong, "Online Fault Diagnosis of Motor Bearing via Stochastic-Resonance-Based Adaptive Filter in an Embedded System," in *IEEE Transactions on Systems, Man, and Cybernetics: Systems*, Vol. 47, pp. 1111-1122, July 2017.

[103] A. Naha, K. R. Thammayyabbabu, A. K. Samanta, A. Routray and A. K. Deb, "Mobile Application to Detect Induction Motor Faults," in *IEEE Embedded Systems Letters*, Vol. 9, no. 4, pp. 117-120, December 2017.

[104] S. M. K. Zaman, X. Liang and L. Zhang, "Greedy-Gradient Max Cut-Based Fault Diagnosis for Direct Online Induction Motors," in *IEEE Access*, Vol. 8, pp. 177851-177862, 2020.

[105] G. Mirzaeva and K. I. Saad, "Advanced Diagnosis of Rotor Faults and Eccentricity in Induction Motors Based on Internal Flux Measurement," in *IEEE Transactions on Industry Applications*, Vol. 54, pp. 2981-2991, June 2018.

[106] T. Yang, H. Pen, Z. Wang and C. S. Chang, "Feature Knowledge Based Fault Detection of Induction Motors Through the Analysis of Stator Current Data," in *IEEE Transactions on Instrumentation and Measurement*, Vol. 65, pp. 549-558, March 2016.

[107] J. A. Antonino-Daviu, J. Pons-Llinares and S. B. Lee, "Advanced Rotor Fault Diagnosis for Medium-Voltage Induction Motors Via Continuous Transforms," in *IEEE Transactions on Industry Applications*, Vol. 52, pp. 4503-4509, October 2016.

[108] W. Sun, R. Zhao, R. Yan, S. Shao and X. Chen, "Convolutional Discriminative Feature Learning for Induction Motor Fault Diagnosis," in *IEEE Transactions on Industrial Informatics*, Vol. 13, pp. 1350-1359, June 2017.

[109] S. B. Jiang, P. K. Wong, R. Guan, Y. Liang and J. Li, "An Efficient Fault Diagnostic Method for Three-Phase Induction Motors Based on Incremental Broad Learning and Non-Negative Matrix Factorization," in *IEEE Access*, vol. 7, pp. 17780-17790, July 2019.

[110] M. Ojaghi, M. Sabouri and J. Faiz, "Analytic Model for Induction Motors Under Localized Bearing Faults," in *IEEE Transactions on Energy Conversion*, Vol. 33, pp. 617-626, June 2018.

BRIEF PROFILE OF RESEARCH SCHOLAR

Kalpana Sheokand is presently working as Assistant Professor in Electronic Engineering Department of J.C. Bose University of Science and Technology, YMCA, Faridabad. She received Bachelor's degree in Electronics & Instrumentation Engineering from Maharshi Dayanand University, Rohtak in 2004 and Master's degree in Signal Processing from Maharshi Dayanand University, Rohtak in 2009. She has supervised various M.Tech thesis and B.Tech projects. She has published several papers in National & International Conferences /Journals. Her research interest is in the fields of signal processing, condition monitoring, fault diagnosis & soft computing and also pursuing her Ph.D. in the relevant field of interest.

LIST OF PUBLICATIONS

LIST OF PUBLISHED PAPERS

Sr. No	Title of the paper along with volume, Issue No, year of Publication	Publisher	Impact factor	Whether Referred or Non-Referred	Whether you paid any money or not for publication	Remarks
1	Classification and Detection of Faults in Induction Motor using DWT with Deep Learning Methods under the time-varying and constant load conditions, International Journal of Recent Technology and Engineering, Vol.-8, Issue- 3, 2019, ISSN No. 2277-3878	BEIESP	1	Referred	No	SCOPUS
2	Behaviour Analysis of Induction Motor under various Fault Conditions of Rotor bar at Different Loading", International Journal of Computer Sciences and Engineering, ISSN No.2347-2693 Vol.-6, Issue 2, 2018	ISROSET	3.802	Referred	No	UGC Approved
3	Fault Diagnosis Of Induction Motor Under Various Fault Conditions Of Stator Winding At Different Loading Level, International journal of Modern Electronics and Communication Engineering, 2018, Vol.6, Issue 2, ISSN No.: 2321-2152	IJMECE Publishing House	1.517	Referred	No	UGC Approved

4	A Review on various Faults and Fault Diagnosis of Induction Motor, Trends in Mechanical Engineering & Technology, ISSN No.: 2347-9965, 2018, Vol.8, Issue- 2	Division of Consortium eLearning Network Pvt. Ltd.	-	Referred	No	UGC Approved
5	Detection of Eccentricity Fault for Induction Motor", Trends in ElectricalEngineering,2018 vol.8, Issue- 2, ISSN No.: 2249–4777	CELNET	-	Referred	No	UGC Approved

LIST OF COMMUNICATED PAPER

Sr. No.	**Title of the Paper**	**Name of the Journal**	**Present Status**	**Year**
6	Diagnosis of Combined Fault Detection in Induction Motor under Loading Conditions using Deep Belief Neural Network Authors: Kalpana Sheokand, Dr. Neelam Turk	SCIE Journal	Under Review	2021

EFFECTS OF TIME VARYING AND CONSTANT LOADS ON EFFECTIVENESS OF FAULT DETECTION METHODS OF ELECTRICAL MACHINE

SYNOPSIS

submitted in fulfillment of the requirement of the degree of

DOCTOR OF PHILOSOPHY

to

J.C.BOSE UNIVERSITY OF SCIENCE & TECHNOLOGY, YMCA, FARIDABAD

by

KALPANA SHEOKAND

Registration No: YMCAUST/Ph23/2011

Under the Supervision of

Dr. NEELAM TURK

PROFESSOR

Department of Electronics Engineering

Faculty of Engineering and Technology

J.C. Bose University of Science & Technology, YMCA, Sector-6, Mathura road

Faridabad, Haryana, India

OCTOBER, 2021

DECLARATION

I hereby declare that this synopsis entitled **EFFECTS OF TIME VARYING AND CONSTANT LOADS ON EFFECTIVENESS OF FAULT DETECTION METHODS OF ELECTRICAL MACHINE** by **KALPANA SHEOKAND,** being submitted in fulfilment of the requirement for the Degree of Doctor of Philosophy in **ELECTRONICS ENGINEERING** under Faculty of Engineering of J. C. Bose University of Science and Technology, YMCA , Faridabad, during the academic years 2020-2021, is a bona fide record of my original work carried out under guidance and supervision of **Dr. NEELAM TURK, PROFESSOR, DEPARTMENT OF ELECTRONICS ENGINEERING,** J. C. Bose University of Science and Technology, YMCA, Faridabad and has not been presented elsewhere.

I further declare that the thesis does not contain any part of any work which has been submitted for the award of any degree either in this university or any other university.

Kalpana Sheokand

Registration No. YMCAUST /Ph 23/2011

CERTIFICATE

This is to certify that this synopsis entitled **EFFECTS OF TIME VARYING AND CONSTANT LOADS ON EFFECTIVENESS OF FAULT DETECTION METHODS OF ELECTRICAL MACHINE by KALPANA SHEOKAND**, submitted in fulfilment of the requirement for the Degree of Doctor of Philosophy in **ELECTRONICS ENGINEERING** under Faculty of Engineering of J. C. Bose University of Science and Technology, YMCA, Faridabad, during the academic years 2020-2021, is a bona fide record of the work carried out under my guidance and supervision.

I further declare that to best of my knowledge the thesis does not contain any part of any work which has been submitted for the award of any degree either in this university or any other university.

Dr. Neelam Turk
Professor
Department of Electronics Engineering
Faculty of Engineering and Technology
J.C. Bose University of Science and Technology,
YMCA, Faridabad

Dated:

TABLE OF CONTENTS

1. INTRODUCTION

The electric motor is an electromechanical device that converts electrical energy into mechanical energy. As a very important part of modern industry, Induction Motors play an important role in important applications such as pump systems, fans, lifting systems, electric vehicles, crushers, cement plants, and many other industrial segments. An asynchronous motor, which is actually an AC motor in which the current required to generate torque, is induced by electromagnetic induction of the magnetic field of the stator winding [1]. Therefore, induction machines generally do not require external mechanical switching, individual excitation, or even self-excitation for part of the energy transferred from the stator to the rotor. The rotors of numerous electrical components in operating induction machines are highly prone to system failure [2].

With a squirrel cage rotor [3], its bars can be damaged by mechanical stresses on the machine. Meanwhile, the bearings in the IM can be affected by extreme wear and fragmentation caused by improper lubrication, unbalanced load on the motor, misalignment of the bearing components with the rotor, etc. Traditionally, most manufacturers and users trust it in a very traditional way approaches to IM protection such as overcurrent or overvoltage estimation to ensure reliable system operation. Fast and immensely complex IM applications in modern industrial applications are alarming for optimized system monitoring and monitoring for induction machines [3]. Even the reduction of the man-machine interface requires requirements for on-line detection, with which motor faults can be diagnosed effectively without danger or process interruptions. The IMs low cost and miniaturized size, low maintenance cost robustness and flexible operation with minimal power supply make this system highly efficient and useful in modern industrial process. Detecting faults in the IM in advance and diagnosing them optimally makes it easier for industry to work with the least unexpected industrial shutdown or maintenance mechanism [4]. This minimizes lost production, financial waste, and even prohibits catastrophic penalties. Condition monitoring and fault diagnosis mechanisms are necessary to formulate a well-defined and qualified map between the motor signals and the IM fault condition indications [4].

Various failure detection methods have been developed and effectively applied to detect machine failures at different stages using various machine variables such as current, voltage, speed, efficiency, temperature, and vibration [5]. Therefore, for economic and safety reasons, it is important to control the behavior of motors of different sizes. As an approach to condition monitoring, a very effective scheme can be offered that can provide the warning device at an early stage and efficiently predict the possibility of errors at an early stage of operation [6]. The monitoring system retrieves the details of the machines in use as raw data or raw details. By implementing advanced and highly efficient signal processing approaches, communicating diagnostic information to operators becomes very easy and straightforward, even well before the catastrophic machine failure. The challenging problem with this approach is that this mechanism requires continuous surveillance with human presence. Automation in the diagnostic process could include the logical progression of condition monitoring methods. To automate the diagnostic process, a series of soft computational diagnostic techniques using fuzzy logic [7, 8], NN [9] and machine learning algorithm [10] have recently been implemented.

In view of the need for a robust and highly efficient system for the detection of faults in IM, the approaches based on the Fourier transform and the wavelet transform can play a decisive role. The precision and spontaneous diagnostic potential of these signal processing approaches make them robust and efficient candidates for use in most induction machine fault detection applications [11]. The work presented considers the Discrete Wavelet Transform (DWT) technique with machine learning algorithms to achieve the objective of detection of errors in IM.

A number of approaches and systems are there for monitoring the IM functions for ensuring the higher consistency. Few leading approaches are as follows [12, 13]:

1. EMF monitoring systems,
2. Systems based on temperature estimation,
3. Monitoring approach based on radio frequency emissions analysis,
4. Approaches based on the estimation of noise and vibration in IM,
5. Approaches considering the speed and torque of rotor,

Despite these approaches and tools mentioned above, there are a number of companies that suffer from unexpected system failures that ultimately result in lower productivity in the industry. Various issues such as the environment, features, and system facilities can cause the system to fail in their combined form. Therefore, any type of optimization and improvement of the system could be of great interest to everyone.

2. BACKGROUND

Extensive research has been conducted over the past 20 years to develop new diagnostic and Fault Detection techniques for IM. The review also covers a wide range of literature in the field including machine modeling, conditioning monitoring, machine health assessment, types of faults in IM and FD techniques. In addition to the methods mentioned above, this literature survey also takes into account the most important developments in this area in recent years. This overview covers techniques related to model-based fault detection techniques, techniques based on signal processing, and techniques based on soft computing.

2.1 Model Based Techniques

In the recent past numerous researches have been conducted and numerous Fault Detection (FD) techniques like Finite Element Method (FEM), and others have been employed by the researchers for fault diagnosis. The major developments in these fields are covered in the review, from early research to the most recent.

Nandi et al. [14] has a broad distribution of the major electrical machines faults:

- Abnormal connection of the stator winding,
- Broken rotor bars or cracked end rings,
- Static and/or dynamic air-gap eccentricities,
- Bent shaft,
- Shorted rotor field winding,
- Bearing and gearbox failures.

These faults produce one or more of the following symptoms [14]:

- Unbalanced voltages and line currents,
- Increased torque pulsation,
- Decreased average torque,
- Increased losses and reduction in efficiency,

Transient analysis of an IM using FEA with predicted transient powers when starting the motor without load [15], when operating the motor with asymmetric stator excitation and during the turn-by-turn fault state, the geometric dimensions of the IM are modeled in the area of the finite elements. Diagnosis and characterization of the influence of broken rotor bars and connectors in squirrel cage motors using the state space sampling method for finite elements in connection with the temporal resolution method, diagnostic effects and characterization of elongation of broken bars and connectors [16]. The models are used to calculate/predict the characteristic frequency components that characterize bus bar and connector breakage. The behavior of electromagnetic properties is also analyzed using the FEM analysis for the occurrence of bus failure [17]. In other research work, flux density and mechanical stress were used to capture motor shaft failure in the mainline fed FEM model [18].

Most of the FD techniques available in the literature are based on the analytical model, which includes various assumptions for current spectrum analysis that does not take into account saturation, non-linear core materials and natural effects etc. To address this problem, the Equivalent Magnetic Circuit (EMC) model [19] was used to take into account the effects of magnetic saturation, the non-linear behavior of the material and the real representation of the air distribution in the stator and grooves rotor. Online diagnosis of squirrel cage motor failures using FEM suggests an approach based on the signature of global and external variables that is used to solve problems related to broken rotor bar and terminal ring [20]. This enables finer analysis using finite element-based implementation, higher precision, and an easier form of recognition. The use of finite element techniques to improve early fault detection techniques in three-phase IM describes how commercial finite element packages can be used to simulate rotor failures and thus improve the capacity of practical condition monitoring systems [21]. Accurate models of machines under failure conditions are developed using finite element packages with fixed mesh and timing. In Martin et al. [22], the influence of non-consecutive line breaks in MCSA to diagnose rotor faults in IM provides modeling to investigate the influence of the number and position of faulty bars on the diagnostic method of traditional MCSA. The analysis is based on the fault current and space vector theory, which provides a physical interpretation of the appearance of the left sideband component at a fraction of two extremes. In other studies, the static two-dimensional analysis of the fault and the results of the stator windings was compared with a healthy motor [23].

Vaseghi et al. [24] proposed IM model with stator winding fault and the model is validated using time steps FEA. The designed model is used to analyze the behavior of the machine under fault conditions. An IM analysis using time-step techniques shows that the equivalent circuit approach generally provides reasonable predictions about torque and current, but not information about flux distribution. This deficiency is remedied by a numerical approach using a nonlinear, time-shifted 2D finite element method to drive a constant voltage source [25]. Comparison of no-load stator current and other load conditions shows good agreement with test values at a large IM.

Ebadi et al. [26] introduced the FEM, a numerical method to solve a differential or integral equation. This is true for a number of physical problems where the relevant differential equations exist. The FEM consists of a continuous function in parts for the solution, so that the fault in the solution is reduced. Ali Ebadi describes the performance evaluation of the three phase squirrel cage induction machine according to FEM.

Lombard et al. [27] discussed some of the benefits of Finite Numerical Method(FEM), widely used for numerically solving differential equations in two or three space variables including higher precision, better design and understanding of critical design parameters, virtual prototypes, fewer hardware prototypes, a faster and more economical design cycle, higher productivity, and more revenue. The basic theory of conventional electromagnetic and direct EMF is given by P Lombard et al. In some research papers, modeling based on state space equations is used to determine the stator current in the IM for FD using the FEA [28].

Fireteanu et al. [29] provide detailed information on the effects of SE on IM in a series of experiments with different strains and eccentricity levels. While this helps to understand the effect of SE, it cannot be used directly to detect eccentricity errors because detailed error testing is not possible on an industrial motor. Researchers have also tried signature (current and air gap magnetic flux) analysis to identify eccentricity failure [30], where the coil sensors are arranged in a different orientation to identify faults. The severity of SE in induction machines diagnosed using the magnetic flux density of airspace [31]. However, due to the difficulty of obtaining air gap magnetic induction, no experimental results were provided to validate the results. The document does not even offer a solution to implement it. An analysis based on flow patterns is presented in some studies [32]. Flow pattern analysis is quite simple and completely non-invasive. In addition, it is more effective than conventional motor current analyzes in identifying the rotor and stator in induction machines.

Isermann [33] presented model-based consistent progressive fault identification and prediction for Multiple Input Multiple Output (MIMO) nonlinear discrete time systems. The proposed scheme handles state and output errors considering separate time profiles. Occurring or abrupt errors are modeled on the basis of the input and output signals of the system. The asymptotic stability of the Failure Detection and Prediction (FDP) scheme improves detection and accuracy of time to failure. The robustness of the proposed method is demonstrated using a MIMO (fourth order) satellite system.

Arkan et al. [34] presented two orthogonal wave models of a tri-phasic IM. Of these two models, the first has asymmetrical windings and the other has inter-turn shorts in the stator winding. The motor is modeled using classical two-axis theory and the equations are modified to account for faults between the stator windings. A form of the system state space is presented for dynamic modeling. The results of the execution of the models are compared with the experiment carried out on a special wound motor with bushings to shorten a different number of turns. Previous models were used successfully to investigate steady-state and transient behavior of IM in short-circuits windings.

Sahraoui et al. [35] have presented an advanced mathematical model for induction machines that operates short circuits between the stator windings. The model is based on the multiple coupled proximity circuit. Inductances are calculated in a 2D extension of the Modified Winding Function (EMWFA) approach, in which spatial harmonics across the slots are taken into account in addition to the effects of rotor bar preload and increasing linear MMF. The results show that the short circuit between the windings causes some spectral components that appear in the spectral line of the current.

Bachir et al. [36] have proposed a new model of squirrel cage motors for stator and rotor failure. First, they processed a model that takes into account the effects of faults between turns that cause a short circuit in one or more stator phase winding circuits.

They then propose a new faulty model dedicated to detecting broken rotor bars. The appropriate diagnostic method is proposed based on the estimation of the defective model parameters of the stator and rotor.

2.2 Signal Processing Techniques

Signal processing techniques have been widely used in recent years to identify various instant messaging errors. These techniques successfully detect certain faults in the IM by analyzing the characteristics or specific parameters generated in the data being sampled. A new method has been introduced to analyze the signature of inductive motors, namely the real-time performance [37]. In this document, real-time energy is used instead of stator current to analyze the motor signature and identify mechanical defects in the drive system. The information carried by energy in real time is the product of voltage and current which is greater than the currently deductible capacity. In the current fixed power spectrum, the highest value is -52 dB, and in the current power spectrum the highest value is -47 dB. From the above, it can be seen that the real-time power is 5 dB greater than the power of the decentralized spectral component. A wavelet package has been proposed to extract useful information from IM vibration signals [38]. Although the measured vibration signals contain a transient part, the Fourier Transform cannot provide enough information to detect some machine faults. The results of using the wavelet packet are used by the statistical feature selection criteria to discard feature components that contain less discriminatory information. The extracted vector with reduced dimensional properties is used as input to the NN classifier. The results show an improvement in the ability to generalize the NN and a significant reduction in training time. The current approach is used to analyze signatures to detect instant messaging errors. This approach uses a power signature to determine that the author has detected many errors, such as breaking rotor bars in the IM squirrel and detecting short revolutions in an industrial motor. In this article, the author has created four case studies that identify various faults in the induction machine. Based on the results, the author made it clear that kinetic current analysis is a powerful technique for monitoring the status of triphasic IMs [39].

Kim et al. [40] has developed a fault diagnosis system without speed sensor for asynchronous motors. In this document, the proposed system is used to detect electrical elements (short circuit in the stator winding) and mechanical elements (broken rotor bars, eccentric air gap, bearings). Here, they used a combination of repetitive NNs and signal processing algorithms, such as wave-based and Fourier-based techniques, to detect faults in IMs. The voltage and currents from the terminals of motors were used as inputs to the diagnostic system. Fourier-based signal processing technology is applicable when the device is in a stable state, and wave-based signal processing technology is applicable when the device is in transition mode.

Douglas et al. [41] introduced a new algorithm that uses the gradient descent method to minimize least squares errors in a series of equations that change with time. The algorithm is used for the analysis of the current signature of the transient motor using waves. Here, the residual currents are analyzed with wavelets to detect broken rotor bars. The advantage of this method is that no parameters such as speed or number of rotor bars are required. In this method, a higher order notch filter is used to separate the fundamental frequency from the rotor bar frequencies. Once the fundamental frequency has been removed, the residual current can be examined using a DWT analysis. Therefore, the 8 Daubechies wavelets are used as a function of the mother wavelet. It can be seen from the results that the rotating rotor bar can be detected using transients measured at maximum current.

T.Yang et al.[42] proposed feature based online diagnostic approach for FD in IM using MCSA with advanced signal processing algorithms. The previously planned system was ready to diagnose IM with four types of defects such as broken rotor bars and also finishing rings, shorting of stator coil windings, bearing cracks and eccentricity defects of the air gap. Motor diagnosis with MCSA is dependent on slip. If the detected slip shows an error, the machine diagnostic results are incorrect. Therefore, to find the correct slip, the best slip hold algorithm estimator supported by the theorem estimation method is used.

A.M. da Silva et al. [43] has presented an IM fault diagnosis method that uses three-phase stator current envelopes for broken rotor bars and shorts between the windings in the stator windings. The above methods not only identify an IM as healthy or faulty, but also identify the severity of the failure by identifying the number of broken bars or the number of short turns in the stator windings. The training and test sets are generated from the tri phasic stator current of an IM under both healthy and faulty operating conditions using Gaussian Mixture Models (GMM) of reconstructed phase space transformations. The author has claimed that the proposed method can be a powerful troubleshooting tool for induction machines due to its higher precision.

M. Riera Guasp [44] proposed a technique based on the transformation of discrete wavelets for the detection of asymmetries in the rotor of an IM using the starting current and the stop-stop current, as well as the mixed eccentricities using the starting current. The author used Daubechies-44 as stem waves for the DWT analysis. To avoid an overlap between two neighboring frequency bands, a higher order mother wavelet was used. The author also found the parameters to quantify the severity of the failure in the case of starter rotor asymmetry and clogged rotor asymmetry.

2.3 Soft Computing Techniques

Various applications of using soft computing techniques in motor fault detection and diagnosis have been published across the different verticals of the industry journals. In most applications, the stator current is used with one of the soft computing classification algorithms to obtain FD accuracy. The Park vector patterns are based on the detection of different types of supply failures, such as voltage imbalance and single-phase adjustment [45]. Furthermore, a NN based back propagation algorithm is used to obtain the state of the machine by testing the shape of the vector patterns of the park. Two NN-based approaches were used, classical and decentralized. The generality of the proposed methodology has been experimentally tested and the authors state that the results provide a satisfactory level of precision. Applications of artificial intelligence in machine monitoring and fault diagnosis are examined in detail [46]. The expert system was used as a tool for the diagnosis of failures and the validity of the use of NN together with the fuzzy logic for the identification of failures and the evaluation of their severity.

Other research introduced a comprehensive adaptive neuro-fuzzy inference system to identify stator shorts in brushless DC motors, with fault diagnosis performed by two independent ANPHYSES. The first is used to find out the shorted turns and the second is used to identify the faulty phase [47]. The inputs to the first Adaptive Fuzzy Neural Inference System (ANFIS) are the diagnostic indices for determining the number of turns shorted, while the output was set to zero during normal operation and integers under fault conditions. The input to the second ANFIS were the identification indices of three phases and its output was an integer indicating the defective phase. In some applications, a generic approach based on a neuro-fuzzy model is based on the detection of flaws in the breaking bar of the rotor in an IM [48]. The data to train the neuro-fuzzy system to model the generic static torque-speed relationship of the IM class used in the practical evaluation of the fault detector. A modeling error was found when comparing the output speed of the neuro-fuzzy model and the speed obtained from the experimental torque-speed equation. This approach overcomes the practical limitations of model-based strategies by reducing the amount of experimental data required to design the flaw detector. This method can also identify the absence / presence of cracked rotor bars under various load conditions.

Ballal et al. [49] proposes ANFIS to detect bearing and insulation wear defects in IM. Here, the authors have given ANFIS five contributions which are as motor input current, speed, winding temperature, bearing temperature, and noise generation. Fuzzy neural architecture takes into account both Artificial Neural Network (ANN) and fuzzy logic technology. Authors have used a multilayer feed forward network as fuzzy rules of the ANN type and fuzzy inference systems.

Rodríguez and Antero Arkkio [50] used a method to detect faults in the stator winding in IM. In this work, the tri phasic mean square values of the stator and the variance were used as input for the fuzzy logic system. The input data is generated by FEM analysis with the engine running under various load conditions. The fuzzy logic method was able to record the state of the motor with and without noise with high precision. The disadvantage of the method is that a current imbalance generated by the power supply can be identified as a motor fault condition.

R.H. Abiyev and O. Kaynak [51] integrated both fuzzy logic systems with NN wavelet for the identification and control of an insecure system. In this article, they used the decent gradient algorithm for parameter settings. Two implementation examples were presented to identify and monitor performance. It was shown that diffuse wave NNs can converge faster and are more adaptable to new data.

Bouzid et. al [52] proposed NN approach for the automatic detection and localization of a short circuit fault between the windings in the stator of an IM. In this, they used a feed-forward multilayer NN perceptron that is trained by the back propagation technique. The phase shift between the phase voltage and the line current of an IM is used as an input to the NN. The desired output is set to one or zero. If a short is detected and it is in one of the three phases, the corresponding output NN is set to one otherwise it is zero.

J. Kurek and S. Osowski [53] presented an automated computerized system for diagnosing the rotor bars of the induction electric motor using the SVM. Two diagnostic system solutions have been developed. The first, called error detection, only detects when an error occurs. The second complex diagnosis can determine which bars have been damaged. The main problem is related to the generation and selection of diagnostic characteristics from which the condition of the rotor bars is detected.

Feng Jia et al. [54] aims to process massive error data immediately and automatically provide accurate diagnostic results. Numerous studies have been carried out on the intelligent diagnosis of failures in rotating machinery. Commonly used among these studies are ANN -based methods that use signal processing techniques to extract features and then input the features into ANN to classify faults.

Zhang W et al. [55] proposed a novel method called deep convolutional neural networks with broad first-layer nuclei. The proposed method uses raw vibration signals as input (data expansion is used to generate more inputs) and uses the wide cores in the first convolution layer to extract characteristics and suppress high frequency noise.

X Yang et al. [56] proposed an effective and practical fault diagnosis algorithm for induction machines, which is based on adaptive weighted votes from various RF classifiers. First, the vibration signals and the stator current signals are obtained and analyzed. The energy characteristics at various characteristic frequencies related to motor failures of each type of signal are extracted and used as input to the appropriate RF classifier. Cluster analysis is then applied to the test and training samples to determine the weight of each classifier to make decisions about the diagnostic result.

T. dos Santos et al. [57] proposed an approach to detect short circuit faults in the stator winding in SCIM based on RF. This is accomplished by evaluating the imbalance in the current and voltage waveforms, as well as in the park's vector for both current and voltage.

Aydin et al. [58] introduced the new feature vector based on park's vector approach. The phase space of this feature vector is constructed using nonlinear time series analysis. Faulty short circuit faults in the rotor rod and stator are rated with SVM in the combined phase space. The experimental data come from a three-phase IM. One, two and three broken rotor bars faults and a 10% short circuit of stator faults are successfully detected. The MCSA technique is based on the analysis of stator current under healthy and faulty conditions. This technique suggested diagnosing stator-to-turn failure in IM using wavelet transform and SVM as tools [59]. The fault diagnosis system using SVM-based classification techniques was developed for the diagnosis of rotor failures of cage induction machines. Subsequently, a classifier based on SVM for various classes will be developed and applied in order to distinguish health status from various rotor failure states [60].

Research based on deep learning is carried out to diagnose and classify the different types of faults in induction machines. For sensitive identification of faults between shifts in IM using deep learning-based methods, the model is trained and tested early on an induction machine to mainly detect short circuit faults between the windings. In the proposed work, models of Convolutional Neural Networks (CNN), recurrent NNs. Long-term Short-term Memory (LSTM), included for Fault Detection. Furthermore, the results show that CNN is superior to LSTM in accuracy, which provides good classification performance for FD in the early stages of fault development [61].

E. Pandarakone et al. [62] took into account the practical occurrence of faults and introduced the scratch on the outer race of the bearing. An online bearing diagnostic method is proposed using a deep learning based approach. The CNN architecture is originally used for fault characterization. In particular, a FFT analysis is performed using the stator load current, followed by the extraction of characteristics of selected frequency components that are used to train the CNN algorithm.

Heydarzadeh et al. [63] in, deep NNs are employed to diagnose five classes of transmission faults that apply to three common supervisory signals, i.e vibration, acoustics, and torque. DWT is used to provide the initial functions as inputs to the network. To validate the proposed method, a test bench built based on a 250W three-phase SCIM shaft which is connected to a single-stage helical gear drive.

John Grezman et al. [64] in, the authors examine the performance of a CNN that is trained using images of time-frequency spectra of vibration signals measured in an IM. The results show that the patterns learned by the CNNs in the time-frequency spectrum images are intuitive and consistent with respect to network retraining.

Mohammad Zawad Ali et al. [65], in this research work, stator currents and vibration signals from motors are selected to develop fault detection methods. Additionally, two signal processing techniques (Matching Pursue and DWT) are selected for feature extraction. Three classification algorithms, SVM, KNN, and Ensemble, with 17 different classifiers offered in the MATLAB toolbox, are used in the modeling to evaluate the performance and suitability of different classifiers for diagnosis of failures.

Tarannum Khan et al [66] in, author suggested Motor Current Signature Analysis (MCSA) using deep learning based one dimensional Convolutional Neural Network(1D-CNN) model and Long Short Term Model (LSTM). The results using these two methods have been compared, and this initial investigation shows that CNN is found to be more suitable than LSTM, for incipient fault diagnosis.

Lots of quality research on fault diagnosis of induction machine and algorithm based detection have been examined. To detect and classify various machine learning based model, fuzzy based model have been implemented and posted commendable results. The literature survey indicates that the individual faults have been the main focused area and combined fault analysis is still an unexplored area. Furthermore, the time varying load operating conditions of IMs are not much researched. Need of considering combination of faults which could be hazardous for the motor is at most.

3. RESEARCH GAPS

Previous research has addressed several aspects related to Fault Detection techniques used for fault diagnosis of Induction Motor like the model based techniques, signal processing techniques and soft computing techniques.

However, majority of the research work which provides outstanding results mainly suggested Motor Current Signature Analysis(MCSA) with stator current as single signature analysis with signal processing techniques like FFT, STFT, Gabor and Hilbert transform etc. to detect presence of fault. But, each technique has some advantages and disadvantages like in case of FFT it has been observed that it cannot diagnose fault in non-loading condition unlike DWT. However, by changing the wavelet transform only a limited amount of work has been done get out.

In addition, model based approaches have their own limitation of characterization of the faults, these methods detect the severe faults and neglect the early stage failure or the faults with diminished magnitude. Previous research suggested primarily fuzzy logic , expert system and ANN soft computing associated with single stator current used for feature extraction. But, rigorous mathematical calculations are done in fuzzy system for fault diagnosis and further, both expert and fuzzy systems have lack of self learning.

Furthermore, the previous research works mainly focus on identification of different types of faults in IM and various methods used to detect these faults using various condition monitoring techniques but the use of advance machine learning techniques in this field still a thrust area now a days. Moreover, earlier research has emphasized largely on fault diagnosis of machine using single stator current signature analysis under full load conditions.

But, the use of multiple signature analysis with signal processing techniques in order to carry out fault detection is still a challenging task.Very little research has been carried out on diagnosis and detection of combined faults and fault detection based on time varying load conditions. Few researchers have used machine learning and deep learning methods for health monitoring of IM.

However, due to the complexity and importance of the systems, there is a need to further improve existing Fault Detection techniques. A major key to the success in FD is the ability to use appropriate technology to effectively fuse the relevant information to provide accurate and reliable results. The advancement in technology will provide opportunities for improving existing FD schemes.

The advance algorithms with feature extraction technique DWT, considering both vibration and stator current signals have not yet been used in this domain of fault diagnosis and detection. The individual faults have been the main focused area and combined fault analysis is still an unexplored area.

Considering the above facts, this present research work includes behavior analysis of motor under healthy and faulty conditions for both individual fault as well as combined faults under different constant and time varying loading conditions in order to validate designed model of IM for carrying out further research work.

The proposed research used hybrid approach of advance machine learning and deep learning algorithms with feature extraction technique applied on both vibration and stator current signals in order to get enhanced accuracy under constant and time varying loading conditions for fault detection of single and combined faults . This approach can identify and aggregate the pertinent information for accurate and authentic motor fault detection and further confirms its effectiveness of fault diagnosis under both constant and time varying loading conditions.

4. MOTIVATION

Induction Motor maintenance is one of the severe problem encounters by various utilities and industries. A number of researches have been done for the issues of automatic and on-line detection of faults in IM. Few of the main research work and recommendations were like, Electric Power Research Institute motor literature of reliability as per the reference [67], states that stator faults are liable for 36% of the IM failures. According to Neale [68], the installation and purchasing cost of the equipment's usually cost less than half of the total expenditure over the life of the machine for maintenance. According to Wowk [69], maintenance expenditure typically presents 15% to 40% of the total cost and it can be up to 80% of the total cost.

The motivation behind this work is to find a methodology which effectively detects faults in induction machine under different constant and time varying loading conditions at an early stage in order to avoid its catastrophic failure which may further lead to system failure. In addition to this, research work involves the stator current with vibration signals for feature selection and proposed framework of novel architecture of DBNN for effective detection of faults under time varying load.

Deep learning techniques are foremost algorithms of artificial intelligence domain. Since after the introduction of deep learning algorithms it over shadows the other machine learning algorithms and are being extensively used in various applications due to its higher accuracy and adaptability to handle data. The ability of the deep neural network's techniques to perform complex correlation among speech signal features, which enhances its performance over traditional approaches.

The deep learning method is the advanced version of the Neural Networks (NNs) which falls under machine learning category and machine learning methods SVM and RF are applied for the comparative analysis of new age deep learning classifier with conventional SVM and RF classifier.

Investigations related to different types of faults like broken rotor bars, stator and eccentric faults in induction machines and various methods to detect these faults are discussed elaborately in the research work.

In this research work, the ANSYS RMxprt & Maxwell 2D and MATLAB software tools were examined using numerous machine learning techniques to diagnose faults in SCIM and identify rotor, stator, eccentric, and combined faults under constant and time-varying load conditions.

After analyzing faults in all conditions, it was concluded that wavelet transformation with machine learning in conjunction with deep learning techniques is very effective in diagnosing various fault related problems. Implementing deep learning methods with DWT can be an important step in optimizing overall system performance.

The idea is to develop a framework to detect and diagnose faults in IM at an early stage. Using deep learning with signal processing technique such as DWT technique can improve the performance of the framework as in Dis short time wavelets allow information to be extracted from high frequency components, which can also diagnose the severity of the fault and its type.

5. RESEARCH OBJECTIVES

The objective of this research work is to develop health monitoring system that can detect and diagnose common faults which are generally occurred in three-phase Squirrel Cage Induction Motor. The main aim is to investigate the use of machine learning and deep learning techniques in the area of motor health monitoring. Since this is an electromechanical system application, the author's objective is to develop a health monitoring system that can detect, classify and diagnose common failures that commonly occur in electrical and mechanical parts of three-phase asynchronous motors. To achieve this objective, the following objectives were established:

- To design and develop the Induction Motor implementation model for behavioral analysis of motor.
- To investigate the motor under various faults like broken rotor bar faults and stator faults under different loading conditions.
- Investigation of eccentricity faults in Induction Motors. Sometimes multiple faults may occur simultaneously in IM during working condition. Less research work has been done on investigation of multiple or combined faults. The new concept of combined fault is introduced and examined under load conditions.
- The implemented model put under varied load conditions and faults conditions to apply machine learning techniques like Deep Belief Neural Network (DBNN), Support Vector Machine (SVM) and Random Forest (RF) to detect and classify the motor faults under different faulty conditions.
- Investigations carried out on effectiveness of proposed fault detection method in research work for detecting how the presence of multiple faults as well as common faults, such as rotor bar fault, stator winding fault, air gap eccentricity and their combinations affects performance of IM under different constant and time varying load conditions.

6. RESEARCH METHODOLOGY

The strategy adapted to carryout research work has been depicted in the Figure 1.1.

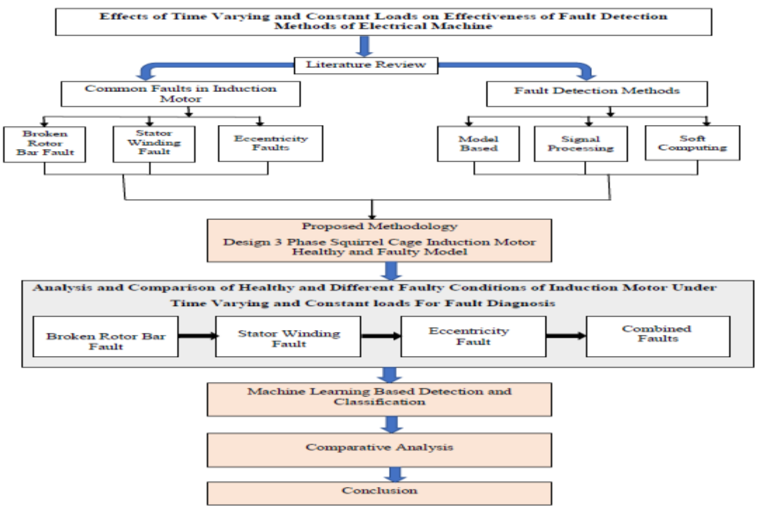

Figure 1.1: Research plan

Further, the following steps provide a brief overview about the work:

- The previous research works mainly focus on identification of different types of faults in IM and various methods used to detect these faults but the use of advance machine learning techniques in this field still a thrust area now a days. In general, broken rotor bars, stator, eccentric and combined faults are discussed elaborately in the research work. Need for monitoring dynamic behavior of the induction machines and combination of the consideration were the two general outcomes of the literature review. In this research work, first the ANSYS RMxprt and Maxwell 2D software tools are used to design the induction machine. The IM healthy characteristics are obtained using the designed model. Parameters like torque, current, and power are analyzed at constant loading condition. Furthermore, various faulty conditions are generated in ANSYS RMxprt designed model and the characteristics of the motor are noted under each fault. The faults considered are rotor broken faults, stator faults, and eccentric faults.

- Analyzed performance characteristics results of healthy and faulty IMs are compared for fault identification under constant loading condition. The MATLAB SCIM model is designed to obtain the health motor performance parameters like torque, speed, stator current and rotor current under time varying load and different constant loading conditions like 100% loading, 50% loading, 25% loading and no loading. Obtained performance characteristics of SCIM healthy and faulty models of rotor bar fault, stator winding fault, eccentric fault and combined faults are compared for fault identification under time varying and different constant loading conditions for further effective fault detection using machine learning methods. Motor vibration and stator current distortion is taken into consideration to detect and diagnose the faulty condition in SCIM. Motor performance degrades as the level of fault increases. So, the DWT is used to extract features of the motor stator current under various faulty conditions like broken rotor bar fault, stator fault, eccentric fault and combination of faults (rotor-stator, stator –eccentric & rotor eccentric).

- To detect and diagnose the type of fault, machine learning algorithms Support Vector Machine and Random Forest are applied on features extracted from analyzed behavior of IM under healthy and faulty conditions for all constant and time varying loading conditions. The accuracies achieved are 96.5% and 97.5% from RF and SVM respectively. The deep learning methods are advanced version of NNs which fall under the machine learning category. These methods are used for effective detection and classification of faults with its type and severity. To enhance the accuracy of detection of fault and its specific type on the results, deep learning techniques are explored. Proposed framework of Deep Belief Neural Network (DBNN) is applied on the extracted features which are based on stator current and vibration of IM. Finally, FD with 99.83% accuracy is achieved from DBNN. The results obtained are compared with other research work for validation.

7. THESIS ORGANIZATION

This thesis includes six chapters and these chapters are summarized as:

CHAPTER 1: INTRODUCTION

This chapter is all about the importance of motors in industry and introduction of motor faults diagnosis methods which can detect the type of faults in motor. This chapter also includes background of a research work which signifies the foundation of research optimization. Numerous reviews have been presented based on systems proposed with Fault detection methods or techniques like model based methods, MCSA with associated signal processing techniques and soft computing based approaches, which performed well in a certain way, but could not get the optimum solution for fault detection and diagnosis optimization. Therefore, research gaps are also mentioned in order to find out the best optimum solution for fault detection with high accuracy. Further, the motivation of the thesis, the research objectives and research methodology are presented in this chapter.

CHAPTER 2: MODELING AND PERFORMANCE OF SQUIRREL CAGE INDUCTION MOTOR UNDER HEALTHY CONDITION

This chapter presents the mathematical modeling of Induction Motor (squirrel cage). The ANSYS RMxprt and Maxwell 2D software tools are used to design the induction machine and furthermore, MATLAB software is used to apply model the mathematical equation of IM and implementation model is designed. Both the software's virtualizes the induction machine for carrying out the further research. Implemented models are operated under healthy operating condition and performance of motor is analyzed in terms of voltage, speed, current and torque. The designed model is subjected to various constant and time varying loading conditions.

CHAPTER 3: FAULT TYPES AND DIAGNOSIS & CLASSIFICATION TECHNIQUES

In this chapter, various faults are discussed in detail which may occur during the operating condition of motors and can cause catastrophic failure of motors if not detected and classified at an early stage. The utilization of classification techniques like SVM and RF in fault detection and classification in motors are discussed. All machine learning algorithms applied to detect the different type of faults generated in the SCIM. Deep learning method like DBNN has performed well as compared to the other machine learning techniques.

CHAPTER 4: BEHAVIORAL ANALYSIS OF INDUCTION MOTOR UNDER DIFFERENT FAULTS

This chapter includes the results obtained from the behavioral analysis of induction machine under different faults such as broken rotor bar faults, stator winding faults, eccentric fault and combined faults like eccentric with stator fault, rotor with stator fault and eccentric with rotor fault. ANSYS RMxprt and Maxwell 2D designed model with different faults discussed and executed. MATLAB model is operated under different faulty conditions and its characteristics performance are analyzed and evaluated under various constant and time varying loading conditions. Loading conditions considered are no load, 25% load, 50% load and 100% load. In order to diagnose the effects of number of broken rotor bars, power spectrum is also obtained for different conditions. Comparison of healthy and faulty conditions is done on the basis of IM parameters current, voltage, speed and torque. It is noted that the motor speed, current and torque distortions increases on account of faults and under heavy loading conditions. Furthermore, the variation of stator current is utilized as features in the Fault Detection and classification.

CHAPTER 5: MACHINE LEARNING ALGORITHM BASED FAULT DIGNOSIS EXPERIMENTATION

This chapter proposes the fault diagnosis of induction machine using Support Vector Machine (SVM), Deep Belief Neural Network (DBNN) and Random Forest (RF) using DWT features of the stator current and vibration signals. The feature extraction process using stator current is described. The dataset prepared of current signature of all the types of faults like rotor faults, stator faults, eccentric faults and combined faults under different constant (100%, 50%, 25% and no load) and time varying loading conditions. The machine learning algorithms are applied on the dataset dividing the complete dataset into training and testing dataset. The total dataset generated is 4000 samples in which 1000 are of healthy operating condition, 500 is of rotor bar faulty condition, 500 samples stator faults, 500 eccentric faults, 500 rotor-stator combined faults, 500 rotor-eccentric combined faults, 500 stator-eccentric combined faults and then the whole dataset is divided into 70% training and 30% testing. On the training and testing dataset the classification approaches DBNN, SVM and RF are applied to get the effectiveness of each algorithm on detection and classification of faults in IM. The comparison is done on the basis of accuracy of fault type detection and time taken in detecting the fault.

CHAPTER 6: CONCLUSIONS, CONTRIBUTIONS AND FUTURE WORK

This chapter covers the benefits that can be derived from the research work undertaken and also concludes the various results obtained during different faults generation and fault diagnosis of induction machine under different constant loads and time varying loading condition. The chapter includes benefactions of the present work in the field of Fault Detection and diagnosis in Induction Motor by applying advanced algorithms of machine learning and deep learning and addresses the future scope to continue with this line of research and development in the field of fault detection and classification of induction machine.

8. OUTCOMES OF THE RESEARCH WORK

The present research work contributes to the field of fault detection and diagnosis in Induction Motor by applying advanced algorithms of machine learning and deep learning. The IMs are the backbone of industrial processes such as power, automotive, machine tools plant processes. Due to the increased use of IM, the need for fault detection and classification has increased significantly. Therefore, the classification of faults of induction motors such as rotor faults, stator faults, eccentric faults, and various combined faults (rotor-stator, stator-eccentric, and rotor-eccentric) are the focus of this research.

The vital prominence of this research work based on methods which effectively detects faults in IM under different constant and time varying loading conditions prior to the system failure. The fault generation and the motor behavior at different range of load condition is executed using Maxwell 2D with FEM technique. MATLAB software is used to apply model the mathematical equation of IM and implementation model is designed. Both the software's virtualizes the induction machine for carrying out the further research. The designed model is subjected to various constant and time varying loading conditions. Machine learning and deep learning algorithms with DWT are applied on MATLAB model to detect and classify the faults. The results of the research work are summarized as follows:

- Literature survey in the field of IM fault diagnosis techniques have been performed which is further categorize in three sections model based methods, signal processing based methods and soft computing algorithm based techniques.
- Healthy SCIM characteristics have been experimentally obtained with the help of ANSYS RMxprt tool and MATLAB software.
- Broken rotor bar faults generation and detection have been successfully performed:
    - Broken rotor bar faults are generated using FEM analysis in ANSYS RMxprt and Maxwell 2D. The vibration in stator, current and speed have been observed by experimenting motor at one, two and three broken rotor bars and it's been analysed that the vibration tends to increase and distortion magnitude increases as broken rotor bar faults.
    - The effects of rotor faults have been observed in comparison to healthy motor behaviour under constant loading condition.

- MATLAB implemented SCIM model has proficiently generated the broken rotor bar faults and motor parameters are obtained.
- The experimentations of effects of constant loads variation (100%, 50%, 25% and no load) on broken bar faulty motor in comparison to healthy motors for fault diagnosis have been successfully presented. Power spectrum of generated faulty conditions has been investigated which concludes the behaviour of motor.
- The effect of time varying loading condition during runtime has been executed conclusively, stating the robustness of the implemented SCIM model.
- The characteristics obtained from different constant loading condition were further used for feature extraction for automatic detection and classification of broken rotor bars.

➢ Stator open and short circuit winding faults detection and classification experimentation was performed:

- Open winding faults have been effectively generated in RMxprt model and its characteristics were obtained using FEM analysis using Maxwell 2D.
- The experimentation on short circuit stator winding fault has been performed using MATLAB implemented model. The effects of different constant load (100%, 50%, 25% and no load) on faulty SCIM motor have been successfully analysed and compared with healthy motor.
- Time varying loading condition experiment has been performed on short circuited stator winding faulty motor and its effect has been observed.
- Obtained characteristics at the time of stator faulty condition have been further utilised to extract features for classification of fault types.

➢ Designed SCIM has been analysed on the presence of eccentric faulty condition both dynamic and static:

- Static and dynamic faults have been successfully generated using Rmxprt designed model and its characteristics behaviour has been observed at constant load condition using Maxwell 2D and also compare with healthy one. Static eccentric fault has been successfully implemented using MATLAB software and its effect under different loading conditions (100%, 50%, 25% and no load) have been presented in this research work. The faulty motor has been positioned under time varying loading condition and the stability performance analysis has been successfully performed.

➢ Considering the gap in research work where the combined faults based research were hard to find, an experimentation on combined faults has been efficiently conducted:

- The distortion of the characteristics of the motor has been analysed on various combined faulty conditions (rotor-stator, stator-eccentric and rotor-eccentric).

- The effect of combined faulty conditions on the different (100%, 50%, 25% and no load) constant loading conditions has been presented effectively and the implemented model stability has been observed from the characteristics obtained.

- The experimentation on the effect of time varying loading condition on different set of combined faults has been conducted positively and all the characteristics have been obtained and presented.

- The characteristics obtained were further more utilised to obtain features for classification process.

The proposed DBNN model framework has been developed successfully to detect and classify the type of fault during the runtime:

- DWT features have been comprehensively extracted using stator current signature at different faulty conditions (rotor, stator, eccentric, and combination of combined faults) under constant and time varying loading conditions.

- Machine learning algorithms SVM and RF have also been used for detection and classification of fault along with proposed DBNN framework.

- The results of proposed method has been compared with other machine learning algorithm, the proposed method has outperformed the previous research work.

- Combined faults have been detected and classified successfully from the proposed DBNN framework.

9. CONCLUSION

From the research work, it is concluded that the motor performance varies drastically when put at different constant and time varying loading conditions and it adversely affect its wear and tear which makes motor prone to get faulty. In order to observe all these effects, in this research work fifty six experiments have been conducted using two different machine learning algorithm and one deep learning algorithm to detect and classify faults like rotor, stator and eccentric and their combinations (rotor-stator, stator-eccentric and eccentric-rotor) at different constant loading conditions and time varying load.

The proposed framework detection and classification performance outcomes obtained in terms of accuracy on change of constant loading conditions are outstanding like the motor at 100% loading condition tends to deteriorate more and its effect on its characteristics parameters are higher due to which the extracted features of the motor at 100% loading helps classification algorithm to detect and classify the type of faults precisely and same for other loading effects even at no load where small effect of faults occur. Also fault detection methods have shown great performance under severe faulty conditions at combined faulty conditions.

The supervised machine learning algorithms such as SVM and RF have performed well in the field of detection of different type of faults at different constant loading conditions and during time varying load in this research work but as the deep learning algorithms utilize the supervised and unsupervised concepts to attain the maximum accuracy for the classification processes due to this reason the DBNN algorithm has achieved higher accuracies as compared to RF and SVM in all different loading conditions for different types of faults in IM which is well investigated during the comparative analysis of all above methods for fault detection in this work.

The present research work outperformed the other existing ones which is only possible due to robust feature extraction using unsupervised learning of features of advance deep learning method to classify the faults more precisely.

REFERENCES

[1] I. M. Culbert and W. Rhodes, "Notice of violation of IEEE publication principles: using current signature analysis technology to reliably detect cage winding defects in squirrel-cage induction motors", *in IEEE Transactions on Industry Applications*, Vol. 43, No. 2, pp. 422-428, March 2007.

[2] N. Bessous, "Reliability surveys of fault distributions in rotating electrical machines, case study of fault detections in IMs", *1st International Conference on Communications, Control Systems and Signal Processing (CCSSP)*, EL OUED, Algeria, pp. 535-543, 2020.

[3] S. Bindu and V. V. Thomas, "Diagnoses of internal faults of three phase squirrel cage induction motor - A review", *International Conference on Advances in Energy Conversion Technologies (ICAECT), Manipal*, pp. 48-54, 2014.

[4] D. Kim, D. Hong, J. Choi, Y. Chun, B. Woo and D. Koo, "An analytical approach for a high speed and high efficiency induction motor considering magnetic and mechanical problems", *in IEEE Transactions on Magnetics*, Vol. 49, No. 5, pp. 2319-2322, May 2013.

[5] A. Siddique, G. S. Yadava and B. Singh, "A review of stator fault monitoring techniques of induction motors", *in IEEE Transactions on Energy Conversion*,

Vol. 20, No. 1, pp. 106-114, March 2005.

[6] A. M. Knight and S. P. Bertani, "Mechanical fault detection in a medium-sized induction motor using stator current monitoring," *in IEEE Transactions on Energy Conversion*, Vol. 20, No. 4, pp. 753-760, December 2005.

[7] S. Altug, Mo-Yuen Chen and H. J. Trussell, "Fuzzy inference systems implemented on neural architectures for motor fault detection and diagnosis", *in IEEE Transactions on Industrial Electronics*, Vol. 46, No. 6, pp. 1069-1079, December 1999.

[8] S. Pharne and A. Patil, "Fault diagnosis of motor using fuzzy logic technique", *International Conference on Energy, Communication, Data Analytics and Soft Computing (ICECDS)*, Chennai, pp. 3110-3115, 2017.

[9] J. F. Martins, V. Ferno Pires and A. J. Pires, "Unsupervised neural-network-based algorithm for an on-line diagnosis of three-phase induction motor stator fault", *in IEEE Transactions on Industrial Electronics*, Vol. 54, No. 1, pp. 259-264, February, 2007.

[10] H. D. L. Rações, F. J. T. E. Ferreira, J. M. Pires and C. V. Damásio, "Application of different machine learning strategies for current and vibration based motor bearing fault detection in induction motors", *IECON 2019 - 45th Annual Conference of the IEEE Industrial Electronics Society, Lisbon, Portugal*, pp. 68-73, 2019.

[11] D. Basak, A. Tiwari and S. P. Das, "Fault diagnosis and condition monitoring of electrical machines - *A Review*", *IEEE International Conference on Industrial Technology, Mumbai*, pp. 3061-3066, 2006.

[12] X. Liang and K. Edomwandekhoe, "Condition monitoring techniques for induction motors", *IEEE Industry Applications Society Annual Meeting, Cincinnati, OH*, pp. 1-10, 2017.

[13] M. J. Castelli, J. P. Fossati and M. T. Andrade, "New methodology to faults detection in induction motors via MCSA", *IEEE/PES Transmission and Distribution Conference and Exposition: Latin America, Bogota*, pp. 1-6, 2008.

[14] Nandi and H. A. Toliyat, “Condition Monitoring and Fault Diagnosis of Electrical Machines – A Review”, *in Proc. 34th Annual Meeting of the IEEE Industry Applications*, pp. 197-204, 1999.

[15] Balamurugan S., Arumugam R., Paramasivam S., Malaiappan M. ,“Transient Analysis of induction motor using finite element analysis”, *IEEE Industrial Electronics Society, 30th annual conference IECON*, pp. 1526-1529, 2004.

[16] J. F. Bangura and N. A. Demerdash, "Diagnosis and characterization of effects of broken bars and connectors in squirrel-cage induction motors by a time-stepping coupled finite element-state space modeling approach," in *IEEE Transactions on Energy Conversion*, Vol. 14, pp. 1167-1176, December 1999.

[17] K. N. Gyftakis, D. V. Spyropoulos, J. C. Kappatou and E. D. Mitronikas, "A Novel Approach for Broken Bar Fault Diagnosis in Induction Motors Through Torque Monitoring," in *IEEE Transactions on Energy Conversion*, Vol. 28, pp. 267-277, June 2013.

[18] Martinez, Javier, Anouar Belahcen, and Antero Arkkio, “Combined FE and two dimensional spectral analyses of broken cage faults in induction motors”, *IECON 39th Annual conference of the IEEE Industrial Electronics Society*, 2013.

[19] Sandarangani and Martinez, C., “Electrical machines–design and analysis of induction and permanent magnet motors”, *Royal Institute of Technology, Stockhol*, 2000.

[20] Bentounsi A. and Nicolas A., “On line diagnosis of defaults on squirrel cage motor using FEM”, *IEEE Transactions on Magnetics*., Vol. 34, No. 5, pp. 3511-3574, 1998.

[21] John F. Watson, Neil C. Paterson, David G. Dorrell, “The use of finite element methods to improve techniques for the early detection of faults in 3- phase induction motors”, *IEEE Transactions on energy conversion*, Vol. 14, No. 3, pp. 655-660, 1999.

[22] Martin Blödt, Jérémi Regnier, and Jean Faucher, “Distinguishing load torque oscillations and eccentricity faults in induction motors using stator current

wigner distributions", *IEEE Transactions on Industry Applications*, Vol. 45, No. 6, 2009.

[23] Aileen Christina. J, Nagarajan. S and S. Rama Reddy. "Detection of broken Bars in three phase squirrel cage induction motor using finite element method", *International Conference on Emerging Trends in Electrical and Computer Technology*, pp. 249-254, 2011.

[24] Vaseghi B., Takorabet N., Meibody-Tabar F., "Modeling of 1M with stator winding inter-turn fault validated by FEM", *Proceedings of the International Conference on Electrical Machines*, 2008.

[25] Preston T. W., Reece A. B. J., Sangha P. S., "Induction motor analysis by time-stepping techniques", *IEEE Transactions on Magnetics*, Vol. 24, No. 1, pp. 471-474. Jan 1988.

[26] Ali Ebadi, Mohammad Mirzaie and Sayyed, "Employing finite element method to analyze performance of three-phase squirrel cage induction motor under voltage harmonics", *Research Journal of Applied Sciences, Engineering and Technology*, Vol 3, pp. 1209-1213, 2011.

[27] P. Lombard, G. Meunier, "A general method for electric and magnetic coupled problem in 2D magneto dynamic domain", *IEEE Transactions on Magnetics*, Vol. 28, No. 2, pp. 1291-1294, March 1992.

[28] J. Grieger, R. Supangat, N.Ertugrul, W.L. Soong, D. A. Gray, C. Hansen, "Estimation of static eccentricity severity in induction motors for online condition monitoring", Proceedings of the 41st *IEEE IAS Annual Meeting Industry Applications Conference*, pp. 2312-2319, October, 2006.

[29] V. Fireteanu and P.Taras, "Diagnosis of induction motor rotor faults based on finite element evaluation of voltage harmonics of coil sensors", *IEEE Sensors Applications Symposium (SAS)*, pp.1-5, February, 2012.

[30] N. Halem, S. E. Zouzou, K. Srairi, S. Guedidi and F. A. Abbood, "Static eecentricity fault diagnosis using signature analysis of stator current and air gap magnetic flux by finite element method saturated induction motors", Vol.4,

No.2, pp.118-128, June 2013.

[31] Yazidi, H. Henao, G. A. Capolino, M. Artioli, F. Filippetti, and D. Casadei, “Flux signature analysis: An alternative method for the fault diagnosis of induction machines”, in Proceedings *IEEE Power Tech, St. Petersburg, Russia,* pp. 1–6, 2005.

[32] Randy R. Schoen, Brian K. Lin, Thomas G. Habetler, Jay H. Schlag, and Samir Farag, “An unsupervised, on-line system for induction motor fault detection using stator current monitoring”, *IEEE Transaction on Industry Applications,* Vol. 31, No. 6, pp. 1280-1286, 1995.

[33] Rolf Isermann, “Model based fault detection and diagnosis status and applications,” *Annual Reviews in Control*, Vol. 29, No. 1, pp. 71–85, 2005.

[34] M. Arkan, D.K. Perović, P. Unsworth, “Online stator fault diagnosis in induction motors”, *IEEE proceedings Electric Power Applications*, Vol. 148, pp. 537 – 547, November 2001.

[35] M. Sahraoui, A. Ghoggal, S. E. Zouzou A. Aboubou and H. Razik, “Modelling and detection of inter-turn short circuits in stator windings of induction motor”, *IEEE Transactions on Energy Conversion*, Vol. 1, No. 1, pp. 4981-4986, 2006.

[36] S. Bachir, S. Tnani, J. C. Trigeassou, and G. Champenois, “Diagnosis by parameter estimation of stator and rotor faults occurring in induction machines”, *IEEE Transactions on Industrial Electron*ics, Vol. 53, No. 3, pp. 963–973, 2006.

[37] F. L. Stanislaw, A .H. M. Sadrul Ula, A. M. Trzynadlowski, “Instantanious power as a medium for the signature analysis of induction motors”, *IEEE Transactions on Industrial Applications,* Vol. 32, No. 4, pp. 904-909, 1996.

[38] G. G. Yen, K. C. Lin, "Wavelet packet feature extraction for vibration monitoring”, *IEEE Transactions on Industrial Electronics,* Vol. 47, No. 3, pp. 650–667, 2000.

[39] Marques M., Martins J., Pires V.F., Jorge R.D., Mendes L.F., “ Fault detection and diagnosis in induction machines: A case study ”, *IFIP Advances in*

Information and Communication Technology, Vol. 394. Springer, Berlin, Heidelberg, 2013.

[40] K. Kim, A. G. Parlos, and R. M. Bharadwaj, “Sensorless fault diagnosis of induction motors”, *IEEE Transactions on Industrial Electronics,* Vol. 50, No. 5, pp. 1038– 1051, 2003.

[41] H. Douglas, P. Pillay, and A.K Ziarani, “A new algorithm for transient motor current signature analysis using wavelets,” *IEEE on Transactions Industrial Applications,* Vol. 40, No. 5, pp. 1361–1368, 2004.

[42] T. Yang, H. Pen, Z. Wang and C. S. Chang, "Feature knowledge based fault detection of induction motors through the analysis of stator current data”, IEEE Transactions on Instrumentation and Measurement, Vol. 65, No. 3, pp. 549-558, March 2016.

[43] A. M. da Silva, R. J. Povinelli and N. A. O. Demerdash, "Induction machine broken bar and stator short-circuit fault diagnostics based on three-phase stator current envelopes”, IEEE Transactions on Industrial Electronics, Vol. 55, No. 3, pp. 1310-1318, March, 2008.

[44] M. Riera- Guasp, J. A. Antonino Daviu, M. Pineda-Sanchez, R. Puche Panadero and J. Perez-Cruz, “A general approach for the transient detection of slip dependent fault components based on the discrete wavelet transform”, *IEEE Transactions on Industrial Electronics,* Vol. 55, No. 12, pp. 4167–4180, 2008.

[45] H. Nejjari and M. H. Benbouzid, “Monitoring and diagnosis of induction motors electrical faults using a current park‘s vector pattern learning approach”, *IEEE Transactions on Industrial Applications,* Vol. 36, No. 3, 2000.

[46] F. Filippetti, G. Franceschini, and C. Tassoni, “Recent developments of induction motor drives fault diagnosis using artificial intelligence techniques”, *IEEE Transactions on Industrial Electronics,* Vol. 47, No.5, pp. 994–1003, 2000.

[47] M. A. Awadallah, and Mon. M. Morcos, “ANFIS- based diagnosis and location of stator inter-turn faults in PM brushless DC Motors,” *IEEE Transactions on*

Energy Conversions, Vol. 19, No. 4, pp. 795-796, 2004.

[48] W. W. Tan and H. Huo, " A generic neuro-fuzzy model-based approach for detecting faults in induction motors," *IEEE Transactions on Industrial Electron*ics, Vol. 52, No. 5, pp. 1420-1427, 2005.

[49] M. S. Ballal, Z. J. Khan, H. M. Suryawanshi, R. L. Sonolikar, "Adaptive neural fuzzy inference system for the detection of inter-turn insulation and bearing wear faults in induction motor," *IEEE Transactions on Industrial Electron*ics, Vol. 54, No. 1, pp. 250–258, 2007.

[50] Pedro Vicente Jover Rodríguez, Antero Arkkio, "Detection of stator winding fault in induction motor using fuzzy logic," *Applied Soft Computing Journal,* Vol. 8, No. 2, pp. 1112–1120, 2008.

[51] R. H. Abiyev, O. Kaynak, "Fuzzy wavelet neural networks for identification and control of dynamic plants- A novel structure and a comparative study," *IEEE Transactions on Industrial Electron*ics, Vol. 55, No. 8, pp. 3133–3140, 2008.

[52] M. B. K. Bouzid, G. Champenois, N. M. Bellaaj, L. Signac, and K. Jelassi, "An effective neural approach for the automatic location of stator inter-turn faults in induction motor," *IEEE Transactions on Industrial Electron*ics, Vol. 55, No. 12, pp. 4277-4289, 2008.

[53] J. Kurek and S. Osowski, "Support vector machine fault diagnosis of the broken rotor bars of squirrel-cage induction motor," *Neural Computing & Applications Journal,* Vol. 19, pp. 557-564, 2010.

[54] Feng Jia, Yaguo Lei, Jing Lin, Xin Zhou, Na Lu, "Deep neural networks A promising tool for fault characteristic mining and intelligent diagnosis of rotating machinery with massive data." *Mechanical Systems and Signal Processing Journal*, Vol 72, pp. 303–315, 2016.

[55] Zhang W, Peng G, Li C, Chen Yand Zhang Z. "A new deep learning model for fault diagnosis with good anti-noise and domain adaptation ability on raw vibration signals". *Sensors (Basel).*17(2):425, February 2017.

[56] X Yang, R Yan, R X Gao., “Induction motor fault diagnosis using multiple class feature selection”. Proceedings of 2015 *IEEE International Instrumentation and Measurement Technology Conference (IIMTC), Pisa, Italy,* pp. 256–260, May 11-15, 2015.

[57] T. dos Santos, F. J. T. E. Ferreira, J. M. Pires and C. Damásio, "Stator winding short-circuit fault diagnosis in induction motors using random forest," *IEEE International Electric Machines and Drives Conference (IEMDC),* Miami, FL, , pp. 1-8, 2017.

[58] Aydin, Ilhan & Karakose, Mehmet & Akin, Erhan. “A new method for early fault detection and diagnosis of broken rotor bars,” *Energy Conversion and Management Journal* , pp :1790-1799, 2011.

[59] Jagadanand, G., Lalgy Gopi, S. George and J. Jacob. “Inter-turn fault detection in induction motor using stator current wavelet decomposition”, *International Journal of Electrical Engineering and Technology*, Vol. 3, pp. 103-122, 2012.

[60] Fang R, “Induction machine rotor diagnosis using support vector machines and rough set”. Lecture Notes in Computer Science, Springer, Berlin, Heidelberg, Vol. 4114, pp. 631–636, June 2006.

[61] Fatima Husari and Jeevanand Seshadrinath, “Sensitive inter-tum fault identification in induction motors using deep learning based methods”, *IEEE International Conference on Power Electronics, Smart Grid and Renewable Energy* (PESGRE2020), 2020.

[62] E. Pandarakone, M. Masuko, Y. Mizuno and H. Nakamura, "Deep neural network based bearing fault diagnosis of induction motor using fast fourier transform analysis," *IEEE Energy Conversion Congress and Exposition (ECCE),* Portland, OR, pp. 3214-3221, 2018.

[63] Heydarzadeh, Mehrdad & Hedayati Kia, Shahin & Nourani, Mehrdad & Henao, Humberto & Andr´, G & Capolino, Gérard-André., “Feature learning using deep neural networks for fault diagnosis in electromechanical systems”, *ASME Dynamic Systems and Control Conference,* November 2019.

[64] John Grezman, Jianjing Zhang, Peng Wang, Kenneth A. Loparo and Robert X. Gao, “Interpretable convolutional neural network through layer-wise relevance propagation for machine fault diagnosis” IEEE Sensors Journal Vol. 20 , No. 6 ,

March15, 2020.

[65] A. Guerra de Araujo Cruz, R. Delgado Gomes, F. Antonio Belo and A. Cavalcante Lima Filho, "A Hybrid System Based on Fuzzy Logic to Failure Diagnosis in Induction Motors," in *IEEE Latin America Transactions*, Vol. 15, , pp. 1480-1489, 2017.

[66] S. Shao, R. Yan, Y. Lu, P. Wang and R. X. Gao, "DCNN-Based Multi-Signal Induction Motor Fault Diagnosis," in *IEEE Transactions on Instrumentation and Measurement*, Vol. 69, pp. 2658-2669, June 2020.

[67] I. Kao, W. Wang, Y. Lai and J. Perng, "Analysis of Permanent Magnet Synchronous Motor Fault Diagnosis Based on Learning," in *IEEE Transactions on Instrumentation and Measurement*, Vol. 68, pp. 310-324, February 2019.

[68] A. Hajary, R. Kianinezhad, S. G. Seifossadat, S. S. Mortazavi and A. Saffarian, "Detection and Localization of Open-Phase Fault in Three-Phase Induction Motor Drives Using Second Order Rotational Park Transformation," in *IEEE Transactions on Power Electronics*, Vol. 34, pp. 11241-11252, November 2019.

[69] B. Gou, Y. Xu, Y. Xia, G. Wilson and S. Liu, "An Intelligent Time-Adaptive Data-Driven Method for Sensor Fault Diagnosis in Induction Motor Drive System," in *IEEE Transactions on Industrial Electronics*, Vol. 66, pp. 9817-9827, December 2019.

[70] S. Lu, Q. He, T. Yuan and F. Kong, "Online Fault Diagnosis of Motor Bearing via Stochastic-Resonance-Based Adaptive Filter in an Embedded System," in *IEEE Transactions on Systems, Man, and Cybernetics: Systems*, Vol. 47, pp. 1111-1122, July 2017.

[71] A. Naha, K. R. Thammayyabbabu, A. K. Samanta, A. Routray and A. K. Deb, "Mobile Application to Detect Induction Motor Faults," in *IEEE Embedded Systems Letters*, Vol. 9, no. 4, pp. 117-120, December 2017.

[72] S. M. K. Zaman, X. Liang and L. Zhang, "Greedy-Gradient Max Cut-Based Fault Diagnosis for Direct Online Induction Motors," in *IEEE Access*, Vol. 8, pp. 177851-177862, 2020.